Université du Québec

INRS-Institut Armand-Frappier

Étude sur la biogenèse et le mouvement des usines virales induites par le virus de la mosaïque du navet

Par

Romain Grangeon

Thèse présentée pour l'obtention

du grade de philosophiae doctor (Ph.D)

Jury d'évaluation

Président du jury	Patrick Labonté
Examinateurs externes	Peter Moffett (université de Sherbrooke)
	Guy Lemay (Université de Montréal)
Directeur de recherche	Jean-François Laliberté

RÉSUMÉ

La capacité infectieuse d'un virus réside dans les interactions qu'il doit réaliser avec des protéines hôtes cibles. Sans ces interactions, il ne peut accomplir son cycle viral qui lui permettra d'infecter son hôte. Les virus à ARN de polarité positive (+) se répliquent en association avec des membranes et provoquent des changements cellulaires. Ces changements conduisent à la formation d'usines virales impliquées dans la réplication des virus. Le virus de la mosaïque du navet (TuMV, turnip mosaic virus), un virus à ARN(+) dont la taille du génome est d'environ 10kb, n'échappe pas à cette règle. Dans ce projet de doctorat, je me suis intéressé à la biogenèse de ces usines virales induites par le TuMV et de l'impact sur la cellule de la formation de telles structures. Je me suis également attardé au rôle que pouvaient jouer ces usines dans le transport intercellulaire du virus.

Dans des travaux publiés dans Journal of Virology (Oct. 2009, Vol.83 n° 20 p. 10460–10471), en collaboration avec Sophie Cotton, nous avons montré que la protéine virale $6K_2$ est responsable de la formation des usines et que plusieurs protéines de l'hôte impliquées dans la traduction sont présentes dans celles-ci. Nous y avons aussi identifié des protéines virales impliquées dans la réplication et la présence d'ARN viral. J'ai contribué à montrer que les usines virales sont mobiles et localisées le long des microfilaments d'actines. Le mouvement intracellulaire de ces vésicules est inhibé lorsque les cellules sont traitées avec de la latrunculin B, une drogue qui dépolymérise les microfilaments. Les résultats obtenus dans cet article suggèrent un couplage de la réplication et de la traduction.

Dans un deuxième article publié également dans Journal of Virology (Sept. 2012 vol. 86 no. 17 p. 9255-9265), j'ai ensuite observé minutieusement la formation des usines virales au cours de l'infection. Il existe deux types de structures bien distinctes: une structure périnucléaire d'environ 10µm de diamètre et de nombreuses vésicules de petites tailles. La structure périnucléaire est un amalgame de membranes issues du système sécrétoire, tandis que les vésicules de petites tailles sont localisées le long du réticulum endoplasmique (RE) du cortex et bougent rapidement. Il existe un lien fonctionnel entre ces deux types de structures, la structure périnucléaire est à l'origine des usines virales mobiles. Bien que les membranes du système sécrétoire se retrouvent dans la structure périnucléaire, le réseau du RE et les corps de Golgi ne semblent pas affectés. La structure périnucléaire est cependant en continuité avec les

membranes du système sécrétoire. De plus, nous avons constaté que le TuMV bloque la sécrétion des protéines dans l'apoplaste.

L'implication des usines virales dans le mouvement intercellulaire du TuMV a été étudiée et les résultats ont été soumis pour publication dans le journal "Proceedings of the National Academy of Sciences". J'ai observé que les vésicules $6K_2$ traversent les plasmodesmes pour se rendre dans les cellules adjacentes. Ce phénomène est rendu possible par l'action de facteurs viraux qui augmentent la taille limite d'exclusion des plasmodesmes et facilitent le passage des vésicules. En collaboration avec Juan Wan, nous avons retrouvé des agrégats membranaires marqués avec $6K_2$ et contenant de l'ARN viral dans le xylème. Ces données suggèrent que le transport symplasmique et vasculaire implique un complexe viral associé à des membranes.

Un clone infectieux permettant de visualiser le site de la réplication virale a été inséré dans un plasmide qui exprime un marqueur du RE. Cette construction permet de suivre les mouvements intercellulaires du TuMV. Grâce à cet outil, avec la collaboration de Maxime Agbeci, nous avons déterminé que le système sécrétoire précoce et tardif est requis pour le mouvement du TuMV. L'endocytose n'est en revanche pas sollicitée. Dans ce travail qui a été soumis à PLoS Pathogens, j'ai calculé que la vitesse de migration du virus est d'une cellule infectée en moyenne toutes les 3 heures.

Dans son ensemble, ce projet apporte des avancées significatives sur la compréhension des mécanismes de réplication des phytovirus et des virus à ARN(+).

Romain grangeon

Jean-François Laliberté

Directeur de recherche

REMERCIEMENTS

Tout d'abord, je tiens à remercier chaleureusement le P[r] Jean-François Laliberté, mon directeur de recherche, de m'avoir accueilli dans son laboratoire. Il a été d'une aide constante, sans sa disponibilité et sa patience je ne pense pas que j'aurais pu mener à bien ce projet. Quand j'ai commencé en septembre 2008, il m'a tout de suite mis en garde, en me disant que je ne m'étais pas engagé dans une course de sprinteurs, mais plutôt dans une course de fond, un marathon. Il a su me pousser et m'encourager à chaque moment où j'en avais besoin. Je me rappelle notamment une de ses fameuses phrases qu'il m'a souvent répétée : "If it's ain't broken, DON'T fix it". Sa bonne humeur, et son enthousiasme perpétuel face aux difficultés que l'on a pu rencontrer, ont été pour moi une source de motivation. Il m'a aussi fait découvrir un pays, une culture, et sur ce point il a été bien plus qu'un simple directeur de recherche.

Je tiens également à remercier les nombreux collègues du laboratoire, Sophie Cotton, Isabelle Mathieu qui étaient déjà présentes dans le laboratoire à mon arrivée. Mais également les collègues avec qui j'ai cohabité plusieurs années en partageant leur quotidien, Maxime Agbeci, Jun Jiang, Juan Wan, et plus récemment Daniel Garcia.

Je remercie également les collaborateurs qui ont contribué à ce projet notamment le P[r] Hugo Zheng de l'université McGill, Gilles Grondin de l'université de Sherbrooke, ainsi que Marcel Desrosiers et Jessy Tremblay de l'IAF pour leur aide irremplaçable au microscope confocal.

Un grand merci aux étudiants du campus avec qui j'ai partagé de bons moments, dans le bus en se rendant à l'IAF le matin, au détour d'un couloir, ou bien tout simplement autour d'un café.

Finalement, je tiens à remercier les membres de ma famille dont le soutien a été sans faille depuis le début dans mes études universitaires.

TABLE DES MATIÈRES

TABLE DES ILLUSTRATIONS

CHAPITRE 1: INTRODUCTION

CHAPITRE 2: PUBLICATIONS

Publication n° 1:

Publication n° 2:

Publication n° 3:

LISTE DES ABRÉVIATIONS

ADN	Acide désoxyribonucléique
ADP	Adénosine diphosphate
ARF	ADP Ribosylation Factors
ARN	Acide ribonucléique
ARNv	ARN viral
BaYMV	Barley yellow mosaic virus, virus de la mosaïque jaune de l'orge
BFA	Brefeldin A
BMV	Brome mosaic virus virus, de la mosaïque du brome
CIRV	Carnation italian ringspot virus, virus des taches annulaires de l'œillet italien
CPMV	Cowpea mosaic virus, virus de la mosaïque du niébé
CymRSV	Cymbidium ringspot virus, virus des taches annulaires du cymbidium
eEF	Eukaryotic translation elongation factor
eIF(iso)4E	Eukaryotic translation initiation factor (iso) 4E
eIF	Eukaryotic translation initiation factor (iso) 4G
ERES	ER exit sites, sites d'export du RE
ESCRT	Endosomal sorting complex required for transport
FRAP	Fluorescence recovery after photobleaching
GFLV	Grapevine fanleaf virus, virus du court-noué
HC-Pro	Helper-component proteinase
Hsc-70-3	Heat shock protein cognate 3
MacMV	Maclura mosaic virus, virus de la mosaïque du Maclura

MNSV	Melon necrotic spot virus, virus de la criblure du melon
MOI	Multiplicity of infection
MP	Movement protein, protéine de mouvement
NIa	Nuclear inclusion a
NIb	Nuclear inclusion b
NLS	Nuclear localization signal
ORF	Open reading frame
PABP	Poly(A)-binding protein
PCaP1	Plasma membrane-associated cation binding protein 1
PDLP1	Plasmodesmata located protein 1
PIPO	Pretty interesting potyviridae ORF
PRSV	Papaya ringspot virus, virus des taches annulaires du papayer
PPV	Plum pox virus, Virus de la charka
PSbMV	Pea seed-borne mosaic virus, le virus de la mosaïque du pois
PVA	Potato virus A, Le virus A de la pomme de terre
PVX	Potato virus X, virus X de la pomme de terre
RCNMV	Red clover necrotic mosaic, virus de la mosaïque nécrotique du trèfle rouge
RdRp	RNA-dependent RNA polymerase
RE	Réticulum endoplasmique
RgMV	Ryegrass mosaic virus, virus de la mosaïque du ray-grass
RHP	Reticulon homology protein
RNP	Ribonucleoprotein, complexe ribonucléoprotéique
RYMV	Rice yellow mottle virus, virus de la panachure jaune du riz

SEL	Size exclusion limit
SPMMV	Sweet potato mild mottle virus, Virus de la marbrure bénigne de la patate douce
TBSV	Tomato bushy stunt virus, virus du rabougrissement buissonneux de la tomate
TEV	Tobacco etch virus, virus de la gravure du tabac
TGBp	Triple gene block protein
TGN	Trans Golgi network, réseau du trans-Golgi
TMV	Tobacco mosaic virus, le virus de la mosaïque du tabac
TuMV	Turnip mosaic virus, virus de la mosaïque du navet
TVMV	Tobacco vein mottling virus, le virus de la marbrure nervaire du tabac
TVMV	Tobacco vein mottling virus
TVS	Transvacuolar strands, filaments transvacuolaires
TYMV	Turnip yellow mosaic virus, virus de la mosaïque jaunissante du navet
VIGS	Virus-induced gene silencing
VPg	Viral protein genome-linked
WSMV	Wheat streak mosaic virus, virus de la mosaïque striée du blé
ZYMV	Zucchini Yellow Mosaic Virus, virus de la mosaïque jaune de la courgette

CHAPITRE 1: INTRODUCTION

1. Généralités sur les virus de plantes

Les virus sont des parasites obligatoires, à ce titre ils n'ont aucune autonomie, et dépendent entièrement de la cellule hôte pour se multiplier. Ils doivent donc détourner la machinerie cellulaire à leur profit. Chez les plantes, une infection réussie implique nécessairement l'entrée du virus dans une première cellule, la synthèse des protéines virales et la formation d'un complexe de réplication qui va permettre la multiplication du virus. Une fois cette première étape effectuée, le virus va pouvoir infecter la cellule voisine et se propager ainsi de cellule en cellule, pour finalement infecter la plante de façon systémique en circulant dans les tissus vasculaires. L'infection virale est caractérisée par l'apparition de symptômes, qui peuvent être plus ou moins sévères dépendamment du virus, de la plante hôte, de sa condition physiologique et de son environnement. Bien souvent les virus provoquent l'apparition de mosaïque sur les feuilles, caractérisée par la décoloration du limbe foliaire formant des motifs de marbrures. Les phytovirus induisent également des retards de croissance, des taches nécrotiques, des taches chlorotiques, la déformation des feuilles et dans certains cas peuvent conduire à la mort de la plante. Globalement les virus réduisent la capacité de croissance de la plante, et peuvent altérer la production de fruit et de légumes, provoquant dans l'agriculture des pertes économiques substantielles. Les mécanismes moléculaires conduisant à l'apparition de symptômes ne sont toujours pas connus, mais ils découlent d'interactions entre des facteurs viraux et des facteurs hôtes interférant avec des processus de développement de la plante. Les maladies virales se propagent en quelques semaines dans la plante entière, et une fois infectée une plante ne peut pas être traitée, elle sera donc infectée durant le restant de sa vie. Les phytovirus provoquent des maladies généralisées qui touchent tous les organes de la plante, feuilles, racines, et tiges, mais certains massifs cellulaires comme les méristèmes ne sont pas touchés.

La dissémination des virus se déroule selon deux modes de transmission, la transmission verticale, et la transmission horizontale :

- La transmission verticale représente le passage du virus, d'une plante à sa descendance. Elle est très fréquente, en particulier chez les plantes qui se reproduisent de façon végétative.

Non- infecté infecté

Le virus de la mosaïque du navet (TuMV)

TuMV par le Dr John Walsh, Université de Warwick

Virus de la sharka (PPV), François Houiller, INRA

Virus de la mosaïque jaune de la courgette (ZYMV),Dominique Blancard, INRA

Figure 1: Symptômes de l'infection par les *Potyvirus*.

De gauche à droite : retard de croissance, taches nécrotiques, défaut de coloration des fruits, rabougrissement, décolorations et déformations sur le feuillage.

Comme l'infection est généralisée, les tubercules, les racines, et les tiges contiennent du virus, donc les boutures prélevées sur une plante mère infectée seront systématiquement infectées. Dans la majorité des cas, le virus ne se transmet pas par les semences. De cette façon les graines issues d'une plante infectée par le virus de la mosaïque du navet (TuMV, turnip mosaic virus) ne donneront pas naissance à un jeune plant infecté. Il existe bien entendu quelques exceptions à cette règle, et certains virus peuvent se transmettre par la graine, c'est le cas du virus de la mosaïque de la tomate (ToMV, tomato mosaic virus), du virus de la mosaïque de la laitue (LMV, lettuce mosaic virus) et du virus de la mosaïque transmise par les semences de pois (PSbMV, pea seed-borne mosaic virus).

- La transmission horizontale désigne la transmission du virus de plante à plante, dans un même champ par exemple. Cette transmission peut être mécanique, c'est à dire lors de pratiques comme la taille, ou simplement par frottement de feuilles infectées contre des feuilles non infectées sous l'action du vent. Mais plus généralement, la transmission horizontale résulte de la transmission du virus par des organismes vivants, champignons, nématodes, ou insectes, appelés vecteurs de la maladie.

Étant donné qu'il n'existe aucun moyen chimique de lutte contre les phytovirus, seule une lutte préventive peut être envisagée, comme l'utilisation de plante résistante, l'utilisation de semences saines, ou l'élimination du vecteur du virus qui dans de nombreux cas est un insecte suceur/piqueur de type aphyde.

La structure du génome des virus de plantes est dans la grande majorité des cas très simple, composée d'un acide nucléique protégé par des protéines de capsides. L'information génétique est contenue dans un acide nucléique sous la forme d'un ARN ou d'un ADN, simple ou double brin, contenant 4-12 gènes viraux (Figure 2).

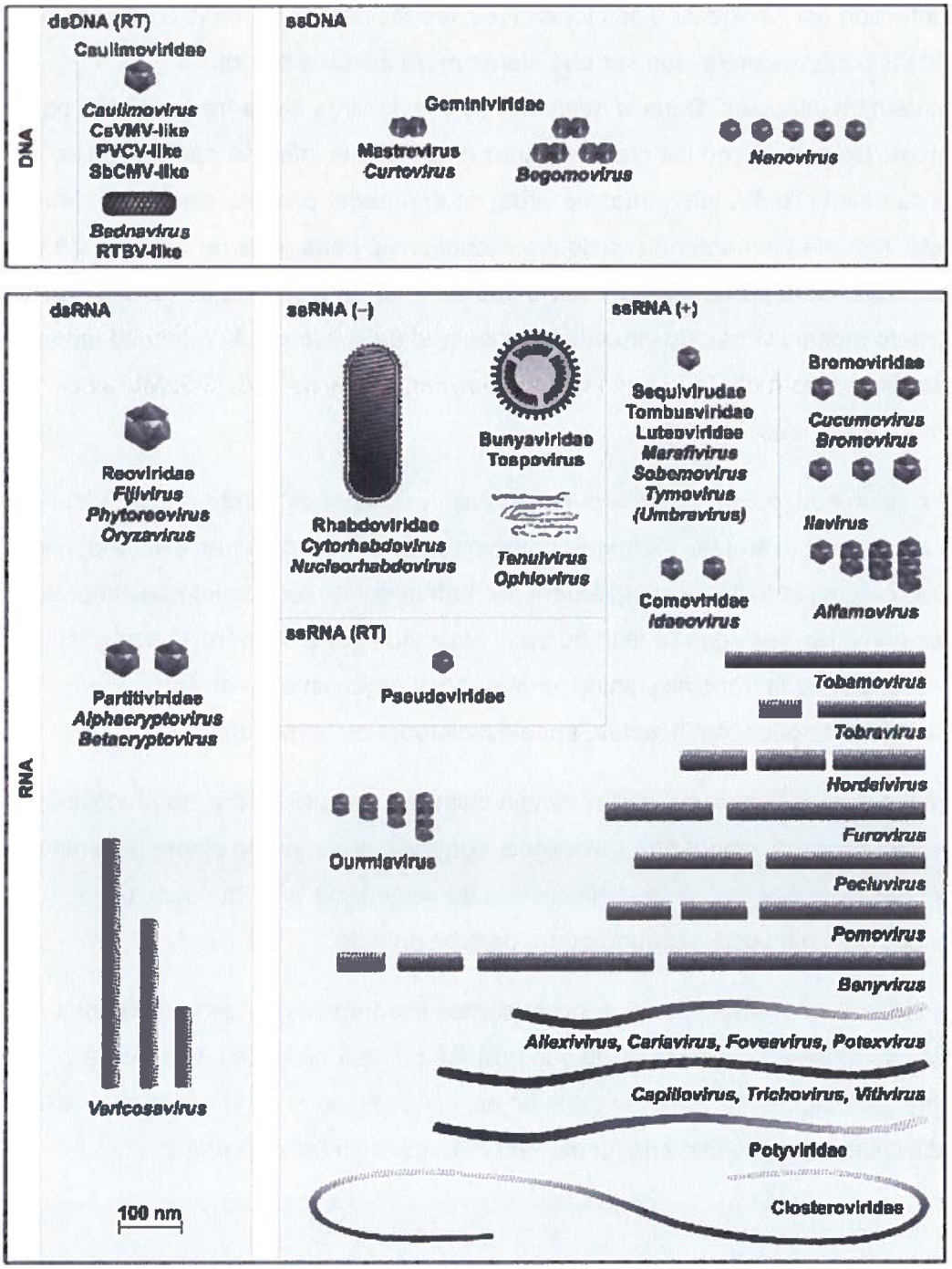

Figure 2: Famille et genre de virus qui infectent les plantes.

Cette représentation distingue les virus selon la nature de leur génome, ADN ou ARN, simple brin ou double brin, de polarité positive ou négative. (tiré de M. H. V. van Regenmortel et al., eds., Virus Taxonomy: 7th Report of the International Committee on Taxonomy of Viruses, p. 33, copyright 2000)

2. Les *Potyvirus*

2.1 Généralités et taxonomie

Le virus de la mosaïque du navet est un *Potyvirus* (Fauquet, 2005). Le genre *Potyvirus* appartient à la famille des *Potyviridae*, qui comprend également les genres Ipomovirus (SPMMV, sweet potato mild mottle virus), Macluravirus (MacMV, maclura mosaic virus), Rymovirus (RgMV, ryegrass mosaic virus), Tritimovirus (WSMV, wheat streak mosaic virus), et Bymovirus (BaYMV, barley yellow mosaic virus) (Astier et al., 2006). Les similarités dans l'organisation du génome et les stratégies de réplication permettent d'inclure les *Potyvirus* dans le super groupe des "picornavirus like", avec les virus bipartites du genre *Comovirus* et *Nepovirus* ainsi que les picornavirus de virus d'animaux (Goldbach, 1992).

Le *Potyvirus* est le genre qui contient le plus de virus chez les plantes, 30% de tous les virus de plantes connus. Économiquement, c'est aussi le groupe de virus qui occasionne les plus grosses pertes en agriculture et en horticulture (Riechmann et al., 1992). Le TuMV infecte principalement les plantes de la famille des brassicacées, anciennement nommées crucifères. Cette grande famille comprend de nombreuses espèces économiquement importantes comme le canola, les choux, la moutarde, le rutabaga, sans oublier le navet. Cette famille comprend aussi de nombreuses plantes adventices susceptibles au TuMV comme *Arabidopsis thaliana* par exemple. Le TuMV peut utiliser ces plantes adventices comme réservoir naturel. Ce virus n'est cependant pas inféodé aux brassicacées, puisqu'il peut infecter certaines plantes de la famille des composés comme la laitue ou la scarole. Les symptômes d'une infection sont des taches chlorotiques, et la présence d'anneaux nécrotiques sur les feuilles.

La transmission du virus se fait de façon non persistante par des insectes suceurs ou piqueurs, de la famille des aphidés, comme le puceron. Dans certains cas, la transmission du virus peut se faire par la graine (PSbMV, pea seed-borne mosaic virus).

Les particules virales sont cylindriques, non enveloppées et filamenteuses, de 680-900 nm de long et 11-15 nm de large (Urcuqui-Inchima et al., 2001) (Figure 3). Le génome viral est protégé par une capside d'environ 2000 unités de la

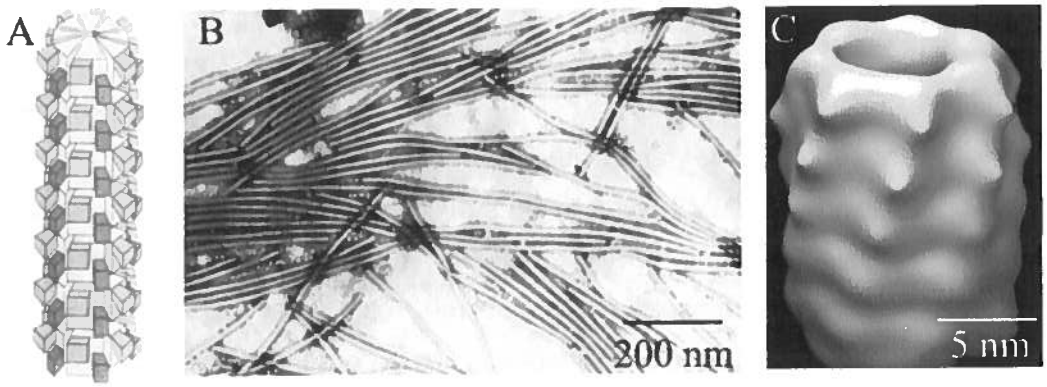

Figure 3: Particule virale d'un *Potyvirus*.

(A) Représentation schématique de la particule d'un *Potyvirus* (Shukla, 1989). (B) Photo de microscopie électronique de la particule virale du TuMV coloré avec du methylamine tungstate (Walsh and Jenner, 2002). (C) Reconstitution d'une particule virale du TuMV en tomographie (Juan Wan, communication personnelle).

protéine CP (coat protein) (Anindya and Savithri, 2004). Une caractéristique commune aux *Potyvirus* est la présence de corps d'inclusions dans le cytoplasme. Également, certains *Potyvirus* induisent la formation de corps d'inclusions nucléaires (excluant le TuMV).

2.2 Structure génomique

Le génome des *Potyvirus* est constitué d'un ARN monocaténaire de polarité positive d'environ 10 kb. À l'extrémité 5', une protéine connue sous le nom de VPg lie l'ARN viral. À l'extrémité 3'du génome se trouve une queue poly (A). Le génome ne possède qu'un seul cadre ouvert de lecture, qui est traduit en une seule polyprotéine de plus 3000 acides aminés. La polyprotéine est clivée co et post-traductionnellement par 3 protéases virales pour donner 11 protéines matures (Figure 4).

Le gène P1 correspond à la partie N-terminale du génome des *Potyvirus* et code pour une protéase qui permet son propre clivage entre elle-même et HC-Pro (helper-component Proteinase)(Riechmann et al., 1992). Le gène P1 est très variable parmi les *Potyvirus*, seule la partie codant pour l'activité catalytique de la protéase est bien conservée. Le centre catalytique de cette protéase est constitué d'une triade His, Asp et Ser correspondant à une protéase de type sérine (Verchot et al., 1992). Une mutation d'un seul de ces 3 acides aminés conduit à l'inactivation du virus (Urcuqui-Inchima et al., 2001). La protéine P1 possède une activité de liaison séquence non-spécifique à l'ARN, identifié chez le TuMV (Soumounou and Laliberte, 1994), le virus A de la pomme de terre (PVA, potato virus A) (Merits et al., 1998) et le virus de la marbrure nervaire du tabac (TVMV, tobacco vein mottling virus) (Brantley and Hunt, 1993).

HC-Pro est une protéine multifonctionnelle. Elle possède une activité auto-protéolytique qui clive la HC-Pro en C-terminal, juste avant la protéine P3. Le centre catalytique de la protéase est semblable aux Cystéines-protéases (Oh and Carrington, 1989). HC-Pro agit comme régulateur lors de la transmission par les aphidés, c'est un facteur de spécificité de la transmission (Maia et al., 1996). HC-Pro est requis lors de l'entrée et la sortie du virion dans le système vasculaire de la plante hôte (Kasschau et al., 1997). HC-Pro induit l'élargissement des plasmodesmes (PD) ce qui facilite le passage de l'ARN viral de cellule en cellule

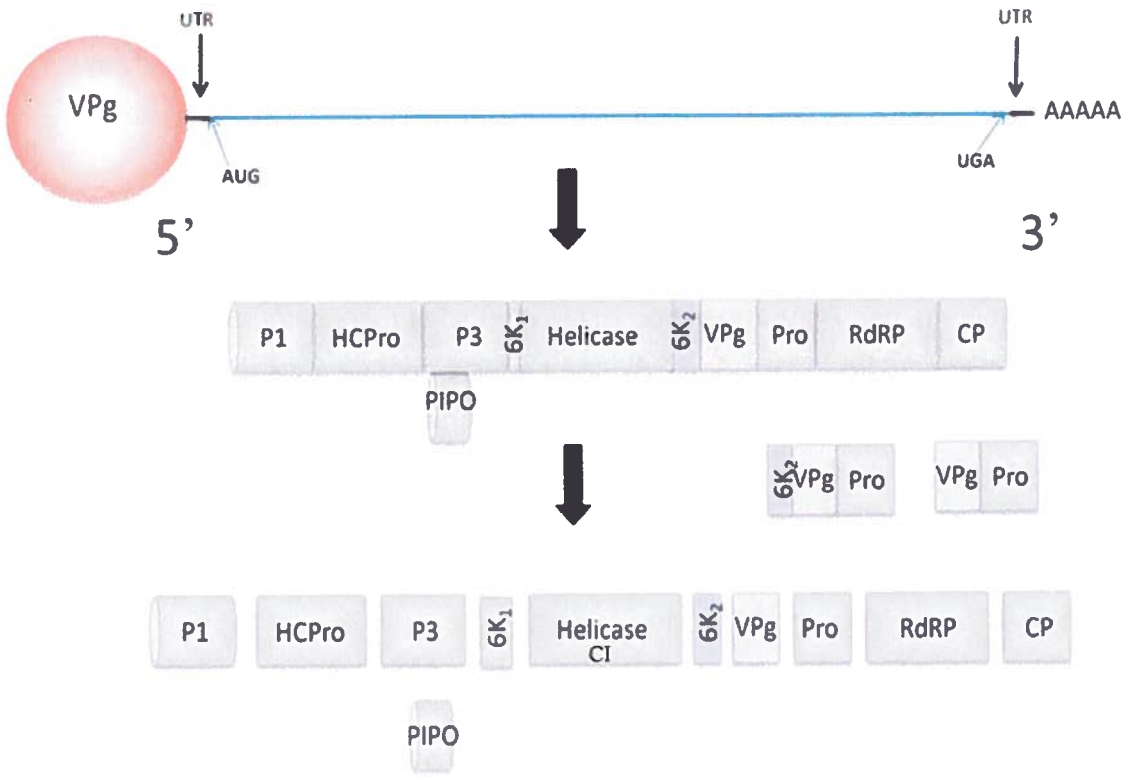

Figure 4: Organisation génomique et stratégie d'expression des *Potyvirus* (exemple du TuMV).

L'ARN de polarité positive du TuMV est lié avec la protéine virale VPg de façon covalente à son extrémité 5', tandis que son extrémité 3' est polyadénylée. L'ARN viral va être traduit en une polyprotéine qui va être clivée sous l'action des protéases virales P1, HC-Pro et VPg-Pro pour finalement générer 10 protéines matures, plus la protéine PIPO qui est issue d'un décalage du cadre de lecture ouvert. La protéine VPg existe aussi sous la forme de précurseurs VPg-Pro et $6K_2$-VPg-Pro.

(Rojas et al., 1997). Une autre fonction important de HC-Pro est la suppression du "gene silencing" (Anandalakshmi et al., 1998). Le "gene silencing" est considéré comme un mécanisme naturel de défense de la plante face à l'accumulation de virus où la plante dégrade l'ARN double brin du virus lors de sa réplication (Covey et al., 1997). HC-Pro joue un rôle important dans le cas d'une infection de la plante par deux virus différents, les symptômes de la maladie s'en trouvent augmentés (Pruss et al., 1997).

P3 et son précurseur P3-$6K_1$ sont libérés de la polyprotéine par l'activité protéolytique de HC-Pro et de VPg-Pro (Riechmann et al., 1992).

Actuellement, P3 est la protéine la moins bien caractérisée parmi les 11 protéines matures des *Potyvirus*. C'est aussi une des protéines virales dont la séquence varie le plus selon les différents *Potyvirus*. P3 semble jouer un rôle lors de la réplication virale. En effet, des mutants d'insertion du TVMV dans le gène codant pour P3 sont incapables de se répliquer dans des plantes et dans des protoplastes (Klein et al., 1994). P3 et 6K1 ne possèdent pas de site de liaison avec l'ARN (Merits et al., 1998) mais seraient impliquées dans la réplication en interagissant avec CI (protéine d'inclusion cytoplasmique)(Rodriguez-Cerezo et al., 1993) . La protéine P3 du virus de la gravure du tabac (TEV,tobacco etch virus) a été détectée dans le noyau en association avec RdRp et VPg-Pro (Langenberg and Zhang, 1997). P3 et son précurseur 6K1-P3 du virus des taches annulaires du papayer (PRSV, papaya ringspot virus) fusionnée avec GFP se localisent dans le RE des cellules d'épidermes d'oignons (Eiamtanasate et al., 2007b). Malgré ces observations qui semblent contradictoires, il existe un consensus pour attribuer à P3 un rôle dans l'amplification du virus. Une étude sur deux isolats de TuMV a révélé que la région codant pour la protéine P3 est impliquée dans l'accumulation du virus, mais également dans les mouvements longue distance du virus lors de l'infection systémique (Suehiro et al., 2004).

La protéine $6K_1$ a été clonée récemment dans notre laboratoire et fusionnée avec GFP. Malgré les prédictions qui attribuent un domaine transmembranaire hydrophobe à $6K_1$, la distribution de cette protéine est cytoplasmique soluble. Des expériences de fractionnement cellulaire ont confirmé cette observation en

retrouvant $6K_1$ dans la fraction soluble S30 (communication personnelle de Jiang Jun).

La protéine PIPO (pretty interesting Potyviridae ORF) est une protéine découverte par bio-informatique, dont on ignorait encore l'existence il y a peu de temps. Sa taille prédite est de 7 kDa. Elle est synthétisée à partir d'un cadre de lecture ouvert (ORF) chevauchant celle de P3 (Vijayapalani et al., 2012). Les virus "Knock-out" pour l'ORF de PIPO ne sont plus infectieux chez *Nicotiana benthamiana* (Chung et al., 2008). Cependant PIPO n'a jamais été détectée toute seule mais fusionnée avec la partie N-terminale de P3, sous la forme P3N-PIPO de ~25 kDa. P3N-PIPO du TuMV exprimée toute seule facilite son propre mouvement de cellules à cellules, et interagit avec la protéine CI pour diriger CI vers les plasmodesmes (PD). Il a été montré que des mutations dans P3 du WSMV qui altèrent PIPO (bien que PIPO n'était pas encore connue) bloquent le mouvement intercellulaire (Choi et al., 2005). P3N-PIPO faciliterait le mouvement intercellulaire d'un complexe contenant l'ARN viral (ARNv) en interagissant avec PCaP1 (plasma membrane-associated cation binding protein 1). P3N-PIPO et PCaP1 se localisent ensemble à la membrane plasmique et aux PDs (Vijayapalani et al., 2012).

CI possède une activité ATPase et hélicase (Urcuqui-Inchima et al., 2001). CI peut se lier à des nucléotides et à l'ARN. Cette protéine participe à la réplication notamment en se liant à l'ARN pour le dérouler. Une étude sur l'activité ATPase de CI dans des plantes de maïs infectées a révélée une activité ATPase dans les vésicules cytoplasmiques de réplication à proximité des inclusions cytoplasmiques et proches des PD suggérant un rôle dans la transmission cellule-cellule (Chen et al., 1994). Pendant l'infection, CI s'accumule et forme des structures coniques qui peuvent fréquemment traverser la paroi de la cellule pour atteindre la cellule voisine (Rodriguez-Cerezo et al., 1993).

$6K_2$ n'a pas d'activité enzymatique propre, mais possède un domaine hydrophobe de 19 acides aminés qui est responsable de sa localisation membranaire (Schaad, 1997). Cette partie transmembranaire est nécessaire à l'ancrage de $6K_2$-VPg-Pro dans les vésicules de réplications. La partie N-terminale de $6K_2$ contient une vingtaine d'acides aminés hydrophiles.

La VPg (Protéine Virale liée au génome) est une protéine d'un poids moléculaire de 20-22 kDa (Laliberté et al., 1992). Cette protéine se retrouve également sous ses formes précurseurs VPg-Pro (49 kDa) et $6K_2$-VPg-Pro (55kDA).

VPg-Pro possède l'activité protéase majeure des *Potyvirus*. Elle est responsable du clivage d'environ deux tiers de la polyprotéine. Il existe un site interne de clivage qui sépare les domaines VPg et Pro. L'activité de protéase provient du domaine Pro qui contient un motif "3C-like" de Picornavirus. Chacune des protéines issues du clivage de la polyprotéine possède des fonctions qui leurs sont propres, la régulation de l'activité protéolytique de VPg-Pro est donc finement régulée.

VPg et ses précurseurs interviennent principalement dans la réplication virale. En effet, en interagissant avec la RdRp, $6K_2$-VPg-Pro permet l'ancrage de la polymérase aux membranes des vésicules où se trouve le complexe de réplication (Li et al., 1997). VPg et ses précurseurs interagissent avec plusieurs protéines virales et cellulaires induisant des spécificités virus-hôtes, ces interactions seront discutées dans la section suivante (2.3) dédiée aux interactions protéines-protéines. Chez certains *Potyvirus* (excluant le TuMV), la protéine VPg-Pro s'accumule dans des inclusions nucléaires (Restrepo-Hartwig and Carrington, 1992;Hajimorad et al., 1996;Urcuqui-Inchima et al., 2001). Cette caractéristique est à l'origine du nom qui lui a été attribué, Nla pour "Nuclear Inclusion a". L'adressage au noyau s'opère grâce à un signal de localisation nucléaire NLS situé dans le domaine VPg (Schaad et al., 1996). Le rôle de VPg-pro dans le noyau n'est pas encore défini, mais ayant une activité de nucléase non spécifique, il a été proposé que VPg-Pro puisse dégrader l'ADN de la cellule hôte (Anindya, 2004).

L'ARN polymérase ARN dépendante (RdRp) est codé par le gène Pol, appelé également Nlb pour "Nuclear Inclusion b", car cette protéine s'accumule dans le noyau chez certains *Potyvirus* (excluant le TuMV). Mais RdRp est également présente au niveau des usines virales, donc avec les membranes associées au complexe de réplication. Cette protéine contient le motif caractéristique GDD (Gly, Asp, Asp) très conservé des réplicases (Hong and Hunt, 1996). Cette enzyme est responsable de la synthèse des brins négatifs et positifs du génome viral (réplicase). La RdRp contient deux domaines indépendants NLS (Li et

al., 1997) mais sa fonction dans le noyau reste mal connue. Plus récemment, il a été montré chez les poliovirus que RdRp permet l'uridylisation de VPg (Steil and Barton, 2008). Sous sa forme urydilée VPg agirait comme une amorce pour l'initiation de la réplication virale.

La protéine de la capside CP a pour principale fonction de protéger le génome du virus. CP est impliquée dans la transmission par les aphidés, les mouvements cellules-cellules, les mouvements systémiques et aussi dans la régulation de l'amplification de l'ARN viral (Urcuqui-Inchima et al., 2001).

2.3 Interaction protéines-protéines

Il est intéressant de remarquer que les protéines des *Potyvirus* sont multifonctionnelles, participant à la réplication, au mouvement du virus, ainsi qu'à la transmission par les aphidés. Pour réaliser toutes ces fonctions, les protéines virales interagissent entre elles.

Une cartographie des interactions entre les différentes protéines du virus de la mosaïque du Soja (Kang SH, 2004), du PVA et du PSbMV (Guo et al., 2001) a été établie à partir du système du double hybride dans des levures. Une forte interaction a été détectée entre CP/CP, HC-Pro/HC-Pro, VPg-Pro/VPg-Pro, CP/HC-Pro, HC-Pro/CI, $6K_2$-VPg-Pro/RdRp et CP/RdRp. L'interaction CP/CP avait déjà été reportée chez le TEV (Hong et al., 1995) et le PVA (Guo et al., 2001). Cette interaction se déroulerait selon toute vraisemblance lors de l'encapsidation du virus. L'interaction HC-Pro/CP jouerait un rôle essentiel lors de la transmission par les Aphidés (Flasinski, 1998).

L'interaction HC-Pro/CI serait impliquée dans le mouvement de cellule à cellule du virus (Cronin et al., 1995;Kasschau et al., 1997).

L'interaction VPg/VPg faciliterait le recrutement du complexe de réplication et/ou de traduction avec l'ARN viral (Guo et al., 2001). Quant à l'interaction $6K_2$-VPg-Pro/RdRp, elle aurait un rôle stimulateur sur l'activité de la RdRp, suggérant un rôle dans la réplication (Hong et al., 1995;Li et al., 1997;Fellers et al., 1998;Daros et al., 1999). La séquestration de la RdRp dans les vésicules met en jeu des

interactions protéines-protéines, c'est vraisemblablement le domaine transmembranaire de $6K_2$ qui permet cet ancrage (Li et al., 1997).

L'interaction entre la protéine de la capside CP et la polymérase RdRp a une fonction inconnue pour l'instant. Elle pourrait contribuer à la régulation de la synthèse d'ARN virale dans les cellules infectées (Hong et al., 1995).

P3N-PIPO et CI interagissent directement *in planta* et coordonnent la formation d'une structure aux PDs qui facilite le mouvement intercellulaire des *Potyvirus* (Wei et al., 2010).

Etant donné le faible nombre de gènes contenus dans le génome des virus à ARN de polarité positive, l'implication de protéines hôtes est nécessaire à l'accomplissement de la majorité des étapes du cycle infectieux (l'entrée du virus, la traduction, la réplication, l'assemblage, ainsi que libération des virions). Les interactions protéines virales avec les protéines hôtes sont donc multiples et diversifiées.

Le complexe de réplication contiendrait en effet de nombreuses protéines cellulaires qui seraient bien souvent des déterminants de spécificité entre le virus et l'hôte (Ortìn and Parra, 2006;Elena and Rodrigo, 2012). Notre laboratoire s'est concentré ces dernières années sur certaines de ces interactions entre protéines virales et protéines hôtes.

La protéine eIF4E est un de ces facteurs. eIF4E lie la coiffe des ARNm et appartient au complexe eIF4F qui a pour rôle de recruter les ribosomes et les ARNm pour initier la synthèse de protéines. En plus de eIF4E, eIF4F inclut eIF4A, une hélicase qui facilite l'accès aux ribosomes en déroulant les structures secondaires des ARNm, et eIF4G qui interagit avec plusieurs autres protéines de la machinerie traductionnelle comme PAPB, eIF3 et eIF4B (un cofacteur de eIF4A) (Nicaise et al., 2007). Chez les plantes, il existe un second complexe eIF4F, nommé eIF(iso)4F qui contient eIF(iso)4E et eIF(iso)4G (Browning, 2004).

L'interaction de VPg avec le facteur eucaryotique d'initiation à la traduction eIF4E a été identifiée avec le système du double hybride pour le TuMV (Wittmann et al., 1997) et aussi pour le TEV (Schaad et al., 2000). Les isomères eIF4E et eIF(iso)4E ont été associés à des gènes récessifs de résistances

naturelles mol¹ et mol² chez la laitue (Nicaise et al., 2003), pvr2 et pvr6 chez le poivron (Ruffel, 2002), sbm-1 chez le pois (Gao et al., 2004) ainsi que pot-1 chez la tomate (Ruffel et al., 2005). La présence de ces gènes récessifs entraîne une accumulation du virus réduite et des symptômes diminués (tolérance) ou une absence d'accumulation du virus (résistance). VPg est le déterminant de virulence des *Potyvirus*, et son interaction avec eIF4E (ou un seul de ces allèles) conduit à une interaction compatible donnant les symptômes typiques de la maladie (Byoung-Cheorl Kang, 2005).

Chez *Arabidopsis thaliana,* les mutants "Knock-out" pour le gène codant eIF(iso)4E sont résistants au TuMV (Duprat, 2002;Lellis et al., 2002). *In planta* l'interaction entre les précurseurs de VPg (ie VPg-Pro et $6K_2$-VPg-Pro) et eIF(iso)4E a également été établi dans le noyau et dans les vésicules de réplications (Beauchemin et al., 2007). L'interaction VPg-Pro avec eIF(iso)4E peut être impliquée dans la perturbation des fonctions cellulaires normales, et l'interaction $6K_2$-VPg-Pro avec eIF(iso)4E serait nécessaire pour la traduction et/ou la réplication virale (Beauchemin et al., 2007). VPg rentre en compétition avec les ARNm pour la liaison à eIF4E (Khan et al., 2006), cette compétition entraînerait une diminution de la synthèse protéique cellulaire (Grzela et al., 2006).

eIF4G a été identifié comme interacteur lors de l'infection par le virus de la mosaïque de la laitue (LMV). eIF4G serait recruté par l'intermédiaire du complexe VPg-Pro/eIF4E, VPg augmentant l'affinité de eIF4E pour eIF4G (Michon, 2006).

Le facteur d'élongation eEF1A interagit aussi bien avec l'ARN viral de virus d'animaux (De Nova-Ocampo et al., 2002) qu'avec celui des virus de plantes (Zeenko et al., 2002). Cette interaction jouerait un rôle dans la traduction et/ou la réplication. L'interaction eEF1A avec RdRp et VPg-Pro chez le TuMV a été identifiée récemment dans les vésicules de réplication (Thivierge et al., 2008) .

In planta PABP interagit avec RdRp (Wang et al., 2000) et avec VPg-Pro dans les vésicules induites par le TuMV, cette interaction jouerait un rôle important lors de l'infection (Leonard et al., 2004;Dufresne et al., 2008).

La protéine Hsc70-3 a elle été identifiée dans les vésicules induites par le TuMV, et interagit avec RdRp (Dufresne et al., 2008).

3. Remodelage cellulaire par les phytovirus

Cette partie de l'introduction fait l'objet d'un article de revue qui a été publié dans la revue française de *Virologie*. Cette section discute du remodelage cellulaire qui survient lors de l'infection par les virus de plantes. Certains résultats obtenus au cours de mon doctorat y sont présentés mais seront abordés de façon plus développée dans les chapitres suivants et dans la discussion finale. Ces résultats sont identifiés par le symbole (*).

3.1 Morphologie générale d'une cellule végétale

Avant d'évoquer le recrutement des endomembranes durant l'infection par les virus à ARN+, il est important de donner aux lecteurs qui ne seraient pas familiers une description rapide d'une cellule végétale. Pour satisfaire leur curiosité, nous suggérons la visite du site internet "The Illuminated Cell" (http://www.illuminatedcell.com) qui décrit de façon détaillée les différents organites que l'on retrouve dans une cellule végétale. Avant tout, il faut savoir que le cytoplasme de la majorité des cellules végétales est un milieu encombré, l'espace y est limité par la présence d'une vacuole dont le volume est imposant et de nombreux chloroplastes. Le réticulum endoplasmique (RE), contrairement à sa distribution dans les cellules animales, ne se cantonne pas seulement autour du noyau, mais constitue un réseau de membranes extrêmement dynamiques qui s'étend dans toute la cellule. On distingue d'une part le RE du cortex qui parcourt le cytoplasme et qui est constitué de tubules et de citernes caractérisées par une structure tout à fait singulière de jonctions à trois points, et d'autre part le RE périnucléaire qui entoure le noyau (Staehelin, 1997). Les filaments transvacuolaires (transvacuolar strands, TVS) établissent une liaison directe entre le RE périnucléaire et le RE du cortex, et permettent l'acheminement de métabolites ainsi que le mouvement d'organites (Ruthardt et al., 2005). Les TVS permettent

également l'ancrage du noyau dans la cellule. L'appareil de Golgi est présent sous la forme de petites vésicules, les corps de Golgi, distribuées un peu partout dans le cytoplasme et dont les mouvements dépendent de l'actine et des tubules du RE. Les corps de Golgi bougent également le long des TVS. Ces organites (RE et l'appareil de Golgi) avec le réseau du trans Golgi (trans Golgi network, TGN), les endosomes et la vacuole composent le système sécrétoire de la cellule végétale (Hanton et al., 2005) (Figure 5). Le système sécrétoire est impliqué dans la synthèse, la modification et le transport des protéines, lipides et polysaccharides. Son bon fonctionnement est donc vital pour le métabolisme de la cellule. Comme nous allons l'évoquer un peu plus loin, la formation d'usines virales va se faire à partir de membranes issues bien souvent du système sécrétoire. Une dernière caractéristique de la cellule végétale est la présence de jonctions entre deux cellules, appelées plasmodesmes. Les PD instaurent une continuité cytoplasmique entres les cellules adjacentes qui permet le passage de molécules de petites tailles.

3.2 Réplication des virus de polarité positive chez les plantes

La structure du génome des virus de plantes est dans la grande majorité des cas très simple, composée d'un acide nucléique protégé par une coque protéique. Le génome viral est un ARN ou un ADN, simple brin ou double brin, codant pour 4 à 12 gènes. En fonction de leur génome, les virus sont classés en sept groupes distincts. Le groupe des virus à ARN+ est le groupe qui contient le plus grand nombre de virus de plantes. Pour certains virus, comme le virus de la mosaïque du tabac (TMV, tobacco mosaic virus) ou le TuMV, toute l'information génétique est contenue sur un seul brin d'ARN. Mais dans d'autres cas, le génome peut être divisé en plusieurs molécules; c'est le cas des virus à génome segmenté comme le

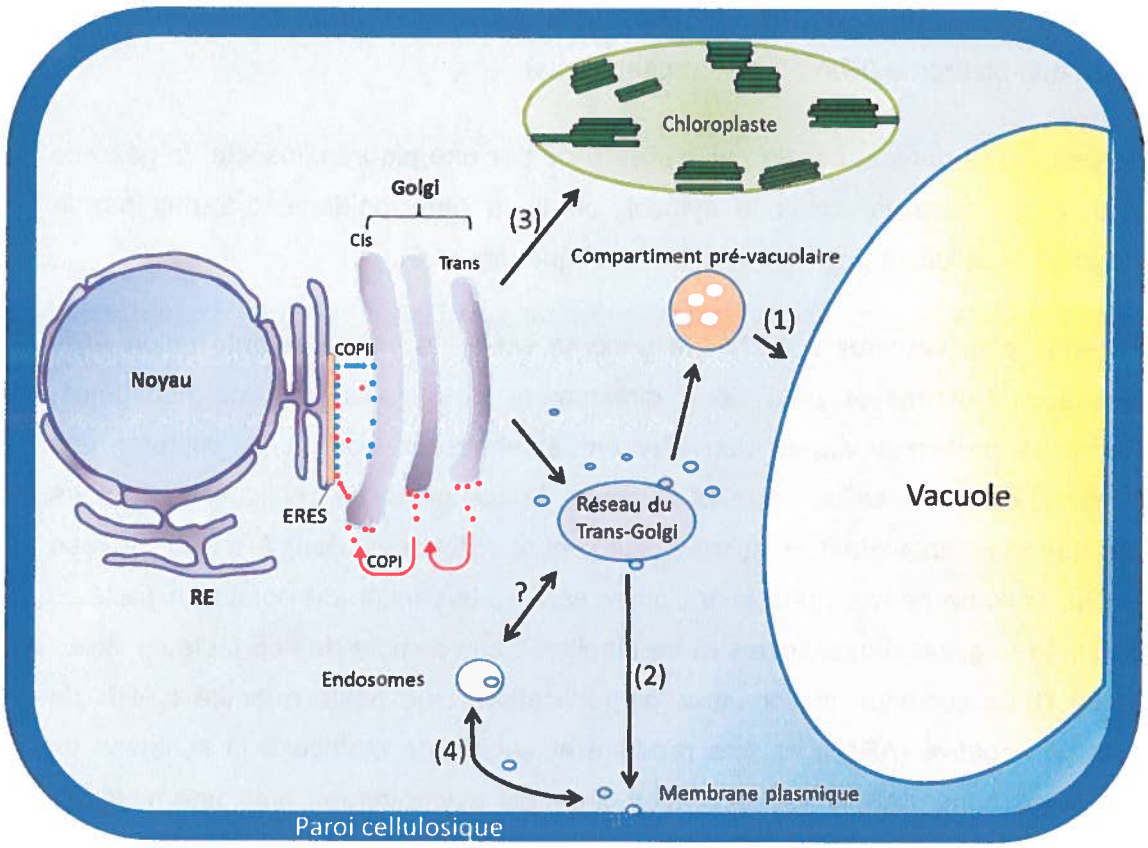

Figure 5: Schéma du système sécrétoire chez les plantes.

Ce schéma représente les différentes routes empruntées par les protéines synthétisées dans le RE. À l'interface entre le RE et l'appareil de Golgi, les vésicules COPII sont impliquées dans l'export des protéines vers le Golgi (voie antérograde), tandis que les vésicules COPI sont impliquées dans le recyclage vers le RE des protéines qui lui sont spécifiques (voie rétrograde). Une fois dans le Golgi les protéines peuvent être acheminées à la vacuole lytique ou de stockage (1), à le membrane plasmique (voie exocytique) (2), ou aux chloroplastes (3). La voie endocytaire (4) permet de recycler les protéines de la membrane plasmique, qui sont ensuite incorporées dans les endosomes et fusionnent avec les compartiments du réseau du trans-Golgi.

virus de la mosaïque du niébé (CPMV, cowpea mosaic virus) ou le virus de la mosaïque du brome (BMV, brome mosaic virus).

Après l'entrée dans la cellule par blessure ou par une piqure d'insecte, le génome viral va se retrouver dans le cytosol, où il va être rapidement traduit par la machinerie cellulaire pour la synthèse protéique (figure 6).

En effet, pour les virus à ARN+, le génome est de la même polarité qu'un ARN messager (ARNm) et peut donc directement être traduit sur les ribosomes. Certaines protéines virales nouvellement synthétisées vont alors recruter des membranes de la cellule hôte et y ancrer le complexe de réplication. Pour se répliquer, les virus à ARN+ utilisent leur propre ARN dépendant ARN polymérase RdRp, mais ne peuvent pas se multiplier sans l'intervention de nombreux facteurs de l'hôte (e.g. protéines, lipides et métabolites). L'ensemble de ces facteurs viraux et de l'hôte constitue le complexe de réplication. Une petite quantité d'ARN de polarité négative (ARN-) va être produite et servira de matrice à la synthèse de nombreux brins d'ARN+. La réplication virale est asymétrique ; pour une molécule d'ARN(-) il y aura environ 40 à 70 molécules d'ARN(+) de produites. Les brins d'ARN(+) nouvellement synthétisés vont être relâchés sous la forme d'un complexe ribonucléoprotéique (RNP) et vont migrer dans la cellule voisine par l'entremise du PD. Nous verrons un peu plus loin que le passage par les PD du complexe RNP peut être facilité par des protéines virales appelées protéines de mouvement (MP).

Il est important de garder en tête qu'à chaque étape de la réplication, les interactions entre les protéines virales et les facteurs de l'hôte vont être déterminantes pour la réussite ou l'échec de l'infection virale.

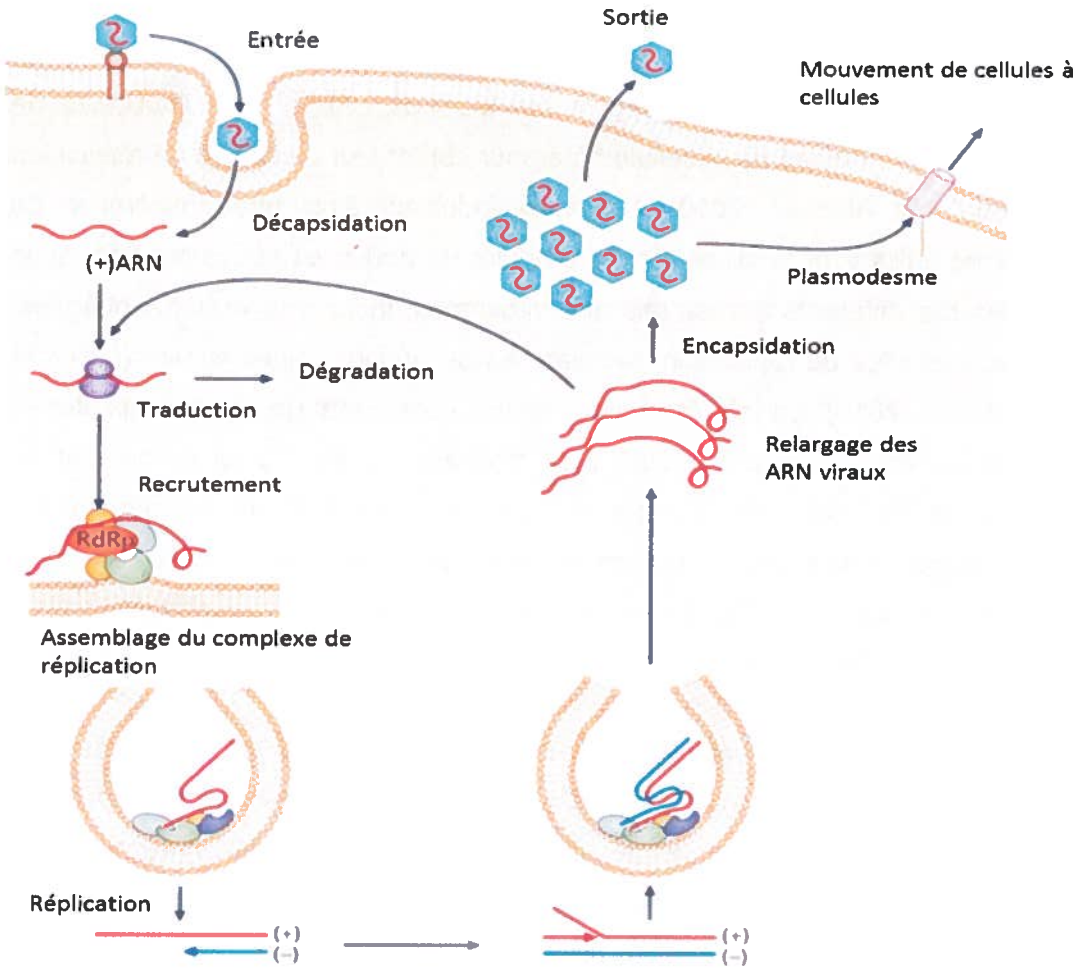

Figure 6: Schéma du cycle d'infection des virus à ARN (+).

Après l'entrée dans la cellule par endocytose (virus animaux) ou par blessure (virus de plantes), le génome des virus à ARN(+) est relargué dans le cytosol, où il va être directement traduit par la machinerie cellulaire de la traduction. Certaines protéines virales vont alors recruter des membranes de la cellule hôte et y ancrer le complexe de réplication. Une petite quantité d'ARN de polarité négative va être produite, qui servira de matrice à la synthèse de nombreux brins d'ARN(+). Les brins d'ARN(+) nouvellement synthétisés vont être relargués dans le cytosol et pourront recommencer un nouveau cycle de traduction/réplication, être encapsidés et sortir de la cellule dans le cas des virus animaux, ou passer dans la cellule voisine par les plasmodesmes sous la forme d'un complexe ribonucléoprotéique dans le cas des virus de plantes. (Adapté de (Nagy, 2012)).

3.3 Les usines virales

Une caractéristique que partagent tous les virus à ARN (+) est l'obligation de mobiliser les membranes de la cellule hôte pour abriter leur complexe de réplication (den Boon and Ahlquist, 2010). Les virus induisent ainsi une prolifération de membranes qu'ils vont modifier afin de produire de nouvelles structures cellulaires désignées par différents termes tels que virosomes, inclusions virales, sphérules, granules, vésicules de réplication, viroplasmes ou encore usines virales (Laliberté and Sanfaçon, 2010). En fait, ces usines virales constituent des quasi-organites et procurent un environnement adapté à la réplication virale : i) en permettant au complexe de réplication de s'ancrer sur une membrane; ii) en augmentant les concentrations locales des composantes requises pour la réplication ; iii) et en confinant la réplication de l'ARN dans une structure bien définie qui permet au virus d'échapper aux défenses de la cellule. .

L'ultrastructure des usines virales de certains virus d'animaux a été observée par tomographie, ce qui a apporté une meilleure compréhension de la réplication des virus à ARN(+) (Kopek et al., 2007;Knoops et al., 2008;Welsch et al., 2009;Belov et al., 2012). La tomographie permet la synthèse d'images en trois dimensions à partir d'une tranche épaisse d'une cellule observée sous différents angles en microscopie électronique (Fridman et al., 2012). Ces études ont révélé l'existence d'un réseau de membranes interconnectées, contenant des tubules et des vésicules à simples et doubles membranes qui proviennent du système sécrétoire ou des mitochondries. Si les membranes constituent une composante essentielle de la réplication, leur origine et leur composition varient grandement en fonction du type de virus. Chez les plantes, la totalité des organites présents dans la cellule peut être remodelée sous l'action d'un virus.

Généralement, l'origine des membranes des usines virales dépend du virus, mais il semble que certains virus peuvent utiliser différents types de membranes sans spécificité propre.

Dans cette section nous allons évoquer la diversité des membranes utilisées pour former les usines de réplication virale chez les plantes.

a) Usines associées aux peroxysomes et aux mitochondries

La réplication du virus du rabougrissement buissonneux de la tomate (TBSV, tomato bushy stunt virus) a été étudiée de façon intensive car le TBSV peut se répliquer dans un certain nombre de plantes, qui sont ses hôtes naturels, mais aussi dans la levure (Nagy, 2008). Le TBSV induit la formation de corps multivésiculaires à partir des membranes du peroxysome. Durant l'infection, les autres organites comme le RE, l'appareil de Golgi, les chloroplastes et les mitochondries restent inchangées (McCartney et al., 2005b). Mais dans des levures mutantes incapables de former des peroxysomes, le TBSV peut malgré tout se répliquer en utilisant des membranes provenant du RE (Jonczyk et al., 2007), ce qui montre une certaine flexibilité d'adaptation du virus à la cellule hôte qu'il infecte.

Le virus des taches annulaires de l'œillet italien (CIRV, carnation italian ringspot virus) et le virus de la criblure du melon (MNSV, melon necrotic spot virus) sont des tombusvirus comme le TBSV. En revanche, ils induisent des usines virales provenant de la membrane externe des mitochondries grâce à un signal d'adressage aux mitochondries contenu dans la protéine p36 (Weber-Lotfi et al., 2002;Mochizuki et al., 2009). Certains isolats du CIRV recrutent préférentiellement les peroxysomes plutôt que les mitochondries, ce qui pourrait s'expliquer par des évènements de recombinaison du signal d'adressage aux peroxysomes entres certaines souches du CIRV et d'autres tombusvirus (Koenig et al., 2009). Il existe aussi des tombuvirus dont les usines sont issues de RE (Turner et al., 2004).

b) Usines associées aux chloroplastes

Le virus de la mosaïque jaunissante du navet (TYMV, turnip yellow mosaic virus) provoque la formation de sphérules sur les membranes des chloroplastes (Hatta et al., 1973). Les usines virales s'assemblent dans ces sphérules qui pourraient contenir des ouvertures connectant l'intérieur de la vésicule avec le cytoplasme, comme cela fût observé pour les usines virales provenant des mitochondries dans le cas d'un virus d'insecte (Kopek et al., 2007).

c) Usines dérivées du réticulum endoplasmique

La biogenèse des usines virales du BMV a été très bien caractérisée. Le BMV possède la particularité de se répliquer aussi bien dans les cellules de ses hôtes naturels, des herbacées, que dans la levure *Saccharomyces cerevisiae*. Les levures sont des organismes eucaryotes unicellulaires pour lesquels de nombreux outils génétiques sont disponibles. Pour cette raison le BMV est un très bon candidat pour étudier les processus de réplication virale. Dans les levures, les usines virales induites, sous la forme de sphérules, proviennent d'une invagination de la membrane du RE périnucléaire (Eiamtanasate et al., 2007a). L'intérieur de ces sphérules est connecté avec le cytoplasme par un petit pore qui permet le passage des ribonucléotides. Dans les plantes, on observe plutôt des vésicules associées au RE (Bamunusinghe et al., 2011).

La prolifération de membranes provenant du RE a également été observée pour d'autres groupes de virus de plantes, incluant les *Potyvirus* (Schaad et al., 1997), les potexvirus (Bamunusinghe et al., 2009), les népovirus (Ritzenthaler et al., 2002;Han and Sanfaçon, 2003), les comovirus (Carette et al., 2000), les tobamovirus (Kawakami et al., 2004) et les réovirus (virus à ARN double brin)(Wei et al., 2006).

Une prolifération de vésicules est observée lors de l'infection par le TuMV (Figure 7A)*. En microscopie confocale, ces vésicules ont l'apparence d'une structure globulaire périnucléaire, qui peut approcher 10 µm de diamètre (Figure 7B). Cette structure est un amalgame de RE, de Golgi, de vésicules COPII mais également de chloroplastes.

Cette structure donne naissance à des vésicules de plus petites tailles (e.g. 100-200 nm) à partir de sites d'export du RE dans un processus dépendant de la machinerie COPI et COPII (Wei and Wang, 2008). Ces vésicules se déplacent rapidement dans la cellule pour atteindre la périphérie de la cellule en association avec les tubules du RE.

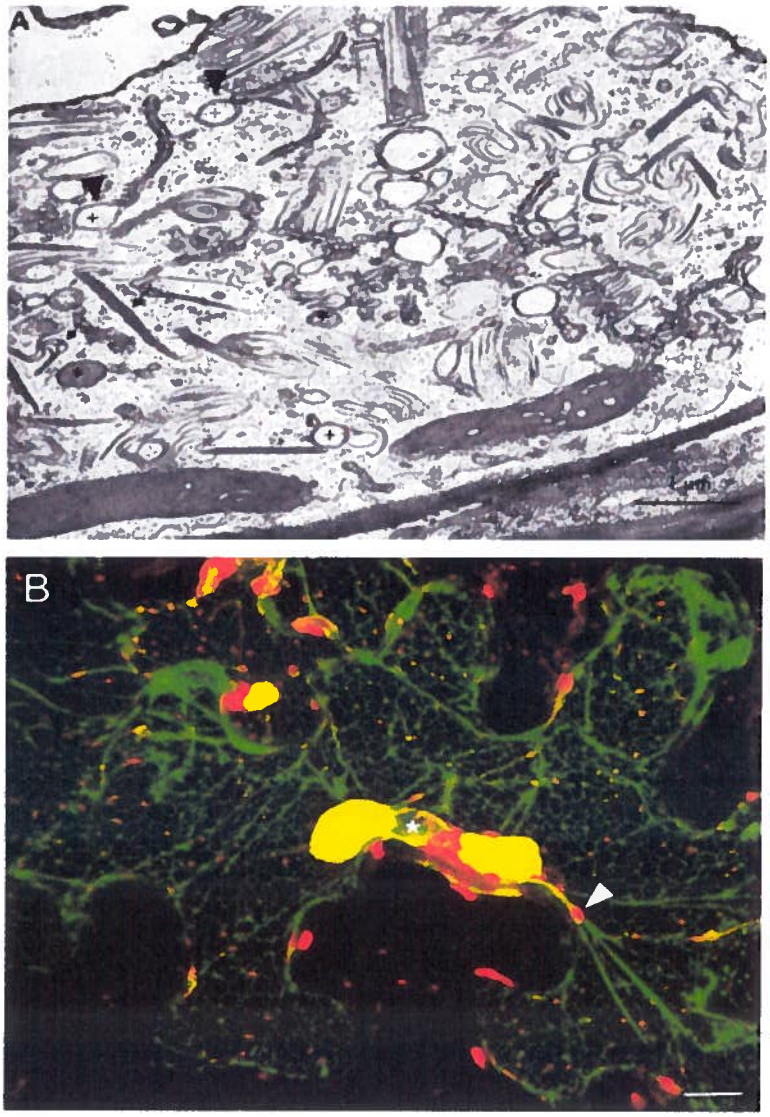

Figure 7: Observation en microscopie électronique et en microscopie confocale de cellules de *Nicotiana benthamiana* infectées par le TuMV.

(A) Cytoplasme montrant des corps d'inclusions typiques du TuMV (flèches noires) et des vésicules translucides (+) ou opaques aux électrons (*). Les têtes de flèches indiquent des vésicules associées aux tubules du RE. (B) Reconstituion 3D d'une cellule de Nicotiana benthamiana exprimant le marqueur de RE HDEL-GFP et infecté par le clone infectieux TuMV qui permet la visualisation des usines virales grâce à une fusion de $6K_2$ avec mCherry. L'astérisque indique la position du noyau, la pointe de flèche blanche indique une vésicule sur un filament transvacuolaire qui relie la structure périnucléaire induite par le TuMV avec le RE du cortex. Échelle=10µm. (Tiré de l'article (Grangeon et al., 2012))

De plus, des expériences de FRAP (Fluorescence Re After Photobleaching) ont montré que cette structure est en communication avec les endomembranes de la cellule (Grangeon et al., 2012). Une structure périnucléaire assez semblable a été observée dans des cellules infectées par le virus du court-noué (GFLV, grapevine fanleaf virus) (Ritzenthaler et al., 2002).

La structure périnucléaire appelée "X-body" induite par le virus X de la pomme de terre (PVX, potato virus X) (Tilsner et al., 2012;Linnik et al., 2013) est assez similaire à la structure induite par le TuMV*. Dans cette usine autour du noyau, on retrouve l'ARN viral, des membranes du Golgi et du RE ainsi que des microfilaments d'actine et des virions à son interface avec le cytoplasme. Des petites granules contenant les protéines virales TGBp2 et TGBp3 sont également visibles dans cette structure. Ces structures virales sont des réservoirs dans lesquels les endomembranes sont réarrangées afin de permettre la réplication et l'assemblage du virus.

d) Protéines virales impliquées dans la biogenèse des usines virales

Chez les plantes, la modification des endomembranes et la formation d'usines virales ne dépendent généralement que d'une ou deux protéines virales (Prod'homme, Jakubiec et al. 2003; Navarro, Rubino et al. 2004; McCartney, Greenwood et al. 2005). L'expression ectopique de ces protéines suffit à induire une modification des endomembranes similaire à celle que l'on observe en contexte infectieux. Ces protéines possèdent un ou plusieurs domaines transmembranaires d'une vingtaine d'acides aminés qui vont permettre leur insertion dans les membranes de façon co-traductionnelle. En plus de ce domaine hydrophobe qui traverse les membranes, ces protéines possèdent une queue N-terminale qui va dépasser de la membrane et permettre leurs interactions avec d'autres facteurs de l'hôte ou viraux. Il faut noter que dans certains cas, les protéines responsables de la formation d'usines virales ne possèdent pas de domaine transmembranaire, une hélice amphiphile permet alors leur attachement à la surface de la membrane (Liu et al., 2009).

Dans le cas des *Potyvirus*, la protéine qui ancre le complexe de réplication dans les membranes est bien caractérisée. Il s'agit de la protéine $6K_2$. Dans les

cellules de *Nicotiana benthamiana* infectées par le TEV ou par le TuMV, les usines virales se localisent en début d'infection aux sites d'export du RE (ERES) probablement en interagissant avec la protéine sec24 de la machinerie COPII.

Pour les tombusvirus, comme le TBSV ou le CIRV, la formation des usines virales dépend respectivement de la protéine virale p33 ou p36. Ces protéines possèdent un signal d'adressage responsable de la formation de sphérules ou de vésicules dans les peroxysomes pour le TBSV et dans les mitochondries pour le CIRV (Rubino et al., 2001;McCartney et al., 2005a;Jonczyk et al., 2007). Les protéines p33/p36 et Pol92 (RdRp) vont ensuite recruter l'ARN viral ainsi que les protéines virales et de l'hôte nécessaires à la formation du complexe de réplication. De plus, si on crée des virus hybrides en échangeant des portions de la protéine p33 du virus des taches annulaires du Cymbidium (CymRSV, cymbidium ringspot virus) responsable du recrutement des membranes des peroxysomes, avec des portions de la protéine p36 du CIRV responsable de la formation d'usines virale à partir de membranes des mitochondries, on observe la formation d'usines virales provenant à la fois des peroxysomes et des mitochondries (Rubino and Russo, 1998).

Pour les tymovirus comme le TYMV, la protéine virale 206K est la protéine requise pour la formation du complexe de réplication. Elle est autoclivée pour donner la protéine 140K qui contient un domaine méthyltransférase, protéase et NTPase/hélicase ainsi que la protéine 66K (RdRp) (Jakubiec et al., 2007). En l'absence de la protéine 140K, la protéine 66K se retrouve dans le cytoplasme de la cellule, mais en présence de 140K, il va y avoir une relocalisation de la 66K dans des usines virales des chloroplastes (Hanton et al., 2005). C'est la protéine 140K qui est responsable de l'ancrage du complexe de réplication dans les membranes des chloroplastes.

Certaines MP possèdent également un domaine transmembranaire et induisent aussi la formation des usines de réplication virales. C'est le cas des protéines TGBp2 et TGBp3 du PVX de la famille des "Triple Gene Block Proteins" (TGBp) (Verchot-Lubicz et al., 2007). TGBp2 et TGBp3 induisent la formation de granules et du X-body lors de l'infection par le PVX, mais sont également nécessaires au mouvement du virus. C'est aussi le cas de p7B, une des deux MP

du MNSV avec p7A (Martínez-Gil et al., 2007). La protéine p7B va induire la formation d'usines virales à partir du RE.

Le BMV possède 3 ARN codant pour 4 protéines distinctes. Les protéines 1a et 2a sont impliquées dans la réplication et partagent de nombreuses similitudes avec leurs homologues chez les Alphavirus qui infectent les vertébrés. La protéine 1a est responsable de la formation des sphérules mais ne possède pourtant pas de domaine transmembranaire. C'est une hélice amphiphile qui permet l'attachement de 1a aux membranes du RE et le recrutement des protéines nécessaires à la réplication. Dans certains cas cependant, les structures induites par une seule protéine virale diffèrent quelque peu de celles produites par le virus. C'est le cas de la protéine 1a du BMV qui lorsqu'elle est exprimée seule ou avec une faible quantité de la protéine 2a (RdRp) induit des sphérules autour du noyau. En revanche, l'expression de la protéine 1a avec une grande quantité de la protéine 2a (RdRp) induit la formation de plusieurs couches de RE périnucléaire (Schwartz et al., 2004). Les réarrangements membranaires dans la cellule infectée semblent donc être modulés en fonction du niveau d'expression des protéines virales.

3.4 Cibles cellulaires

Il semblerait que le système sécrétoire soit au cœur des changements morphologiques de la cellule. Chez les phytovirus, bien que peu d'information soit disponible sur le détournement du système sécrétoire au profit de la réplication virale, de nombreuses protéines de l'hôte impliquées dans la voie sécrétoire ont été identifiées comme indispensables à la réplication. Ces protéines sont de véritables cibles pour les protéines virales, et lorsque ces dernières manquent leurs cibles, le virus perd sa capacité infectieuse. C'est cet ensemble d'interactions entre protéines virales et protéines cibles qui définit en partie le tropisme du virus.

Pour les tobamovirus, c'est le cas des protéines TOM1 et TOM3 associées aux tonoplastes et d'ARL8 une protéine de la famille des protéines ARF (ADP ribosylation factor) (Nishikiori et al., 2011). Il a été montré que pour le TEV que la formation des usines virales dépend de la machinerie COPI et COPII, donc de l'interface RE/appareil de Golgi (Wei and Wang, 2008). Dans le cas du TuMV et du

MNSV, le traitement à la Brefeldin A (BFA), une drogue qui inhibe le système sécrétoire, ne bloque pas la réplication virale mais plutôt le mouvement de cellule à cellule* (Genovés et al., 2010;Grangeon et al., 2012). Mais un traitement à la BFA sur des cellules infectées par le GFLV inhibe cependant la réplication virale et la formation de la structure périnucléaire. Il a été proposé que la perturbation de la formation des vésicules COPII à l'interface RE/Golgi peut conduire à la formation d'un amas périnucléaire contenant un amalgame de membranes provenant du RE et du Golgi (Faso et al., 2009). Une interaction entre la RdRp du virus de la mosaïque nécrotique du trèfle rouge (red clover necrotic mosaic, RCNMV) et le facteur Arf1 (ADP ribosylation factor 1) a aussi été mise en évidence (Hyodo et al., 2013). Arf1 est impliqué dans la formation du complexe COPI sur les membranes du Golgi.

Les virus utilisent les membranes de la cellule de l'hôte pour se protéger des défenses de la cellule et parfois séquestrent des protéines de l'hôte impliquées dans leur dégradation. C'est le cas des protéines ESCRT (endosomal sorting complex required for transport) qui sont impliquées dans la reconnaissance et le transport des protéines ubiquitinylées. En absence de certaines composantes du complexe ESCRT, l'activité de la réplicase p92 du TBSV est réduite et l'ARN est accessible au ribonucléases (Barajas et al., 2009). Il a été proposé que le TBSV nécessite l'action des ESCRT pour stabiliser son complexe de réplication. Également en séquestrant ces protéines de l'hôte, le virus se protège de la dégradation.

Le maintien de l'architecture des membranes réarrangées par les virus est encore mal connu, mais il a été montré que le BMV cible les protéines RHP (reticulon homology proteins) pour former le pore des sphérules qu'il induit. Normalement les réticulons sont les protéines responsables du maintien de la structure du RE. La formation des sphérules le long du RE périnucléaire se fait par polymérisation de la protéine virale 1a, qui donne une courbure négative aux sphérules. Le BMV recrute les RHP pour former une courbure positive et créer ainsi un pore. Ce pore va permettre l'échange de molécules avec le cytoplasme.

3.5 Impact sur le métabolisme de la cellule végétale

Tous ces changements morphologiques observés dans la cellule infectée ne sont pas sans conséquence sur le métabolisme de la cellule.

Il est connu pour les virus de mammifères, qui sont pour la plupart enveloppés, que la prise de contrôle du système sécrétoire est cruciale pour l'assemblage des particules virales, mais aussi pour le mouvement intra- et intercellulaire du virus. De plus, il a été montré que l'inhibition du système sécrétoire lors de l'infection réduit la réponse immunitaire de la cellule hôte. Par exemple, les picornavirus modifient le système sécrétoire pour produire leurs usines virales en interagissant avec la protéine Arf1, ce qui a pour effet de bloquer la formation de vésicules COPI et d'inhiber le système sécrétoire (Hsu et al., 2010). Pour l'instant, seul le TuMV a été montré comme inhibant la sécrétion de protéines* (Wei and Wang, 2008;Grangeon et al., 2012).

Un autre impact de l'infection de la cellule est une production accrue de membranes pour la réplication virale. Pour le PVX, le GFLV et le CPMV, il a été rapporté que la synthèse des lipides est nécessaire à l'infection (Carette et al., 2000;Ritzenthaler et al., 2002;Bamunusinghe et al., 2009). En effet, la cérulenine, une drogue qui inhibe la synthèse *de novo* des lipides, inhibe la réplication virale. Suite à l'infection par le BMV, on observe une hausse de la production lipidique de 25 à 33% (Lee and Ahlquist, 2003). Une mutation dans la séquence codante pour une désaturase, enzyme responsable de la transformation des acides gras saturés en acides gras insaturés, inhibe grandement la réplication du BMV. Cette mutation affecte la fluidité et la plasticité des membranes qui dépendent de la composition en lipides saturés et insaturés. Un phénomène similaire est observé pour le TBSV (Sharma et al., 2011).

3.6 Mouvement intracellulaire des virus

Les interactions entre les protéines virales et les protéines de l'hôte du système sécrétoire perturbent le fonctionnement normal de la cellule au profit de la multiplication du virus. Dans la prochaine section, nous allons voir que le système

sécrétoire est également utilisé par le virus pour se déplacer dans la cellule puis de cellule en cellule.

Chez les plantes, une infection réussie implique qu'une entité infectieuse doit se propager de cellules en cellules et dans les tissus vasculaires pour finalement infecter la plante de façon systémique. La première phase du transport viral est le mouvement intracellulaire d'un complexe protéique associé à l'ARN viral. Pour certains virus, il semblerait que ce complexe ait son origine dans la structure périnucléaire. En effet pour le PVX, les granules contenant les protéines TGBp2 et TGBp3 et l'ARN viral partent de la structure périnucléaire pour se diriger vers le RE du cortex (Tilsner et al., 2012). Un phénomène similaire est observé pour le TuMV où les usines virales périphériques peuvent sortir de la structure périnucléaire et bouger le long des TVS pour rejoindre la membrane plasmique. Les usines virales du TuMV bougent de façon unidirectionnelle et irrégulière, s'arrêtent puis repartent, mais leur vitesse de mouvement moyenne est de 0.35µm/sec*. Dans le cas du TMV, l'ARN viral associé avec la protéine de mouvement et la RdRP se déplacent le long du RE du cortex sous forme de corps membranaires. Ces structures se déplacent à travers le cytoplasme à des vitesses avoisinants 0.16 µm/sec à 14 heures post infection (hpi). À 16 hpi, ces structures se déplacent plus lentement (0.04 µm/sec) le long de la membrane plasmique, vraisemblablement sur des microfilaments d'actine impliquant la myosine (Kawakami et al., 2004). Les mouvements intracellulaires des usines virales peuvent être inhibés par un traitement avec la latrunculine B, une drogue qui dépolymérise les microfilaments (Cotton et al., 2009). Les protéines TGBp2 et TGBp3 du virus de la fasciation de la pomme de terre *(Potato mop-top virus* PMTV) bougent sous forme de granules et utilisent le réseau RE/actine pour se déplacer (Haupt et al., 2005). Les usines virales induites par p7B du MNSV sont également mobiles et utilisent également le réseau RE/actine (Genovés et al., 2010). Il semble que le système sécrétoire soit également requis pour le transport intracellulaire (Genovés et al., 2010). Le résultat de ce mouvement intracellulaire est l'accumulation de ces structures membranaires à proximité des PD.

3.7 Modification des plasmodesmes

Les PD sont une porte d'entrée dans la paroi cellulosique rigide qui sépare deux cellules, assurant le passage des molécules nécessaires au bon développement de la plante. Ils s'étendent à travers la paroi cellulaire et contiennent en leur centre une structure dérivée du RE (le desmotubule), plusieurs micro-domaines enrichis de protéines, de callose et des microfilaments (Figure 8A) (Maule et al., 2011). La limite de diffusion des molécules au travers des PD (SEL, size exclusion limit) est définie par la taille de la plus petite molécule qui peut diffuser passivement à travers les PD.

La SEL oscille généralement entre 800 et 1000 daltons. Mais les PD sont hautement régulés et peuvent se dilater pour permettre le passage de molécules supérieures à 10 000 Da. La taille d'une particule virale ou d'un génome virale est généralement 3 à 4 fois supérieure à la limite de diffusion normale des PD. Pour pouvoir les traverser, les virus codent pour des protéines de mouvement (MP, mouvement protein) qui vont modifier la SEL des PD. Bien que le virus pour sa propagation n'ait pas d'autre choix que de passer par les PD, il existe cependant une grande diversité de stratégies employées qui peut dépendre des différents types de particules virales, filamenteuses, cylindriques ou icosaédriques (Figure 8). L'entité virale qui circule d'une cellule à l'autre n'est pour la plupart des phytovirus pas connus, et sa nature varie en fonction du virus.

Le TMV ne nécessite qu'une seule MP pour dilater les PD (Figure 8B). Ce n'est pas le cas de tous les virus de plantes. Certains virus nécessitent l'action combinée de la MP et de la protéine de coque (CP, capsid protein), notamment pour le CMV (Salánki et al., 2011). Chez les *Potyvirus*, il n'y a pas de MP clairement identifiée. Le mouvement du virus nécessite l'action des protéines HC-Pro, VPg, CI et P3N-PIPO (Vijayapalani et al., 2012). La protéine CI est responsable de la formation de corps d'inclusions observés de part et d'autre de la paroi, ce qui suggère une implication directe dans le mouvement intercellulaire du virus. P3N-PIPO a été découverte récemment et elle ressemble le plus à une MP, mais on ne sait pas si elle a la capacité de lier l'ARN viral. Cette protéine interagit aux PD avec CI et une protéine de l'hôte appelée "plasma membrane-associated cation binding protein" (PCAP1). Le recrutement de PCAP1 faciliterait le mouvement du virus.

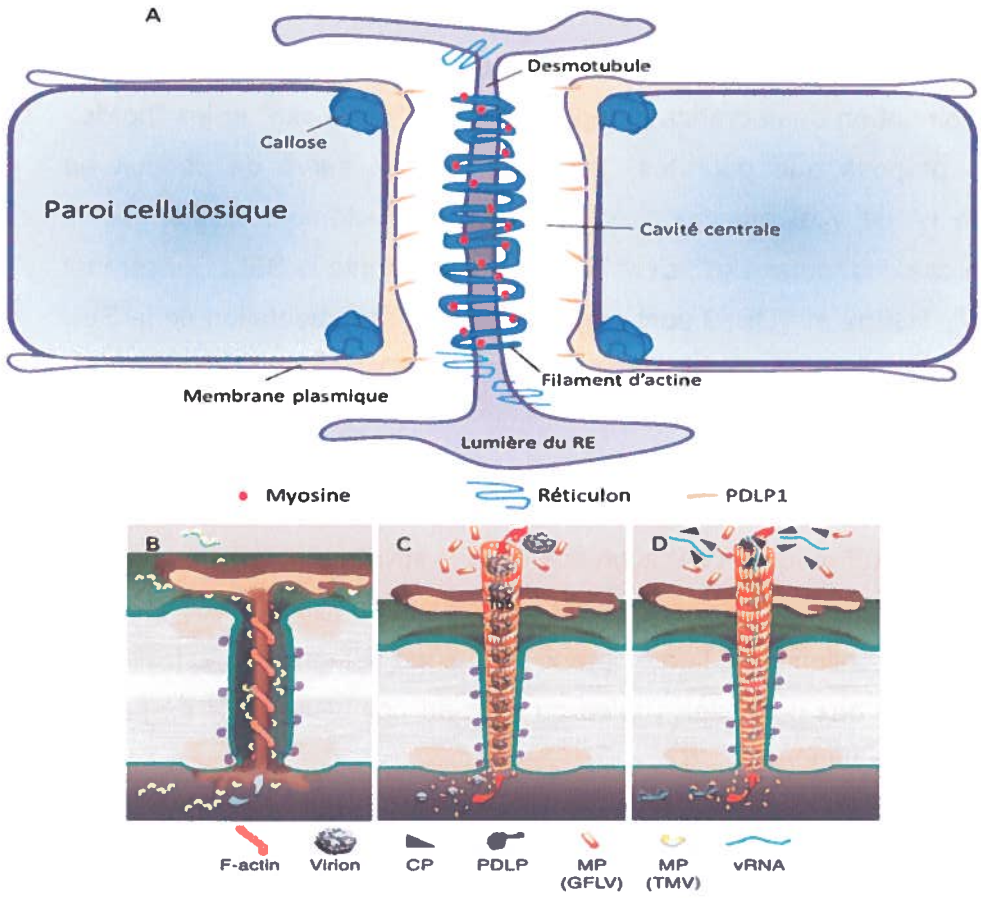

Figure 8: Schéma d'un plasmodesme et modification par les MP.

(A) Lors de la formation de la paroi durant la cytocinèse, des composantes du RE vont se retrouvées piégées dans la paroi et deviendront les desmotubules. Le desmotubule est entouré par la membrane plasmique et permet la continuité cytoplasmique entre deux cellules adjacentes. La circulation des molécules qui transitent par le PD se déroule dans la cavité centrale, entre la membrane plasmique et le desmotubule. Ce flux est régulé par l'actine (représentée en bleu), l'accumulation de callose et probablement d'autres protéines qui restent à identifier. Les protéines de la famille des réticulons sont impliquées dans le maintien de la structure du RE. (B) Modification des PD par l'action de la MP du TMV, augmentation de la SEL suite à une réduction de la callose et mouvement d'un complexe RNP. (C) et (D) formation de tubules à partir de l'interaction entre les MP et PDLP1 (Plasmodesmata located protein 1), qui conduit à la disparition du desmotubule. Le tubule peut ensuite transporter le virus déjà assemblé sous forme encapsidée (C), ou un complexe RNP (D). [(A) inspiré de Maule, Benitez-Alfonso et al. 2011 (Maule et al., 2011); (B) tiré de Ritzenthaler 2011 (Ritzenthaler, 2011)].

Certains virus utilisent un groupe de 3 protéines de mouvement soit TGBp1, TGBp2, et TGBp3. Les virus qui utilisent les protéines TGBp pour leurs mouvements sont divisés généralement en deux grands groupes, les virus "potex-like" et les "hordei-like". Il a été proposé que pour les "potex-like" le RE serve de conduit au mouvement de l'ARN viral attaché directement ou indirectement aux protéines TGBp. Dans le cas des "potex-like", c'est TGBp1 qui augmente la SEL. Concernant les "hordei-like", TGBp2 et TGBp3 sont responsables de l'augmentation de la SEL et aident le complexe TGBp1-ARN à passer par les PD (Verchot-Lubicz et al., 2010).

Dans le cas de certains virus à particule icosaédrique, comme les comovirus et les népovirus, les MP modifient de façon drastique la structure des PD en formant un tubule à travers la cavité centrale. Lors de cette transformation, le desmotubule disparait et seule la continuité de la membrane plasmique est conservée. Le tubule va ensuite permettre aux particules virales ou bien au complexe RNP de passer dans la cellule voisine (Figure 7C, 7D).

Le mécanisme de dilatation du PD par les MP n'est pas bien connu. La protéine 30K du TMV interagit avec une protéine appelée ankyrine, ce qui a pour effet de diminuer la présence de callose aux PD et ainsi d'augmenter la SEL (Liu and Nelson, 2013). Il a aussi été montré que le mouvement du TMV est corrélé avec une augmentation de la quantité de β-1,3-glucanase qui dégrade la callose. Une étude récente a montré que le TMV et le CMV dégradent les microfilaments d'actine-F, ce qui aurait pour conséquences d'augmenter la SEL et de permettre au virus de passer à travers les PD (Su et al., 2010). Une famille de protéines récemment identifiée, les PDLP, semble jouer le rôle de récepteur pour faciliter l'attachement des MP aux PD (Amari et al., 2010).

Maintenant il reste à savoir quelle est l'entité virale qui passe au travers des PD pour infecter les cellules voisines. Dans le cas de certains virus icosaédriques, c'est la particule virale qui passerait d'une cellule à l'autre pour d'autres ca serait un complexe RNP. Dans le cas du TMV, les avis sont partagés. Il est admis que c'est un complexe RNP qui passe d'une cellule à l'autre, mais il n'est pas exclu que ce soit le complexe de réplication associé à une structure membranaire qui transite

d'une cellule à l'autre (Kawakami et al., 2004) ouvrant la voie à un couplage de la réplication virale et du mouvement de cellule à cellule.

3.8 Couplage entre la réplication et mouvement du virus

La grande majorité des études menées sur le mouvement intercellulaire se sont concentrées sur l'adressage des MP au PD. Elles ont traité la réplication comme un évènement séparé et distinct du mouvement intercellulaire. Cependant, il y a des évidences qui suggèrent que ces deux évènements sont intimement liés. Exprimées de façon ectopique, les MP sont capables de se déplacer de cellules en cellules. Mais si un ARN viral fluorescent du TMV est inséré par microinjection dans des plantes transgéniques exprimant la MP, cela ne suffit pas à le faire passer dans la cellule voisine (Christensen et al., 2009). Dans cette étude, les auteurs montrent que le mouvement intercellulaire du TMV nécessite au préalable un évènement de réplication. À quel endroit dans la cellule les MP interagissent-elles avec les ARN viraux produits par le complexe de réplication ? Est-ce possible d'imaginer que les MP interagissent directement dans les usines virales ? Pour le TuMV, il a été proposé que la traduction virale se déroule dans les usines virales induites par $6K_2$* (Cotton et al., 2009). Par conséquent, les protéines virales nécessaires au mouvement du virus peuvent directement interagir avec l'ARN viral nouvellement synthétisé. Dans le cas du PVX, la situation est similaire : les usines virales qui se forment à partir du RE sont également le site de la traduction et de la réplication virale (Tilsner and Oparka, 2012). La MP du RCNMV se localise au PD quand on l'exprime seule. Mais en conditions infectieuses, la MP se relocalise dans les usines virales issues du RE. Ce virus segmenté possède deux ARN, l'ARN1 code pour les protéines 27K et 88K impliquées dans la réplication, et CP, tandis que l'ARN2 code pour la MP 35K. Comme 27K et 88K répliquent les deux ARN, ceux-ci se retrouvent dans le même compartiment membranaire provenant du RE. Dans le cas du RCNMV, la MP doit recruter les deux ARN afin d'infecter la cellule voisine. Il n'est donc pas impossible que le MP interagisse directement avec les usines virales afin de faciliter le mouvement du virus.

Les usines virales du TMV recrutent aussi la MP et des observations suggèrent que des usines virales intactes peuvent passer d'une cellule à une autre (Kawakami et al., 2004). Les mouvements intercellulaires apparaissent rapidement

après l'entrée du virus, bien avant que la charge virale devienne importante dans la cellule, vraisemblablement autour de 10 h après l'arrivée du virus dans la cellule (Tilsner and Oparka, 2012). Ces exemples illustrent bien le besoin d'un couplage réplication/mouvement pour les virus (Kaido et al., 2011).

La multiplicité d'infection cellulaire chez les plantes (cellular MOI, multiplicity of infection) définit le nombre de génomes requis pour infecter une cellule. Cette définition diffère légèrement de la MOI chez les virus d'animaux, qui équivaut au rapport entre le nombre de particules infectieuses sur le nombre de cellules soumises à l'infection.

Récemment, la MOI d'un virus à ADN et de deux virus à ARN de plantes a été déterminée (González-Jara et al., 2009;Gutiérrez et al., 2010). Il apparaît que la MOI varie grandement entre les premières cellules infectées et les cellules infectées suite à un mouvement du virus. Dans les cellules secondairement infectées, lorsque le virus bouge rapidement d'une cellule à l'autre, la MOI tend vers 1. Le mécanisme d'exclusion virale est un phénomène encore mal compris, mais limite les super infections (cellules infectées par plusieurs virus). À partir de ces observations, on peut penser que si le mouvement du virus est couplé à la réplication virale, cela lui permet de rapidement mettre en place un mécanisme d'exclusion, qui expliquerait la faible MOI observée dans les cellules secondairement infectées. Les virus en adoptant cette stratégie gagnent du temps et limitent également leur taux de mutation, puisque la cellule est infectée par un seul génome viral qui est copié plusieurs fois.

3.9 Modèle de réplication et de transport viral

La Figure 9 résume les informations données précédemment et propose un modèle qui intègre la réplication virale avec le transport intercellulaire des virus. Dès l'entrée du virus dans la cellule, la traduction et la réplication virale commencent. Pour certains virus, comme le TuMV* et possiblement le PVX et le TMV, ces processus se déroulent dans une structure périnucléaire induite par le virus. Cette structure est un amalgame de membranes provenant du RE, du Golgi, de vésicules

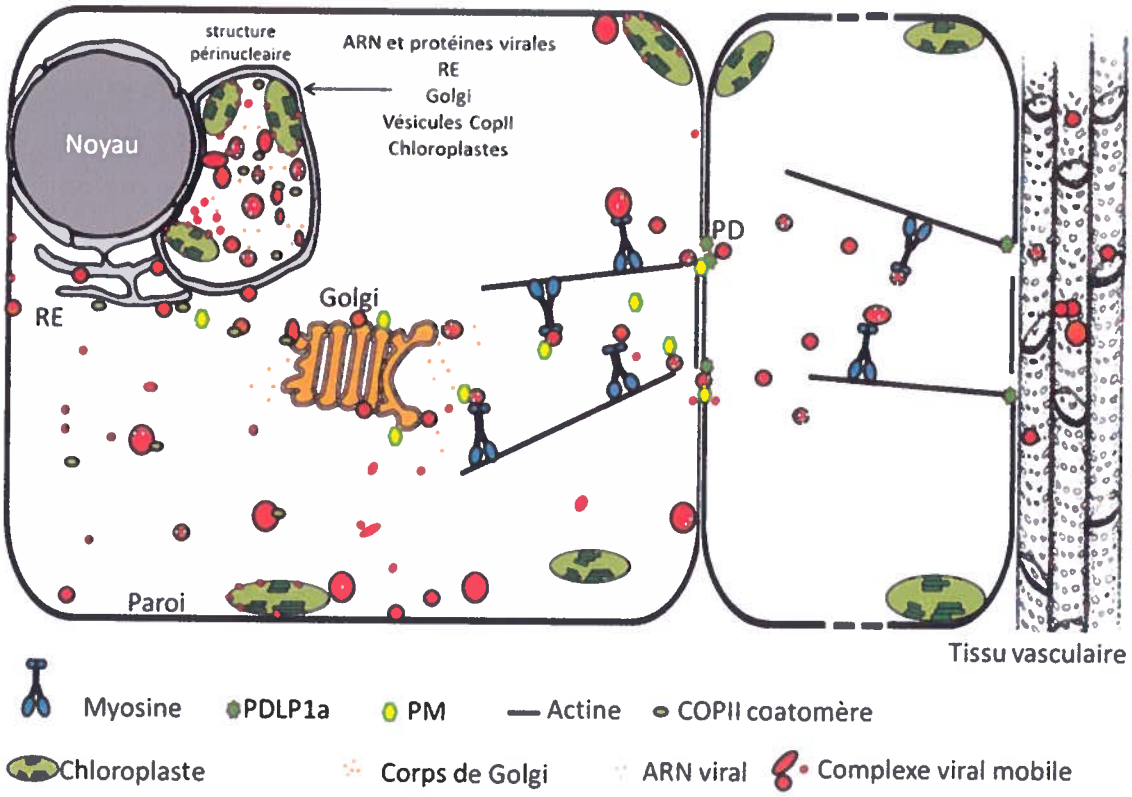

Figure 9: Modèle qui intègre la réplication virale, le mouvement intercellulaire et l'infection systémique des virus à ARN(+).

Voir la description dans la section modèle de réplication et de transport viral de cette revue.

COPII et de chloroplastes. Pour d'autres virus, la réplication a lieu dans des usines associées à d'autres organites cellulaires. Après un certain temps, des complexes viraux mobiles se forment aux sites de réplication et utilisent la voie sécrétoire et les microfilaments pour se rendre à la membrane plasmique et traverser les PD et infecter les cellules voisines. La nature du complexe viral mobile peut changer en fonction du virus (complexe RNP, usine de réplication intacte ou particule virale). Une fois dans la cellule contigüe le virus recommence un cycle d'infection. Ce mouvement symplasmique (intracellulaire) continu jusqu'à ce que le virus atteigne les tissus vasculaires.

4. Problématique, hypothèses et objectifs de travail

Avant d'entreprendre mon doctorat, les précédents membres du laboratoire ont identifié des protéines hôtes présentes dans les usines virales induites par le TuMV et dont l'interaction est nécessaire à l'infection. Ils ont notamment trouvé la protéine eIF(iso)4E (*eukaryotic translation initiation factor 4E*), qui s'est avérée plus tard être le produit d'un gène de résistance récessif. Nous savons également qu'un certains nombre de facteurs de traduction comme PABP [*Poly(A)-binding protein*], eIF(iso)4G (*Eukaryotic translation initiation factor iso 4G*), eEF1a (*Eukaryotic translation elongation factor iso1A*), et Hsc-70-3 (*Heat shock protein cognate 3*) sont recrutés dans les usines virales par l'intermédiaire de VPg-Pro (Jiang and Laliberté, 2011). Ces résultats suggèrent que les usines virales abritent la réplication et potentiellement la traduction virale. Bien que certaines protéines contenues dans les usines virales soient connues, le contenu et le rôle exact de ces vésicules sont loin d'être totalement élucidés.

La protéine $6K_2$ est responsable de la formation des usines virales, mais nous ne savons que peu de choses sur la biogenèse, le mouvement et l'architecture de ces usines virales. Des observations antérieures ont révélé que ces usines virales sont mobiles dans la cellule. Nous savons que le cytosquelette et les myosines sont des éléments essentiels du trafic des organites dans les cellules végétales, et que le cytosquelette est intimement lié au système de sécrétion de la

cellule. D'autre part dans le cas du TuMV les usines virales ont déjà été observées en mouvement dans la cellule.

Dans le cadre de mes études de doctorat, nous avons émis une hypothèse qui a été le fil conducteur tout au long de mes travaux :

- La protéine $6K_2$ induit la formation d'une structure membranaire nécessaire à la réplication de l'ARN viral et au transport de cellule à cellule du virus.

Afin de répondre à cette hypothèse nous nous sommes fixés plusieurs objectifs :

a) Caractériser le mouvement intracellulaire de ces usines virales.
b) Étudier l'impact de la biogenèse d'usines virales sur le système de sécrétion de la cellule infectée.
c) Définir l'implication des usines virales dans le mouvement du virus de cellule à cellule.

Le premier objectif a été réalisé en collaboration avec une étudiante du laboratoire qui achevait son doctorat, Sophie Cotton. Pour les deux derniers objectifs, j'ai travaillé en collaboration avec le professeur Hugo Zheng de l'université McGill, qui est un spécialiste du système sécrétoire chez les plantes et j'ai bénéficié de l'aide de Maxime Agbeci, un étudiant à la maîtrise dans notre laboratoire.

CHAPITRE 2: PUBLICATIONS

Publication n° 1

Turnip Mosaic Virus RNA Replication Complex Vesicles Are Mobile, Align with Microfilaments, and Are Each Derived from a Single Viral Genome

Journal of Virology

Oct. 2009, Vol.83 n° 20 p. 10460–10471

Sophie Cotton[1], Romain Grangeon[2], Karine Thivierge[1], Isabelle Mathieu[2], Christine Ide[1], Taiyun Wei[3], Aiming Wang[3], and Jean-François Laliberte´ [2]*

[1] Department of Plant Science, McGill University, 21,111 Lakeshore, Ste-Anne-de-Bellevue, Quebec H9X 3V9, Canada.

[2] INRS-Institut Armand-Frappier, 531 Boulevard des Prairies, Laval, Quebec H7V 1B7, Canada[2*].

[3] Southern Crop Protection and Food Research Centre, Agriculture and Agri-Food Canada,1391 Sandford Street, London, Ontario N5V 4T3, Canada[3].

* Corresponding author : Jean-François Laliberté

Email: jeanfrancois.laliberte@iaf.inrs.ca

Contribution

Ma première publication s'insère dans le projet de Sophie Cotton, une ancienne étudiante au doctorat de notre laboratoire. À mon arrivée dans le laboratoire Sophie venait de soumettre une première version de ce papier qui a été refusée. Étant sur la fin de son doctorat et de surcroit en congés de maternité, mon directeur de thèse m'a proposé de remettre à plat toutes les expériences du papier, et de travailler sur une nouvelle version. J'ai passé ma première année et demie à travailler sur ce projet en apportant des changements significatifs qui ont permis de publier cette étude.

Bien que deuxième auteur, ma contribution à cet article est majeure, en effet j'ai contribué directement à toutes les figures de ce papier excepté les figures 6 et 8. J'ai défini et mené les expériences à faire avec les conseils de mon directeur de thèse.

Résumé

Des plants de *Nicotiana benthamiana* ont été agroinfiltrés avec un clone infectieux du virus de la mosaïque du navet (TuMV) exprimant une protéine fluorescente GFP ou mCherry fusionnée avec la protéine virale $6K_2$, connue pour être responsable de la formation de vésicules. Dans le cytoplasme des cellules infectées, nous avons détecté des structures ponctuées, correspondant à des vésicules abritant le complexe de réplication viral. Ces vésicules sont mobiles et localisées le long des microfilaments d'actines. Le mouvement intracellulaire de ces vésicules est inhibé lorsque les cellules sont traitées avec de la Lantraculine B, une drogue qui dépolymérise les microfilaments. Ce traitement induit également une réduction de l'accumulation virale. Ces données indiquent que les microfilaments sont utilisés pour les mouvements des vésicules et nécessaires pour la production virale. La biogenèse de ces vésicules a été investiguée en exprimant dans les mêmes cellules un clone infectieux du TuMV qui exprime $6K_2$GFP et un autre clone infectieux du TuMV qui exprime $6K_2$mCherry. Des vésicules vertes et rouges ont été observées, indiquant que les vésicules proviennent d'un seul génome. Mais certaines vésicules exhibant des portions rouges, vertes, ou jaunes ont également été observées, suggérant une fusion possible entre les vésicules. Des protoplastes

ont été isolés à partir de cellules de *N. benthamiana* infectées par le TuMV. Par immunofluorescence en microscopie confocale, nous avons pu visualiser les sites de réplication virale, qui sont des structures ponctuées localisées dans le cytoplasme. Nous avons également identifié dans ces structures les protéines virales VPg-Pro, RdRp, CI ainsi que des facteurs hôtes de traduction. Ces observations suggèrent que la réplication virale et la traduction virale se déroulent dans ces vésicules.

Summary

Nicotiana benthamiana plants were agroinoculated with an infectious cDNA clone of Turnip mosaic virus (TuMV) that was engineered to express a fluorescent protein (green fluorescent protein [GFP] or mCherry) fused to the viral $6K_2$ protein known to induce vesicle formation. Cytoplasmic fluorescent discrete protein structures were observed in infected cells, corresponding to the vesicles containing the viral RNA replication complex. The vesicles were motile and aligned with microfilaments. Intracellular movement of the vesicles was inhibited when cells were infiltrated with latrunculin B, an inhibitor of microfilament polymerization. It was also observed that viral accumulation in the presence of this drug was reduced. These data indicate that microfilaments are used for vesicle movement and are necessary for virus production. Biogenesis of the vesicles was further investigated by infecting cells with two recombinant TuMV strains: one expressed $6K_2$GFP and the other expressed $6K_2$mCherry. Green- and red-only vesicles were observed within the same cell, suggesting that each vesicle originated from a single viral genome. There were also vesicles that exhibited sectors of green, red, or yellow fluorescence, an indication that fusion among individual vesicles is possible. Protoplasts derived from TuMV-infected *N. benthamiana* leaves were isolated. Using immunofluorescence staining and confocal microscopy, viral RNA synthesis sites were visualized as punctate structures distributed throughout the cytoplasm. The viral proteins VPg-Pro, RNA-dependent RNA polymerase, and cytoplasmic inclusion protein (helicase) and host translation factors were found to be associated with these structures. A single-genome origin and presence of protein synthetic machinery components suggest that translation of viral RNA is taking place within the vesicle

Introduction

Positive-strand RNA viruses replicate their genomes on intracellular membranes. Extensive membrane rearrangements leading to cytoplasmic membranous structure production are observed during the infection cycle of many of these viruses (for a review, see reference **32**). These virus-induced membrane structures vary greatly in origin, size, and shape. For instance, Flock House virus induces the formation of 50-nm vesicles (spherules), which are outer mitochondrial membrane invaginations with interiors connected to the cytoplasm by a necked channel of approximately 10-nm diameter (**24**). On the other hand, poxviruses replicate in 1- to 2-μm cytoplasmic foci known as DNA factories (**43**), which are bounded by rough endoplasmic reticulum (ER). These factories are not only the site of DNA synthesis but also of DNA transcription and RNA translation (**21**). Similarly, mimiviruses are huge double-stranded DNA viruses that replicate in giant cytoplasmic virus factories (**45**). Three-dimensional electron microscopic imaging has shown that coronavirus-induced membrane alterations define a reticulovesicular network of modified ER that integrates convoluted membranes, numerous interconnected double-membrane vesicles, and vesicle packets (**23**), similar to what was observed for dengue viruses (**52**). These virus-induced structures are known to shelter the virus replication complex, which carries out viral RNA synthesis. The replication complex contains the viral RNA-dependent RNA polymerase (RdRp), positive- and negative-strand viral RNAs, accessory nonstructural viral proteins, and host cell factors. The role of these virus-induced membrane vesicles in regard to viral RNA synthesis is not well understood. They have been proposed to increase the local concentration of components required for replication, to provide a scaffold for anchoring the replication complex, to confine the process of RNA replication to specific cytoplasmic locations, and to aid in preventing the activation of certain host defense functions. The mechanisms that are responsible for the formation of these structures have begun to be deciphered. Several studies have shown that the specific viral proteins are responsible for the formation of the membrane vesicles (**3**, **42**). However, how individual proteins promote their formation is still unexplained. The full role of cellular factors also remains to be investigated in terms of both membrane vesicle formation and viral RNA synthesis. Finally, intracellular trafficking of these vesicles has been reported (**15**, **25**, **29**, **54**).

Turnip mosaic virus (TuMV) belongs to the genus *Potyvirus* in the family*Potyviridae* (**44**). The TuMV genome is composed of a positive-sense single-stranded RNA molecule of about 10 kb in length (**36**). The 5′ terminus of the viral RNA is linked covalently to a viral protein known as VPg and the 3′ terminus is polyadenylated. The TuMV RNA is translated into a long polyprotein of 358 kDa and is processed into at least 10 mature proteins by three different virus-encoded proteases. It was demonstrated for *Tobacco etch virus* (TEV) and *Plum pox virus*, also members of the *Potyvirus* genus, that viral RNA synthesis is associated with membranes of the ER (**30**, **42**). In the case of TuMV, the $6K_2$-VPg-Pro polyprotein, through its hydrophobic $6K_2$ domain, was shown to be responsible for the formation of cytoplasmic vesicles derived from the ER (**4**), similar in structure to those observed during TEV infection (**42**, **51**). Besides being involved in vesicle formation, $6K_2$-VPg-Pro binds a number of proteins of viral and host origin. Interaction with the viral RdRp and the host translation eukaryotic initiation factor (iso) 4E [eIF(iso)4E], poly(A)-binding protein (PABP), heat shock cognate 70-3 (Hsc70-3), and the eukaryotic elongation factor 1A (eEF1A) has been shown to take place within the $6K_2$-VPg-Pro-induced vesicles (**4**, **5**, **9**, **48**). Although these vesicles have been referred to as sites for TuMV replication (**48**), the presence of viral RNA in these vesicles has not been reported. The presence of translation factors with virus replication proteins also brings the question of the physical relationship between viral RNA translation and replication.

In the present study, the biogenesis of the TuMV-induced vesicles was investigated. It was observed that the TuMV-induced vesicles, tagged with a fluorescent protein fused to $6K_2$, were mobile and aligned with microfilaments. In addition, results using depolymerizing compounds supported the contention that vesicles trafficked on microfilaments and that microtubules were not involved. Evidence is also provided indicating that each vesicle is derived from a single viral genome. Finally, the association of host translation factors with viral RNA synthesis sites was confirmed by double immunofluorescence staining in TuMV-infected protoplasts. The single-genome origin and the presence of translation factors within the replication complex vesicles suggest that viral translation is taking place within the vesicles.

Materials and Methods

Plasmid constructions

pCambiaTunos was obtained by digesting p35Tunos (**41**) with KpnI and StuI, followed by ligation with pCambiaTunos/6KGFP (**48**), also digested with KpnI and StuI. Kanamycin-resistant *Escherichia coli* colonies were screened for plasmids deleted in the region encoding $6K_2GFP$ (i.e., pCambiaTunos/6KGFP). pUC19/6KGFP was obtained by digestion of p35Tunos/ΔNsil-6KGFP (**48**) with BamHI and KpnI and the 1458-bp fragment was ligated in pUC19 digested with the same enzymes and in which the HindIII restriction site had previously been destroyed. The mCherry coding region was amplified by PCR from pCambia/mCherry (**9**) by using the forward primer 5′-ATTCGGATCCGTGAGCAAGGGCGAGGAG-3′ and the reverse primer 5′-ATTCAAGCTTCCTTGTACAGCTCGTCCATG-3′ (the restriction sites are underlined). The PCR product was digested with BamHI and HindIII and ligated in pUC19/6KGFP (**48**), which was also digested with the same enzymes. Ampicillin-resistant *E. coli* colonies were screened for plasmids containing the fragment encoding $6K_2$mCherry (i.e., pUC19/6KmCherry). This plasmid was then cut with BamHI and KpnI and the 1451-bp fragment was ligated with p35Tunos/ΔNsil-6KGFP (**48**) cut with the same enzymes. Ampicillin-resistant *E. coli* colonies were screened for plasmids containing the fragment encoding $6K_2$mCherry (i.e., p35Tunos/ΔNsil-6KmCherry). p35Tunos/ΔNsil-6KmCherry was digested with SmaI and KpnI and was ligated with pCambiaTunos/6KGFP, also digested with the same enzymes. Kanamycin-resistant *E. coli* colonies were screened for plasmids containing the fragment encoding $6K_2$mCherry (i.e., pCambiaTunos/ 6KmCherry). All plasmid constructs were verified by sequencing.

Antibodies

Rabbit antisera were used at the following dilutions: for immunoblot analysis, anti-CP at 1:2,500; and for immunofluorescence labeling, anti-CP at 1:300, anti-RdRp at 1:100 (**9**), anti-VPg-Pro at 1:200 (**27**), anti-PABP2 at 1:300 (**28**), anti-eIF(iso)4E at 1:150 (**7**), anti-eEF1A at 1:500 (**57**), and anti-CI at 1:300. Recombinant clones pET-CP and pET-CI in *E. coli* BL21(DE3) cells were used for anti-CP and

anti-CI serum production. Full-length coding sequences of TuMV CP and CI were cloned in frame in the pET11d vector (Novagen). The recombinant proteins were overproduced in *E. coli* and purified as insoluble inclusion bodies. Inclusion bodies were resuspended in Tris-buffered saline and used for rabbit injection and serum production at McGill University Animal Resources Center. The mouse monoclonal antibody dilutions were as follows: anti-actin8, 1:1000 (Sigma); anti-BrdU, 1:100 (Sigma); and anti-dsRNA, 1:300 (English & Scientific Consulting Bt.). The secondary antibodies were goat anti-mouse conjugated to Alexa Fluor 568 at 1:500 (Molecular Probes) and goat anti-rabbit conjugated to Alexa Fluor 488 at 1:1,000 (Molecular Probes). For immunoblot analysis, the antigen-antibody complexes were visualized by using a horseradish peroxidase-coupled goat anti-rabbit immunoglobulin G (IgG).

Protein expression in plants

Constructs containing genes for proteins fused to fluorescent tag were introduced by electroporation into *Agrobacterium tumefaciens* AGL1 and selected on LB ampicillin-kanamycin plates. The pellet of an overnight culture was gently resuspended in water supplemented with 10 mM $MgCl_2$ and 150 µM acetosyringone and left at room temperature for 3 h. The solution was then diluted to an optical density at 600 nm of 0.6. Three-week-old*N. benthamiana* plants were agroinfiltrated with the fusion construct. Plants were kept for 4 days in growth chamber until observation.

Drug treatments

Stock solutions of latrunculin B (LatB; 2.5 mM [Calbiochem]), cytochalasin D (CytD; 20 mM [Calbiochem]), trifluralin (20 mM [ChemService]), and oryzalin (10 mM [ChemService]) were prepared in dimethyl sulfoxide (DMSO) and diluted to the desired concentration in water prior to their infiltration into 3-week-old *N. benthamiana* leaves.

Protoplast isolation and immunofluorescence labeling

*N. benthamiana*was agroinfiltrated with pCambiaTunos/6KGFP. Leaves obtained at 4 days postinfection were sliced in 1-mm wide stripes, followed by

incubation in an enzyme solution (1.5% cellulose R10, 0.2% macerozyme R10, 0.5 M mannitol, 20 mM KCl, 20 mM MES [pH 5.7], 10 mM $CaCl_2$, 0,1% bovine serum albumin [BSA]) for 3 h in the dark under a vacuum. The protoplast suspension was filtered through a 45-µm-pore-size nylon filter and centrifuged for 4 min at 100 × *g*. The supernatant was removed. Protoplasts were incubated for 15 min at room temperature with 1 volume of fixing solution (4% paraformaldehyde, 0.25 M mannitol, and 50 mM sodium phosphate in phosphate-buffered saline [PBS]). They were centrifuged and resuspended for 30 min with 2 volumes of fixing solution at room temperature. Protoplasts were washed three times with PBS for 10 min. They were then put on cover slide pretreated with 0.1% poly-L-lysine (Sigma), treated with Triton X-100 0.5% in PBS for 10 min, and incubated for 20 min in a blocking solution of 5% BSA in PBS. The samples were then incubated for 1 h with the primary antibody, washed three times with PBS for 10 min, incubated for another hour with Alexa Fluor 568- or Alexa Fluor 488-conjugated secondary antibody (Molecular Probes), and finally washed three times with PBS for 10 min. Pro-long Gold Antifade (Invitrogen) was used to prepare the slides.

In vivo RNA labeling

Protoplasts were isolated from plants agroinfiltrated at 4 days postinfection with *A. tumefaciens* containing pCambiaTunos. They were incubated for 30 min with 10 µg/ml of actinomycin D in order to block RNA transcription from cellular DNA-dependent RNA polymerases. Two mM 5-bromouridine 5′-triphosphate (BrUTP; Sigma) was then added for 3 h. The reaction was stopped by the addition of fixing solution (described above) for 15 min, washed once with PBS, and fixed again for another 30 min. The immunofluorescence labeling was processed as described above using anti-BrdU (1:100), and the detection was done using Alexa Fluor 568-conjugated secondary antibody (Molecular Probes) at a 1:500 dilution.

Immunoblot analysis

Total proteins were extracted from *N. benthamiana*agroinfiltrated with pCambiaTunos/6KGFP 4 days before and treated previously with drugs with an extraction buffer (50 mM Tris-HCl [pH 7.6], 50 mM KCl, 0.5 mM EDTA, 20 mM NaCl,

5% glycerol, 0,1% Triton X-100, 0.01% sodium dodecyl sulfate [SDS], and plant protease inhibitor cocktail [Sigma]). Plant tissue (0.5 g) was ground in 500 µl of extraction buffer with a Dounce homogenizer and centrifuged for 1 min at 5,000 × *g*. The concentration of the supernatant was determined by using a Bradford assay (Bio-Rad) using BSA as a standard. Then, 2 µg of total protein preparation was used to perform an immunoblot analysis after SDS-polyacrylamide gel electrophoresis. The antigen-antibody complexes were visualized using a horseradish peroxidase-coupled goat anti-rabbit IgG or goat anti-mouse IgG according to the manufacturer's recommendations. Immunoreactions were detected with the SuperSignal West Pico chemiluminescent substrate (Pierce).

Confocal microscopy

Agroinfiltrated leaf sections were placed on a microscope coverslide using immersion oil. Coverslides were inverted on depression slides, aligning the leaf tissue in the well. Cells were observed using a 40X oil immersion objective on a Radiance 2000 confocal microscope (Bio-Rad). Argon-krypton laser was used to excite fluorescent proteins and data from both green and red channels were collected at the same time. A charge-coupled-device camera was used to collect the images. Protoplasts were observed by using a 63X oil immersion objective on a LSM 510 Meta confocal microscope (Zeiss). Argon and HeNe lasers were used to excite fluorescent proteins and data from both green and red channels were collected at sequential time. After acquisition, images were processed by using Metamorph (6.2r6), ImageJ (1.41o), Carl Zeiss LSM Image Browser, and/or Adobe Photoshop software. The Manual Tracking pluging (**http://rsbweb.nih.gov/ij/plugins/track/track.html**) was used for displaying vesicle movement paths.

Results

Movement of replication complex vesicles

There are reports indicating that virus replication complexes are motile (**15**, **25**, **29**, **54**). Trafficking of TuMV-induced vesicles was thus investigated with an

infectious clone of TuMV (pCambiaTunos/6KGFP) (Fig. 1) that was previously engineered for tagging replication complexes with green fluorescent protein (GFP) (48). The coding sequence of GFP was fused with the gene encoding $6K_2$ and inserted between the P1 and HCPro coding genes as an in-frame translational fusion containing flanking P1 and VPg-Pro cleavage site coding sequences: $6K_2$GFP is thus released when the polyprotein is processed during infection. The resulting recombinant TuMV induced the formation of fluorescent discrete structures in *N. benthamiana* (Fig. 2). They were irregular in shape and heterogeneous in size, ranging from 0.6 to 4.3 µm in diameter, the mean being 1.68 µm ± 0.91 µm (n = 52). Optical cross-sections show that generally GFP fluorescence fill the whole vesicle structure, with occasional observation of ringlike vesicles (described in reference 51) (Fig. 2C). These $6K_2$GFP-tagged structures were previously shown to contain $6K_2$-VPg-Pro, RdRP, eIF(iso)4E, PABP, and eEF1a (9, 48) and were reminiscent of those induced by $6K_2$-VPg-Pro alone (4). To confirm that the $6K_2$GFP fluorescence matched with viral replication sites, these were visualized by staining with antibodies directed against double-stranded RNA (dsRNA) (1, 10).*N. benthamiana* leaves were agroinfiltrated with A. tumefaciens AgI1 strain containing pCambiaTunos/6KGFP, and protoplasts were isolated from infiltrated leaves 4 days later. The fixed and permeabilized protoplasts were then reacted with a mouse antibody recognizing dsRNA and Alexa Fluor 586 (red)-conjugated anti-mouse antibodies. Protoplasts were subsequently observed by confocal microscopy. dsRNA was associated with punctate structures of 2.1 µm ± 0.5 µm in diameter distributed throughout the cytoplasm in TuMV-infected protoplasts (see Fig. 8I). No immunofluorescence was observed in uninfected protoplasts (data not shown). The presence of dsRNA coincided with fluorescence emitted by GFP, confirming that $6K_2$GFP tagging constitutes a good marker for the visualization of TuMV replication complexes.

These discrete structures are likely to be membrane-bound vesicles and not protein aggregates. First, $6K_2$-VPg-Pro, which has been shown to colocalize with $6K_2$GFP (48), and RdRp "float" in membrane flotation experiments (5, 9), indicating that these replication-associated proteins are membrane associated and not aggregates or inclusions. Furthermore, Schaad et al. (42) have shown that the $6K_2$ protein of the related tobacco etch virus fused to GFP and expressed using the same approach as here was associated with large vesicular compartments derived from the ER. Although

some are relatively large and akin to mini-organelles, these TuMV-induced structures will be designated as vesicles from now on. The large size of the $6K_2$GFP-tagged TuMV-induced vesicles suggests that they are linked to chloroplasts or Golgi bodies. The Bio-Rad confocal microscope used in the present study possesses three detectors with filter sets calibrated to absorb light at wavelengths of 515 nm ± 15 nm (GFP fluorescence [green channel]), of 600 nm ± 20 nm (mCherry fluorescence [red channel]), and of >660 nm (chlorophyll autofluorescence [blue channel]). Such setup allows chlorophyll fluorescence to be separated from the fluorescence emitted by GFP and mCherry.

Observation of serial optical images showed that the bulk of the chloroplasts were generally found near the surface of the plasma membrane, whereas the virus-induced vesicles were located more in the interior of the cell, often near the nucleus. Figure **2A** shows a single 1-µm optical slice where $6K_2$GFP-tagged vesicles can be seen concomitantly with chloroplasts. Some vesicles were found in close association with chloroplasts, which possibly contribute along the ER to membrane structures at least in the case of plum pox virus replication (**30**). However, more often, vesicles and chloroplasts were seen as different entities. Golgi localization was based on the cytoplasmic tail and transmembrane domain (first 49 amino acids) of the soybean α-1,2-mannosidase I (**40**) fused to mCherry (**34**). This Golgi marker consists of a large number of small (<1 µm) independent stacks (**34**) that appeared as round discs of uniform size (Fig. **2B**). The Golgi marker also showed ER labeling, resulting from the continuous recycling of Golgi resident proteins through the ER round discs (**6**). The $6K_2$GFP-tagged vesicles were found to align with the ER (as expected) but generally did not colocalize with the Golgi bodies. Occasional association with Golgi is explained by the biogenesis of *Potyvirus* replication vesicles occurring at ER exit sites in a COPI- and COPII-dependent manner (**51**). The $6K_2$GFP-tagged TuMV-induced vesicles are thus distinct from Golgi bodies.

The intracellular trafficking of vesicles induced by TuMV and tagged with either fluorescent protein was then investigated. Three-week-old *N. benthamiana*leaves were agroinfiltrated with *A. tumefaciens* AgI1 containing pCambiaTunos/6KGFP, and movement of the fluorescing vesicles was investigated by time-lapse imaging after 4 days. The vesicles were motile, but each vesicle

moved at different speed, with average velocities of 0.45 µm/s ± 0.27 µm/s (n = 10) (Fig. **3** and see Movie S2 in the supplemental material). Movement was unidirectional, which was accompanied with stop-and-go activity. Although the exact destination was not known, occasional fusion with perinuclear vesicles was observed, as shown in Fig. **3**. Similar data were obtained when vesicles were tagged with mCherry. In comparison, cauliflower mosaic virus (CaMV) P6 inclusion bodies move with an average velocity of 2 µm/s (maximum of approximately 8 µm/s) (**15**), and the average velocities are ~1 µm/s for tobacco mosaic virus 126K bodies and viral replication complexes (maximum of 8 µm/s) (**29**).

Since $6K_2$-VPg-Pro alone induces vesicle formation (**4**), their trafficking was also investigated. *N. benthamiana* plants were agroinfiltrated with pGreen6KVPgProGFP, and the movement of the green fluorescing vesicles was observed after 3 days. $6K_2$-VPg-Pro-induced vesicles were also motile (see Movie S3 in the supplemental material), suggesting that the virus molecular determinant for movement lies within $6K_2$-VPg-Pro. Stop and go movement is indicative of Golgi and was consequently compared directly to that of TuMV-induced vesicles. The Golgi stacks can be seen moving extensively along the polygonal cortical ER network (see Movie S4 in the supplemental material) with an estimated speed of 0.35 µm/s. These data indicated that TuMV-induced $6K_2$GFP-tagged and Golgi vesicles are distinct structures.

Vesicle alignment with microfilaments

Since the protein content and organized nature of the cytoplasm restrict diffusion of large molecular complexes, movement of virus-induced vesicles is likely to require cytoskeleton elements (**17**). To determine whether TuMV vesicle movement is associated with microfilaments, an *A. tumefaciens* AgI1 mixture containing pCambiaTunos/6KmCherry (Fig. **1**) and a pCambia vector containing the 35S::GFP-ABD2-GFP construct (**50**) was agroinfiltrated in *N. benthamiana*. The latter construct codes for GFP fused to both termini of the actin-binding domain of fimbrin (GFP-ABD2-GFP) and provides improved imaging of actin filaments. Figure **4A** shows the positioning of the mCherry-tagged vesicles with respect to the GFP-ADB2-GFP-labeled actin filaments. A dense filament network is seen radiating from the nucleus (denoted by an asterisk in the figure) to the cell periphery, and the TuMV vesicles are randomly distributed in the cell. Alignment of the vesicles with the ABD2 filaments is readily observed, with each vesicle concurrently interacting with

several filaments. Vesicles seen not to align with ABD2 filaments are from adjoining cells that were not expressing the latter protein.

It must be noted that in cells expressing both proteins, no vesicles were observed in subcompartments of the cell devoid of ABD2 filaments, suggesting that alignment of the vesicles with the filaments is not the indirect consequence of the density of the network trapping any large structures. The red vesicles cannot be interpreted as being chloroplasts, as explained above. Moreover, no mCherry fluorescence is observed in the red channel in mock-inoculated plants or in cells expressing GFP fusions only. Furthermore, experiments using mCherry fusions developed previously (**9, 48**) showed that the red fluorescence does not result from chlorophyll autofluorescence.

Movement of the vesicles was investigated in the presence of GFP-ABD2-GFP. Trafficking of the vesicles was difficult to discern, a phenomenon observed also for the movement of the CaMV P6 inclusion bodies (**15**). It has been reported that the use of live markers to visualize actin in plants could affect motility of cellular compounds because of the overexpression of the markers (**19**). However, despite this inhibition, TuMV vesicles were seen to traffic along GFP-ABD2-GFP filaments (Fig. **5**; see also Movie S5 in the supplemental material).

To confirm the implication of microfilaments in viral vesicle movement, LatB was used to disassemble microfilaments. Since LatB's effect on microfilaments is likely to affect several processes, which indirectly might affect vesicle trafficking, movement was first evaluated on preestablished vesicles as soon as possible after drug application. *N. benthamiana* leaves were agroinfiltrated with *A. tumefaciens* AgI1 suspensions containing pCambiaTunos/6KGFP and the 35S::GFP-ABD2-GFP construct. At 4 days postinfection and 4 h before confocal observation, the agroinfiltrated leaves were treated with 5 μM LatB or 1% DMSO solvent control. The DMSO infiltration did not affect the microfilament network (data not shown), but after LatB treatment the ABD2 filaments had begun the depolymerization process, as noted by the blurred appearance of the filaments near the nucleus (Fig. **4B**). When LatB was infiltrated 4 h prior to TuMV agroinfection, the network, when observed by confocal microscopy 4 days later, was sparser, the filaments were thicker, and several microfilament bundles were observed (Fig. **4C**). Within that time period, it is expected that plant cells had metabolized some of the

LatB molecules and that the microfilament network is in the process of regaining its normal state. Interestingly, the $6K_2$mCherry-tagged TuMV-induced vesicles were tightly enclosed within the microfilament bundles (4C).

Movement was assessed with *N. benthamiana* leaves agroinfiltrated with *A. tumefaciens* AgI1 suspensions containing pCambiaTunos/6KGFP or the GFP-labeled Golgi marker construct. The latter marker was used as a drug control since Golgi trafficking in dependent on myosin (**2**). DMSO had no inhibitory effect on Golgi body and TuMV vesicle movement (data not shown). On the other hand, LatB treatment 4 h before
confocal microscope observation abolished trafficking of Golgi bodies (see Movie S6 in the supplemental material) and TuMV vesicles (see Movie S7 in the supplemental material).

TuMV infection is inhibited by LatB treatment

To assess the effect of cytoskeleton-affecting drugs on the initiation of TuMV infection, *N. benthamiana* leaves were infiltrated either with LatB, CytD, oryzalin, trifluralin, or DMSO 24 h prior to agroinfiltration with *A. tumefaciens* AgI1 containing pCambiaTunos/6KGFP. CytD depolymerizes microfilaments, while oryzalin and trifluarin are agents that disassemble microtubules. Plant tissues were collected 4 days later, and the total proteins were extracted, separated by SDS-polyacrylamide gel electrophoresis, and subjected to immunoblot analysis. Virus accumulation was assessed using a rabbit serum raised against the TuMV coat protein (CP). Figure **6** shows virus accumulation in plants following different drug treatments. Treatment with 5 µM LatB or 20 µM CytD reduced CP production below the level of detection by the Western immunoblot, whereas treatment with 20 µm oryzalin or trifluralin did not significantly inhibit CP production. Diminished virus production was correlated by confocal observation of agroinoculated leaves. The number of vesicles per cell was reduced after treatment with LatB and CytD compared to untreated plants or plants treated with DMSO, oryzalin, or trifluralin (data not shown). The presence of vesicles (albeit to a decreased level) suggests that translation and initial vesicle formation is possible in the presence of microfilaments depolymerization drugs. However, an intact microfilament network appears to be required for the

establishment of a fully productive TuMV infection, whereas microtubules do not appear to be involved.

Vesicles derive from single genome

Intracellular movement of and likely fusion (see Fig. 3) among the vesicles raise the question on the biogenesis of the vesicles. TuMV-induced vesicles contain viral proteins (and also host proteins), but how these proteins are imported in these vesicles is not known. One possibility is that viral RNA is translated in the surrounding cytoplasm and the viral proteins exported to growing $6K_2$-VPg-Pro-induced vesicles. Because of the presence of translation factors within the vesicles (4, 5, 9, 48), the other possibility is that viral protein synthesis is taking place within the virus-induced vesicles. To resolve this issue, two recombinant TuMV were used: one that expressed $6K_2$GFP and the other that expressed $6K_2$mCherry.

The rational was that in a cell that is simultaneously infected with the two recombinant viruses, if the viral RNA is translated in the cytoplasm and the viral proteins are indiscriminately exported to the vesicles, one should observe vesicles that are both green and red fluorescing. On the other hand, if the vesicles are derived from a single genome and translation occurs within the vesicle, one should observe green- and red-only fluorescing vesicles. Leaves were agroinfected with a 1:1 mixture of the two viruses and individual cells that exhibited both green and red fluorescing vesicles were screened for. Among these cells were examples with individual green and red vesicles (Fig. 7A and B), suggesting that each vesicle originated from a single viral genome. Interestingly, there were vesicles that exhibited both green and red fluorescence (Fig. 7C). However, $6K_2$GFP and $6K_2$mCherry were not always perfectly colocalizing, resulting in variegated vesicles (i.e., a mixture of red, green, and yellow sectors). This uneven mixing of the fluorescent proteins is an indication that fusion among individual vesicles is also possible, a phenomenon that was observed during vesicle movement (see Fig. 3).

Localization of host and viral proteins within virus replication complexes

Formation of a large vesicle derived from a single viral genome presupposes that a *cis* mechanism is involved: proteins synthesized from the same viral RNA are incorporated in the same vesicle, with no outside contribution from other genomes. This is possible if viral RNA translation is taking place within the vesicle. It was

previously shown that $6K_2$-VPg-Pro of TuMV induces the formation of vesicles that contain host translation factors such as eIF(iso)4E, PABP, eEF1A, and Hsc70 (**4**, **5**, **9**, **48**). The question however remains whether these same vesicles are also the sites of viral RNA synthesis. RNA replication sites can be visualized by immunofluorescence staining using antibodies either directed against dsRNA or neosynthesized 5-bromouridine-labeled RNA (**1**, **10**).

To confirm that the above-listed host proteins colocalize with viral replication sites, double immunofluorescence staining of TuMV-infected protoplasts was performed as described above. The fixed and permeabilized protoplasts were then reacted with rabbit sera raised against viral or plant proteins and mouse antibodies recognizing dsRNA or bromouridine. For bromouridine labeling, protoplasts were treated with actinomycin D prior to BrUTP incorporation in order to block host DNA transcription without affecting TuMV-directed RNA-dependent RNA synthesis. Rabbit and mouse antibodies were labeled with Alexa Fluor 488 (green)- and Alexa Fluor 586 (red)-conjugated secondary antibodies, respectively, and protoplasts were observed by confocal microscopy. To assess the background fluorescence, protoplasts from mock-inoculated leaves were subjected to the same immunofluorescence labeling conditions, and fluorescent signals were adjusted to set the background threshold level. For virus-specific elements, no significant background was detected in uninfected protoplasts (data not shown). Figure **8** shows the intracellular localization of dsRNA or bromouridine-labeled RNA, along with plant and viral proteins in TuMV-infected protoplasts. As mentioned above, dsRNA was associated with punctate structures distributed throughout the cytoplasm. Similar structures were also observed for bromouridine-labeled RNA, indicating that the presence of dsRNA likely corresponds to area of active RNA synthesis. No immunofluorescence was observed in uninfected protoplasts (data not shown). If the dsRNA punctate structures are true indicators of the virus replication complex, viral proteins known to be involved in virus replication must be associated with these structures. The anti-VPg-Pro antibodies react with VPg-Pro, its precursor (6K-VPg-Pro), as well as processed forms (VPg and Pro) (**4**). Staining with this serum was observed throughout the cytoplasm, as expected from previous cell fractionation data (**4**, **28**). However, a subpopulation of the proteins recognized by the anti-VPg-Pro antibodies was also associated with the dsRNA or bromouridine-

labeled RNA punctate structures (Fig. **8A and B**). A similar fluorescent pattern was observed for RdRp (Fig. **8C**). Interestingly, the cytoplasmic inclusion protein (CI), which has helicase activity (**26**), was associated with punctate structures that did not always coincide with the presence of dsRNA. However, dsRNA structures always correlated with the presence of CI (Fig. **8D**). This suggests that CI may have additional roles besides being involved with the replication complex. The CP, which is not known to be directly involved in RNA replication, was very rarely associated with dsRNA punctate structures (Fig. **8E**), suggesting that RNA synthesis and capsid-related events (e.g., virion assembly) are physically separated.

Host proteins that were shown to be enclosed within 6K-VPg-Pro-induced vesicles were then tested. eIF(iso)4E, PABP, and eEF1A were distributed throughout the cytoplasm (Fig. **8F to H**), as expected from the fractionation data (**4**, **28**, **48**), but subpopulations of the different proteins were found to colocalize with the dsRNA punctate structures. Taken together, these results indicate that TuMV RNA replication sites not only contained viral proteins expected to be involved in RNA synthesis but also host factors implicated in protein synthesis.

Discussion

A major finding of this investigation is that a TuMV-induced vesicle originates from a single viral genome. Infecting cells simultaneously with two recombinant viruses, one tagging vesicles with $6K_2$GFP and the other with $6K_2$mCherry, showed that green- and red-only vesicles were observed within the same cell. Vesicles tagged with both $6K_2$GFP and $6K_2$mCherry were also found and were often characterized by uneven mixing of the fluorescent protein (i.e., the presence of green, red, and yellow sectors). This indicates that fusion between vesicles is taking place, a phenomenon that has been regularly observed while looking at vesicle trafficking. A single-genome origin means that there is a *cis*-acting mechanism that incorporates the proteins resulting from the translation of a viral RNA into the same vesicle and also prevents the importation of viral proteins synthesized from surrounding viral RNAs. The *cis*-acting mechanism that naturally comes to mind is that viral RNA translation is taking place within the vesicle. As soon as the polyprotein is undergoing synthesis and processing, sufficient copies of $6K_2$-VPg-Pro are produced after a few rounds of translation to induce the formation of a

membrane vesicle. Upon its formation, it encloses the viral RNA and the protein synthetic machinery through protein interaction with viral proteins, notably $6K_2$-VPg-Pro and RdRp (**4**, **5**, **9**, **48**). Viral RNA translation continues within the vesicle and the viral proteins produced in situ contribute to the size increase of the vesicle and its maturation.

One requirement for this hypothesis is the presence of translation initiation factors within the replication complex vesicles. PABP, eIF(iso)4E, Hsc70, and eEF1A have been shown to interact with RdRp and/or VPg-Pro within $6K_2$-VPg-Pro-induced vesicles (**4**, **5**, **9**, **48**, **53**). PABP and Hsc70 undergo intracellular redistribution and a population of the proteins becomes associated with membranes during TuMV infection (**5**, **9**). Here, colocalization of viral RNA with these host proteins has been demonstrated. Viral RNA synthesis sites were visualized as punctate structures distributed throughout the cytoplasm, likely enclosed within membrane vesicles induced by $6K_2$-VPg-Pro. This dsRNA punctate distribution is commonly observed for plant positive-strand RNA viruses (**10**, **31**). As expected, TuMV proteins suspected to be involved in RNA replication, such as VPg-Pro, RdRp, and CI (helicase), were found to colocalize with these same punctate structures. Thus, the presence of three translation proteins enclosed within vesicles containing actively transcribing RNA was confirmed. Association of PABP or eEF1A with viral replication sites has been reported (**8**, **18**, **20**, **55**, **57**), and this association has generally been linked to replication of the viral genome. Here, at least three factors (and possibly Hsc70) were found with actively replicating RNA. Although a role in viral RNA synthesis cannot be excluded, the presence of so many translation factors is an indication that they are probably involved in viral protein synthesis.

An electron microscopy tomography study showed that coronavirus replication is supported by a reticulovesicular network of modified ER (**23**). This network integrates convoluted membranes, numerous interconnected double-membrane vesicles and vesicle packets. Although not found within them, the presence of ribosomes on the outer membrane of double-membrane vesicles and vesicle packets was noted. It is possible that the TuMV-induced vesicles at a higher resolution may show a similar assemblage of membrane structures and vesicles. Consequently, instead of translation taking place within the vesicles, viral proteins may be synthesized in the vicinity of the vesicle (i.e., on the cytoplasmic side) and being preferentially imported to the same vesicle.

In the case of positive-sense RNA viruses, virology textbooks generally depict viral RNA translation and synthesis as distinct processes that are physically separated (for example, see Fig. 12 and its legend in the appendix of reference **12**). In this model, viral RNA is translated on ribosomes distributed randomly in the cytoplasm and resulting viral proteins necessary for viral RNA replication are exported to vesicle-enclosed replication complexes. In the case of poliovirus, it was even suggested that the viral RNA intended to be translated is structurally different (i.e., it does not have a VPg) from the RNA found associated with the replication complex (**37**). However, there are increasing reports indicating that viral RNA translation and replication are tightly coupled events. This is the case for picornaviruses (**13**) or ambisense viruses (**35**), where viral replication and/or transcription necessitates continuous viral protein synthesis. Egger et al. (**11**) demonstrated that preformed poliovirus vesicles could not accept viral RNA and proteins involved in replication and concluded that vesicle formation, viral RNA translation, and replication are *cis*-linked events. Inefficient complementation activity of poliovirus 2C and 3D proteins for the rescue of lethal mutations in the viral genome indicates that poliovirus RNA replication shows marked preference for proteins contributed in *cis* (**47**). Efficient *Brome mosaic virus* RNA1 replication requires 1a synthesis from RNA1 in *cis* (**56**), and eIF3 is associated with purified *Brome mosaic virus* replication complexes (**38**). Finally, it was found that coupling between translation and replication of RNA2 may occur in cells infected with *Red clover necrotic mosaic virus* (**33**). However, no physical mechanism responsible for the coupling of viral RNA translation with replication and/or transcription has been proposed for these studies.

Recently, Katsafanas and Moss showed that the host protein synthetic machinery can be sequestered within virus-induced structures (**21**). Poxviruses are large DNA viruses that replicate in cytoplasmic foci known as DNA factories. Poxvirus infection redistributes associated components of eIF4F and concentrates them within these factories (**21**, **49**). To demonstrate that the factories were not only sites of DNA replication and transcription but also of viral RNA translation, these authors coinfected cells with two engineered viruses, each of which expressed a different fluorescent protein (yellow or cyan) fused to a late virion structural protein. The factories that stained uniquely with either yellow or cyan were readily observed, thus demonstrating that protein synthesis was taking place within the factories. This

observation parallels the one obtained for TuMV. It will be interesting to learn for other viruses whether RNA translation is taking place in replication complex vesicles.

Another hallmark of TuMV-induced vesicles is their motility, which is dependent on microfilaments. Numerous examples of microtubule- or microfilament-mediated transport of viral components have been reported (**14**, **17**). In plant-virus interactions, viruses appears to utilize the plant cytoskeleton for disease spread (**46**). For instance, viral movement proteins interact with actin microfilaments and microtubules and evidence has accumulated that both cytoskeletal systems may act as conduits not only for viral RNAs and virions but also for plant macromolecules to reach plasmodesmata (**16**). Recently, movement of RNA virus replication complexes has been documented. Hepatitis C virus replication complexes showed microtubule- and microfilament-dependent transport (**25**, **54**). Tobacco mosaic virus replication complex trafficking is dependent on actin filaments (**29**) and is able to move in a cell-to-cell manner (**22**). The CaMV protein P6 forms motile inclusions that traffic along actin microfilaments and stabilize microtubules (**15**). Furthermore, initiation of viral infection requires an intact microtubule or microfilament network (**15**, **39**). The biological function of TuMV vesicle movement is not clear but appears to be a requirement for the virus replication cycle since disruption of microfilaments inhibited virus production. One possible mechanism for inhibition of virus production appears to be the confinement of the vesicles in microfilament bundles, which is perhaps preventing fusion of vesicles among themselves. Because microfilament disassembly results in a collapse of the ER network, replication defect can also be attributed to the inability of virus to recruit ER membranes for replication or other processes.

Acknowledgements

We thank Marcel Desrosiers and Christian Charbonneau for helping with confocal microscopy, Karen S. Browning for the anti-eEF1A serum, Andreas Nebenführ for the Golgi organelle marker, and Elison B. Blancaflor for the GFP-

ABD2-GFP construct. We thank Hélène Sanfaçon for critical reading of the manuscript and the anonymous reviewers of a previous submission.

This study was supported the National Science and Engineering Research Council of Canada and from Le Fonds de la Recherche sur la Nature et les Technologies from the Government of Québec.

References

1. Aizaki, H., K. S. Choi, M. Liu, Y. J. Li, and M. M. Lai. 2006. Polypyrimidinetract-binding protein is a component of the HCV RNA replication complex and necessary for RNA synthesis. J. Biomed. Sci. 13:469–480.

2. Avisar, D., M. Abu-Abied, E. Belausov, E. Sadot, C. Hawes, and I. A. Sparkes. 2009. A comparative study of the involvement of 17 Arabidopsis myosin family members on the motility of Golgi and other organelles. Plant Physiol. 150:700–709.

3. Barco, A., and L. Carrasco. 1995. A human virus protein, poliovirus protein 2BC, induces membrane proliferation and blocks the exocytic pathway in the yeast Saccharomyces cerevisiae. EMBO J. 14:3349–3364.

4. Beauchemin, C., N. Boutet, and J.-F. Laliberte´. 2007. Visualization of the interaction between the precursors of VPg, the viral protein linked to the genome of turnip mosaic virus, and the translation eukaryotic initiation factor iso 4E in planta. J. Virol. 81:775–782.

5. Beauchemin, C., and J.-F. Laliberte´. 2007. The poly(A) binding protein is internalized in virus-induced vesicles or redistributed to the nucleolus during turnip mosaic virus infection. J. Virol. 81:10905–10913.

6. Brandizzi, F., E. L. Snapp, A. G. Roberts, J. Lippincott-Schwartz, and C. Hawes. 2002. Membrane protein transport between the endoplasmic reticulum and the Golgi in tobacco leaves is energy dependent but cytoskeleton independent: evidence from selective photobleaching. Plant Cell 14:1293–1309.

7. Browning, K. S., J. Humphreys, W. Hobbs, G. B. Smith, and J. M. Ravel. 1990. Determination of the amounts of the protein synthesis initiation and elongation factors in wheat germ. J. Biol. Chem. 265:17967–17973.

8. Davis, W. G., J. L. Blackwell, P. Y. Shi, and M. A. Brinton. 2007. Interaction between the cellular protein eEF1A and the 3'-terminal stem-loop of West Nile virus

genomic RNA facilitates viral minus-strand RNA synthesis. J. Virol. 81:10172–10187.

9. Dufresne, P. J., K. Thivierge, S. Cotton, C. Beauchemin, C. Ide, E. Ubalijoro, J.-F. Laliberte´, and M. G. Fortin. 2008. Heat shock 70 protein interaction with turnip mosaic virus RNA-dependent RNA polymerase within virusinduced membrane vesicles. Virology 374:217–227.

10. Dunoyer, P., C. Ritzenthaler, O. Hemmer, P. Michler, and C. Fritsch. 2002. Intracellular localization of the Peanut clump virus replication complex in tobacco BY-2 protoplasts containing green fluorescent protein-labeled endoplasmic reticulum or Golgi apparatus. J. Virol. 76:865–874.

11. Egger, D., N. Teterina, E. Ehrenfeld, and K. Bienz. 2000. Formation of the poliovirus replication complex requires coupled viral translation, vesicle production, and viral RNA synthesis. J. Virol. 74:6570–6580.

12. Flint, S. J., L. W. Enquist, V. R. Racaniello, and A. M. Skalka. 2009. Principles of virology: molecular biology, pathogenesis, and control of animal viruses, 3rd ed. ASM Press, Washington, DC.

13. Gamarnik, A. V., and R. Andino. 1998. Switch from translation to RNA replication in a positive-stranded RNA virus. Genes Dev. 12:2293–2304.

14. Greber, U. F., and M. Way. 2006. A superhighway to virus infection. Cell 124:741–754.

15. Harries, P. A., K. Palanichelvam, W. Yu, J. E. Schoelz, and R. S. Nelson. 2009. The cauliflower mosaic virus protein P6 forms motile inclusions that traffic along actin microfilaments and stabilize microtubules. Plant Physiol. 149:1005–1016.

16. Heinlein, M. 2002. The spread of tobacco mosaic virus infection: insights into the cellular mechanism of RNA transport. Cell Mol. Life Sci. 59:58–82.

17. Henry, T., J.-P. Gorvel, and S. Me´resse. 2006. Molecular motors hijacking by intracellular pathogens. Cell. Microbiol. 8:23–32.

18. Herold, J., and R. Andino. 2001. Poliovirus RNA replication requires genome circularization through a protein-protein bridge. Mol. Cell 7:581–591.

19. Holweg, C. L. 2007. Living markers for actin block myosin-dependent motility of plant organelles and auxin. Cell Motil. Cytoskelet. 64:69–81.

20. Johnson, C. M., D. R. Perez, R. French, W. C. Merrick, and R. O. Donis. 2001. The NS5A protein of bovine viral diarrhoea virus interacts with the (Goodin et al.) subunit of translation elongation factor-1. J. Gen. Virol. 82:2935–2943.

21. Katsafanas, G. C., and B. Moss. 2007. Colocalization of transcription and translation within cytoplasmic poxvirus factories coordinates viral expression and subjugates host functions. Cell Host Microbe 2:221–228.

22. Kawakami, S., Y. Watanabe, and R. N. Beachy. 2004. Tobacco mosaic virus infection spreads cell to cell as intact replication complexes. Proc. Natl. Acad. Sci. USA 101:6291–6296.

23. Knoops, K., M. Kikkert, S. H. Worm, J. C. Zevenhoven-Dobbe, Y. van der Meer, A. J. Koster, A. M. Mommaas, and E. J. Snijder. 2008. SARS-coronavirus replication is supported by a reticulovesicular network of modified endoplasmic reticulum. PLoS Biol. 6:e226.

24. Kopek, B. G., G. Perkins, D. J. Miller, M. H. Ellisman, and P. Ahlquist. 2007. Three-dimensional analysis of a viral RNA replication complex reveals a virus-induced mini-organelle. PLoS Biol. 5:e220.

25. Lai, C.-K., K.-S. Jeng, K. Machida, and M. M. C. Lai. 2008. Association of hepatitis C virus replication complexes with microtubules and actin filaments is dependent on the interaction of NS3 and NS5A. J. Virol. 82:8838–8848.

26. Lain, S., M. T. Martin, J. L. Riechmann, and J. A. Garcia. 1991. Novel catalytic activity associated with positive-strand RNA virus infection: nucleic acid-stimulated ATPase activity of the plum pox potyvirus helicaselike protein. J. Virol. 65:1–6.

27. Laliberte´, J.-F., O. Nicolas, H. Chatel, C. Lazure, and R. Morosoli. 1992. Release of a 22-kDa protein derived from the amino-terminal domain of the 49-kDa NIa of turnip mosaic potyvirus in Escherichia coli. Virology 190:510–514.

28. Léonard, S., C. Viel, C. Beauchemin, N. Daigneault, M. G. Fortin, and J.-F.Laliberte´. 2004. Interaction of VPg-Pro of Turnip mosaic virus with the translation initiation factor 4E and the poly(A)-binding protein in planta. J. Gen. Virol. 85:1055–1063.

29. Liu, J.-Z., E. B. Blancaflor, and R. S. Nelson. 2005. The Tobacco mosaic virus 126-kilodalton protein, a constituent of the virus replication complex, alone of within the complex aligns with and traffics along microfilaments. Plant Physiol. 138:1853–1865.

30. Martin, M. T., M. T. Cervera, and J. A. Garcia. 1995. Properties of the active plum pox potyvirus RNA polymerase complex in defined glycerol gradient fractions. Virus Res. 37:127–137.

31. McCartney, A. W., J. S. Greenwood, M. R. Fabian, K. A. White, and R. T. Mullen. 2005. Localization of the tomato bushy stunt virus replication protein p33 reveals a peroxisome-to-endoplasmic reticulum sorting pathway. Plant Cell 17:3513–3531.

32. Miller, S., and J. Krijnse-Locker. 2008. Modification of intracellular membrane structures for virus replication. Nat. Rev. Microbiol. 6:363–374.

33. Mizumoto, H., H.-O. Iwakawa, M. Kaido, K. Mise, and T. Okuno. 2006. Cap-independent translation mechanism of Red clover necrotic mosaic virus RNA2 differs from that of RNA1 and is linked to RNA replication. J. Virol. 80:3781–3791.

34. Nelson, B. K., X. Cai, and A. Nebenfuhr. 2007. A multicolored set of in vivo organelle markers for colocalization studies in Arabidopsis and other plants. Plant J. 51:1126–1136.

35. Nguyen, M., and A.-L. Haenni. 2003. Expression strategies of ambisense viruses. Virus Res. 93:141–150.

36. Nicolas, O., and J.-F. Laliberté. 1992. The complete nucleotide sequence of Turnip mosaic potyvirus RNA. J. Gen. Virol. 73:2785–2793.

37. Nomoto, A., N. Kitamura, F. Golini, and E. Wimmer. 1977. The 5'-terminal structures of poliovirion RNA and poliovirus mRNA differ only in the genome-linked protein VPg. Proc. Natl. Acad. Sci. USA 74:5345–5349.

38. Quadt, R., C. C. Kao, K. S. Browning, R. P. Hershberger, and P. Ahlquist. 1993. Characterization of a host protein associated with brome mosaic virus RNA-dependent RNA polymerase. Proc. Natl. Acad. Sci. USA 90:1498–1502.

39. Roohvand, F., P. Maillard, J.-P. Lavergne, S. Boulant, M. Walic, U. Andreo, L. Goueslain, F. Helle, A. Mallet, J. McLauchlan, and A. Budkowska. 2009. Initiation of hepatitis C virus infection requires the dynamic microtubule network: role of the viral nucleocapsid protein. J. Biol. Chem. 284:13778–13791.

40. Saint-Jore-Dupas, C., A. Nebenführ, A. Boulaflous, M.-L. Follet-Gueye, C. Plasson, C. Hawes, A. Driouich, L. Faye, and V. Gomord. 2006. Plant Nglycan processing enzymes employ different targeting mechanisms for their spatial arrangement along the secretory pathway. Plant Cell 18:3182–3200.

41. Sanchez, F., D. Martinez-Herrera, I. Aguilar, and F. Ponz. 1998. Infectivity of Turnip mosaic potyvirus cDNA clones and transcripts on the systemic host Arabidopsis thaliana and local lesion hosts. Virus Res. 55:207–219.

42. Schaad, M. C., P. E. Jensen, and J. C. Carrington. 1997. Formation of plant RNA virus replication complexes on membranes: role of an endoplasmic reticulum-targeted viral protein. EMBO J. 16:4049–4059.

43. Schramm, B., and J. K. Locker. 2005. Cytoplasmic organization of POXvirus DNA replication. Traffic 6:839–846.

44. Shukla, D. D., C. W. Ward, and A. A. Brunt. 1994. The Potyviridae. CAB International, Wallingford, United Kingdom.

45. Suzan-Monti, M., B. L. Scola, L. Barrassi, L. Espinosa, and D. Raoult. 2007. Ultrastructural characterization of the giant volcano-like virus factory of Acanthamoeba polyphaga mimivirus. PLoS ONE 2:e328.

46. Takemoto, D., and A. R. Hardham. 2004. The cytoskeleton as a regulator and target of biotic interactions in plants. Plant Physiol. 136:3864–3876.

47. Teterina, N., W. Zhou, M. Cho, and E. Ehrenfeld. 1995. Inefficient complementation activity of poliovirus 2C and 3D proteins for rescue of lethal mutations. J. Virol. 69:4245–4254.

48. Thivierge, K., S. Cotton, P. J. Dufresne, I. Mathieu, C. Beauchemin, C. Ide, M. G. Fortin, and J.-F. Laliberte´. 2008. Eukaryotic elongation factor 1A interacts with turnip mosaic virus RNA-dependent RNA polymerase and VPg-Pro in virus-induced vesicles. Virology 377:216–225.

49. Walsh, D., C. Arias, C. Perez, D. Halladin, M. Escandon, T. Ueda, R. Watanabe-Fukunaga, R. Fukunaga, and I. Mohr. 2008. Eukaryotic translation initiation factor 4F architectural alterations accompany translation initiation factor redistribution in poxvirus-infected cells. Mol. Cell. Biol. 28:2648–2658.

50. Wang, Y.-S., C.-M. Yoo, and E. B. Blancaflor. 2008. Improved imaging of actin filaments in transgenic Arabidopsis plants expressing a green fluorescent protein fusion to the C and N termini of the fimbrin actin-binding domain 2. New Phytologist 177:525–536.

51. Wei, T., and A. Wang. 2008. Biogenesis of cytoplasmic membranous vesicles for plant potyvirus replication occurs at endoplasmic reticulum exit Sites in a COPI- and COPII-dependent manner. J. Virol. 82:12252–12264.

52. Welsch, S., S. Miller, I. Romero-Brey, A. Merz, C. K. Bleck, P. Walther, S. D. Fuller, C. Antony, J. Krijnse-Locker, and R. Bartenschlager. 2009. Composition and three-dimensional architecture of the dengue virus replication and assembly sites. Cell Host Microbe 5:365–375.

53. Wittmann, S., H. Chatel, M. G. Fortin, and J.-F. Laliberté. 1997. Interaction of the viral protein genome linked of Turnip mosaic potyvirus with the translational eukaryotic initiation factor (iso) 4E of Arabidopsis thaliana using the yeast two-hybrid system. Virology 234:84–92.

54. Wolk, B., B. Buchele, D. Moradpour, and C. M. Rice. 2008. A dynamic view of hepatitis C virus replication complexes. J. Virol. 82:10519–10531.

55. Yamaji, Y., T. Kobayashi, K. Hamada, K. Sakurai, A. Yoshii, M. Suzuki, S. Namba, and T. Hibi. 2006. In vivo interaction between Tobacco mosaic virus

RNA-dependent RNA polymerase and host translation elongation factor 1A. Virology 347:100–108.

56. Yi, G., and C. Kao. 2008. cis- and trans-acting functions of brome mosaic virus protein 1a in genomic RNA1 replication. J. Virol. 82:3045–3053.

57. Zeenko, V. V., L. A. Ryabova, A. S. Spirin, H. M. Rothnie, D. Hess, K. S. Browning, and T. Hohn. 2002. Eukaryotic elongation factor 1A interacts with the upstream pseudoknot domain in the 3' untranslated region of tobacco mosaic virus RNA. J. Virol. 76:5678–5691.

Figures legends

Figure 1: Schematic representation of recombinant TuMV expressing $6K_2$GFP or $6K_2$mCherry. At the top, the TuMV genome is shown as a rectangle, and an arrow represents the CaMV 35S promoter. Start and stop codons are represented, and An indicates the position of the polyadenylated tail. At the bottom, a TuMV polyprotein is shown as a rectangle in which individual proteins are delineated by vertical lines. The position within the polyprotein of $6K_2$GFP and $6K_2$mCherry is indicated.

Figure 2: $6K_2$GFP-tagged TuMV-induced vesicles. *N. benthamiana* cells expressing 6K2GFP-tagged TuMV-induced vesicles observed by confocal microscopy at 4 days after agroinfiltration. (A) Optical images (1-µm thick) showing $6K_2$GFP-tagged vesicles (green) with chloroplasts (in blue), with merge colors in the right panel. (B) Optical images (1-µm thick) showing $6K_2$GFP-tagged vesicles (green) and the Golgi marker fused to mCherry (red), with merge colors in the right panel. (C) Consecutive 1-µm thick single plane images (from left to right) of the depicted square in B that show GFP distribution within the vesicles. Scale bar, 10 µm.

Figure 3: Movement of TuMV-induced vesicles. *N. benthamiana* cells expressing $6K_2$GFP-tagged TuMV-induced vesicles observed 4 days after agroinfiltration by confocal microscopy. Time-lapse images illustrate the movement of the vesicles over the indicated time periods. Lines depict the path taken by individual vesicles. Scale bar, 10 µm.

Figure 4: Coalignment of vesicles with microfilaments. (A) *N. benthamiana* cells expressing $6K_2$mCherry-tagged TuMV-induced vesicles and GFP-ABD2-GFP

observed by confocal microscopy at 4 days after agroinfiltration. (A) No treatment was applied. (B) Leaves were infiltrated with 5 µM LatB 4 h prior to confocal microscope observation. (C) Leaves were infiltrated with 5 µM LatB 4 h prior to agroinfiltration. Photographs are three-dimensional renderings of 40 1-µm-thick slices that overlap by 0.5 µm. An asterisk indicates the position of the nucleus. The inset image is a close-up view of the depicted square. Arrows indicate the presence of TuMV vesicles "trapped" within microfilament bundles. Scale bar, 10 µm.

Figure 5: Vesicle trafficking along microfilaments. *N. benthamiana* cell expressing $6K_2$GFP-tagged TuMV-induced vesicles and GFP-ABD2-GFP observed 4 days after agroinfiltration by confocal microscopy. Time-lapse images illustrate the movement of a vesicle over the indicated time periods. A line depicts the path taken by the vesicle. An asterisk denotes the position of the nucleus, and arrows indicate the position of a single microfilament. Scale bar, 10 µm.

Figure 6: Effect of cytoskeleton-affecting drugs on the initiation of TuMV infection. *N. benthamiana* leaves were infiltrated with 5 µM LatB or 20 µM CytD, oryzalin, or trifluralin 24 h prior to infiltration with A. tumefaciens Agl1 containing pCambiaTunos/6KGFP. Total proteins were extracted 4 days after agroinfiltration, and 2 µg was analyzed by immunoblot analysis with antibodies raised against TuMV CP. Antibody against actin-8 was used as a loading control.

Figure 7: Presence of TuMV-induced vesicles tagged with $6K_2$:GFP and $6K_2$:mCherry within the same cell. *N. benthamiana* leaves were agroinfiltrated with A. tumefaciens Agl1 containing pCambiaTunos/6KGFP and pCambiaTunos/6KmCherry in a 1:1 mixture and observed 4 days after agroinfiltration. (A to C) Three different cells infected by both viruses. Photographs are consecutive 1-µm-thick single optical images (from left to right) taken every 1 µm (A and C) or 2 µm (B). Arrowheads delimit cellular membrane between two cells in panel B. Arrows highlight chimeric vesicles. Scale bar, 10 µm.

Figure 8: Localization of dsRNA and BrUTP-labeled RNA with plant and viral proteins in TuMV-infected protoplasts. *N. benthamiana* leaves agroinfiltrated with A. tumefaciens Agl1 containing pCambiaTunos were collected for protoplast isolation. TuMV-infected protoplasts were processed for double-label immunofluorescence with antisera raised against dsRNA and VPg-Pro (A), BrdU and VPg-Pro (B), dsRNA

and RdRp (C), dsRNA and CI (helicase) (D), dsRNA and CP (E), dsRNA and eIF(iso)4E (F), dsRNA and PABP2 (G), and dsRNA and eEF1A (H). Goat anti-mouse conjugated to Alexa Fluor 568 (red, for visualization of dsRNA and BrdU) and goat anti-rabbit conjugated to Alexa Fluor 488 (green, for visualization of viral or host proteins) were used as secondary antibodies. (I) *N. benthamiana* leaves agroinfiltrated with A. tumefaciens Agl1 containing pCambiaTunos/6KGFP and protoplasts were processed for dsRNA immunofluorescence detection as described above. The left panels show fluorescence emitted by the green channel only, the middle panels show fluorescence emitted by the red channel only, and the right panels show the merging of the red and green channels. The inset in panel E (left panel) is a close-up view of depicted square. Scale bar, 10 μm.

Figures

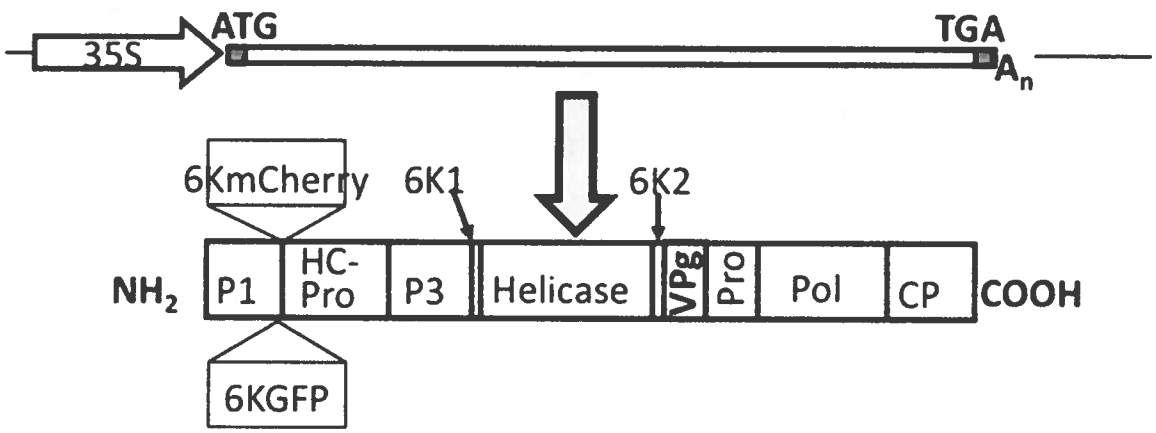

Figure 1: Schematic representation of recombinant TuMV expressing $6K_2$GFP or $6K_2$mCherry.

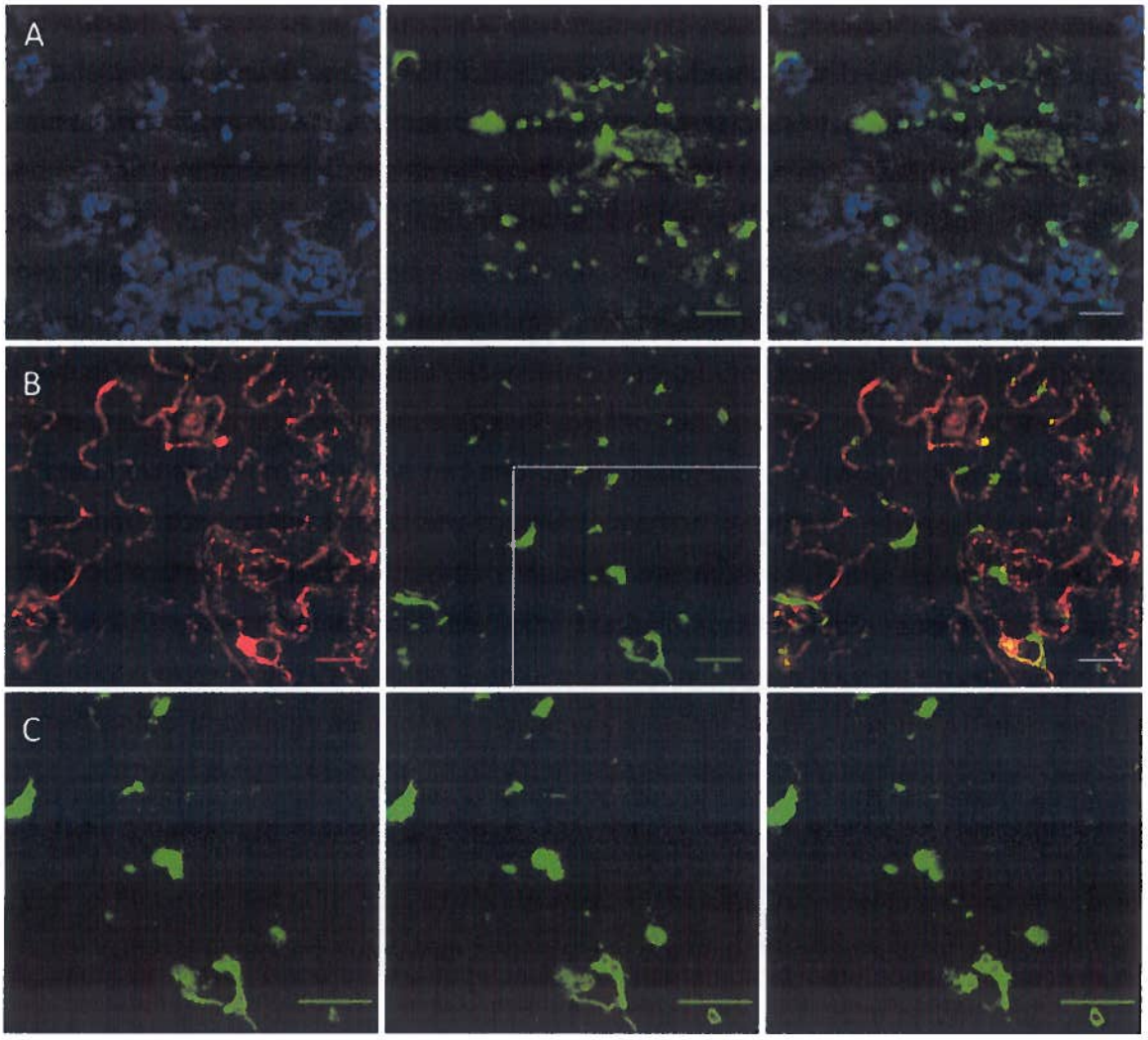

Figure 2: $6K_2$GFP-tagged TuMV-induced vesicles.

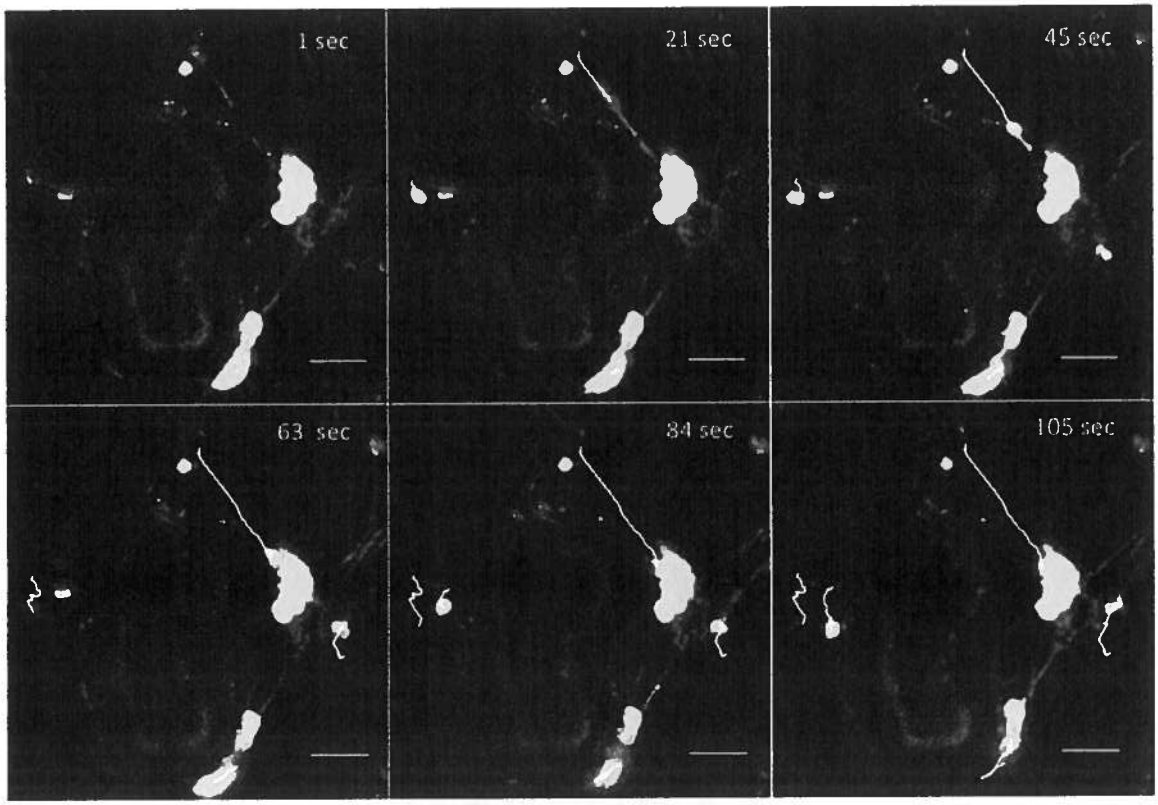

Figure 3: Movement of TuMV-induced vesicles.

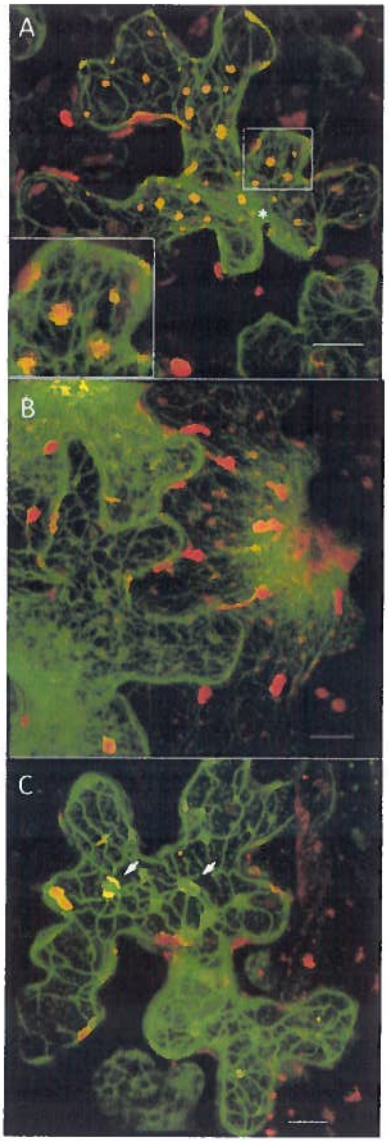

Figure 4: Coalignment of vesicles with microfilaments.

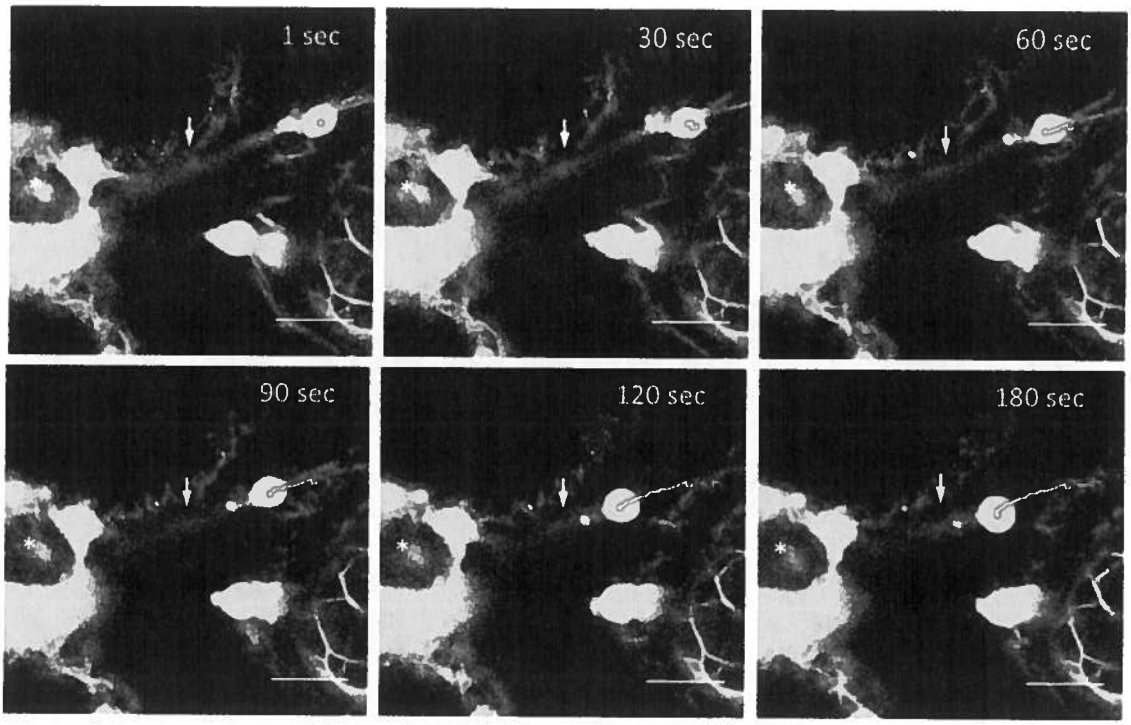

Figure 5: Vesicle trafficking along microfilaments.

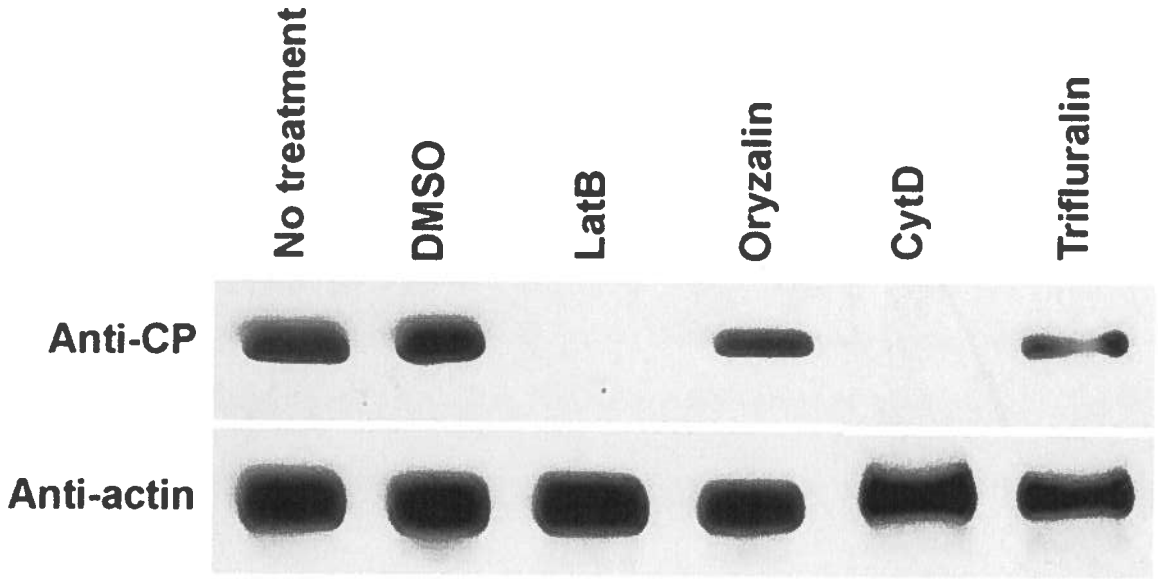

Figure 6: Effect of cytoskeleton-affecting drugs on the initiation of TuMV infection

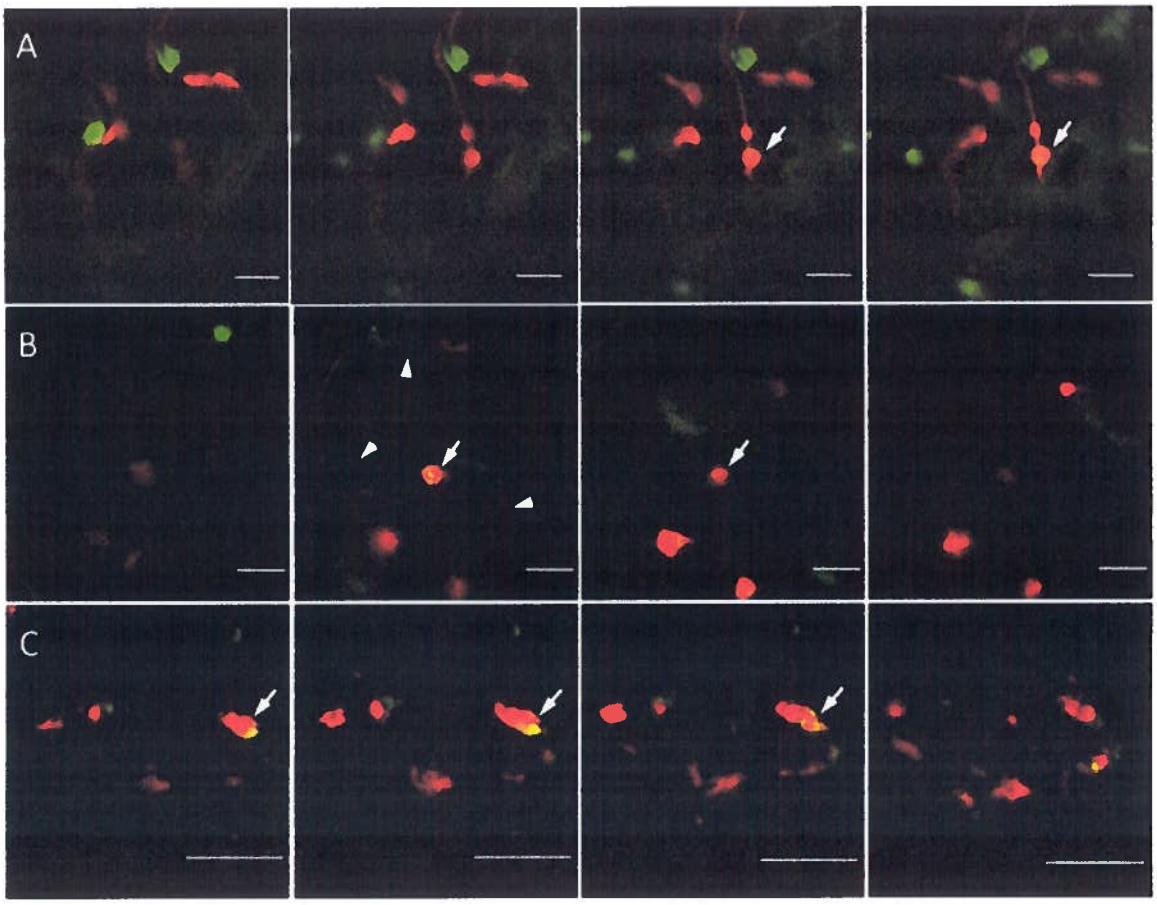

Figure 7: Presence of TuMV-induced vesicles tagged with $6K_2$:GFP and $6K_2$:mCherry within the same cell.

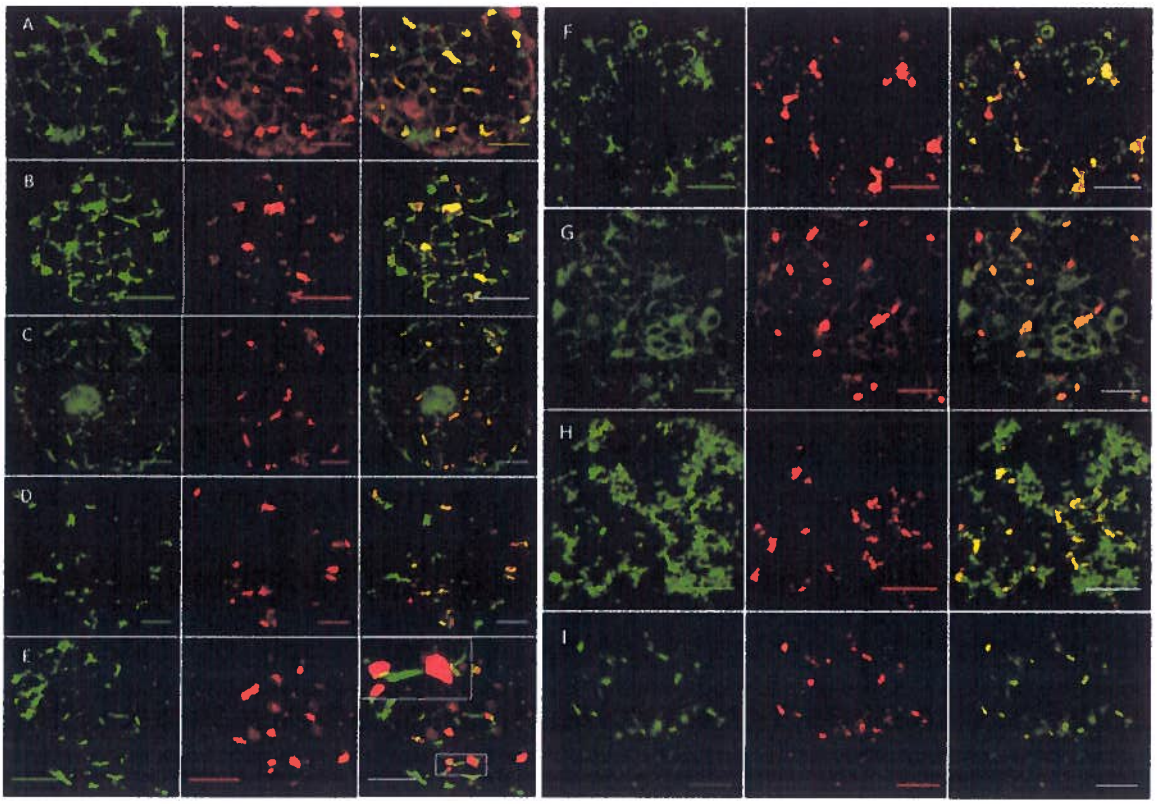

Figure 8: Localization of dsRNA and BrUTP-labeled RNA with plant and viral proteins in TuMV-infected protoplasts.

Publication n°2

Impact on the Endoplasmic Reticulum and Golgi Apparatus of Turnip Mosaic Virus Infection

Journal of Virology

Sep. 2012, p. 9255-9265

Running title : TuMV factories

Romain Grangeon[1], Maxime Agbeci[1], Jun Chen[2], Gilles Grondin[3], Huanquan Zheng[2] and Jean-François Laliberté[1*]

[1] INRS-Institut Armand-Frappier, Institut National de la Recherche Scientifique, Laval, Québec, Canada.

[2] Department of Biology, McGill University, Montréal, Québec, Canada

[3] Département de Biologie, Université de Sherbrooke, Sherbrooke, Québec, Canada

* Corresponding author : Jean-François Laliberté
Email: jeanfrancois.laliberte@iaf.inrs.ca

Contribution

Dans cet article, nous nous sommes concentrés sur les effets pour la cellule de la formation d'usines virales. J'ai conçu et réalisé les expériences de cet article. J'ai également écrit cet article avec l'aide de mon directeur de recherche. Maxime Agbeci, un étudiant à la maîtrise dans notre laboratoire m'a fourni la construction qui sert à visualiser le mouvement intercellulaire du TuMV que j'ai utilisé dans la figure 7.

Résumé

L'impact de l'infection du virus de la mosaïque du navet (TuMV) sur les endomembranes de la voie sécrétoire de la cellule hôte a été examiné en utilisant un clone infectieux qui a été conçu pour visualiser les usines virales de réplication en fusionnant une protéine fluorescente avec la protéine virale $6K_2$. L'infection par le TuMV conduit à une amalgamation du réticulum endoplasmique (RE), de l'appareil de Golgi, de vésicules COPII, et de chloroplastes dans une structure globulaire périnucléaire qui contient également des protéines virales. Une des conséquences de l'Infection par le TuMV est l'inhibition de la sécrétion, bloquée à l'interface RE-Golgi. Des expériences de recouvrement de fluorescence après photoblanchiment (FRAP) ont indiqué que la structure périnucléaire ne peut pas être réapprovisionnée par des protéines virales après photoblanchiment. En revanche, la structure est reliée dynamiquement à l'appareil de Golgi et au RE. Des expériences avec la protéine $6K_2$ fusionnée à la protéine fluorescente verte photoactivable (GFP) ont montré que les vésicules $6K_2$ périphériques, mobiles, sont liés fonctionnellement à la structure périnucléaire. La perturbation de la voie sécrétoire précoce par un traitement à la BFA n'a pas empêché la formation de la structure globulaire périnucléaire. Ce traitement augmente la colocalisation entre les vésicules $6K_2$ périphériques et les vésicules COPII, et conduit à l'inhibition du mouvement du virus de cellule à cellule. Ceci suggère qu'une voie de sécrétion fonctionnelle n'est pas nécessaire pour la formation de la structure globulaire TuMV périnucléaire et des vésicules périphériques, mais est nécessaire pour la réussite de la propagation virale.

Summary

The impact of turnip mosaic virus (TuMV) infection on the endomembranes of the host early secretory pathway was investigated using an infectious clone that has been engineered for tagging viral membrane structures with a fluorescent protein fused to the viral protein $6K_2$. TuMV infection led to the amalgamation of the endoplasmic reticulum (ER), Golgi apparatus, COPII coatamers, and chloroplasts into a perinuclear globular structure that also contained viral proteins. One consequence of TuMV infection was that protein secretion was blocked at the ER-Golgi interface. Fluorescence recovery after photobleaching (FRAP) experiments indicated that the perinuclear structure cannot be restocked in viral components but was dynamically connected to the bulk of the Golgi apparatus and the ER. Experiments with $6K_2$ fused to photoactivable green fluorescent protein (GFP) showed that production of motile peripheral $6K_2$ vesicles was functionally linked to the perinuclear structure. Disruption of the early secretory pathway did not prevent the formation of the perinuclear globular structure, enhanced the clustering of peripheral $6K_2$ vesicles with COPII coatamers, and led to inhibition of cell-to-cell virus movement. This suggests that a functional secretory pathway is not required for the formation of the TuMV perinuclear globular structure and peripheral vesicles but is needed for successful viral intercellular propagation.

Introduction

Vertebrate positive-strand RNA viruses are known to remodel the endomembrane system of the host cell (for a review, see references **16** and **42**). These membrane alterations are associated with the viral RNA replication complex, and the resulting organization has been given the name virus factory. Electron tomography has been used to generate three-dimensional images of virus-induced alterations (for a review, see reference **19**). Analyses of coronavirus, dengue virus, and picornavirus factories (**8**, **27**, **34**, **58**) have revealed a reticulovesicular/tubular network of modified endoplasmic reticulum (ER) that integrates convoluted membranes, numerous double-membrane vesicles (DMVs) that may be interconnected, and vesicle packets that apparently arise from the merging of DMVs. The biogenesis of these virus factories affects the function of the host

secretory pathway by interacting with or interfering with cellular membrane trafficking proteins in the case of the Norwalk virus (**50**), foot-and-mouth disease virus (**37**), and poliovirus (**6**, **7**). In the past, research on vertebrate virus infection suggests that the modifications of the host secretory pathway usually result from the action of one or two viral proteins (**52**, **60**). Generally, these viral proteins have one or several transmembrane domains that consist of stretches of approximately 20 hydrophobic amino acid residues. They also possess other molecular determinants that interact with host components necessary for the subversion of the host secretory pathway (**6**, **7**, **24**, **37**, **50**).

Membrane rearrangements involving the ER have also been observed in virus-infected plant cells (for a review, see references **29** and **55**). These virus-induced cellular alterations are required for viral genome replication or for virus cell-to-cell movement. The modifications generally involve the formation of spherules, vesicles, and/or multivesicular bodies, which may be bound by a double-layer membrane and are often connected by a narrow channel to the surrounding cytosol. However, there are fundamental differences in the endomembrane system between plant and animal cells. In animal cells, the ER is tightly associated with microtubules, and Golgi bodies are clustered at the microtubule-organizing centers (MTOCs) near the nucleus. In plant cells, the ER is associated with actin microfilaments, and no MTOCs have been found near the nuclei. Furthermore, Golgi stacks in plant cells are not clustered but are singly distributed throughout the cytoplasm and are in close association with highly dynamic interconnected ER tubules and actin tracks (**9**, **36**, **39**, **51**). Plant cells are also characterized by the presence of plasmodesmata that provide cytoplasmic continuity between adjacent cells. These plasma membrane-lined channels contain ER-derived desmotubules and actin filaments and are used for virus cell-to-cell spread (for a review, see reference **44**). These distinctive features have been thought to be an underlying reason that may explain the relationship between ER-associated virus replication centers and virus egress, which is exemplified by the observation that tobacco mosaic virus replication takes place in ER-derived compartments that move from cell to cell (**26**).

It has been shown that infection by tobacco etch virus (TEV) (genus *Potyvirus*) is associated with a vesiculation of the ER network into a series of discrete aggregated structures (**48**). The viral protein $6K_2$ of TEV is an integral membrane protein and is associated with the punctate structures reminiscent of the structures observed

during viral infection (**48**). Wei and Wang (**57**) observed in *Nicotiana benthamiana* cells expressing only TEV $6K_2$ fused to the cyan fluorescent protein (CFP) the production of small punctae along with larger ring-like structures. The punctae localized at endoplasmic reticulum exit sites (ERES), and their formation depended on retrograde and anterograde transport in the ER-Golgi interface (**33**, **57**). Expression of nonfunctional Sar1 and Arf1 mutants, which block the secretory pathway, affected virus yield (**57**), but the enzyme-linked immunosorbent assay (ELISA) used to measure virus production could not distinguish whether viral RNA synthesis or virus cell-to-cell movement was affected.

Ectopic expression of a single viral protein does not take into consideration the contribution of other viral proteins that are likely to affect the viral process under study. In order to investigate the action of $6K_2$ during infection, an infectious clone of turnip mosaic virus (TuMV) (genus *Potyvirus*) has been engineered to coproduce $6K_2$ as a fluorescent protein (**15**). The coding sequence of the fluorescent protein was fused with the gene encoding $6K_2$ and inserted between the P1- and HCPro-coding genes as an in-frame translational fusion containing flanking P1 and VPg-Pro cleavage site-coding sequences: $6K_2$-GFP ($6K_2$ fused to green fluorescent protein [GFP])/$6K_2$-mCherry is thus released when the polyprotein is processed during infection. Cytoplasmic fluorescent discrete protein structures were observed in infected *N. benthamiana* cells and contained double-stranded RNA (dsRNA) (a marker for viral RNA replication), the viral proteins VPg-Pro, RNA-dependent RNA polymerase, cytoplasmic inclusion protein (helicase), and host translation factors (**15**, **17**, **25**, **53**, **56**). Similar to what had been noted with the ectopic expression of TEV $6K_2$, the TuMV-induced $6K_2$-tagged vesicles moved along microfilaments and the cortical ER (**15**) and were additionally associated with chloroplasts (**56**). Finally, larger irregularly shaped $6K_2$-tagged static structures were found in the midsection of the cell near the nucleus (**15**, **53**). These last structures were not observed after ectopic expression of $6K_2$ only (**33**, **57**).

The above studies focused mainly on the membrane origin and involvement of the secretory pathway and microfilaments on the formation of the $6K_2$-associated vesicular structures. In the present investigation, we looked at the impact TuMV infection has on the overall architecture and dynamics of the early secretory endomembranes. We found that TuMV infection was accompanied by modifications of the ER, COPII coatamers, and Golgi apparatus. We noted that there was an

amalgamation of the ER and Golgi apparatus within a perinuclear globular structure, in addition to the generation of motile peripheral viral vesicles associated with the transvacuolar and cortical ER. Experiments with $6K_2$ fused to photoactivable GFP (PAGFP) indicated that the peripheral vesicles were functionally linked to the perinuclear structure. The formation of the perinuclear structure was not dependent on an operational secretory pathway, while the functionality of the peripheral $6K_2$ vesicles and intercellular virus movement were.

Materials and Methods

Fluorescent proteins and molecular clones

TuMV infectious clones pCambiaTunos/6KGFP and pCambiaTunos/6KmCherry were described previously (**15**, **53**). The introduction of the 35S-GFP-HDEL gene cassette into pCambiaTunos/6KmCherry was done as follows. pBIN/20-ER-gk (**41**) was digested with AseI and ligated with similarly digested pCambiaTunos/6KmCherry. Kanamycin-resistant *E. coli* colonies were screened for CambiaTunos/6KmCherry/HDELGFP. To make yellow fluorescent protein (YFP)-Sec24, the gene coding for Sec24A (At3g07100) was amplified from *Arabidopsis thaliana* Col-0 ecotype cDNA library with the following two primers: Sec24-Forward (GGGGACAACTTTGTACAAAAAAGTTGGAATGGGTACG GAGAATCAGGGC) and Sec24-Reverse (GGCGGCCGCACAACTTTGTACAAGAAAGT TGGGTATTAGTTTGTTGAACTTGGCGG). Amplified *Sec24* was cloned into the pDONR222 vector by BP recombination (Gateway cloning). The cloned gene was sequenced and then subcloned into the Gateway compatible destination vector pEarlyGate104 (ABRC stock DB3-686) by LR recombination to yield YFP-Sec24. $6K_2$ was fused to photoactivable GFP (PAGFP) as follows. Plasmid pMDC32 calnexin fused to PAGFP (CX-PAGFP) (**46**) was PCR amplified using the forward primer GCTGGATCCGGTGTGAGCAAGGGCGAGGAGCTGTTC (the BamHI site is underlined) and the reverse primer AACTGCAGTTACTTGTACAGCT (the PstI site is underlined). The amplified fragment was digested with BamHI and PstI and ligated with similarly restricted pCambia/$6K_2$ to obtain pCambia/$6K_2$-PAGFP.

Protein expression in plants

Transient expression was performed by agroinfiltration on 3-week-old *N. benthamiana* plants as described in reference**15**. The *Agrobacterium tumefaciens* suspension was diluted to an optical density at 600 nm (OD_{600}) of 0.03 for secreted GFP (secGFP) and GFP-HDEL (**61**), to 0.1 for p24δ1d-YFP (**12**), ERD2-GFP (**47**), GFP fused to the transmembrane domain of the rat sialyl transferase (ST-GFP) (**9**), and YFP-Sec24, to 0.05 for Arf1 constructs (**43**), and to 0.2 for the viral infectious clones. For coexpression, we agroinfiltrated a 1:1 mixture of the two AGL1 bacteria containing the plasmid of interest. Plants were kept for 3 or 4 days postagroinfiltration (dpa) in a growth chamber until observation.

Brefeldin A (BFA) (Sigma-Aldrich) was used at a final concentration of 10 μg/ml in dimethyl sulfoxide (DMSO). *N. benthamiana* leaves were agroinfiltrated with pCambiaTunos/6KmCherry/HDELGFP or with pCambiaTunos/6KmCherry along with pYFP-Sec24. The leaves were infiltrated with BFA 66 h later and observed by confocal microscopy after a 24-h incubation period.

Confocal microscopy

Agroinfiltrated leaf sections were mounted on a depression microscope slide, aligning the leaf tissue in the well. The cells were observed using a 10× objective, 40×, and/or 63× oil immersion objective on a Radiance 2000 confocal microscope (Bio-Rad) and/or on a LSM 510 Meta confocal microscope (Zeiss). For the Radiance 2000 microscope experiments, an argon-krypton laser was used to excite fluorescent proteins, and for LSM 510 Meta microscope experiments, argon and HeNe lasers were used. Data from both green and red channels were collected at the same time. Photobleaching and photoactivation of GFP was done with a Zeiss LSM 510 Meta system. Ten to fifteen pulses of the 405-nm laser were sufficient to activate PAGFP so that it produced very bright fluorescence emission that was detected by excitation at 488 nm using a 500- to 530-nm band pass filter. A 25-mW blue diode 405-nm laser was used at high output (50 to 100% transmission) to target globular structure or small region in the cytoplasm using the photobleaching function of the Zeiss software in time-lapse mode. Generally, 20 to 30 iterations were enough to bleach fluorescents proteins with the 488-nm laser.

After acquisition, images were processed using Metamorph to quantify the average intensity of fluorescence (6.2r6), and ImageJ (1.46k), Carl Zeiss LSM Image Browser, and/or Adobe Photoshop software for postcapture imaging processes.

Electron microscopy

Transmission electron microscopy (TEM) was performed essentially as described previously (**23**). Three-week-old *N. benthamiana* leaves were cut into fine pieces (3 mm by 3 mm) using a clean sharp razor blade. Leaves were fixed for 24 h in 2.0% glutaraldehyde, 4% paraformaldehyde, and 0.05% tannic acid in 0.1 M sodium cacodylate buffer (pH 7.4), washed three times in cacodylate buffer, and postfixed in 1% osmium tetroxide in the same buffer for 7 h, washed three times in buffer, and postfixed a second time in 1% osmium tetroxide and 1% potassium ferrocyanide overnight at 4°C. For a control, we rapidly fixed our samples just once in 3% $KMnO_4$ for 4 h, and we observed the same structures but with fewer details, indicating that our fixation method did not induce any artifacts. The samples were washed four times in water, dehydrated in a series of ethanol solutions (30%, 40%, and 50%), and block stained overnight in 1% uranyl acetate in 50% ethanol at 4°C. The samples were dehydrated in ethanol, embedded in Epon 812 resin, and sliced into thin sections (70 nm thick) with an ultramicrotome Ultracut E of Reichert Jung. In addition, semithin sections (1 µm thick) were stained in toluidine blue for light microscope examination with a Zeiss microscope. Staining of thin sections was performed in 2% aqueous uranyl acetate for 7 min followed by treatment with lead citrate for 3 min. The sections were observed with a TEM Philips 201.

Results

ER, Golgi bodies, COPII coatamers, and chloroplasts are amalgamated in a perinuclear globular structure during TuMV infection

To obtain an overall view of the structural changes that the endomembranes of the early secretory pathway undergo during infection, we examined the distribution of well characterized ER and Golgi organelle markers in TuMV-infected *N. benthamiana*cells by confocal microscopy. We first analyzed the morphology of the ER using GFP-HDEL, a lumenal ER marker (**61**). In noninfected

cells, the marker showed the characteristic cortical polygonal network of short interconnected tubules, transvacuolar strands, and labeling around the nucleus (**Fig. 1A**). In TuMV-infected cells, the cortical ER did not show any apparent modification, but the ER marker was additionally recruited into a large irregularly shaped globular-like structure juxtaposed to the nucleus in the midsection of the cell that also contained $6K_2$-mCherry (**Fig. 1B**). The ER was compacted within this structure and did not show a polygonal tubular pattern. Occasionally, the globular structure was distant from the nucleus, or two structures were seen in the same cell. The largest section of this structure was estimated to be 16 μm ± 4 μm long (n = 30). By comparison, we calculated the nuclear diameter to be 12 μm ± 3 μm (n = 30). The globular structure was linked to the cortical ER by transvacuolar strands (**Fig. 1B**, white arrowhead), and $6K_2$-mCherry-tagged vesicles essentially devoid of the GFP-HDEL marker were seen traveling along these strands and the polygonal ER tubules (see Movie S1 in the supplemental material). A similar result was obtained with P24σ1d-YFP, a resident membrane ER marker (**12**) (data not shown).

The morphology of the Golgi apparatus was analyzed using the *cis*-Golgi marker ERD2-GFP (**47**) and GFP fused to the transmembrane domain of the rat sialyl transferase (ST-GFP) (**9**), which is targeted to the *trans*-Golgi. In healthy cells, ST-GFP and ERD2-GFP were mainly found as Golgi bodies (**9**, **47**). In TuMV-infected cells, in addition to Golgi bodies, ST-GFP was also localized to a large globular structure near the nucleus (**Fig. 1D**) that overlapped with the $6K_2$-mCherry fluorescent signal (**Fig. 1C**). Some individual bodies were seen, but the ST-GFP marker was predominantly diffuse within this structure. The ring-like configuration for some of the $6K_2$-mCherry fluorescent signals denoted the presence of chloroplasts (see below). Similarly, ERD2-GFP was found as individual Golgi bodies (not shown) but was recruited in the globular structure in a diffused form (**Fig. 1G**) along with $6K_2$-mCherry (**Fig. 1F**). Production of punctate motile structures induced by TEV $6K_2$ occurred in a COPII- and COPI-dependent manner (**57**). We consequently investigated the distribution of the COPII coatamer component Sec24 (**18**) in the globular structure. YFP-Sec24 in healthy epidermal leaves were characteristically distributed as punctate structures (**18**). Although the punctate appearance of YFP-Sec24 was still observed in TuMV-infected cells (not observable in **Fig. 1H**), YFP-Sec24 was also detected in the globular structure induced by the virus (**Fig. 1H**).

Finally, the presence of chloroplasts in the globular structure was investigated as $6K_2$ vesicles were reported to associate with chloroplasts early in infection (56).Figure 1I to K show that the globular structure contained several chloroplasts, with $6K_2$-GFP labeling their contours.

To analyze the host membrane modifications at the ultrastructural submicron-resolution level, we performed electron microscopy analyses on 4-week-old *N. benthamiana* plants that had been agroinfected with TuMV 6 days before. The structural modifications that were observed cannot be attributed to*Agrobacterium*, since no detectable effect on the morphology of cellular organelles and on the endomembrane network was observed following agroinfiltration with an empty vector (and confirmed in reference 3). **Figure 2A** shows that infected cells contained characteristic "pinwheel" cytoplasmic inclusion bodies (black arrows) (**30**) and electron-translucent (+) and electron-opaque (*) vesicles of 90 to 340 nm in diameter (average of 170 nm ± 13 nm for 25 vesicles). On some occasions, vesicles were found in direct continuity with tubular ER coated with ribosomes (**Fig. 2A**, black arrowheads). Some chloroplasts were distorted and formed pseudopodium-like extrusions (**Fig. 2B**, black arrow), an observation that was previously reported (**56**). Vesicle clustering in the proximity of the nucleus was also observed (**Fig. 2C**).

The presence of both lumenal and membrane-associated endomembrane markers in the same $6K_2$-containing globular compartment suggests that the ER, COPII coatamers, and Golgi apparatus are heavily reorganized near the nucleus during TuMV infection, being amalgamated possibly as dense membrane stacks surrounding chloroplasts. On the other hand, the transvacuolar and cortical ER and the rest of the Golgi bodies were not affected.

TuMV infection inhibits protein secretion at the ER-Golgi interface

Because of the amalgamation of the ER and Golgi apparatus into a $6K_2$-tagged globular structure, we investigated the impact of infection on the overall functionality of the host secretory pathway. After its synthesis in the ER, secreted GFP (secGFP) is transported via the Golgi apparatus to the apoplast where its fluorescence is dim. When secretion is inhibited, the protein accumulates intracellularly where it can be readily visualized by fluorescence microscopy (**61**,**62**). Four days following agroinfiltration, we examined *N. benthamiana* leaves for secGFP fluorescence emission by confocal microscopy at a 10× objective

magnification (**Fig. 3**). For a positive control for intracellular retention, we expressed GFP-HDEL. The fluorescence emitted by GFP-HDEL was strong (**Fig. 3A**), in contrast to the fluorescence of secGFP, which was generally weak or undetectable (**Fig. 3B**) due to the apoplast acidic pH (**61**, **62**). On the other hand, expression of secGFP in TuMV-infected cells resulted in increased GFP fluorescence (**Fig. 3C**). We quantified the GFP fluorescence for each treatment using the MetaMorph software, and the data are shown in **Fig. 3F**. Compared to secGFP alone, we observed higher average intensity fluorescence when secGFP was expressed in infected cells. These data are in agreement with those observed during TEV infection (**57**). High-magnification observations of secGFP in infected cells indicated that it was retained in the ER, with additional accumulation in the perinuclear globular structure (compare **Fig. 3E** and **D**). These results indicate that TuMV infection not only has important consequences for the morphology of the ER and Golgi apparatus but also has an impact on the secretory pathway by blocking protein secretion at the ER-Golgi interface.

The globular structure is not an isolated subcellular compartment

TuMV peripheral vesicles travel along microfilaments (**15**), ER transvacuolar strands, and tubules (see Movie S1 in the supplemental material), but the perinuclear globular structure is generally a static entity. However, the ER and Golgi apparatus are highly dynamic organelles, constantly undergoing remodeling (**9**, **39**). Since the perinuclear globular structure observed in infected cells contains an amalgam of condensed ER and Golgi membranes, we wanted to investigate whether this compartment is nevertheless functionally linked to the bulk of nonmodified endomembranes. We consequently performed a fluorescence recovery after photobleaching (FRAP) experiment on TuMV-infected cells expressing ST-GFP. In one experiment, we selected a cell harboring two distinct globular structures around the nucleus and we used a 488-nm laser at high intensity to bleach the ST-GFP and $6K_2$-mCherry fluorophores in one of the two globular structures. We then monitored fluorescence recovery and redistribution every 10 s for 5 min. As shown in **Fig. 4** and Movie S2 in the supplemental material, the recovery of $6K_2$-mCherry fluorescence did not occur over the 5-min time period, but ST-GFP fluorescence returned to near prebleach level within less than 2 min. In another experiment, we

bleached half of the globular structure and observed the same results (data not shown).

Photoactivable GFP (PAGFP) is used for fluorescent pulse-labeling of fusion proteins at a specific position within a cell, which allows their subsequent cellular redistribution to be monitored. PAGFP fused to the *A. thaliana* ER-resident protein calnexin (CX-PAGFP) (**46**) was used to monitor the dynamics of the ER membrane with reference to the globular structure in TuMV-infected cells. Expression of CX-PAGFP in TuMV-infected cells that produced $6K_2$-mCherry was observed by confocal microscopy 4 days after agroinfiltration of *N. benthamiana* plants. Photoactivation was performed in an area close to or within the globular structure in a 10- to 20-s pulse, and activated CX-PAGFP distribution was followed by time-lapse photography. The localized background level of green fluorescence observed prior to activation is attributed to the high concentration of CX-PAGFP in the globular structure. Following activation in an area next to the globular structure (**Fig. 5A**), CX-PAGFP fluorescence drastically increased and was found to move rapidly away from the site of activation toward the cortical ER and also into the globular structure. After less than 1 min, the fluorescence from CX-PAGFP became weak at the site of activation and in the globular structure, suggesting rapid depletion ofthe pulsed activated protein. When activation was performed within the globular structure (**Fig. 5B**), activated CX-PAGFP fluorescence was seen to rapidly fill up and then to exit the globular structure toward the cortical ER. Throughout a 15-min observation period, the fluorescence due to CX-PAGFP remained high in the globular structure, indicating that this compartment is a reservoir that can hold a large quantity of ER membranes.

These data indicate that the perinuclear globular structure was not restocked in viral components, with no input of viral proteins from nearby perinuclear structures following photobleaching. On the other hand, the TuMV-induced globular structures were dynamically connected to the bulk of the ER and Golgi apparatus. The ER, although amalgamated with Golgi bodies and compacted in the globular structure, still retained its dynamic membrane properties and moved in and out of the virus-induced compartment.

The globular structure is functionally linked to motile peripheral $6K_2$ vesicles

$6K_2$ was also fused to PAGFP ($6K_2$-PAGFP) and expressed in TuMV-infected *N. benthamiana* cells that produced $6K_2$-mCherry. Weak localized background of green fluorescence was observed in the globular structure prior to activation, probably due to the high concentration of $6K_2$-PAGFP in the structure (**Fig. 6A**). Photoactivation was performed for 10 to 20 s within the globular structure, and the dynamics of activated $6K_2$-PAGFP was then monitored by time-lapse photography (**Fig. 6A**). Following activation, $6K_2$-PAGFP fluorescence was found to rapidly fill up the globular structure, and after a delay of 25 s, a green fluorescing motile $6K_2$ vesicle was seen to originate and to move away from the structure. This experiment was repeated several times, and although few in numbers, vesicles exiting from the globular structure were consistently observed. When activation was performed next to the globular structure (**Fig. 6B**), motile vesicles were seen trafficking away or toward the globular structure. In the example provided in **Fig. 6B**, one vesicle was seen to move toward and subsequently exit from the globular structure. These experiments then provide evidence for a functional link between the perinuclear globular structure and peripheral $6K_2$ vesicles. Not only do the vesicles have their origin in the globular structure, but they can also be recycled back to it.

Brefeldin A does not abrogate the formation of the perinuclear globular structure

We next investigated the importance of ER-to-Golgi transport on the biogenesis of the globular structure. For this purpose, we treated cells with brefeldin A (BFA), a lactone antibiotic that primarily inhibits transport of proteins from the Golgi apparatus back to the ER (**40**). *N. benthamiana* leaves were agroinfected with TuMV expressing $6K_2$-GFP and were treated 66 h postinfection with DMSO or BFA at a concentration of 10 μg/ml before the globular structure could be observed. The cells were examined 24 h later by confocal microscopy. Treatment with BFA did not affect the formation of the perinuclear globular structure (**Fig. 7C**) and the production of peripheral vesicles, whose morphology was similar to that observed in untreated cells (compare the middle panels of **Fig. 7A** and **B**). However, when YFP-Sec24 was expressed in infected cells, the COPII marker punctate structures were larger and were found to be more frequently clustered with the peripheral vesicles

(**Fig. 7B**) than in the absence of the drug (**Fig. 7A**). Using the JACoP plugin in ImageJ (**10**), the Pearson's correlation coefficient Rr values were 0.38 ± 0.02 and 0.14 ± 0.02 in the presence or absence of BFA, respectively (**Fig. 7D**), which confirms increased clustering of $6K_2$vesicles with the COPII marker after BFA treatment. BFA was shown to decrease the yield of TuMV particles produced during infection (**56**), but the assays used could not differentiate between inhibition of viral RNA replication/synthesis or inhibition of virus cell-to-cell movement. In order to discriminate between agroinfiltrated primary infected cells from secondary infected cells and thus assaying for viral intercellular movement, we introduced a gene cassette encoding GFP-HDEL under the control of the cauliflower mosaic virus (CaMV) 35S promoter next to the TuMV cassette expressing $6K_2$-mCherry, both of which are flanked by the left and right borders of the T-DNA in pCambia (**Fig. 7E**). Since both gene cassettes are delivered in the same cells and GFP-HDEL does not move between cells (**4**), primary infection foci were characterized by concomitant green and red fluorescence, while secondary infection foci exhibited red fluorescence only (**Fig. 7F**). No delay in virus infection and virus production was observed with this additional gene cassette, and cell-to-cell movement was observed 4 days after agroinfiltration (M. Agbeci et al., unpublished data manuscript in preparation). *N. benthamiana* leaves were agroinfiltrated with the TuMV-$6K_2$mCherry/GFP-HDEL dual-cassette construct and were treated with DMSO or BFA at a concentration of 10 μg/ml 66 h postinfiltration. The treated leaf cells were examined 24 h later by confocal microscopy with a 10× objective. Virus cell-to-cell movement was readily observed in leaves treated with DMSO but was inhibited in BFA-treated leaf samples (compare **Fig. 7F** and **G**). The surface area for foci expressing mCherry only (n = 20) was quantified, and the data indicated higher average intensity fluorescence for leaves treated with DMSO than for leaves treated with BFA (**Fig. 7H**). In the case of primary infection foci, no difference in mCherry fluorescence intensity was detected between the two treatments (data not shown), suggesting that viral replication was unaffected by the drug. Since BFA may have unexpected effects on other cellular transport pathways, we repeated the experiment by expressing along with TuMV the dominant-negative Arf1 mutant (**43**), which primarily inhibits Golgi recycling back to the ER. Expression of this mutant had the same inhibitory effect on TuMV cell-to-cell movement as BFA did (**Fig. 7I** to **K**). Since the dominant Arf1 had the same effect as BFA, the globular structure

was still observed. The above data suggest that the secretory pathway is not required for the formation of the TuMV-induced perinuclear structure and viral protein production. On the other hand, disruption of ER-to-Golgi transport caused the retention of $6K_2$ vesicles with COPII coatamers and blocked virus cell-to-cell movement.

Discussion

It was previously shown that the $6K_2$ protein of TuMV induced the production of membrane-associated vesicular structures (5, 15, 17, 25, 53, 56). In the present investigation, we have investigated the impact of this production on the endomembranes of the early secretory pathway. The formation of a virus-induced perinuclear globular structure was characterized by the amalgamation of ER, Golgi, and COPII markers as well as chloroplasts within this structure, which also contained $6K_2$ and hence replication complex components. However, the cortical ER and the bulk of Golgi bodies were apparently not affected. Even though the ER and Golgi apparatus had lost their characteristic organization in this globular structure, they remained connected to the host secretory pathway. This connection is likely important for the generation of peripheral $6K_2$ vesicles, which have been shown to exit from the globular structure and possibly are recycled back. A similar functional link between peripheral bodies and their origin from the perinuclear ER has been noted in the case of Bamboo mosaic virus (31) and Potato mop-top virus (22), and in the latter case, recycling through the endocytic pathway has been suggested.

TuMV $6K_2$-induced structures are associated with viral RNA and contain viral replication and host proteins known to be required for virus production (5, 15,17, 25, 53, 56). The production of endomembrane aggregates in the perinuclear region has been reported for a few plant viruses (2, 11, 35, 45, 54). For instance, Potato virus X (PVX) infection induced the formation of a single large inclusion body known as "X-body" localized next to the nucleus that contained ribosomes, virions, and the viral RNA-dependent RNA polymerase (2). Recently, Tilsner et al. (54) have shown that X-body biogenesis resulted in the reorganization and accumulation of host actin, ER, and Golgi apparatus into that structure for the compartmentalization of viral gene products needed for virus replication. Similarly, Grapevine fanleaf virus (GFLV) (45) and Cowpea mosaic virus (CPMV) (11) infection led to the redistribution of the ER to generate a perinuclear viral

compartment where replication took place. It is then likely that the perinuclear structure is a major site for viral RNA replication. Curiously, Golgi bodies were not found in the perinuclear compartments for GFLV and CPMV, which is different from what is observed for TuMV and PVX. This noticeable discrepancy suggests the existence of different mechanisms for host endomembrane recruitment during infection.

One question is whether formation of the perinuclear structure is a result of redistribution of existing ER and Golgi membranes or of *de novo* synthesis. First, we did not notice any changes in the morphology of the cortical ER, and the number of Golgi bodies outside the globular structure appeared to be of the same order, whether the cell was infected or not. Additionally, the lack of depletion of CX-GFP fluorescence over an extended period (at least 15 min) when activation was done within the structure suggests that the globular structure is a large reservoir of ER membranes. Finally, it has been reported that plant viral infections stimulate *de novo* membrane synthesis (**2**, **11**, **32**, **45**). These observations would suggest that the recruitment of organelles into the TuMV globular structure results from an increase in ER and Golgi synthesis, which would reflect a need for the sustained high synthetic activity that is required for virus production.

Interestingly, aberrant perinuclear globular structures entwined by actin cables and composed of ER, Golgi apparatus, and soluble secreted markers were also observed in mutant *A. thaliana* lines (**18**, **38**). These lines have a defect in one of the Sec24 isomers that causes a partial loss of function for the binding of cargo protein destined for secretion. The mutation led to impaired traffic of proteins at the ER-Golgi interface, accompanied with the formation of aberrant endomembrane clusters near the nucleus. These clusters are morphologically and dynamically very similar to those observed in TuMV-infected cells. Inhibition of protein transport at the ER and Golgi interface has been noted during vertebrate RNA virus infections (**13**, **14**, **37**, **50**). The Norwalk virus nonstructural p22 and the picornaviral 3A and/or 2BC proteins are responsible for this phenomenon. In the case of p22, a YXΦESDG motif that mimics a diacidic ER export signal plays a critical role as an ER/Golgi trafficking antagonist (**50**). Alternatively, the 3A protein inhibits GBF1, a guanine nucleotide exchange factor that activates small Arf1 GTPase involved in COPI vesicle formation (**59**). In the case of TuMV, we also think that the inhibition of protein secretion is a consequence of viral modification of the ER-Golgi interface.

The TuMV $6K_2$ protein shares some characteristics with these viral proteins (e.g., presence of a transmembrane domain responsible for vesicle formation) and may have an ER export signal (**33**). It will be interesting to investigate whether $6K_2$ targets a component of the early secretory pathway at the ER-Golgi interface that leads to inhibition of protein secretion and formation of the perinuclear globular structure.

BFA treatment or the coexpression of a dominant-negative mutant of Arf1 did not affect the formation of the globular structure or the production of viral proteins in primary infected cells, suggesting that viral replication proceeded normally. It thus appears that the ER-Golgi interface does not play a direct role in the globular structure morphogenesis or functionality. This situation is analogous to what has been observed during coronavirus infection where virus-induced remodeling of endoplasmic reticulum membranes and viral replication, albeit reduced, still took place in the presence of BFA (**28**). Additionally, production of peripheral $6K_2$ vesicles was not affected, although they showed increased overlap with the COPII marker Sec24. The importance of the secretory pathway for viral movement protein-induced vesicle trafficking and for intercellular virus movement has been demonstrated for many plant viruses (**1**, **20**, **21**, **35**). In the case of Poa semilatent virus, trafficking may involve an unconventional mechanism, since treatment with secretory pathway inhibitors had no detectable effect on peripheral body formation (**49**). This is analogous to what we observed in the case of TuMV, but the increased clustering of Sec24 with the peripheral vesicles indicates that the latter may have become dysfunctional. This suggests that disruption of the early secretory pathway slows down the budding of $6K_2$ vesicles at ERES, which is then reflected in the inhibition of virus intercellular movement.

On the basis of the data generated in the present investigation, we suggest the following model to describe cellular remodeling during TuMV infection (**Fig. 8**). Early in the infection process, the incoming viral RNA is translated and the viral gene products contribute to the formation of the perinuclear globular structure. Replication events (i.e., negative- and positive-sense RNA transcription) take place within this globular structure, and these events would still happen even if the ER-Golgi interface is disrupted during viral infection. After this step, viral egress is initiated by the budding of $6K_2$ vesicles at ERES in the globular structure, which then traffic along the ER/microfilaments toward the plasma membrane and

plasmodesmata for ultimate delivery of the virus into neighboring cells. At that point, some peripheral vesicles may be recycled back to the globular structure. Future investigations will aim at identifying host proteins that are involved in the formation of the perinuclear structure and why in the absence of MTOC, such a large viral structure can be formed near the nucleus.

Acknowledgements

We thank M. Desrosiers and J. Lacoste for helping with confocal microscopy, C. Hawes for ERD2-GFP, and J. Runions for CX-PAGFP. We thank H. Sanfaçon for critically reading the manuscript.

This study was supported by the Natural Sciences and Engineering Research Council of Canada and from Le Fonds de recherche du Québec – Nature et technologies to H.Z. and J.-F.L.

References

1. Amari K, Lerich A, Schmitt-Keichinger C, Dolja VV, Ritzenthaler C. 2011. Tubule-guided cell-to-cell movement of a plant virus requires class XI myosin motors. PLoS Pathog. 7:e1002327. doi:10.1371/journal.ppat.1002327.

2. Bamunusinghe D, et al. 2009. Analysis of potato virus X replicase and TGBp3 subcellular locations. Virology 393:272–285.

3. Bamunusinghe D, Seo J-K, Rao ALN. 2011. Subcellular localization and rearrangement of endoplasmic reticulum by brome mosaic virus capsid protein. J. Virol. 85:2953–2963.

4. Batoko H, Zheng HQ, Hawes C, Moore I. 2000. A rab1 GTPase is required for transport between the endoplasmic reticulum and Golgi apparatus and for normal Golgi movement in plants. Plant Cell 12:2201–2218.

5. Beauchemin C, Boutet N, Laliberté J-F. 2007. Visualization of the interaction between the precursors of VPg, the viral protein linked to the genome of Turnip mosaic virus, and the translation eukaryotic initiation factor iso 4E in planta. J. Virol. 81:775–782.

6. Belov GA, et al. 2007. Hijacking components of the cellular secretory pathway for replication of poliovirus RNA. J. Virol. 81:558 –567.

7. Belov GA, Feng Q, Nikovics K, Jackson CL, Ehrenfeld E. 2008. A critical role of a cellular membrane traffic protein in poliovirus RNA replication. PLoS Pathog. 4:e1000216. doi:10.1371/journal.ppat.1000216.

8. Belov GA, et al. 2012. Complex dynamic development of poliovirus membranous replication complexes. J. Virol. 86:302–312.

9. Boevink P, et al. 1998. Stacks on tracks: the plant Golgi apparatus traffics on an actin/ER network. Plant J. 15:441–447.

10. Bolte S, Cordelieres FP. 2006. A guided tour into subcellular colocalization analysis in light microscopy. J. Microsc. (Oxford) 224:213–232.

11. Carette JE, Stuiver M, Van Lent J, Wellink J, Van Kammen AB. 2000. Cowpea mosaic virus infection induces a massive proliferation of endoplasmic reticulum but not Golgi membranes and is dependent on de novo membrane synthesis. J. Virol. 74:6556 –6563.

12. Chen J, Stefano G, Brandizzi F, Zheng H. 2011. Arabidopsis RHD3 mediates the generation of the tubular ER network and is required for Golgi distribution and motility in plant cells. J. Cell Sci. 124:2241–2252.

13. Choe SS, Dodd DA, Kirkegaard K. 2005. Inhibition of cellular protein secretion by picornaviral 3A proteins. Virology 337:18 –29.

14. Cornell CT, Kiosses WB, Harkins S, Whitton JL. 2006. Inhibition of protein trafficking by coxsackievirus b3: multiple viral proteins target a single organelle. J. Virol. 80:6637–6647.

15. Cotton S, et al. 2009. Turnip mosaic virus RNA replication complexvesicles are mobile, align with microfilaments, and are each derived from a single viral genome. J. Virol. 83:10460 –10471.

16. den Boon JA, Ahlquist P. 2010. Organelle-like membrane compartmentalization of positive-strand RNA virus replication factories. Annu. Rev. Microbiol. 64:241–256.

17. Dufresne PJ, et al. 2008. Heat shock 70 protein interaction with Turnip mosaic virus RNA-dependent RNA polymerase within virus-induced membrane vesicles. Virology 374:217–227.

18. Faso C, et al. 2009. A missense mutation in the Arabidopsis COPII coat protein Sec24A induces the formation of clusters of the endoplasmic reticulum and Golgi apparatus. Plant Cell 21:3655–3671.

19. Fu CY, Johnson JE. 2011. Viral life cycles captured in three-dimensions with electron microscopy tomography. Curr. Opin. Virol. 1:125–133.

20. Harries PA, et al. 2009. Differing requirements for actin and myosin by plant viruses for sustained intercellular movement. Proc. Natl. Acad. Sci. U. S. A. 106:17594 –17599.

21. Harries PA, Schoelz JE, Nelson RS. 2010. Intracellular transport of viruses and their components: utilizing the cytoskeleton and membrane highways. Mol. Plant Microbe Interact. 23:1381–1393.

22. Haupt S, et al. 2005. Two plant-viral movement proteins traffic in the endocytic recycling pathway. Plant Cell 17:164 –181.

23. Hayat MA. 1981. Fixation for electron microscopy. Academic Press, New York, NY.

24. Hsu N-Y, et al. 2010. Viral reorganization of the secretory pathway generates distinct organelles for RNA replication. Cell 141:799 –811.

25. Huang TS, Wei T, Laliberté J-F, Wang A. 2010. A host RNA helicase-like protein, AtRH8, interacts with the potyviral genome-linked protein, VPg, associates with the virus accumulation complex, and is essential for infection. Plant Physiol. 152:255–266.

26. Kawakami S, Watanabe Y, Beachy RN. 2004. Tobacco mosaic virus infection spreads cell to cell as intact replication complexes. Proc. Natl. Acad. Sci. U. S. A. 101:6291–6296.

27. Knoops K, et al. 2008. SARS-coronavirus replication is supported by a reticulovesicular network of modified endoplasmic reticulum. PLoS Biol. 6:e226. doi:10.1371/journal.pbio.0060226.

28. Knoops K, et al. 2010. Integrity of the early secretory pathway promotes, but is not required for, severe acute respiratory syndrome coronavirus RNA synthesis and virus-induced remodeling of endoplasmic reticulum membranes. J. Virol. 84:833–846.

29. Laliberté J-F, Sanfaçon H. 2010. Cellular remodeling during plant virus infection. Annu. Rev. Phytopathol. 48:69 –91.

30. Langenberg WG. 1991. Cylindrical inclusion bodies of wheat streak mosaic virus and three other potyviruses only self-assemble in mixed infections. J. Gen. Virol. 72:493–497.

31. Lee SC, Wu CH, Wang CW. 2010. Traffic of a viral movement protein complex to the highly curved tubules of the cortical endoplasmic reticulum. Traffic 11:912–930.

32. Lee WM, Ahlquist P. 2003. Membrane synthesis, specific lipid requirements, and localized lipid composition changes associated with a positivestrand RNA virus RNA replication protein. J. Virol. 77:12819 –12828.

33. Lerich A, Langhans M, Sturm S, Robinson DG. 2011. Is the 6 kDa tobacco etch viral protein a bona fide ERES marker? J. Exp. Bot. 62:5013–5023.

34. Limpens RW, et al. 2011. The transformation of enterovirus replication structures: a three-dimensional study of single- and double-membrane compartments. mBio 2(5):e00166 –11. doi:10.1128/mBio.00166-11.

35. Liu JZ, Blancaflor EB, Nelson RS. 2005. The tobacco mosaic virus 126-kilodalton protein, a constituent of the virus replication complex, alone or within the complex aligns with and traffics along microfilaments. Plant Physiol. 138:1853–1865.

36. Marti L, Fornaciari S, Renna L, Stefano G, Brandizzi F. 2010. COPIImediated traffic in plants. Trends Plant Sci. 15:522–528.

37. Moffat K, et al. 2007. Inhibition of the secretory pathway by foot-andmouth disease virus 2BC protein is reproduced by coexpression of 2B with 2C, and the site of inhibition is determined by the subcellular location of 2C. J. Virol. 81:1129 –1139.

38. Nakano RT, et al. 2009. GNOM-LIKE1/ERMO1 and SEC24a/ERMO2 are required for maintenance of endoplasmic reticulum morphology in Arabidopsis thaliana. Plant Cell 21:3672–3685.

39. Nebenfuhr A, et al. 1999. Stop-and-go movements of plant Golgi stacks are mediated by the acto-myosin system. Plant Physiol. 121:1127–1142.

40. Nebenfuhr A, Ritzenthaler C, Robinson DG. 2002. Brefeldin A: deciphering an enigmatic inhibitor of secretion. Plant Physiol.130:1102–1108.

41. Nelson BK, Cai X, Nebenfuhr A. 2007. A multicolored set of in vivo organelle markers for co-localization studies in Arabidopsis and other plants. Plant J. 51:1126 –1136.

42. Netherton CL, Wileman T. 2011. Virus factories, double membrane vesicles and viroplasm generated in animal cells. Curr. Opin. Virol.1:381–387.

43. Phillipson BA, et al. 2001. Secretory bulk flow of soluble proteins is efficient and COPII dependent. Plant Cell 13:2005–2020.

44. Ritzenthaler C. 2011. Parallels and distinctions in the direct cell-to-cell spread of the plant and animal viruses. Curr. Opin. Virol. 1:403–409.

45. Ritzenthaler C, et al. 2002. Grapevine fanleaf virus replication occurs on endoplasmic reticulum-derived membranes. J. Virol. 76:8808 –8819.

46. Runions J, Brach T, Kuhner S, Hawes C. 2006. Photoactivation of GFP reveals protein dynamics within the endoplasmic reticulum membrane. J. Exp. Bot. 57:43–50.

47. Saint-Jore CM, et al. 2002. Redistribution of membrane proteins between the Golgi apparatus and endoplasmic reticulum in plants is reversible and not dependent on cytoskeletal networks. Plant J. 29:661–678.

48. Schaad MC, Jensen PE, Carrington JC. 1997. Formation of plant RNA virus replication complexes on membranes: role of an endoplasmic reticulum-targeted viral protein. EMBO J. 16:4049 –4059.

49. Schepetilnikov MV, et al. 2008. Intracellular targeting of a hordeiviral membrane-spanning movement protein: sequence requirements and involvement of an unconventional mechanism. J. Virol. 82:1284 –1293.

50. Sharp TM, Guix S, Katayama K, Crawford SE, Estes MK. 2010. Inhibition of cellular protein secretion by Norwalk virus nonstructural protein p22 requires a mimic of an endoplasmic reticulum export signal. PLoS One 5:e13130. doi:10.1371/journal.pone.0013130.

51. Sparkes IA, Ketelaar T, De Ruijter NCA, Hawes C. 2009. Grab a Golgi: laser trapping of Golgi bodies reveals in vivo interactions with the endoplasmic reticulum. Traffic 10:567–571.

52. Suhy DA, Giddings TH, Jr, Kirkegaard K. 2000. Remodeling the endoplasmic reticulum by poliovirus infection and by individual viral proteins: an autophagy-like origin for virus-induced vesicles. J. Virol. 74:8953–8965.

53. Thivierge K, et al. 2008. Eukaryotic elongation factor 1A interacts with Turnip mosaic virus RNA-dependent RNA polymerase and VPg-Pro in virus-induced vesicles. Virology 377:216 –225.

54. Tilsner J, et al. 2012. The TGB1 movement protein of potato virus X reorganizes actin and endomembranes into the X-Body, a viral replication factory. Plant Physiol. 158:1359 –1370.

55. Verchot J. 2011. Wrapping membranes around plant virus infection. Curr. Opin. Virol. 1:388–395.

56. Wei T, et al. 2010. Sequential recruitment of the endoplasmic reticulum and chloroplasts for plant potyvirus replication. J. Virol. 84:799 –809.

57. Wei T, Wang A. 2008. Biogenesis of cytoplasmic membranous vesicles for plant potyvirus replication occurs at endoplasmic reticulum exit sites in a COPI- and COPII-dependent manner. J. Virol. 82:12252–12264.

58. Welsch S, et al. 2009. Composition and three-dimensional architecture of the Dengue virus replication and assembly sites. Cell Host Microbe5:365–375.

59. Wessels E, et al. 2006. A viral protein that blocks Arf1-mediated COP-I assembly by inhibiting the guanine nucleotide exchange factor GBF1. Dev. Cell 11:191–201.

60. Wolk B, Buchele B, Moradpour D, Rice CM. 2008. A dynamic view of hepatitis C virus replication complexes. J. Virol. 82:10519 –10531.

61. Zheng H, et al. 2005. A Rab-E GTPase mutant acts downstream of the Rab-D subclass in biosynthetic membrane traffic to the plasma membrane in tobacco leaf epidermis. Plant Cell 17:2020 –2036.

62. Zheng H, Kunst L, Hawes C, Moore I. 2004. A GFP-based assay reveals a role for RHD3 in transport between the endoplasmic reticulum and Golgi apparatus. Plant J. 37:398 –414

Figures legends

Figure 1: TuMV infection causes amalgamation of endomembranes in the perinuclear area. (A and B) Three-dimensional confocal microscopy images of leaf epidermal cells of *N. benthamiana* showing GFP-HDEL in healthy cells (A) or in TuMV-infected cells expressing $6K_2$-mCherry (B) 4 days after agroinfiltration. The images are three-dimensional renderings of >40 1-µm-thick slices that overlap by 0.5 µm. (C to K) Single optical confocal images showing individual cells infected with TuMV. Panels C to E show coexpressed $6K_2$-mCherry, ST-GFP, and their merged fluorescent signals, respectively. Panels F and G show coexpressed $6K_2$-mCherry and its signal merged with ERD2-GFP signal, respectively. Panel H shows coexpressed $6K_2$-mCherry and its signal merged with YFP-Sec24 signal. Panels I to K show coexpressed $6K_2$-GFP, chloroplast autofluorescence, and their merged fluorescent signals, respectively. Bars = 10 µm. A white asterisk shows the position of the nucleus, and the white arrowhead points to the transvacuolar ER strand linking the globular structure with cortical ER.

Figure 2: Observations of infected cells by TEM. (A) Cytoplasm of a TuMV-infected cell showing typical inclusion bodies (thin black arrows) and electron-translucent (+) and -opaque (*) vesicles. The large black arrowheads denote vesicles closely associated with tubular ER. (B) Micrograph showing a distorted chloroplast encircling a vesicle (black

arrow). (C) Cytoplasm of a TuMV-infected cell with the nucleus close to a cluster of vesicles (black arrow).

Figure 3: TuMV infection inhibits the secretion of secGFP. (A to C) Single-slice confocal microscopy images at a low magnification of leaf epidermal cells of *N. benthamiana* expressing GFP-HDEL (A), secGFP (B), and secGFP and TuMV (C). Bars = 200 µm. (D and E) Confocal microscopy images at a high magnification showing the distribution of secGFP expressed in healthy cells (D) or in infected cells producing $6K_2$-mCherry (E). Panels D and E are three-dimensional renderings of 40 1-µm-thick slices that overlap by 0.5 µm. Bars = 20 µm. (F) Average GFP fluorescence intensity of *N. benthamiana* epidermal cells expressing the indicated proteins. Statistical differences are indicated by brackets and asterisks as follows: **, 0.001 < P value < 0.01 (very significant); ***, P value < 0.001 (extremely significant).

Figure 4: FRAP experiments on perinuclear globular structure. (A and B) Confocal microscopy images of leaf epidermal cells of *N. benthamiana* infected by TuMV producing $6K_2$-tagged vesicles (A) and ST-GFP (B). T (C) Merged images from panels A and B. A cell harboring two different globular structures was chosen, and at time point T −10 s, a rectangular region corresponding to a globular structure was bleached by a 488-nm laser for 10 s. Images were collected every 10 s. The numbers at the top of the figure show the time when fluorescence was recorded. Bars = 20 µm. (D and E) Average intensity of fluorescence emitted by $6K_2$-mCherry (D) and ST-GFP (E) before bleaching or during the recovery period.

Figure 5: Photoactivation of CX-PAGFP shows connection between the globular structure induced by TuMV and the ER. Time series images of cells infected with TuMV expressing $6K_2$-mCherry showing dispersal of calnexin fused to photoactivatable GFP (CX-PAGFP) after activation with a 405-nm laser by 10 to 15 iterations using the bleach mode of the LSM 510 Meta confocal microscope (Zeiss). Activation was performed in an area next to the globular structure (A) or within the globular structure (B). The white rectangle in panel A and the white circle in panel B outline the activation area. Bars = 10 µm.

Figure 6: The globular structure is functionally linked to motile $6K_2$ vesicles. Time series images of $6K_2$-PAGFP expressed in TuMV-infected *N. benthamiana* cells that produced $6K_2$-mCherry. (A) Activation of 6K2-PAGFP occurred within the globular structure, and

time lapse images were taken. The white arrowhead shows the movement of one vesicle originating from the globular structure. (B) Activation was performed next to the globular structure in the cytoplasm, and the movement of activated $6K_2$-PAGFP vesicles is shown using the plugin MTrackJ of ImageJ. The white circle in the Activation panel in panel A and the white rectangle in the Activation panel in panel B represent the activation spot. The circle around the vesicle shows the position at the indicated time. Bars = 10 µm.

Figure 7: Effect of BFA treatment on the formation of $6K_2$-tagged vesicles and on virus cell-to-cell movement. (A and B) *N. benthamiana* leaves were infiltrated with A. tumefaciens containing plasmids with genes encoding TuMV producing $6K_2$-mCherry-tagged vesicles and YFP-Sec24. The leaves were infiltrated with DMSO (A) or 10 µg/ml BFA (B) 66 h after agroinfiltration. The cells were analyzed 24 h later with a LSM 510 Meta confocal microscope (Zeiss). The left panels show the green fluorescence channel for YFP-Sec24, the middle panels show the red fluorescence channel for TuMV producing $6K_2$-mCherry-tagged vesicles, and the right panels show the merged images. The images are three-dimensional (3D) renderings of 15 1-µm-thick slices that overlap by 0.5 µm. (C) Image showing that the globular structure is produced in the presence of BFA. (D) Quantification of clustering between YFP-Sec24 COPII marker and the $6K_2$-mCherry-tagged vesicles by calculation of the Pearson's correlation coefficient Rr values. (E) Schematic representation of the plasmid used to discriminate primary agroinfiltrated infected cells from secondary infected cells. Primary infection foci are characterized by concomitant green and red fluorescence, while secondary infection foci show red fluorescence only. (F and G) Viral movement was assayed in the absence (F) or presence (G) of BFA. (H) The surface area of only the foci with red fluorescence was calculated and expressed in arbitrary fluorescence units. (I and J) The effect of Arf1 expression on virus cell-to-cell movement was assayed in the presence of wild-type Arf1 (I) or in the presence of the dominant-negative mutant NI of Arf1 (J). (K) The surface area of only the foci with red fluorescence was calculated and expressed in arbitrary fluorescence units. Statistical differences are indicated by brackets and asterisks as follows: **, $0.001 < P \text{ value} < 0.01$ (very significant); ***, $P \text{ value} < 0.001$ (extremely significant).

Figure 8: Model to describe the formation of the perinuclear globular structure. Early in the infection process, the incoming viral RNA is translated, and the viral gene products contribute to the formation of the perinuclear globular structure. Replication events (i.e., negative- and positive-sense RNA transcription) take place within this globular structure. After this step, viral egress is initiated by the budding of $6K_2$ vesicles at ERES in the globular structure, which then traffic along the ER/microfilaments toward the plasma membrane and plasmodesmata for ultimate delivery of the virus into neighboring cells. At that point, some peripheral vesicles may be recycled back to the globular structure.

Figures

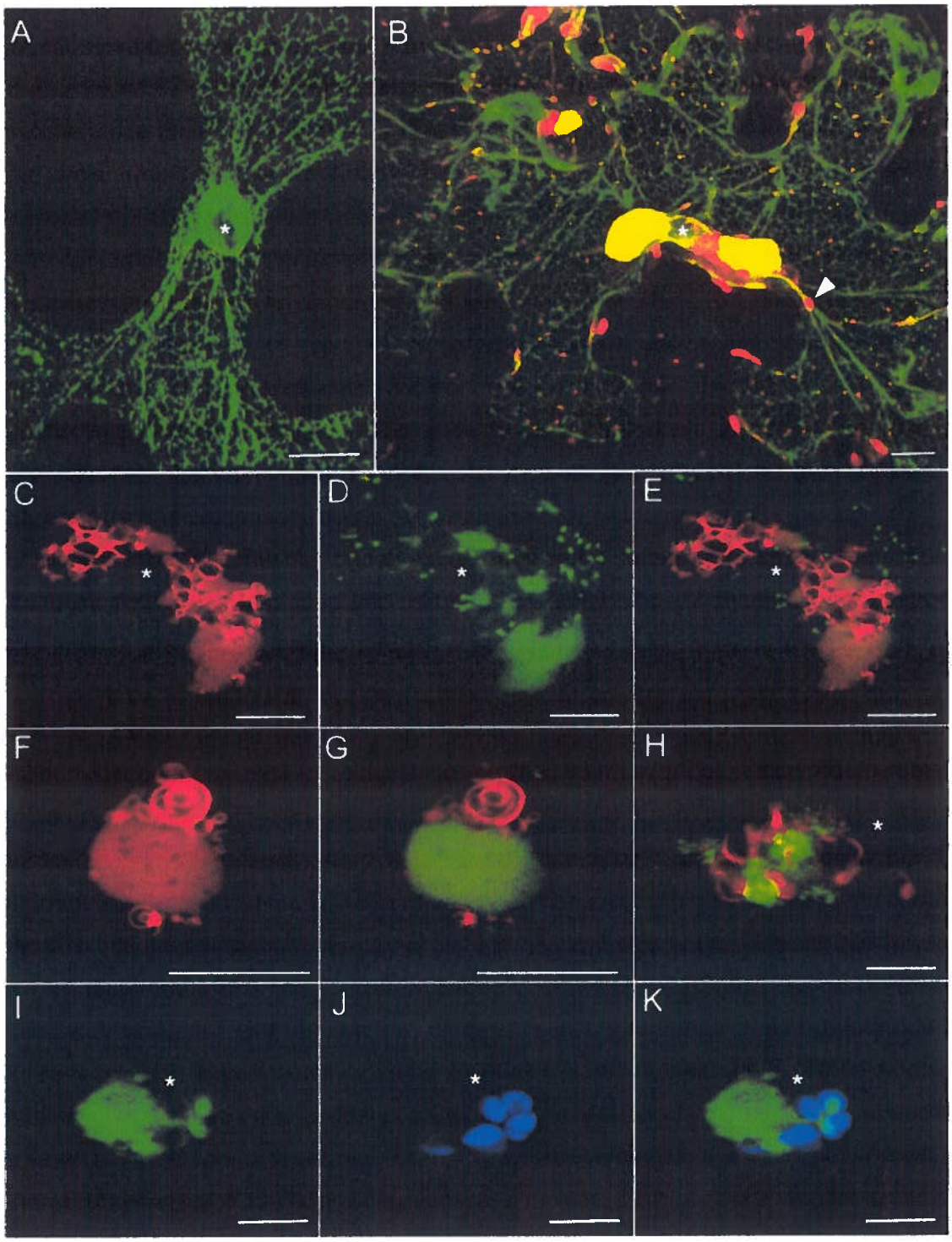

Figure 1: TuMV infection causes amalgamation of endomembranes in the perinuclear area.

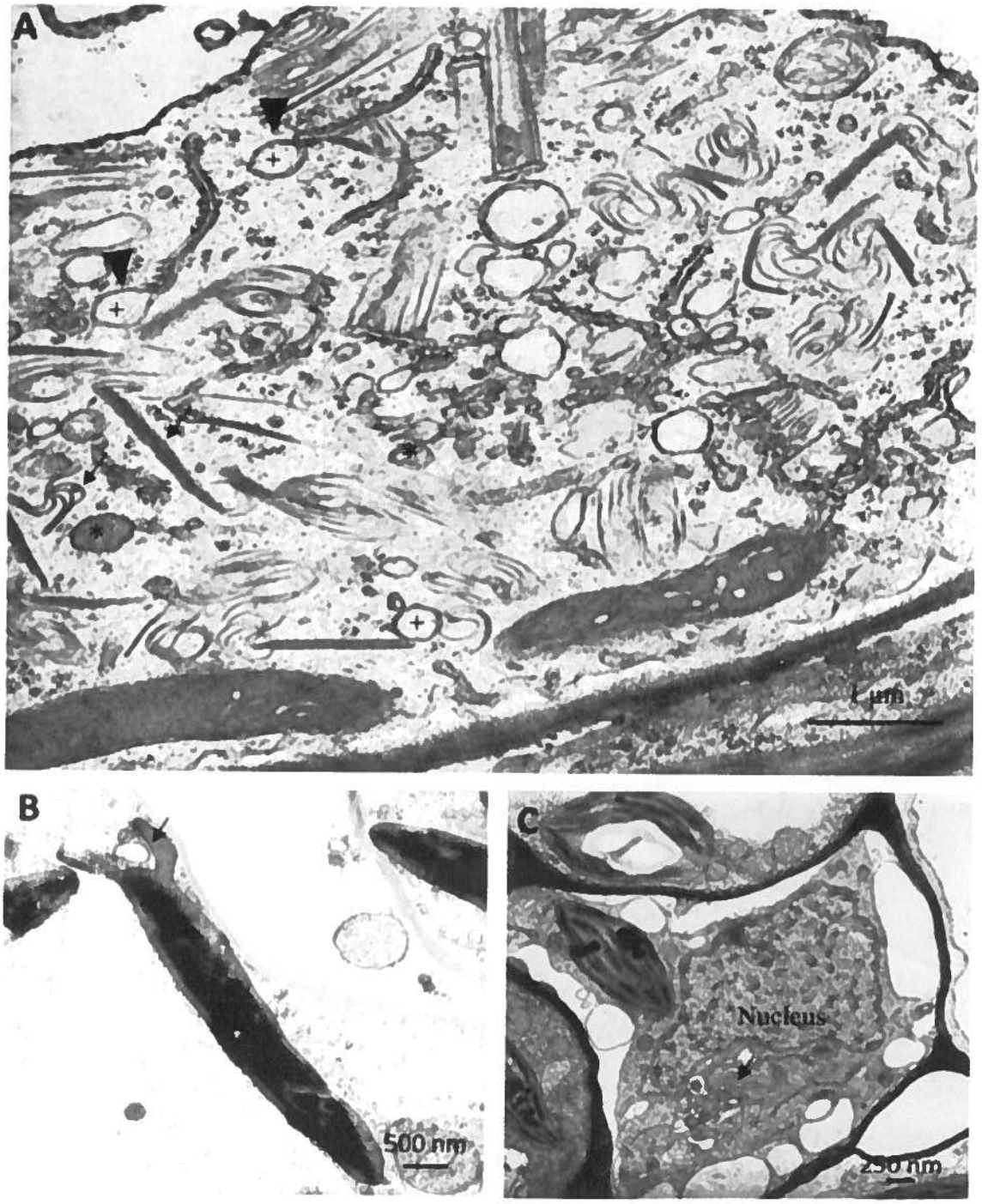

Figure 2: Observations of infected cells by TEM.

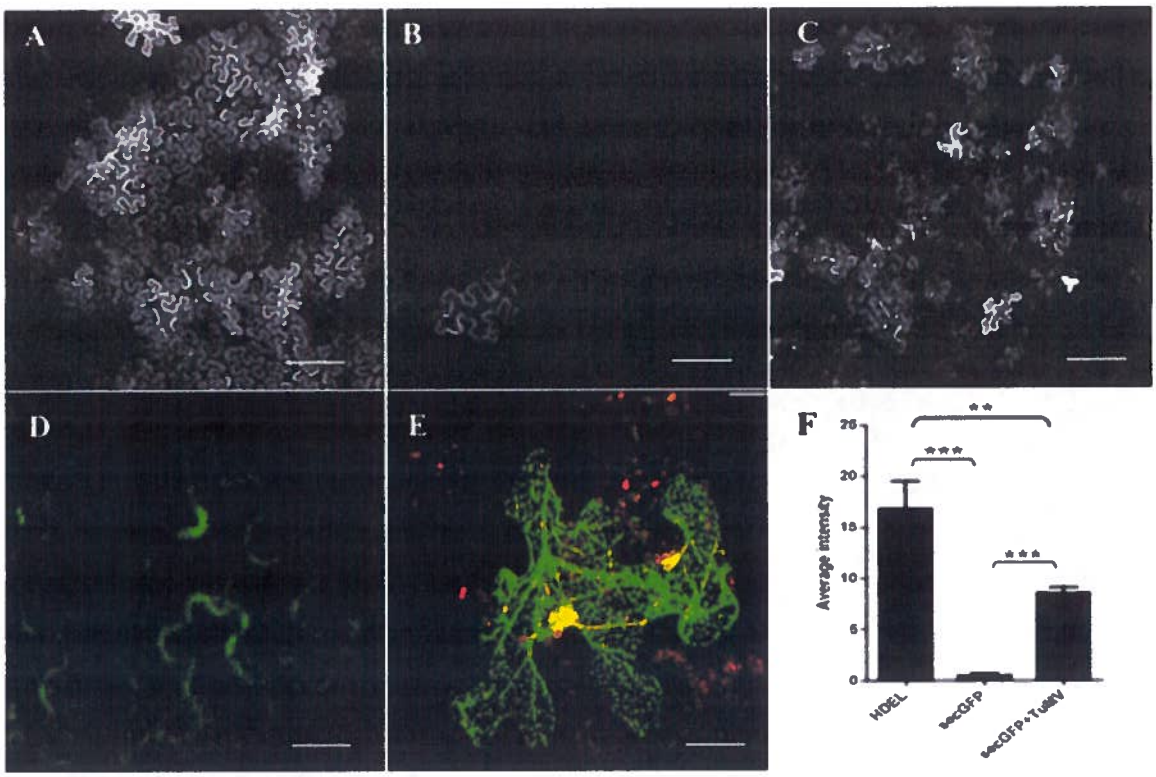

Figure 3: TuMV infection inhibits the secretion of secGFP.

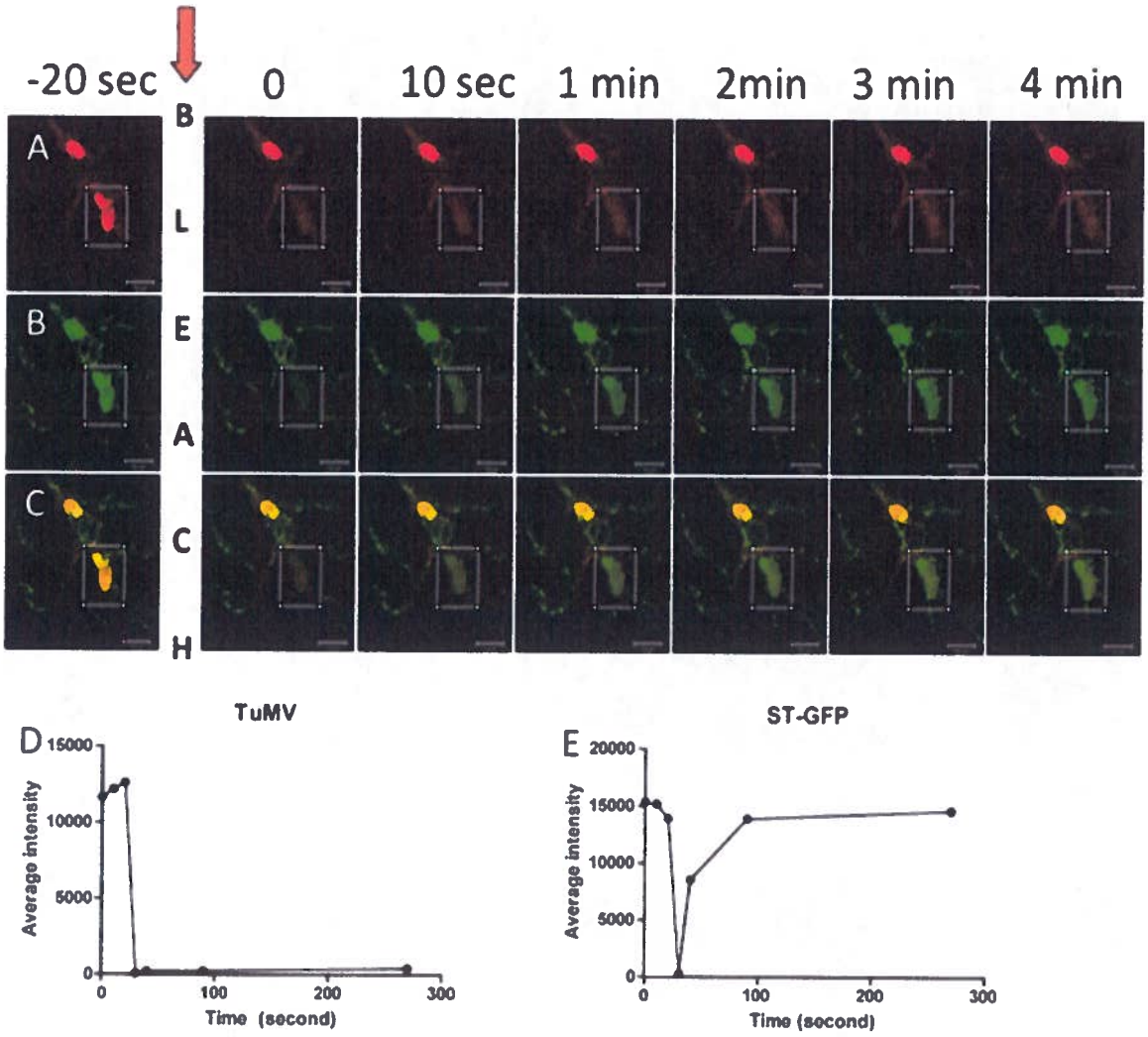

Figure 4: FRAP experiments on perinuclear globular structure.

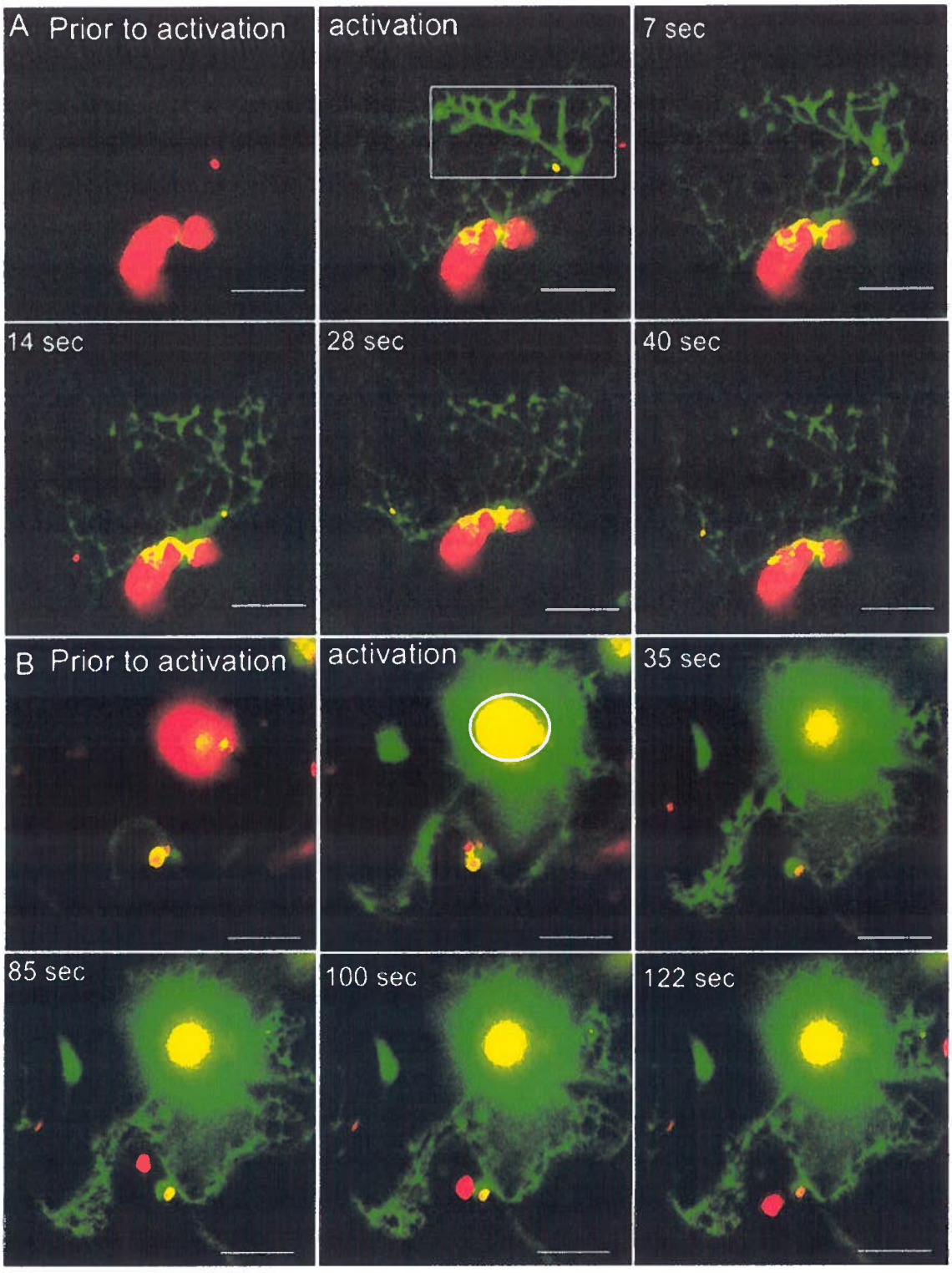

Figure 5: Photoactivation of CX-PAGFP shows connection between the globular structure induced by TuMV and the ER.

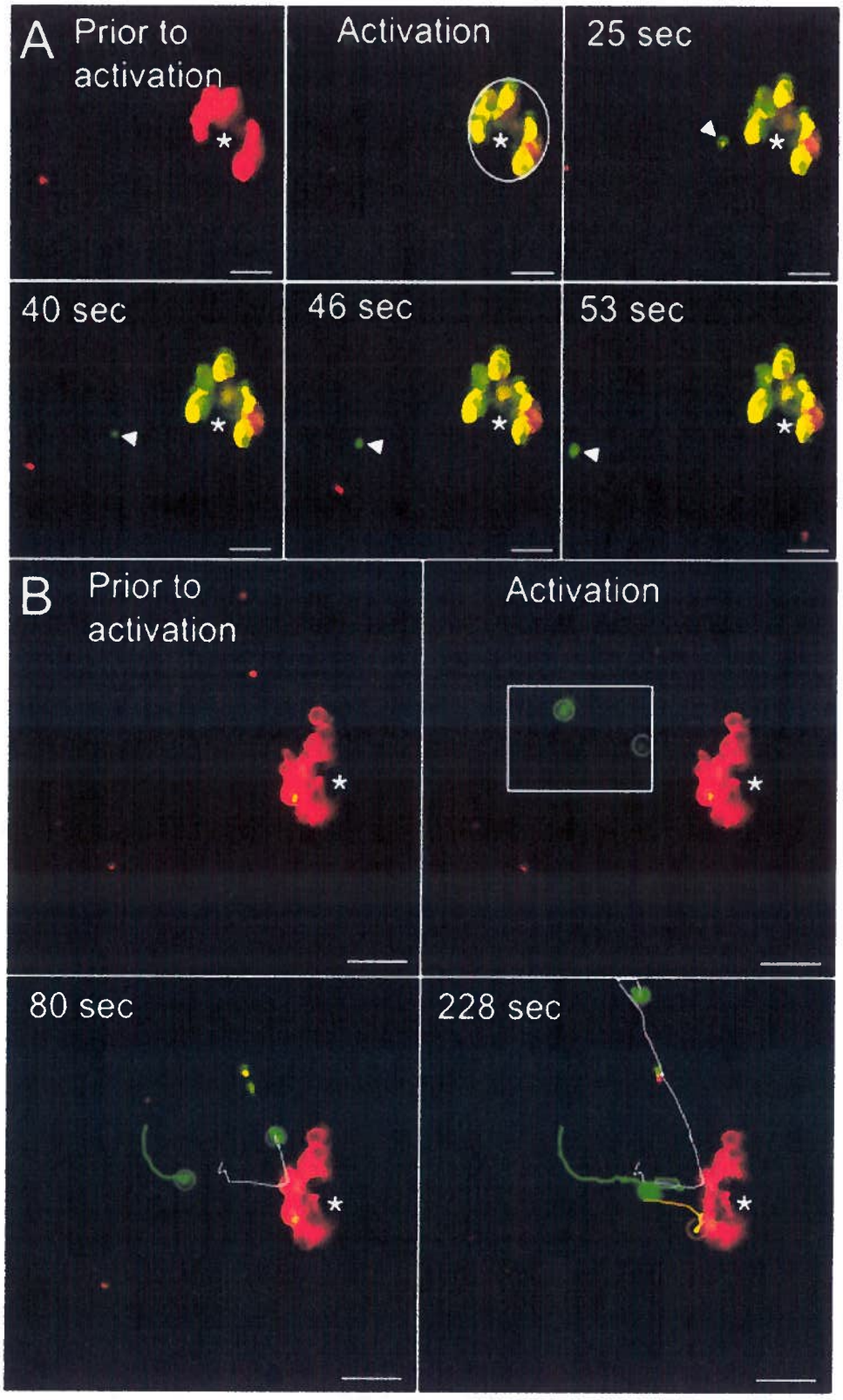

Figure 6: The globular structure is functionally linked to motile $6K_2$ vesicles. Time series images of $6K_2$-PAGFP expressed in TuMV-infected *N. benthamiana* cells that produced $6K_2$-mCherry.

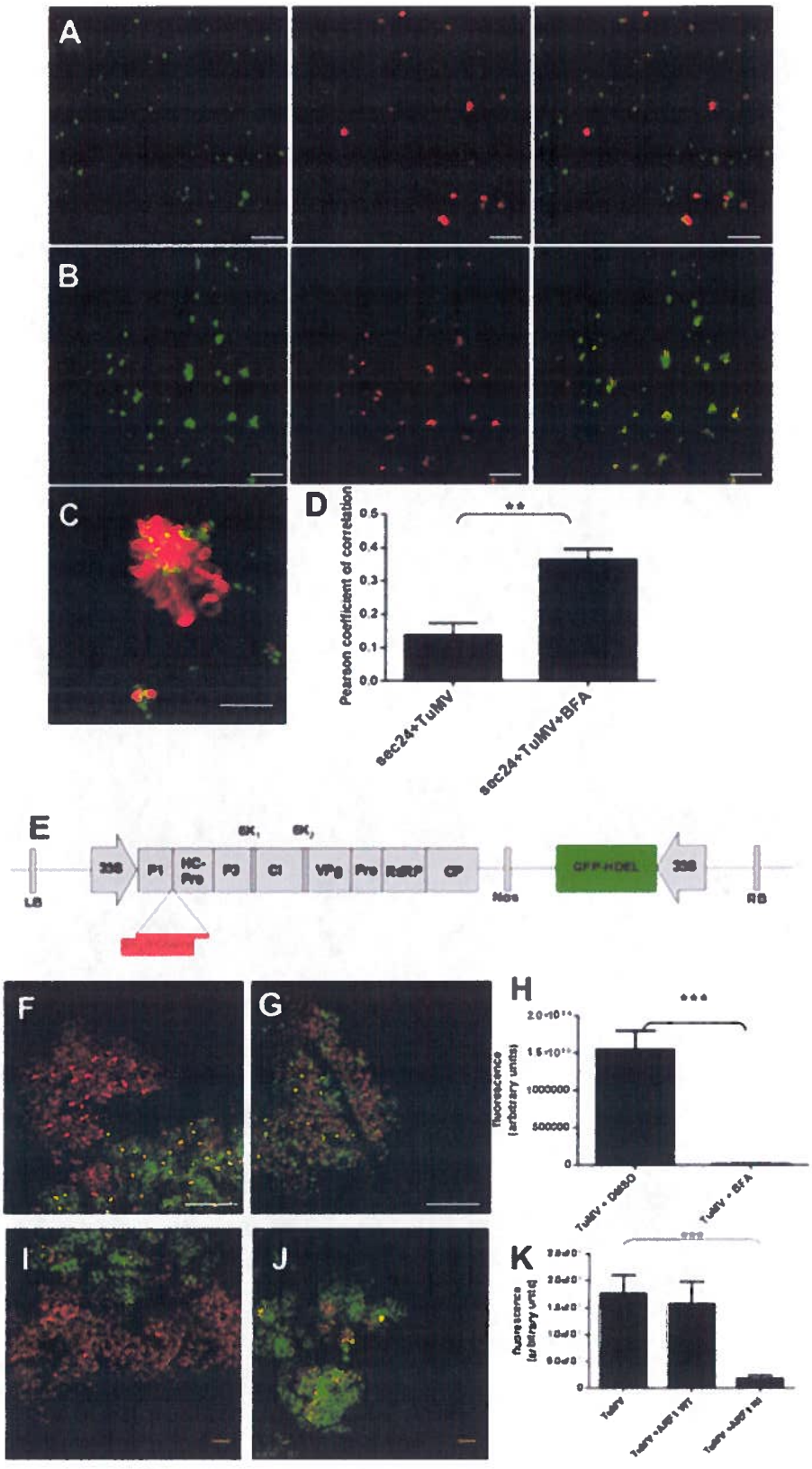

Figure 7: Effect of BFA treatment on the formation of $6K_2$-tagged vesicles and on virus cell-to-cell movement.

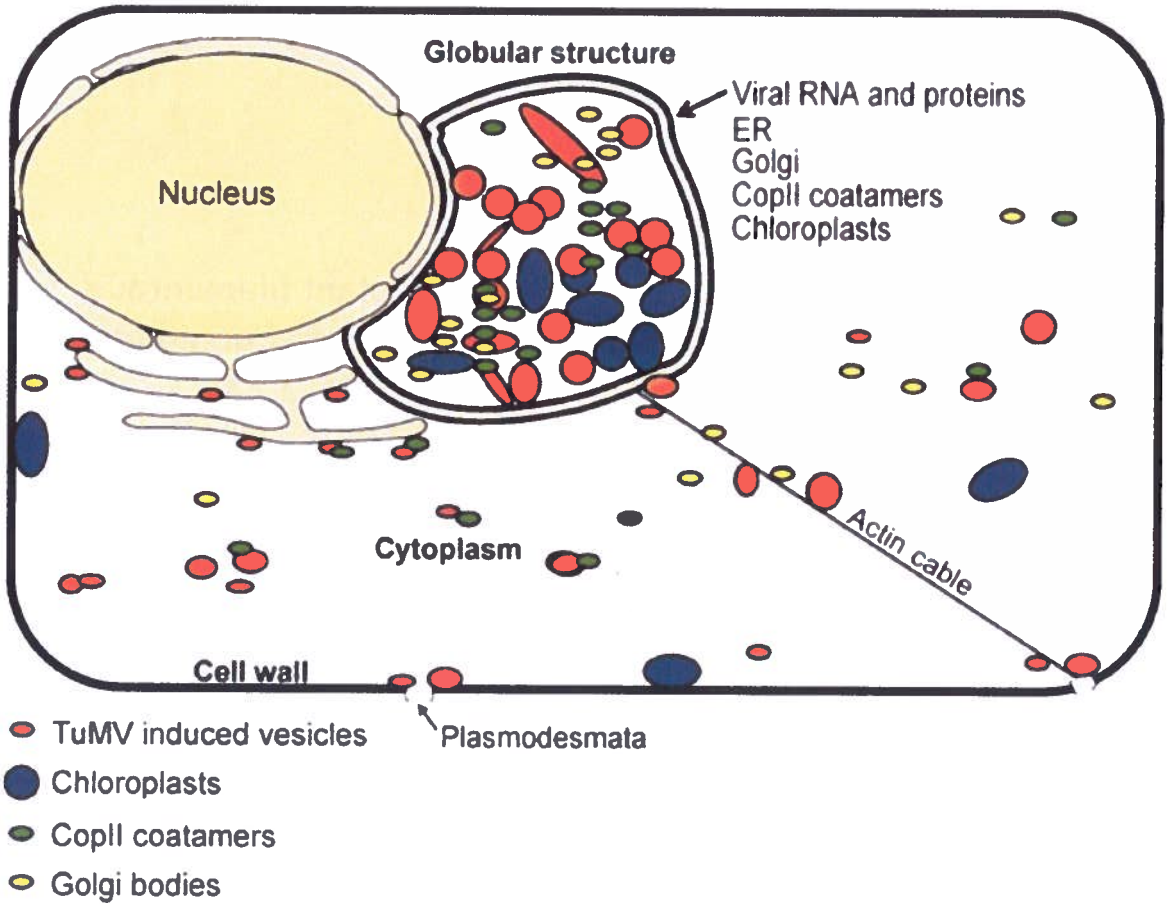

Figure 8: Model to describe the formation of the perinuclear globular structure.

Publication n°3

Symplasmic and vascular movement of a plant filamentous virus proceed through membrane-associated viral complexes

Soumis à PNAS le 10 avril 2012

Romain Grangeon[1], Juan Wan[1] Maxime Agbeci[1], Jun Jiang[1], Huanquan Zheng[2], and Jean-François Laliberté[1]*

[1] INRS-Institut Armand-Frappier, Institut National de la Recherche Scientifique, Laval, Québec, Canada.

[2] Department of Biology, McGill University, Montréal, Québec, Canada

* Corresponding author : Jean-François Laliberté

Email : jeanfrancois.laliberte@iaf.inrs.ca

Contribution

J'ai défini et mené les expériences de cet article avec les conseils de mon directeur de thèse. J'ai réalisé toutes les figures excepté la figure 5. J'ai effectué le travail d'écriture avec l'aide et la supervision de mon directeur de recherche. La figure 5 a été faite par Juan Wan qui a développé une technique de cryosection des feuilles et des tiges de *Nicotiana benthamiana* afin de visualiser nos échantillons en coupes transversales ou longitudinales.

Résumé

La réplication des virus de plantes à ARN de polarité positive induit la formation dans la cellule infectée de réarrangements membranaires complexes qui soutiennent la synthèse d'ARN viral. La protéine $6K_2$ du virus de la mosaïque du navet (TuMV) est une protéine membranaire qui provoque la formation de vésicules impliquées dans le mouvement intracellulaire de l'ARN viral. Cette étude montre que les vésicules induites par $6K_2$ utilisent les filaments transvacuolaires pour gagner la membrane plasmique et s'amarrer au plasmodesme (PD). Le TuMV augmente la taille limite d'exclusion des PD, ce qui permet aux vésicules marquées par $6K_2$ de passer dans les cellules voisines. La protéine $6K_2$ a été fusionnée à la GFP photo-activable ($6K_2$:PAGFP) pour visualiser le mouvement intercellulaire des vésicules $6K_2$ au cours de l'infection. Après activation, les vésicules étiquetées par $6K_2$:PAGFP se déplaçent rapidement (0,3 µm/s) à la périphérie de la cellule, et traversent la paroi de la cellule pour rejoindre les cellules adjacentes. Des observations supplémentaires en microscopie confocale ont indiqué que les vésicules contiennent la protéine virale RdRp et sont donc potentiellement active pour la réplication. Des agrégats de vésicules $6K_2$ contenant l'ARNv ont également été trouvés dans les vaisseaux du xylème. Nous proposons un modèle dans lequel le mouvement symplasmique et vasculaire de TuMV est réalisé par un complexe viral associé à des membranes marquées par $6K_2$.

Summary

Replication by plant positive-sense RNA viruses induces the formation in the infected cell of elaborate membranous organelle-like platforms that sustain viral RNA synthesis. The turnip mosaic virus (TuMV) $6K_2$ protein is a membrane protein and induces the formation of vesicles that are involved in intracellular movement of viral RNA. This study shows that $6K_2$-induced vesicles trafficked on transvacuolar strands towards the plasma membrane and docked at the plasmodesmata (PD). TuMV infection increased the size exclusion limit of PDs, which allowed transit into adjoining cells of $6K_2$-tagged vesicles. $6K_2$ was fused to photo-activable GFP ($6K_2$:PAGFP) to visualize by live cell imaging the intercellular movement of $6K_2$ vesicles during infection. Rapidly after activation, $6K_2$:PAGFP-tagged vesicles moved rapidly (0.3 µm/s) to the cell periphery, and moved across the cell wall into adjacent cells. Additional confocal observations of the motile $6K_2$ vesicles indicated that they contain RdRp and are thus potentially active for replication. $6K_2$-tagged and membrane-bound aggregates that contained viral RNA were also found in xylem vessels. We propose a model whereby symplasmic and vascular movement of TuMV is achieved by a membrane-associated viral complex associated with $6K_2$.

Introduction

Viruses are obligatory intracellular parasites that need host factors for replication and dissemination. To be successful, plant viruses have to enter and replicate in an initial cell, move to the adjoining cells and finally spread systemically in the host through vascular tissues (**1**-**3**). For intercellular movement, viruses must overcome the cell wall barrier by dilating plasmodesmata (PD), which are symplasmic tunnels between cells and the gateway for viral cell-to-cell movement (**4**, **5**). Plant viruses encode movement proteins (MPs) that interact with PDs to mediate intercellular spread of virus infection (**6**). What viral component goes through PDs is not fully known. A viral RNA-protein complex involving MPs among other proteins is suspected to cross over into non-infected cells. For some icosahedral viruses, viral particles transit through MP-induced tubules that go through PDs for their delivery into non-infected cells (**7**-**10**). In the case of filamentous viruses, the viral entity that enters the neighboring cells has not yet

been extensively studied but it does not appear to be encapsidated. So far, there is only one report stating that tobacco mosaic virus (TMV) infection spreads intercellularly as intact viral replication complexes (VRCs) (**11**).

Plant RNA viruses induce the remodeling of the secretory pathway (**12**-**18**) or of organelles such as chloroplasts (**19**-**21**), mitochondria (**22**, **23**) and peroxisomes (**24**) for viral replication. These « quasi-organelles » are often referred to as virus factories and harbor VRCs. However, the function of virus factories may be more than a simple replication complex associated with membranes. Recently, it has been suggested that replication and intercellular movement of some plant viruses are coordinated events that are mediated by membrane-associated motile vesicular structures (**13**, **25**, **26**). Turnip mosaic virus (TuMV) (genus *Potyvirus*) is a filamentous virus with a positive-sense RNA genome. TuMV infection leads to significant rearrangements of the early secretory pathway of the host cell (**27**). The infection is associated with the formation of at least two distinct types of sub-cellular compartments induced by the membrane-associated viral protein $6K_2$: a perinuclear globular structure and cortical endoplasmic reticulum (ER)-associated motile vesicular structures (**27**). The perinuclear globular structure contains ER, Golgi, chloroplasts and COPII coatamers (**27**), along with viral RNA and replication proteins (**28**). These structures are not isolated organelles and are dynamically connected to the bulk of non-modified endomembranes. The motile vesicular structures are derived from the globular structure, move along transvacuolar ER and associate with cortical ER. Thus, the $6K_2$ vesicles are likely the vehicles that mediate intracellular movement of viral RNA.

In this study, we report that during TuMV infection $6K_2$ vesicles were associated with the plasma membrane and docked at Pds, and then crossed over into adjacent cells. Furthermore, we found $6K_2$-tagged membrane aggregates containing viral RNA in xylem vessels of systemically infected plants. These data suggest that the viral entity of TuMV that moves from cell-to-cell and through vascular tissues is associated with membranes that are recruited by $6K_2$.

Results

$6K_2$-induced vesicles use transvacuolar strands to reach the plasma membrane and dock at plasmodesmata

Cotton et al (**28**) showed that TuMV-induced $6K_2$-tagged vesicles moved along actin microfilaments but the final destination of this intracellular movement was not determined. To examine if any of $6K_2$-tagged vesicles were associated with the plasma membrane, we stained *N. benthamiana* leaves infected with TuMV producing $6K_2$:GFP-tagged vesicles with the red FM4-64 dye, a lipophilic styryl compound used to label the plasma membrane (**29**). Numerous $6K_2$:GFP-tagged vesicles were observed at the plasma membrane (**Fig 1A**). Occasionally, vesicles appeared to have crossed the plasma membrane of the infected cell to reach a non-infected one because this cell did not contain a substantial amount of $6K_2$ vesicles (**Fig 1A**, arrows).

To observe how $6K_2$-induced vesicles reach the plasma membrane, we infected *N. benthamiana* plants with TuMV that produced $6K_2$:mCherry-tagged vesicles and co-expressed the plasmodesmata located protein 1 (PDLP1) fused to GFP (**30**). PDLP1 is dependent on the host secretory pathway for reaching PDs (**7**, **31**). PDLP1 :GFP and $6K_2$:mCherry-tagged vesicles were found to traffic on transvacuolar strands (TVS), which were visualized by bright-field illumination (**32**) (**Fig. 1B and Movie S1**). Since $6K_2$ vesicle formation were shown to depend also on the host secretory pathway (**27**), it is possible that they use the same path as PDLP1 for reaching the plasma membrane.

To determine if $6K_2$-tagged vesicles are localized at PDs, we infected plants with TuMV producing $6K_2$:GFP vesicles and co-expressed the plasmodesmata callose binding protein 1 (PDCB1) fused to mCherry (**7**) (**Fig 1C**). Some TuMV-induced $6K_2$:GFP-tagged vesicles were found adjacent to PDCB1. In several instances, $6K_2$ vesicles were present at opposite ends of PDCB1-labeled PD (**Fig. 1C**, arrows), suggesting a possible transit of $6K_2$ vesicles through this organelle. These data suggest that $6K_2$ vesicles move intracellularly towards the plasma membrane and dock at PDs for their likely transit into neighboring cells.

TuMV infection leads to an increase of PD size exclusion limit

PDs have a size exclusion limit (SEL) that is calculated by the molecular weight of the largest dye that can move from cell to cell (**33**). The SEL of PD is normally 1 kDa, which is too small to allow the passive transit of a virus complex (**34**). MPs are known to increase the SEL of the PD, allowing the cell-to-cell spread of much larger molecular complexes (**35-37**). For potyviruses, HCPro and CP were shown to increase the SEL of PD (**38**). To determine if TuMV can sufficiently increase the SEL of PD to allow the passage of $6K_2$ vesicles, we first introduced a gene cassette encoding GFP-HDEL under the control of the cauliflower mosaic virus (CaMV) 35S promoter next to a mCherry-encoding cassette. The two gene cassettes are flanked by the left and right borders of the T-DNA in the binary vector pCambia (pCambia/mCherry/GFP-HDEL) (**Fig. 2A**). Since both gene cassettes are delivered in the same cells and GFP-HDEL does not move between cells (**39**), agroinfiltrated cells should be characterized by concomitant green and red fluorescence. We used the Tile Scanning function of the confocal microscope to collect a series of adjoining images (the "tiles") and merged them digitally to get a larger leaf sample area. At 6 day post-agroinfiltration, all cells were emitting both green and red fluorescence when observed under the confocal microscope at low magnification. No red-only fluorescence foci were observed, indicating that mCherry did not move out by diffusion from agroinfiltrated cells (**Fig 2B**). When pCambia/mCherry/GFP-HDEL was expressed with a non-fluorescent TuMV infectious clone, in addition to cells emitting both red and green fluorescence, cells emitting only red fluorescence were readily observed (**Fig 2C**). This is an indication that TuMV infection leads to an increase in PD SEL that allows diffusion of cytosolic soluble proteins.

We then determined if the SEL increase observed during TuMV infection could allow the transit of $6K_2$:mCherry vesicles by constructing the expression vector pCambia/$6K_2$:mCherry/GFP-HDEL (**Fig. 2A**). Confocal and electron microscopy images indicated that $6K_2$ vesicles have an average diameter of 170 nm ± 13 nm (**27**). No intercellular movement of $6K_2$:mCherry was observed in the absence of TuMV (**Fig. 2D**), but movement was readily observed in TuMV infected cells (**Fig. 2E**). Quantitative analysis of intercellular movement was performed by measuring surface area of red fluorescence-only foci of 15 leaf samples containing a

minimum of 4 x 4 tiles and was shown to be statistically significant (**Fig. 2F**). No intercellular movement of $6K_2$:mCherry was observed when the dual gene cassette was expressed along with a non-replicative TuMV cDNA clone in which the GDD motif of the RdRp was replaced by a VNN motif (**Fig. 2F**). These data indicates that TuMV infection dilate PDs to allow cell-to-cell movement not only of soluble individual proteins but also of large membrane-associated multi-protein complexes.

TuMV-induced $6K_2$-tagged vesicles move intercellularly

Photoactivable GFP (PAGFP) is used for fluorescent pulse labeling of fusion proteins at a specific position within a cell, which allows their subsequent cellular redistribution to be monitored (**40**). PAGFP fused to $6K_2$ ($6K_2$:PAGFP) was used to monitor their intercellular movement in TuMV infected cells. Expression of $6K_2$:PAGFP in TuMV-infected cells that produced $6K_2$:mCherry-tagged vesicles was observed by confocal microscopy 5 days after agroinfiltration of *N. benthamiana* plants. Photoactivation was done for 20 s within a single cell, and time-lapse imaging was performed for to monitor $6K_2$:PAGFP vesicle intercellular movement. Following activation, $6K_2$:PAGFP vesicles were found to rapidly move out from the region of activation. In Fig. 3, a green fluorescing motile $6K_2$ vesicle (designated by the arrow) moved rapidly on a TVS towards the activated cell border, then disappeared for few seconds through the cell wall to reappear in the adjacent cell. This vesicle moved for a distance of at least 70 µm after activation, with an average velocity of 0.3 µm/s (movie S2). This real-time intercellular movement was seen in 5 different experiments, which confirms that this event occurred consistently.

We also activated $6K_2$:PAGFP in 39 different cells over 4 separate experiments and we monitored vesicles transport into adjoining cells (**Figure 3B**) two hours after activation. We found that 62% of the activated cells (24/39 cells) had vesicles moving into adjoining cells. Of these 24 activated cells, 63 vesicles moved into 38 different neighboring cells. On average, every activated cell produced 2.6 vesicles that moved into 1.6 adjoining cells. Furthermore, some vesicles that had travelled through 2 cell layers were observed (**Figure 3B**, red arrow). These experiments provide direct evidence that $6K_2$ vesicles can move cell to cell.

The viral RNA-dependent RNA polymerase is found within cortical motile $6K_2$ vesicles

Immunofluorescent experiments on protoplasts isolated from TuMV infected *N. benthamiana* leaves showed that $6K_2$ structures contained viral RNA and viral proteins such as VPg-Pro and the RNA-dependent RNA polymerase (RdRp) as well as host translation factors (**28**). To ascertain that the motile $6K_2$ vesicles on their way to the plasma membrane are potentially active for replication, we investigated whether or not they contain the TuMV RdRp. We infected *N. benthamiana* with TuMV producing $6K_2$:mCherry-tagged vesicles and co-expressed the viral RdRp fused to GFP (RdRp :GFP). We found that all motile $6K_2$:GFP/mCherry vesicles were associated with the GFP fluorescence, confirming the presence of RdRp in these structures (**Fig 4A**). As expected, co-localization of red and green fluorescence was also found in the large perinuclear structure. We also looked at $6K_2$ vesicles near the cell border (shown by bright-field illumination) and found them to be associated with RdRp (**Fig. 4B**). Since all motile $6K_2$ vesicles contained RdRp, it is likely that vesicles that move over into non-infected cells are active for replication.

Membranous viral complexes associated with $6K_2$ are found in xylem vessels

Since $6K_2$ vesicles can move between cells through PDs, we wondered if they could also be released in the vascular tissues of the plant for long-distance movement. We performed longitudinal cryo-sectioning of mock and TuMV/$6K_2$:GFP infected stems to observe the distribution of the virus in systemically infected tissues where the cell wall was labeled with Fluorescent Brightener 28 (Calcofluor, Sigma) and shown in magenta. Green fluorescence was distributed in epidermal cells, pith cells, cortex, trichomes and vein tissues of infected stem (**Fig 5A**). As expected, no green fluorescence was observed in mock-infected stems (data not shown). We looked into the vein tissue region and found large $6K_2$:GFP aggregates in the xylem vessels easily recognizable by their typical perforation (**Fig 5B**). 3D reconstruction shows that $6K_2$:GFP aggregates can have a substantial volume with respect to the xylem vessel diameter and were an amalgam of what looks like smaller vesicles (Movie S3). We then performed immunostaining using a monoclonal antibody that recognizes double-stranded (ds) RNA, which is an indication for the presence of viral RNA. Fig. 5C shows punctate dsRNA labeling (in red) in $6K_2$:GFP-tagged

vesicles found in the xylem, indicating that the aggregates are potentially infectious. We also used the membrane dye DiOC6(3) (Molecular Probes®) (in green) to stain the xylem and observed labeling of the $6K_2$:mCherry aggregates by DiOC6(3) (**Fig. 5D**), confirming the membranous nature of the $6K_2$-tagged structure. This suggests that long distance TuMV movement in the xylem may take the form of a $6K_2$-recruited membrane-associated viral complex.

Discussion

Several studies have identified viral proteins and host processes that are involved in intra- and intercellular movement of plant viruses. These have highlighted the importance of PDs, MPs, the host secretory pathway and actomyosin motors in viral movement (**5**). However, it is not clear what is the nature of the viral entity that crosses over the cell barrier of the infected cell into non-infected ones. In case of TMV, it is been proposed that non-encapsidated infectious RNA molecules associated with MPs are being transported (**41**). But the exact composition of this RNA-protein complex has yet to be defined, in particular the contribution of other viral proteins and host components (e.g. proteins and lipids).

Potyvirus infection is associated with the remodeling of the endomembrane systems and formation of large perinuclear structures that leads to the release of motile viral vesicles (**27**). Formation of these structures is induced by the viral 6 kDa membrane protein $6K_2$ (**17**). Several viral proteins (e.g. VpgPro, HCPro, P3, helicase and RdRp) and host proteins (e.g. eukaryotic initiation factor 4^E, polyA binding protein, eukaryotic elongation factor 1a), in addition to the viral RNA, are found within or associated with these membrane structures (**28, 42-44**). We show in this study that TuMV-induced $6K_2$-tagged vesicles could carry this viral RNA-protein cargo to PDs. The $6K_2$ vesicles trafficked along TVS [**Fig. 1B**, Movie S1 and (**27**)], which connect the nuclear region with the cell periphery (**45**), for docking at PDs (**Fig. 1D**). Although there is no single dedicated MP, several potyviral proteins with MP-like function have been identified. For instance, HCPro and CP can increase PD SEL (**38**), while the CI helicase and P3N-PIPO interact with PDs (**46**, **47**). With the exception of P3N-PIPO (**46**), these viral proteins have been found to be associated with $6K_2$ vesicles (**28**, **44**), which may be the factors that contribute to PD docking of

$6K_2$ vesicles. In the case of P3N-PIPO, it may reach PD independently of $6K_2$ vesicles (**47**) and at that point interacts with the CI helicase (**46**), possibly associated with $6K_2$ vesicles. Normally, transport vesicles fuse with their target membrane and release their cargo over the trans side of the target membrane (e.g. either organelle luminal space or apoplast) (**48**). Here, $6K_2$ vesicles when they reached the plasma membrane did not fuse with this membrane but instead they docked and entered PDs and exited intact into the next cell as shown by live cell imaging (**Fig. 3** and Movie S2). The size of these vesicles was rather large (e.g. 170 nm ± 13 nm in diameter) (**27**) but the increase in SEL of PDs during TuMV infection was sufficient to allow the passage of such structures (**Fig. 2**). This suggests that the viral entity of TuMV that transits into non-infected cells is a highly intricate RNA-protein complex bounded by a lipid membrane. Kawakami et al (**11**) proposed similar transport mode for TMV, which moved intercellularly as intact VRCs associated with MP membrane bodies. However, the lack of live cell imaging experiment showing intact VRC transiting through PD in real time may however cast some doubts as to the real nature of the viral entity that moved intercellularly. The work shown here could be viewed as a support for membrane-bound MP body-associated TMV RNA-protein complex is indeed capable of going though PD.

Another significant finding of this investigation is that not only was a membrane-bound TuMV complex found to transit through PD but it was also released in conducting tissues. Indeed, large membrane aggregates of $6K_2$-vesicles were found in xylem vessels (**Fig. 5**). Smaller $6K_2$ vesicles were occasionally seen throughout the conducting tube and may have clumped together as they traveled up the plant along with xylem sap to become aggregated. Presence of viral RNA within these aggregates (**Fig. 5b**) is an indication that these structures are potentially active for replication. Although viruses normally use the phloem, it is not uncommon to see viruses move in the xylem for systemic infection (**49**-**56**). For potyviruses, the presence of viral particles in the xylem has been reported for papaya ringspot virus and zucchini yellow mosaic virus (**57**). To explain the movement of rice yellow mottle virus between xylem cells, Opalka et al (**50**) proposed that during the differentiation of parenchyma cells into vascular elements, cells undergo programmed cell death that results in the loss of cellular contents. In this process, virus particles are passively transported to vessels. This may well take place for TuMV but the viral

entity would be membrane bound. This agrees with the early observation of membrane-associated particle aggregates in the sap of potyvirus infected plants (58).

Fig. 6 illustrates our current model for intercellular and systemic spread of TuMV. Upon TuMV entering a cell, translation and synthesis of viral RNA takes place in the perinuclear structure, an amalgam of viral RNA and protein as well as ER, Golgi, COPII coatamers and chloroplasts (27). At some point, small motile $6K_2$ vesicles exit from the perinuclear structure in a COPII/COPI dependent manner (27) and traffic in the TVS along actomyosin filaments (28, 43) for plasma membrane targeting and docking at PDs by possibly interacting with the helicase conical structures and P3N-PIPO. Intact $6K_2$ vesicles then enter dilated PDs through combined interactions of viral and host factors and move into adjoining non-infected cell as a membranes-associated complex ready to begin a new round of infection. This symplasmic spread proceeds until infection reaches parenchyma cells, which then undergo programmed cell death to release $6K_2$-recruited membrane-bound TuMV in xylem vessels for systemic infection of the plant, and possibly uptake by aphid vectors.

In conclusion, this study highlights the contribution of host membrane structures in symplasmic and systemic movement of a filamentous virus. It has been reported that plant viral infections stimulate de novo membrane synthesis, presumably for replication (59-62). It may also well be important for systemic movement. It will be interesting to identify other viral and host factors that are associated with formation, intracellular transport, PD docking/transit and aggregation of $6K_2$ –tagged structures during their movement in plants.

Materials and Methods

Molecular cloning and construction of fluorescent fusion proteins

The construction of pCambiaTunos/$6K_2$:GFP, pCambiaTunos/$6K_2$:mCherry, pCambia/$6K_2$:PAGFP, and pCambia/GFP :RdRp was described previously (27, 63). The cloning of PDLP1 :GFP and PDCB1 :mCherry were described in (7, 31). pCambia/$6K_2$:mCherry was generated by a PCR amplification of $6K_2$ from

pCambia/Tunos UK1 strain, using the following primer pairs (Forward : 5'-GCTCTAGAATGAACACCAGCGACATGA-3'; Reverse : 5'-CGGGATCCTTCATGGGTT ACGGGTTCGGA-3'). The PCR product was digested with XbaI and BamHI and inserted into pCambia/mCherry (**64**).

The introduction of the 35S-GFP-HDEL gene cassette into pCambia/mCherry or pCambia/$6K_2$:mCherry were done as follows. pBIN/20-ER-gk (**31**) was digested with AseI and ligated with similarly digested pCambia/mCherry or pCambia/$6K_2$:mCherry. Kanamycin-resistant Escherichia coli colonies were screened for either pCambia/mCherry/GFP-HDEL or pCambia/$6K_2$:mCherry/GFP-HDEL. For pCambiaTunosVNN, the Stratagene QuikChange II XL Multi Site-Directed Mutagenesis Kit and the primer pairs (Forward : 5'-CATCATCAGATTCTTCGTCAATGTAAATAA TTTACTGCTAAGCGTACACCCA-3'; Reverse : 5'-TGGGTGTACGCTTAGCAGTAAATT ATTTACATTGACGAAGAATCTGATGATG-3') were used to create the mutation from p35Tunos (**65**). The resulting mutant p35TunosVNN was digested with SmaI and ApaI, and then cloned into binary vector pCambia0390. The mutant was verified by sequencing.

Protein expression in plants

Transient expression studies were performed by agroinfiltration on three-week-old *Nicotiana benthamiana* plants. Plasmids were introduced into Agrobacterium tumefaciens AGL1 by electroporation and selected on LB ampicillin-kanamycin plates. The pellet of an overnight culture was gently suspended in water supplemented with 10 mM $MgCl_2$ and 150 µM acetosyringone and left at room temperature for 3 h. The solution was then diluted to an OD600 of 0.6 for pCambia/$6K_2$:mCherry/GFP-HDEL, pCambia/mCherry/GFP-HDEL, pCambiaTunosVNN, pCambia/$6K_2$-PAGFP, pCambia/GFP-RdRp; 0.1 for PDLP1-GFP and PDCB1-mCherry for infiltration. For co-expression, 1 :1 mixture of the two AGL1 bacteria containing the plasmids of interest was used for infiltration. Infiltrated plants were kept for 3-7 days post-agroinfiltration (dpa) in a growth chamber until observation. For FM4-64 staining, small pieces of *N. benthamiana* leaves were cut and dipped in 1 µg/µl of FM4-64 (Molecular Probes). Leaves were incubated at room temperature for 40-45 minutes and observed by confocal laser microscopy.

Confocal microscopy

Agroinfiltrated leaf sections were mounted on a depression microscope slide, aligning the leaf tissue in the well. The cells were observed using a 10× objective, 40×, and/or 63× oil immersion objective on a LSM-780 confocal microscope (Zeiss). For LSM-780 microscope experiments, argon and HeNe lasers were used. Data from both green and red channels were collected at the same time. Photoactivation of GFP was done using ten to fifteen pulses of the 405-nm laser to activate PAGFP so that it produced very bright fluorescence emission that was detected by excitation at 488 nm using a 495- to 540-nm band pass filter. A 25-mW blue diode 405-nm laser was used at high output (50 to 100% transmission) to region in the cytoplasm using the photobleaching function of the Zeiss software in time-lapse mode. After acquisition, images were processed using ImageJ (1.46k) and Carl Zeiss ZEN software. Area quantification of red fluorescence was performed using Image J, and statistically analyzed using GraphPad Prism®.

Stem sections preparation, staining and immunofluorescence labeling

N. benthamiana was agroinfiltrated with pCambiaTunos/$6K_2$:GFP or pCambiaTunos/$6K_2$:mCherry. Systemic infected stems were fixed at 6 day post infiltration. Fixation, cell wall coloration with fluorescent brightener 28, sucrose gradient and cryosectioning were processed as described previously (**66**). For immunofluorescence labeling, slides were pre-treated with Poly-L-lysine solution (Sigma-Aldrich®). Stem cryosections were then dried 2 h, prior to add PBS for 20 min. Then cryosections were incubated for 1 h in a blocking solution (phosphate-buffered saline [PBS], pH 7.4, containing 5% bovine serum albumin [BSA], 0.3% Triton X-100). After this, the cryosections were incubated for 1 h with the mouse anti-dsRNA J2 antibody (1 :300, English & Scientific Consulting Bt.) and washed three times with PBS for 10 min. The labeled cryosections were then incubated for 1 h with Alexa Fluor 568 goat anti-mouse IgG (1 :500, Invitrogen), followed by washing four times with PBS for 10 min. SlowFade Gold (Molecular Probes®) was mounted on the samples, and the covered slices were sealed with nail polish. For membrane staining, slides were pre-treated with Poly-L-lysine solution (Sigma-Aldrich®). Fixation, cell wall coloration with fluorescent brightener 28, sucrose gradient and cryosectioning were done as described above. Stem cryosections were dried 2h, prior to add PBS for 20 min. We theb added 10µM of the lipophilic dye

DioC6(3) (Molecular Probes®) for 30 min at room temperature. We washed the sample 3 times for 10 min with PBS. SlowFade Gold (Molecular Probes®) was mounted on the samples, and the covered slices were sealed with nail polish.

Acknowledgments

We thank Jessy Tremblay for helping with confocal microscopy, A. Maule for PDLP1-GFP, C. Ritzenthaler for PDCB1-mCherry, and J. Runions for CX-PAGFP. We thank Hélène Sanfaçon for critically reading the manuscript. This study was supported by the Natural Sciences and Engineering Research Council of Canada and from Le Fonds de recherche du Québec – Nature et technologies to H.Z. and J.-F.L.

References

1. Epel BL (2009) Plant viruses spread by diffusion on ER-associated movement-protein-rafts through plasmodesmata gated by viral induced host β-1,3-glucanases. Seminars in Cell & Developmental Biology 20(9) :1074-1081.

2. Liu C & Nelson RS (2013) The cell biology of Tobacco mosaic virus replication and movement. Frontiers in Plant Science 4 :12.

3. Tilsner J, Amari K, & Torrance L (2011) Plasmodesmata viewed as specialised membrane adhesion sites. Protoplasma 248(1) :39-60.

4. Harries P & Ding B (2011) Cellular factors in plant virus movement : At the leading edge of macromolecular trafficking in plants. Virology 411(2) :237-243.

5. Schoelz JE, Harries PA, & Nelson RS (2011) Intracellular Transport of Plant Viruses : Finding the Door out of the Cell. Molecular Plant 4(5) :813-831.

6. Niehl A & Heinlein M (2011) Cellular pathways for viral transport through plasmodesmata. Protoplasma 248(1) :75-99.

7. Amari K, Lerich A, Schmitt-Keichinger C, Dolja VV, & Ritzenthaler C (2011) Tubule-guided cell-to-cell movement of a plant virus requires class XI myosin motors. PloS Pathog 7(10) :e1002327.

8. van Lent J, Storms M, van der Meer F, Wellink J, & Goldbach R (1991) Tubular structures involved in movement of cowpea mosaic virus are also formed in infected cowpea protoplasts. Journal of General Virology 72 (Pt 11) :2615-2623.

9. Chen Q, et al. (2012) Tubular structure induced by a plant virus facilitates viral spread in its vector insect. PloS Pathog 8(11) :e1003032.

10. Pouwels J, et al. (2003) Identification of distinct steps during tubule formation by the movement protein of Cowpea mosaic virus. Journal of General Virology 84(Pt 12) :3485-3494.

11. Kawakami S, Watanabe Y, & Beachy RN (2004) Tobacco mosaic virus infection spreads cell to cell as intact replication complexes. Proc Natl Acad Sci U S A 101(16) :6291-6296.

12. Bamunusinghe D, Seo J-K, & Rao ALN (2011) Subcellular Localization and Rearrangement of Endoplasmic Reticulum by Brome Mosaic Virus Capsid Protein. Journal of Virology 85(6) :2953-2963.

13. Linnik O, Liesche J, Tilsner J, & Oparka KJ (2013) Unraveling the structure of viral replication complexes at super-resolution. Frontiers in Plant Science 4 :6.

14. Cui X, Wei T, Chowda-Reddy RV, Sun G, & Wang A (2010) The Tobacco etch virus P3 protein forms mobile inclusions via the early secretory pathway and traffics along actin microfilaments. Virology 397(1) :56-63.

15. Welsch S, et al. (2009) Composition and Three-Dimensional Architecture of the Dengue Virus Replication and Assembly Sites. Cell Host & Microbe 5(4) :365-375.

16. Wei T & Wang A (2008) Biogenesis of cytoplasmic membranous vesicles for plant potyvirus replication occurs at endoplasmic reticulum exit sites in a COPI- and COPII-dependent manner. Journal of Virology 82(24) :12252-12264.

17. Schaad MC, Jensen PE, & Carrington JC (1997) Formation of plant RNA virus replication complexes on membranes : role of an endoplasmic reticulum-targeted viral protein. EMBO Journal 16(13) :4049 – 4059.

18. Patarroyo C, Laliberte JF, & Zheng H (2012) Hijack it, change it : how do plant viruses utilize the host secretory pathway for efficient viral replication and spread? Front Plant Sci 3 :308.

19. Jonczyk M, Pathak KB, Sharma M, & Nagy PD (2007) Exploiting alternative subcellular location for replication : Tombusvirus replication switches to the endoplasmic reticulum in the absence of peroxisomes. Virology 362(2) :320-330.

20. Prod'homme D, Jakubiec A, Tournier V, Drugeon G, & Jupin I (2003) Targeting of the Turnip Yellow Mosaic Virus 66K Replication Protein to the Chloroplast Envelope Is Mediated by the 140K Protein. Journal of Virology 77(17) :9124-9135.

21. Prod'homme D, Le Panse S, Drugeon G, & Jupin I (2001) Detection and Subcellular Localization of the Turnip Yellow Mosaic Virus 66K Replication Protein in Infected Cells. Virology 281(1) :88-101.

22. Hwang Y, McCartney A, Gidda S, & Mullen R (2008) Localization of the Carnation Italian ringspot virus replication protein p36 to the mitochondrial outer membrane is mediated by an internal targeting signal and the TOM complex. BMC Cell Biology 9(1) :54.

23. Kopek BG, Perkins G, Miller DJ, Ellisman MH, & Ahlquist P (2007) Three-Dimensional Analysis of a Viral RNA Replication Complex Reveals a Virus-Induced Mini-Organelle. PloS Biol 5(9) :e220.

24. McCartney AW, Greenwood JS, Fabian MR, White KA, & Mullen RT (2005) Localization of the Tomato Bushy Stunt Virus Replication Protein p33 Reveals a Peroxisome-to-Endoplasmic Reticulum Sorting Pathway. The Plant cell 17(12) :3513-3531.

25. Tilsner J & Oparka KJ (2012) Missing links? — The connection between replication and movement of plant RNA viruses. Current Opinion in Virology 2(6) :705-711.

26. Tilsner J, et al. (2012) The TGB1 movement protein of Potato virus X reorganizes actin and endomembranes into the X-body, a viral replication factory. Plant physiology 158(3) :1359-1370.

27. Grangeon R, et al. (2012) Impact on the Endoplasmic Reticulum and Golgi Apparatus of Turnip Mosaic Virus Infection. Journal of Virology 86(17) :9255-9265.

28. Cotton S, et al. (2009) Turnip mosaic virus RNA replication complex vesicles are mobile, align with microfilaments, and are each derived from a single viral genome. Journal of Virology 83(20) :10460-10471.

29. Bolte S, et al. (2004) FM-dyes as experimental probes for dissecting vesicle trafficking in living plant cells. Journal of Microscopy 214(2) :159-173.

30. Thomas CL, Bayer EM, Ritzenthaler C, Fernandez-Calvino L, & Maule AJ (2008) Specific Targeting of a Plasmodesmal Protein Affecting Cell-to-Cell Communication. PloS Biol 6(1) :e7.

31. Amari K, et al. (2010) A Family of Plasmodesmal Proteins with Receptor-Like Properties for Plant Viral Movement Proteins. PloS Pathog 6(9) :e1001119.

32. Ruthardt N, Gulde N, Spiegel H, Fischer R, & Emans N (2005) Four-dimensional imaging of transvacuolar strand dynamics in tobacco BY-2 cells. Protoplasma 225(3-4) :205-215.

33. Radford JE & White RG (2001) Effects of tissue-preparation-induced callose synthesis on est plasmodesma size exclusion limits. Protoplasma 216(1-2) :47-55.

34. Zambryski P (1995) Plasmodesmata : Plant Channels for Molecules on the Move. Science 270(5244) :1943.

35. Poirson A, et al. (1993) Effect of the alfalfa mosaic virus movement protein expressed in transgenic plants on the permeability of plasmodesmata. Journal of General Virology 74 (Pt 11) :2459-2461.

36. Deom CM, et al. (1990) Molecular characterization and biological function of the movement protein of tobacco mosaic virus in transgenic plants. Proc Natl Acad Sci U S A 87(9) :3284-3288.

37. Wolf S, Deom CM, Beachy RN, & Lucas WJ (1989) Movement protein of tobacco mosaic virus modifies plasmodesmatal size exclusion limit. Science 246(4928) :377-379.

38. Rojas MR, Zerbini FM, Allison RF, Gilbertson RL, & Lucas WJ (1997) Capsid Protein and Helper Component-Proteinase Function as Potyvirus Cell-to-Cell Movement Proteins. Virology 237(2) :283-295.

39. Lewis JD & Lazarowitz SG (2010) Arabidopsis synaptotagmin SYTA regulates endocytosis and virus movement protein cell-to-cell transport. Proc Natl Acad Sci U S A 107(6) :2491-2496.

40. Runions J, Brach T, Kuhner S, & Hawes C (2006) Photoactivation of GFP reveals protein dynamics within the endoplasmic reticulum membrane. Journal of Experimental Biology 57(1) :43-50.

41. Pena EJ & Heinlein M (2012) RNA transport during TMV cell-to-cell movement. Front Plant Sci 3 :193.

42. Jiang J & Laliberté J-F (2011) The genome-linked protein VPg of plant viruses; a protein with many partners. Current Opinion in Virology 1(5) :347-354.

43. Wei T, et al. (2010) Sequential recruitment of the endoplasmic reticulum and chloroplasts for plant potyvirus replication. Journal of Virology 84(2) :799-809.

44. Ala-Poikela M, Goytia E, Haikonen T, Rajamaki ML, & Valkonen JP (2011) Helper component proteinase of the genus Potyvirus is an interaction partner of translation initiation factors eIF(iso)4^E and eIF4E and contains a 4^E binding motif. Journal of Virology 85(13) :6784-6794.

45. Reisen D, Marty F, & Leborgne-Castel N (2005) New insights into the tonoplast architecture of plant vacuoles and vacuolar dynamics during osmotic stress. BMC Plant Biology 5 :13.

46. Wei T, et al. (2010) Formation of Complexes at Plasmodesmata for Potyvirus Intercellular Movement Is Mediated by the Viral Protein P3N-PIPO. PloS Pathog 6(6) :e1000962.

47. Vijayapalani P, Maeshima M, Nagasaki-Takekuchi N, & Miller WA (2012) Interaction of the trans-frame potyvirus protein P3N-PIPO with host protein PcaP1 facilitates potyvirus movement. PloS Pathog 8(4) :e1002639.

48. Drakakaki G & Dandekar A (2013) Protein secretion : how many secretory routes does a plant cell have? Plant Science 203-204 :74-78.

49. Opalka N, et al. (2000) Structure of native and expanded sobemoviruses by electron cryo-microscopy and image reconstruction. Journal of Molecular Biology 303(2) :197-211.

50. Opalka N, et al. (1998) Movement of rice yellow mottle virus between xylem cells through pit membranes. Proc Natl Acad Sci USA 95(6) :3323-3328.

51. Dubois F, Sangwan RS, & Sangwan-Norreel BS (1994) Spread of beet necrotic yellow vein virus in infected seedlings and plants of sugar beet (Beta vulgaris). Protoplasma 179(1-2) :72-82.

52. Fribourg CE, Koenig R, & Lesemann DE (1987) A new tobamovirus from Passiflora edulis in Peru. Phytopathology 77(3) :486-491.

53. Khan JA, Lohuis H, Goldbach RW, & Dijkstra J (1994) Distribution and localization of bean common mosaic virus and bean black root virus in stems of doubly infected bean plants. Archives of Virology 138(1-2) :95-104.

54. Robertson NL & C TW (1989) Electron microscopy of the novel barley yellow streak mosaic virus. Journal of Ultrastructure and Molecular Structure Research 102(2) :139-146.

55. Moreno IM, Thompson JR, & García-Arenal F (2004) Analysis of the systemic colonization of cucumber plants by Cucumber green mottle mosaic virus. Journal of General Virology 85(3) :749-759.

56. Ding XS, Boydston CM, & Nelson RS (2001) Presence of Brome mosaic virus in Barley Guttation Fluid and Its Association with Localized Cell Death Response. Phytopathology 91(5) :440-448.

57. French CJ & Elder M (1999) Virus particles in guttate and xylem of infected cucumber (Cucumis sativus L.). Annals of Applied Biology 134(1) :81-87.

58. Brunt AA & Atkey PT (1974) Membrane-associated particle aggregates in extracts of plant : infected with some viruses of the potato Y group. Annals of Applied Biology 78(3) :339-341.

59. Bamunusinghe D, et al. (2009) Analysis of potato virus X replicase and TGBp3 subcellular locations. Virology 393(2) :272-285.

60. Carette JE, Stuiver M, Van Lent J, Wellink J, & Van Kammen A (2000) Cowpea mosaic virus infection induces a massive proliferation of endoplasmic reticulum but not Golgi membranes and is dependent on de novo membrane synthesis. J Virol 74(14) :6556-6563.

61. Lee WM & Ahlquist P (2003) Membrane synthesis, specific lipid requirements, and localized lipid composition changes associated with a positive-strand RNA virus RNA replication protein. J Virol 77(23) :12819-12828.

62. Ritzenthaler C, et al. (2002) Grapevine fanleaf virus replication occurs on endoplasmic reticulum-derived membranes. J Virol 76(17) :8808-8819.

63. Dufresne PJ, et al. (2008) Heat shock 70 protein interaction with Turnip mosaic virus RNA-dependent RNA polymerase within virus-induced membrane vesicles. Virology 374(1) :217-227.

64. Beauchemin C & Laliberte JF (2007) The poly(A) binding protein is internalized in virus-induced vesicles or redistributed to the nucleolus during turnip mosaic virus infection. Journal of Virology 81(20) :10905-10913.

65. Sánchez F, Martínez-Herrera D, Aguilar I, & Ponz F (1998) Infectivity of turnip mosaic potyvirus cDNA clones and transcripts on the systemic host Arabidopsis thaliana and local lesion hosts. Virus Research 55(2) :207-219.

66. Elisabeth Knapp RF, David Scheiblin, Shannon Modla, Kirk Czymmek, and Vidadi Yusibov (2012) A cryohistological protocol for preparation of large plant tissue sections for screening intracellular fluorescent protein expression. BioTechniques Vol. 52(No. 1) :31–37.

Figure Legends

Figure 1: $6K_2$-induced vesicles use transvacuolar strands to reach the plasma membrane and dock at plasmodesmata. (A) Confocal images of *N. benthamiana* leaves infected by pCambiaTunos/$6K_2$:GFP and stained with FM4-64 for plasma membrane labeling. Arrows indicate presence of $6K_2$ vesicles in adjacent apparently non-infected cell. (B) Confocal images of *N. benthamiana* leaves infected with TuMV producing $6K_2$:mCherry-tagged expressing PDLP1-GFP, with bright-field illumination. Arrows indicate the positioning of PDLP1-GFP and one $6K_2$ vesicle on a transvacuolar strand. (C) Confocal images of *N. benthamiana* leaves infected with TuMV producing $6K_2$:GFP-tagged vesicles expressing PDCB1mCherry. Arrow indicates docking of a $6K_2$ vesicle on either side of a PDCB1:mCherry-labelled PD.

Figure 2: TuMV infection leads to an increase of PD size exclusion limit. (A) Schematic representation of the pCambia/mCherry/GFP-HDEL and pCambia/$6K_2$:mCherry/GFP-HDEL. Confocal images of leaves expressing pCambia/mCherry/GFP-HDEL in healthy (B) or TuMV-infected (C) *N. benthamiana* plant. Confocal images of leaves expressing pCambia/$6K_2$:mCherry/GFP-HDEL in healthy (D) or TuMV-infected (E) *N. benthamiana* plant. Areas of protein movement are indicated by the white dotted line. All images in this figure have been taken using the "tile" function of the LSM 780 confocal microscope. (F) Area of movement has been quantified for 15 *N. benthamiana* epidermal samples expressing the indicated proteins. Statistical differences are indicated by brackets and asterisks as follows: **, 0.001 < P value < 0.01 (very significant); ***, P value < 0.001 (extremely significant).

Figure 3: TuMV-induced $6K_2$-tagged vesicles move intercellularly. (A) Time series images of a photoactivated cell infected with TuMV producing $6K_2$:mcherry-tagged vesicles and expressing $6K_2$:PAGFP. Top left panel shows cell prior to photoactivation, and top right panel shows cell after activation with a 405-nm laser by 10 to 15 iterations using the bleach mode of the LSM 780 confocal microscope (Zeiss). Green line indicates activation area. The following panels show position of an activated $6K_2$:PAGFP vesicle (arrow) at the indicated time. In the 52 s panel, vesicle is not seen as fluorescence is quenched during transit in PD (see Movie S2). (B) Cell infected with TuMV producing $6K_2$:mcherry-tagged vesicles and expressing $6K_2$:PAGFP that was photoactivated 2 h before. Green line indicates activation area. White arrows point to vesicles that have moved through one cell layer. Red arrow points to a vesicle that has moved through two cell layers.

Figure 4: The viral RNA-dependent RNA polymerase is found within cortical motile $6K_2$ vesicles. Confocal images of leaf epidermal cells of *N. benthamiana* showing RdRp:GFP (A and D) in TuMV-infected cells producing $6K_2$:mCherry-tagged vesicles (B and E) and merged data (C and F). A, B, C are three-dimensional renderings of >30 1-µm-thick slices that overlap by 0.5 µm. D, E, F are single images with bright-field illumination. Arrowheads indicate a TVS and arrows show a $6K_2$-induced vesicle containing RdRp close to the plasma membrane.

Figure 5: $6K_2$:GFP aggregates are found in xylem vessels of TuMV infected plants. (A) Longitudinal cross-section of a *N. benthamiana* stem infected with TuMV producing $6K_2$:GFP vesicle viewed using the 20X objectives of the LSM 680 confocal microscope. (B) is an higher magnification of (A) using the 63X objective focusing on a xylem vessel. (C) Infected xylem containing $6K_2$:GFP aggregate (left panel) is immunostained for dsRNA using monoclonal antibody J0 (middle panel). Right panel is a merge version. (D) Infected xylem containing $6K_2$:mCherry aggregates (left panel) stained with the membrane dye DiOC6(3) (middle panel). Right panel is a merge version. Cell wall was stained with Fluorescent Brightener 28 and shown in magenta. Ep=Epidermal cell; Pi= Pith cells; C=Cortex; T=Trichome; X=Xylem cell.

Figure 6: Model to describe the process of intercellular and systemic spread by the TuMV. See Discussion section for description.

Movie S1: Times lapse experiment of *N. benthamiana* leaves infected with TuMV producing $6K_2$:mCherry-tagged vesicles and expressing PDLP1-GFP, with bright-field illumination. PDLP1:GFP and one 6K2 vesicle can be seen trafficking on a transvacuolar strand. Images were acquired every 4 seconds using the 40X of the LSM 680 confocal microscope.

Movie S2: Time lapse images of a photoactivated cell infected with TuMV producing $6K_2$:mcherry-tagged vesicles and expressing $6K_2$:PAGFP. Green line indicates activation area. Blue line depicts tracking of a single $6K_2$:PAGFP vesicle. Images were acquired every 3 seconds using the 40X of the LSM 680 confocal microscope.

Movie S3: 3D rendering of $6K_2$:GFP aggregates found in a xylem vessel of a TuMV infected plant. Cell wall was stained using Brightener 28 (magenta), and images were acquired using the 63X of the LSM 680 confocal microscope.

Figures

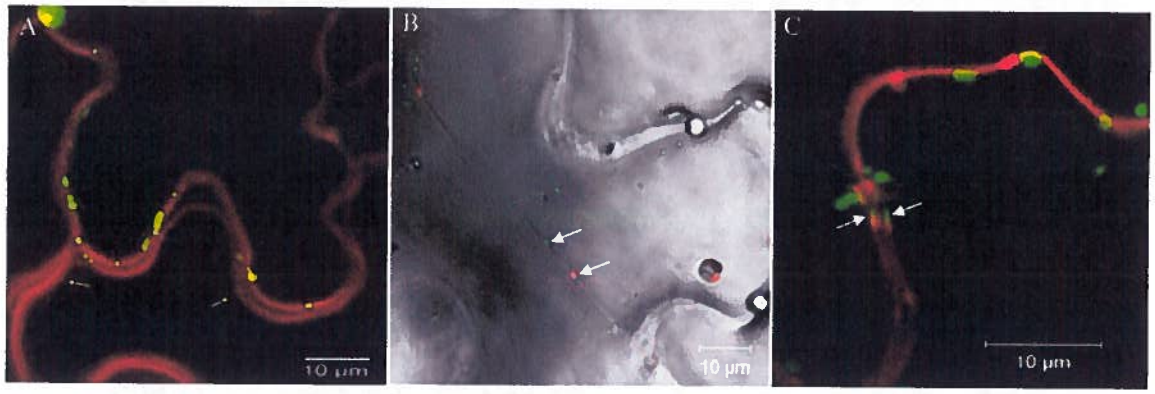

Figure 1: $6K_2$-induced vesicles use transvacuolar strands to reach the plasma membrane and dock at plasmodesmata.

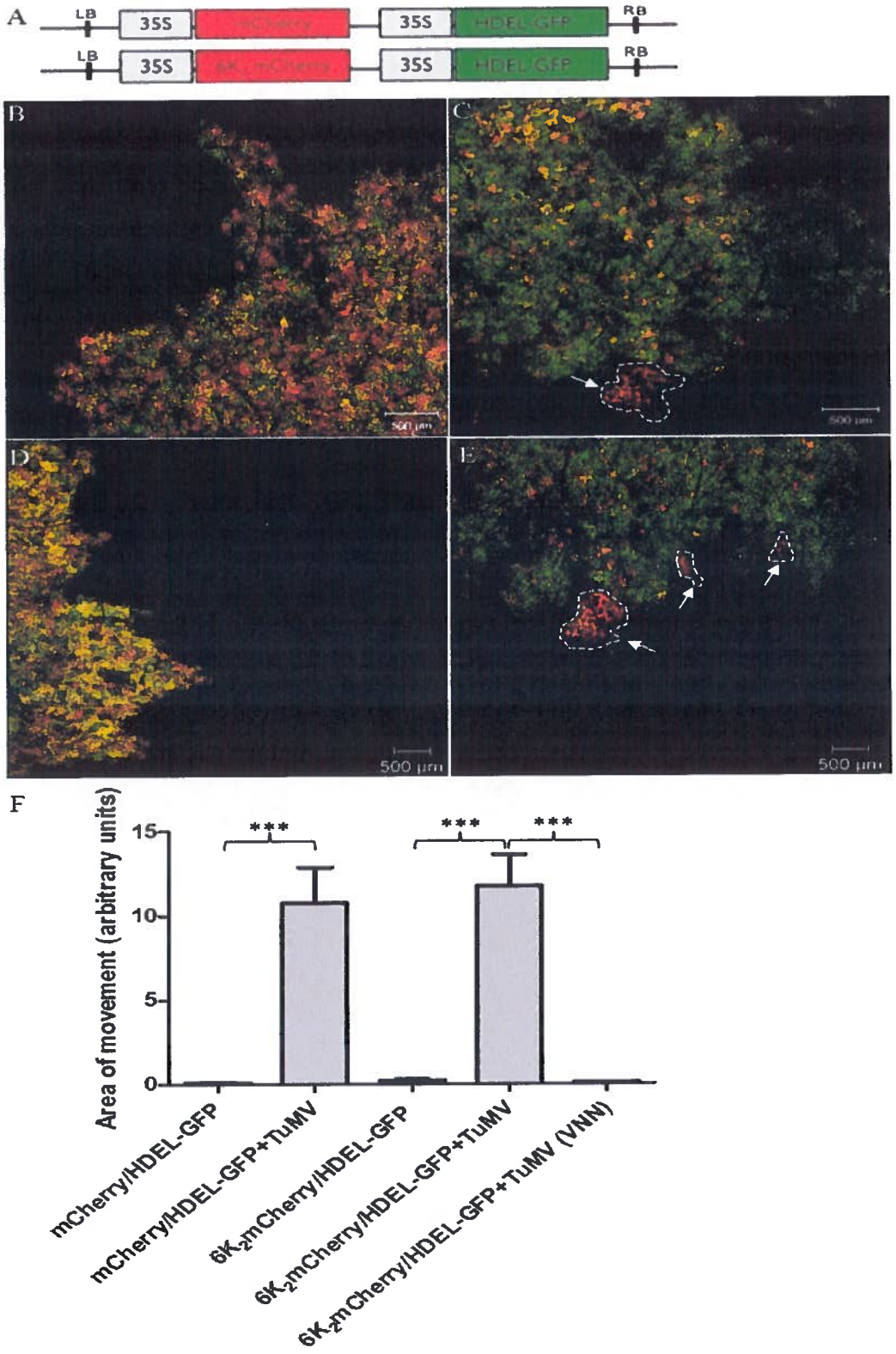

Figure 2: TuMV infection leads to an increase of PD size exclusion limit.

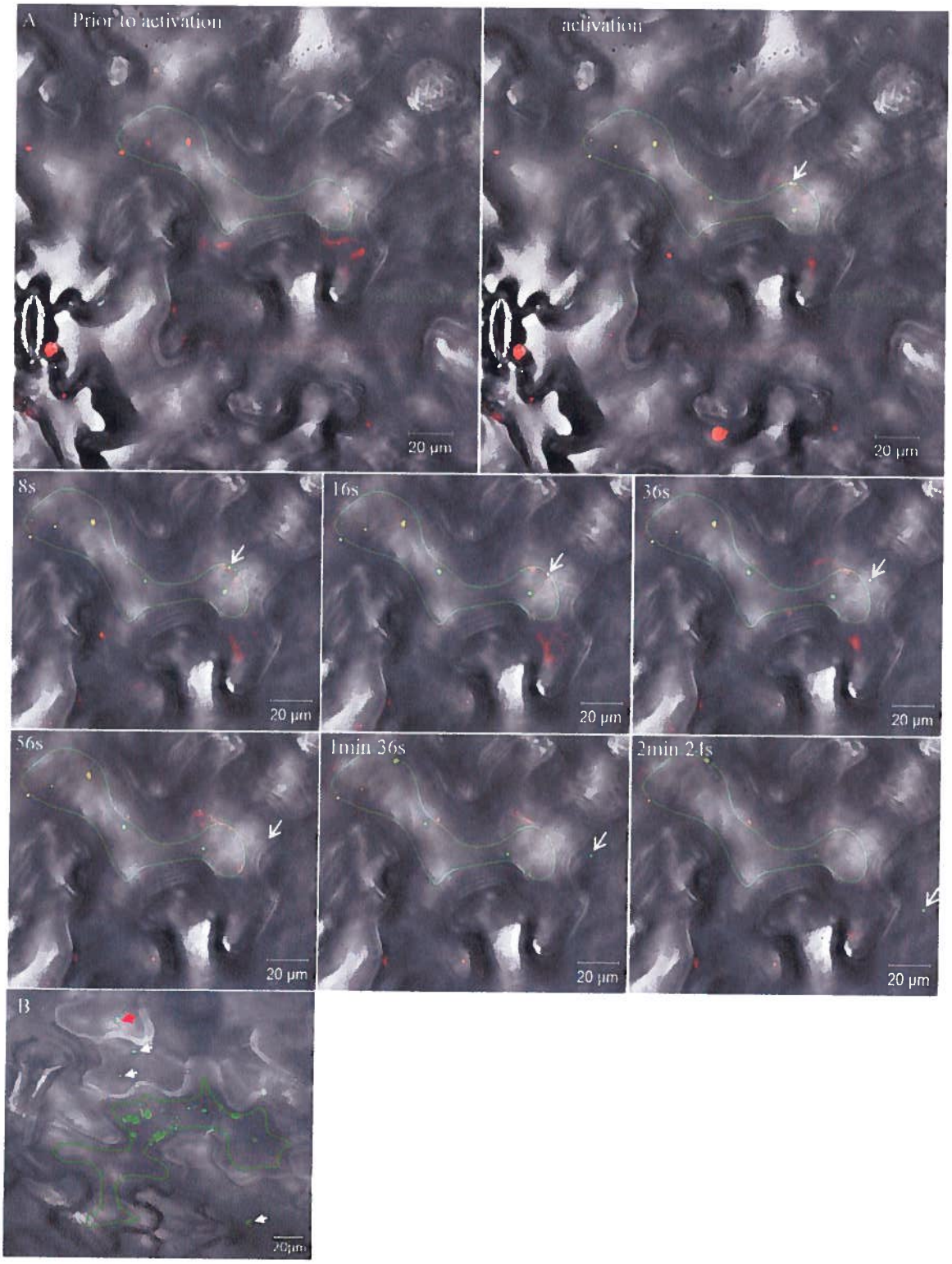

Figure 3: TuMV-induced 6K$_2$-tagged vesicles move intercellularly.

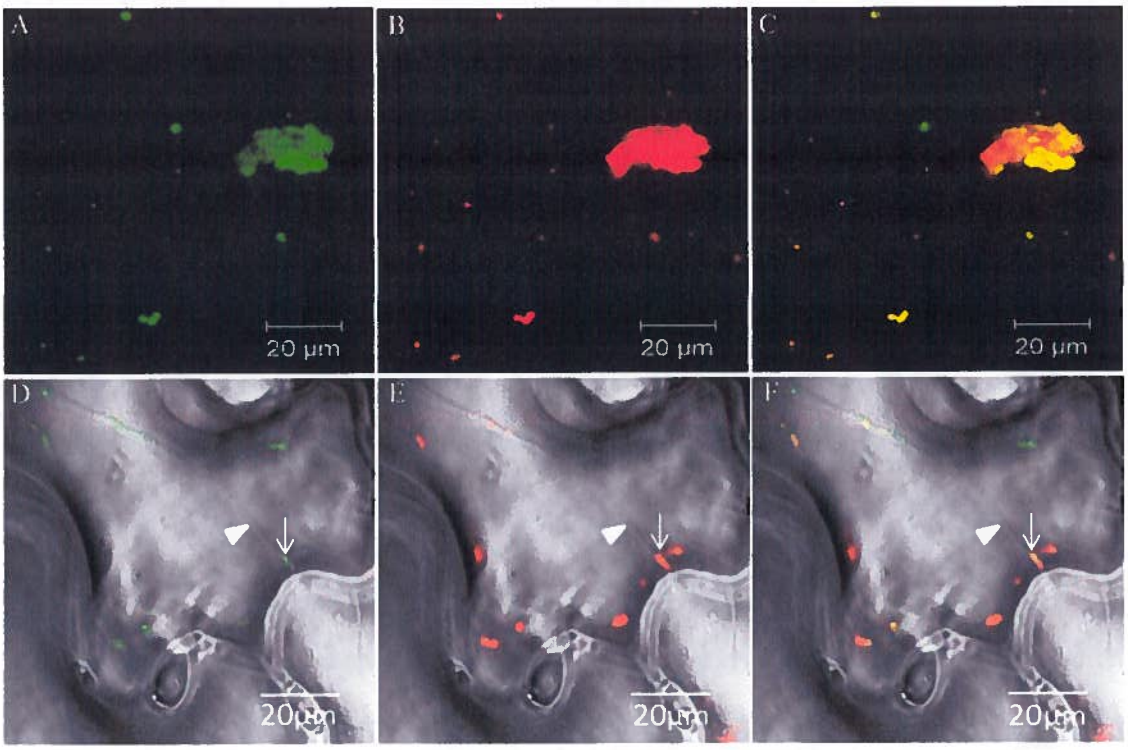

Figure 4: The viral RNA-dependent RNA polymerase is found within cortical motile $6K_2$ vesicles.

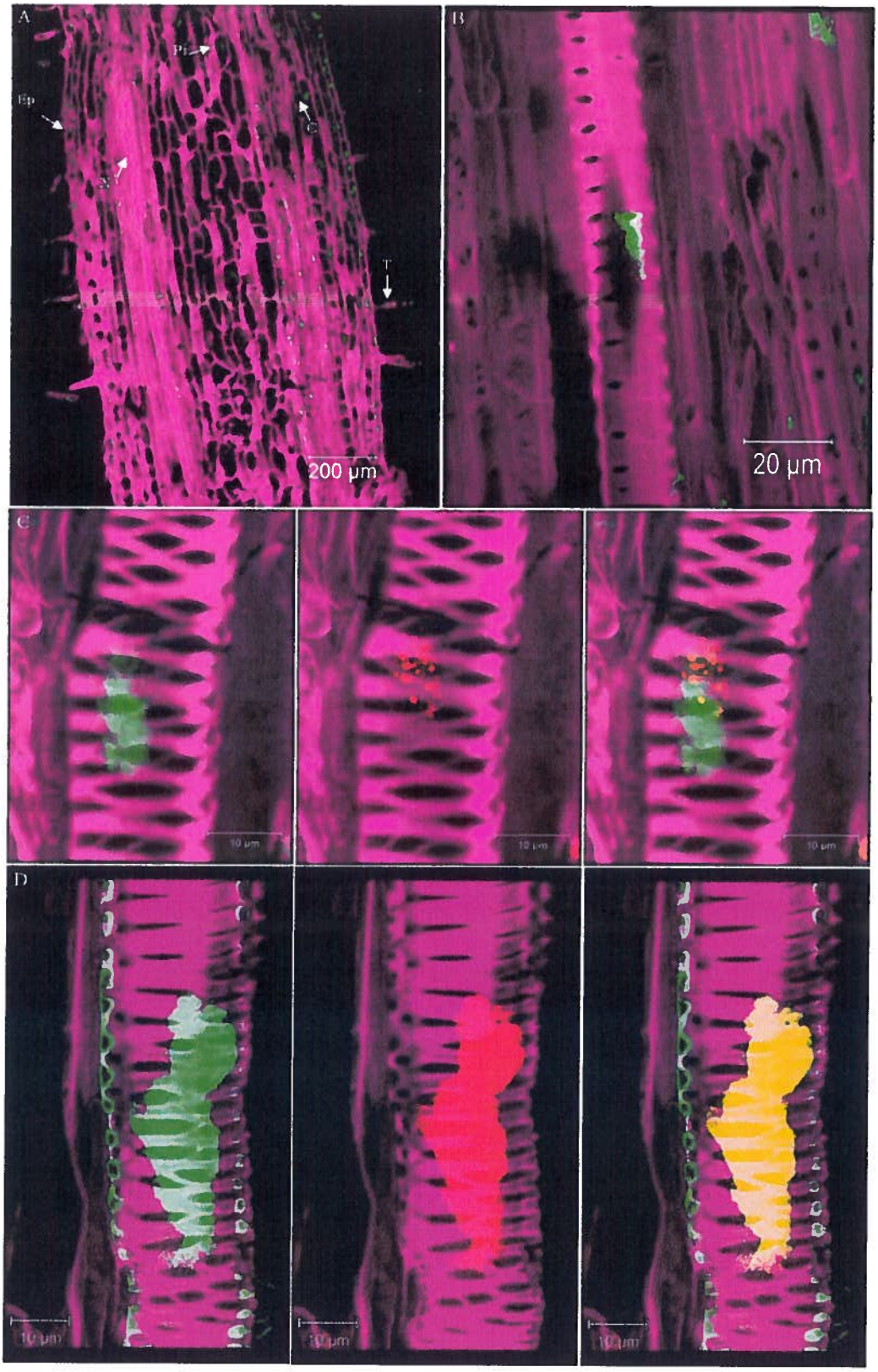

Figure 5: $6K_2$:GFP aggregates are found in xylem vessels of TuMV infected plants.

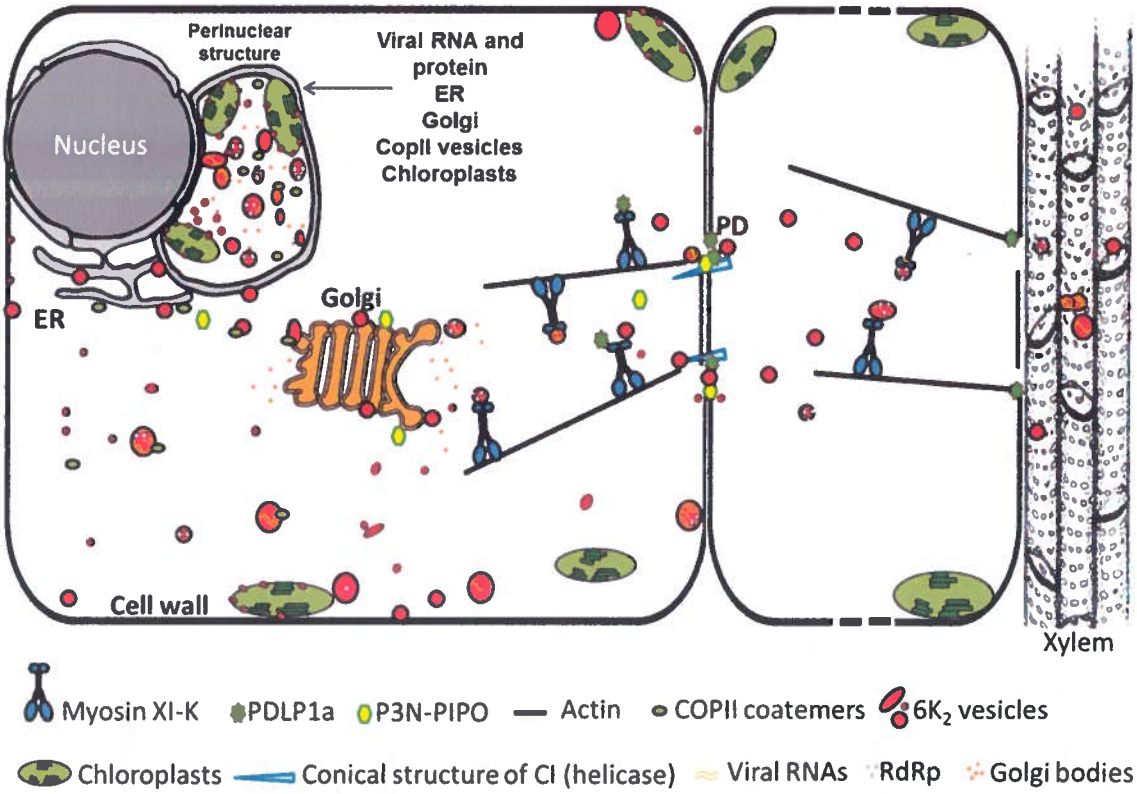

Figure 6: Model to describe the process of intercellular and systemic spread by the TuMV.

Publication n°4

Contribution of host intracellular transport machineries to intercellular movement of Turnip mosaic virus

En préparation de re-soumission

Maxime Agbeci[1*], Romain Grangeon[1*], Rick S. Nelson[2], Huanquan Zheng[3] and Jean-François Laliberté[1*]

*These authors contributed equally to this work

[1] INRS-Institut Armand-Frappier, 531 Boulevard des Prairies Laval, Québec H7V 1B7, Canada

[2] Plant Biology Division, Samuel Roberts Noble Foundation, Inc., Ardmore, OK 73401, USA

[3] Department of Biology, McGill University, 1205 Dr. Penfield Avenue, Montréal, Québec, H3A 1B1, Canada

Author for correspondence: Jean-François Laliberté

Email: jean-francois.laliberte@iaf.inrs.ca

Contribution

Cet article a été soumis une première fois dans "PLOS pathogen", et a été rejeté. Les relecteurs de cet article ont soulevé un certain nombre de questions et de nouvelles expériences ont été exigées. Notamment il nous a été demandé de démontrer que notre système d'expression du TuMV par agroinfiltration, ne ralentit pas la vitesse de migration du virus. J'ai réalisé les expériences demandées et nous avons re-soumis cet article, toujours dans "PLOS pathogen". Cette fois il a été accepté avec modifications mineures. Je suis co-auteur de cet article, car bien que c'est principalement les résultats du projet de maîtrise de Maxime Agbecci, j'ai supervisé ces travaux en participant à l'acquisition des images de microscopie confocale de toutes les figures, j'ai fait intégralement la figure 1 ainsi que les nouvelles expériences exigées qui ne figurent pas dans cette version du papier. J'ai aussi réalisé toutes les modifications de texte demandées par les relecteurs et requises pour son acceptation. J'ai mis au point une méthode en microscopie confocale qui permet d'observer le mouvement du TuMV sur plusieurs jours, et ainsi déterminer la vitesse de migration du TuMV, qui infecte une cellule environ toutes les 3h. La vitesse de migration obtenue est dans le même ordre de grandeur que ce que d'autres équipes ont obtenu avec d'autres virus de plantes.

Résumé

La contribution des différents mécanismes de transport de la cellule hôte dans le mouvement intercellulaire du virus de la mosaïque du navet (TuMV) a été étudiée. Pour discriminer entre les cellules infectées par agroinfiltration et les cellules dont l'infection résulte d'un mouvement du virus, une cassette exprimant la protéine GFP-HDEL a été insérée dans le plasmide contenant la cassette du clone infectieux du TuMV exprimant $6K_2$-mCherry. Lors de l'agroinfiltration, les deux cassettes de gènes sont délivrées à la même cellule, les cellules primo-infectées émettent à la fois de la fluorescence verte et rouge tandis que les cellules par le mouvement du virus sont seulement rouges. Le mouvement intercellulaire a été suivi pendant 17 heures consécutives. Nous avons calculé que le virus infecte une nouvelle cellule toute les 3h en moyenne. Pour déterminer si la voie de sécrétion est importante pour le mouvement intercellulaire du TuMV, des inhibiteurs et des

mutants dominants négatifs qui bloquent la voie de sécrétion précoce et tardive ont été utilisés. Le traitement à la Brefeldin A, à la concanamycine A ainsi que l'expression des mutants dominants négatifs d'ARF1 et RAB-E1D ne perturbe pas la réplication virale, mais réduit significativement le mouvement du TuMV. Les traitements à la Tyrphostin A23 et à la Wortmannin, des inhibiteurs de l'endocytose, n'ont pas d'effet sur le mouvement intercellulaire du TuMV. Ce résultat a été confirmé par une absence de colocalisation entre les vésicules marquées par $6K_2$ et le colorant de la membrane plasmique FM4-64, ou le marqueur des endosomes Ara7 (AtRabF2b). Un traitement avec un agent de dépolymérisation des microfilaments bloque également le mouvement intercellulaire du TuMV. Finalement des expériences d'inactivation de gène induite par un virus a montré (VIGS) que le mouvement du virus dépend des myosines de la classe XI-2, et non pas de celles de la classe VIII.

Summary

The contribution of different transport machineries of the host cell in the intercellular movement of *Turnip mosaic virus* (TuMV) was investigated. To discriminate between primary infected from secondary infected cells associated with viral intercellular movement, a gene cassette expressing GFP-HDEL was inserted adjacent to a TuMV infectious cassette expressing $6K_2$-mCherry, both within the T-DNA borders of the binary vector pCambia. Since both gene cassettes were delivered to the same cell, primary infection foci emitted both green and red fluorescence while secondary infected cells emitted red-only fluorescence. Intercellular movement was followed for 17 consecutive hours. Sustained intercellular movement was observed at a rate of one cell being infected every 3 hours. To determine if the secretory pathway was important for TuMV intercellular movement, chemical and protein inhibitors that block both early and late secretory pathways were used. Treatment with Brefeldin A or Concanamycin A and expression of ARF1 or RAB-E1d dominant negative mutants reduced cell-to-cell movement of the virus but did not hamper virus replication in primary infected cells. A pharmacological interference assay using Tyrphostin A23 and Wortmannin showed that endocytosis in TuMV intercellular movement was not important. Lack of co-localization with the FM4-64 and Ara7 (AtRabF2b) and TuMV-induced $6K_2$-tagged vesicles further indicated that these endocytic pathways were not important for TuMV local cellular

spread. Microfilament depolymerising drugs also blocked intercellular movement of TuMV. Interestingly, virus-induced gene silencing showed that movement relied on myosin XI-2, but not on myosin VIIIs.

Authors's summary

Plant viruses move from the initially infected cell to neighboring cells during local movement and then over long distances through vascular tissues to establish a systemic infection in the plant. Transport between cells involves moving a viral RNA-protein complex through plasmodesmata (Pds) that requires viral and host factors. Virus intercellular movement is normally assessed by assays that cannot always differentiate between reduced viral RNA replication and intercellular movement. By using a dual gene cassette construct encoding fluorescent proteins that can differentiate between primary infected cells from cells infected after intercellular transport, we provide evidence that turnip mosaic virus (TuMV) needs a functional secretory pathway where post-Golgi traffic and the actinomyosin network are involved. Interestingly, disruption of the host transport machinery had no impact on TuMV accumulation in initially infected cells. These results support the idea that virus replication activities can be influenced separately from those involved in other virus activities such as movement, although aspects of both are likely coordinated.

Introduction

Plant viruses move from the initially infected cell to neighboring cells for local movement and then over long distances through vascular tissues to establish a systemic infection in the plant. Transport of viruses between cells first involves the intracellular movement of the viral RNA from the site of replication to plasmodesmata (Pds) and then its delivery into neighboring cells through Pds. Pds are tunnels in the cell wall that connect the cytoplasm, the endoplasmic reticulum (ER) and the plasma membrane between adjoining cells (reviewed in [1]). The normal size exclusion limit (SEL) of Pd is too small to allow passive transport of large molecular complexes, but plant viruses encode movement proteins (MPs) that increase the SEL of PDs to allow passage of the viral RNA (reviewed in [2,3]). Intracellular movement involves a membrane-associated viral RNA-protein complex involving MPs but the exact configuration of the viral entity that enters the neighboring cells has not yet been extensively studied. In the case of

tobacco mosaic virus (TMV), the viral RNA spreads intercellularly as membrane MP-associated viral replication complexes (VRCs) [4]. For some icosahedral viruses, viral particles transit through MP-induced tubules that go through PDs for their delivery into non-infected cells [5-8].

Although MPs are at the core of viral RNA intra- and intercellular movement, it is clear that host factors are required. The cytoskeleton is an essential component of organelle trafficking in plant cells (reviewed in [9]) and it has been shown to be involved in vertebrate virus intracellular movement (reviewed in [10]). In the case of TMV, several studies have shown that microtubules and microfilaments are necessary to anchor and release, or propel the movement of the VRC within the ER (reviewed in [2,11,12]). Involvement of microfilaments in MP or virus movement has also been shown for other plant viruses [13-18]. Myosin motors are also required for MP or viral trafficking [5,19-22]. The secretory pathway is involved in intra- and intercellular trafficking for several viruses [14,15,18,19,23,24]. Finally, recent studies suggest that the endocytic transport pathway may also be involved in viral movement [25,26].

However, not all viruses or MPs use the cytoskeleton or the secretory pathway for movement. For example, Pd targeting of the tubule-forming MP of cowpea mosaic virus (CPMV) is not affected by the disruption of either protein transport between the ER and Golgi or the cytoskeleton [27]. Similarly, the targeting of the triple gene block protein 3 (TGBp3) of poa semilatent virus to Pd does not require a functional cytoskeleton or the secretory pathway [28].

The genome of potyviruses is a single ~10 kb RNA molecule that codes for a polyprotein that is processed into 10 mature proteins. In addition to polyprotein-derived polypeptides, a ~7 kDa protein termed PIPO is produced in infected cells [29] and is also found as a trans-frame protein consisting of the amino-terminal half of P3 fused to PIPO (P3N-PIPO) [30]. Potyviruses have no designated MP but many viral proteins have been reported to have MP-related functions. For instance, HCPro and CP can increase PD SEL [31]. In addition, the coat protein (CP) and cylindrical inclusion (CI) protein are required for intercellular movement [32-34] and are associated with Pd [35,36]. Recently, the targeting of CI to Pd was shown to be mediated by P3N-PIPO [37], which itself is targeted to the plasma membrane through an interaction with the host protein PCaP1 [30]. One last protein to be involved in viral movement is the 6 kDa membrane-

associated $6K_2$ protein. It induces the production of motile vesicles that contain viral RNA [38] and are the likely vehicle for intracellular trafficking of potyviral RNA. This suggests that the potyviral genome is transported to Pds and into non-infected cells by a complex of several viral proteins. However, contribution of cellular processes on potyviral movement during infection still needs to be addressed.

In this study, by using a dual gene cassette construct that can differentiate between primary infected cells from cells infected after intercellular virus movement, we provided in vivo quantitative evidence that TuMV requires both early and late secretory pathways to move from one cell to another. We also investigated the role of microfilament myosin motor proteins for TuMV intercellular movement and determined that class XI but not VIII myosins were required for this activity. Although these cellular components are required for intercellular movement, they do not appear to be involved in virus protein production in primary infected cells.

Results

An in vivo quantitative assay for TuMV intercellular movement

A recombinant tobacco etch virus (TEV) (genus Potyvirus) was previously engineered to express the reporter protein ß-glucuronidase for direct observation of viral spread in leaves [32]. Viral spread is a function of the rate of viral RNA replication and of the speed of intercellular movement. Reduction of viral spread under experimental conditions may thus be the consequence of reduced viral RNA replication or inhibition of viral intercellular movement, or both. Hence, the use of the above viral system is limited since it cannot ascertain if a given treatment affected viral replication or intercellular movement. In order to discriminate primary infected from secondary infected cells and thus differentiate virus intercellular movement from viral RNA replication, we introduced a gene cassette encoding the ER-localized GFP-HDEL under the control of the cauliflower mosaic virus (CaMV) 35S promoter adjacent to a TuMV infectious cassette expressing $6K_2$:mCherry, both flanked by the T-DNA borders in the binary vector pCambia (**Fig. 1A**) [39]. Since both gene cassettes are delivered to the same cells and GFP-HDEL does not move between cells [26], primary infected cells should display concomitant green and red fluorescence while secondary infected cells should display red-only fluorescence.

A single inoculation with an A. tumefaciens suspension containing the above plasmid was performed on three-week old *N. benthamiana* leaves, resulting in an agroinfiltrated area of 5-10 mm in diameter (**Fig. 1B**). Movement was then assayed by observing protein fluorescence at the perimeter of the infiltrated area by confocal microscopy. Fluorescence emitted by GFP-HDEL was generally observed at approximately 36 hrs post infiltration (hpi) and mCherry fluorescence resulting from TuMV replication was detected at approximately 60 hpi. Systemic TuMV infection was observed at 4-5 days post infiltration (dpi). A similar outcome was obtained when more dilute agrobacterium suspensions (e.g. 0.01-0.001) were infiltrated. *N. benthamiana* cells displayed the expected green polygonal ER pattern and virus-induced $6K_2$-tagged red vesicles (**Fig. 1C**). At 60 hpi, all cells that emitted green fluorescence also showed red fluorescence and no red-only cells were observed (**Fig. 1D**), indicating that viral movement had not yet begun. Intercellular movement was followed by observing the progression of red fluorescence over 17 consecutive hours. This was achieved by putting a TuMV-infected leaf at the 72 hpi stage still attached to the plant under the confocal microscope objective. Images were taken every hour throughout the observation period. When the perimeter of the agroinfiltrated area was initially pictured, intercellular movement was already under progression as indicated by the presence of red-only fluorescent patches (**Fig. 1E**). At the end of the observation period, the surface area of GFP-HDEL fluorescence did not change, indicating that this marker did not diffused into neighboring cells. On the other hand, red-only fluorescence, indicative of TuMV secondary infection, had spread an average distance of 311 µm in the xy plane (**Fig. 1F**). Movie S1 shows the sustained progression of the infection front. We calculated that there is on average 17.6 epidermal cells per linear mm in the xy plane. Using this parameter, we estimated that new cells were infected on average every 3.0 hrs, within the range calculated for TEV [**32**]. This TuMV rate of infection is also very close to the cell infection rate of TMV, which was estimated to be 3.5 hrs [4]. This experiment was repeated five times and similar results were obtained. The increase in red fluorescence surface area was not due to the diffusion of $6K_2$:mCherry from agroinfected cells because replacement of the TuMV gene cassette by the cDNA encoding $6K_2$:mCherry in the above plasmid did not produce red-only fluorescent foci (**Fig. S1A**). These experiments then indicate that the use of the above double-gene cassette is valid to follow intercellular movement of TuMV.

Intercellular movement of TuMV requires both the early and late secretory pathways

Chemical and protein inhibitors were used to evaluate the role of the early and late secretory pathway in the intercellular movement of TuMV. The plant secretory pathway consists of the nuclear envelope, the ER, the Golgi apparatus, various post-Golgi intermediate compartments, the vacuoles/lysosomes and the small vesicular transport carriers that shuttle between these compartments. The early secretory pathway embraces the ER–Golgi interface while the Golgi apparatus and the various post-Golgi organelles that control plasma membrane or vacuolar sorting is categorized as the late secretory pathway (reviewed in [40]).

Brefeldin A (BFA) is an inhibitor that interferes with protein transport in the ER-Golgi interface [41]. Concanamycin A (CMA) inhibits protein transport around the trans-Golgi network (TGN) [42] by inhibiting the function of TGN-localized proton-ATPases, which leads to the acidification of the TGN lumen [43]. *N. benthamiana* leaves were treated with DMSO, 10 µg/mL BFA or 0.5 µM CMA 4h before pCambiaTunos/6K_2:mCherry/GFP-HDEL agroinfiltration. **Fig. S1B** shows that BFA at this concentration is effective at blocking the secretory pathway. At 4 dpi, confocal observation showed that DMSO had no inhibitory effect on TuMV movement (**Fig. 2A**). On the other hand, BFA and CMA treatment reduced cell-to-cell movement (**Fig. 2B-C**). The surface area for mCherry-only expressing foci from twenty leaf samples for each treatment was measured and the analysis confirmed the inhibitory effect of BFA and CMA on TuMV intercellular movement (**Fig. 2D**). To assess whether or not BFA and CMA inhibited the replication of TuMV that might influence the intercellular movement of the virus, we quantified mCherry fluorescence intensity over GFP fluorescence intensity in primary infection foci for all treatments. **Fig. 2E** shows that that there was no significant difference in the ratio of red over green fluorescence for all tested conditions at 4 dpi, indicating that viral protein production in the primary infected cells was not affected by the drug treatments. The level of green fluorescence with DMSO was similar to the level of fluorescence in the BFA- and CMA-treated primary cells, indicating that production of GFP was not affected by the treatments (data not shown).

Protein inhibitors were used to confirm the role of the secretory pathway in TuMV intercellular transport. The ADP-ribosylation factor 1 (ARF1) is a small GTPase regulating the recruitment of COPI coatomer proteins. A dominant negative mutant of

ARF1 [ARF1(NI)] impaired in GTP/GDP binding has been shown to affect the transport of soluble markers from the ER to Golgi, and cause a re-absorbance of Golgi membrane proteins into the ER [44]. RAB-E1d is a small Rab GTPase acting at a post-Golgi trafficking pathway and the dominant negative mutant RAB-E1d(NI) inhibits trafficking from the Golgi apparatus to the plasma membrane [45]. These two dominant-negative mutants were co-expressed with pCambiaTunos/6K_2:mCherry/GFP-HDEL. Four days post-agroinfiltration, confocal observation of red-only foci showed that the two mutant proteins reduced intercellular movement of TuMV (Fig. 3B-C). Surface area measurements for mCherry-only expressing patches from twenty leaf samples for each treatment confirmed the inhibitory effect of both ARF1(NI) and RAB-E1d(NI) on TuMV intercellular movement (Fig. 3D). On the other hand, expression of these two mutant proteins did not hamper virus protein production in primary infected cells as measured by red over green fluorescence ratios in the dual expressing regions of the infected leaves (Fig. 3E). We therefore conclude that inhibition of both early and late secretory pathways blocks TuMV intercellular movement but does not affect viral replication in primary infected cells. The last assertion is in line with the prior observation that BFA treatment did not affect the production of TuMV-induced 6K_2-tagged perinuclear structures and peripheral vesicles [39].

Cell-to-cell transport of TuMV is independent of the endocytic pathway

We examined if endocytosis was involved in TuMV intercellular movement. To this end, we first used a pharmacological interference assay with Tyrphostin A23, Tyrphostin A51 and Wortmannin. In mammalian cells, Tyrphostin A23 inhibits the recruitment of endocytic cargo into clathrin-coated vesicles formed at the plasma membrane by preventing the interaction between the clathrin-binding AP-2 adaptor complex μ2 subunit and the sorting motif within the cytoplasmic domain of plasma membrane proteins [46]. Tyrphostin A51 is a structural analog of Tyrphostin A23 but has no inhibitory effect and is routinely used as negative control [46]. Tyrphostin A23 also works in plant cells [47] and it has been shown that the drug inhibits endocytosis of some plasma membrane proteins [48]. Wortmannin is a phosphatidylinositol 3-kinase inhibitor that inhibits in mammalian cells receptor sorting and/or vesicle budding required for delivery of endocytosed material to "mixing" endosomes [49]. In plant cells, it has been shown that the drug inhibits endocytosis of FM4-64 (an amphiphilic styryl dye used to monitor endocytosis) [50] and morphogenesis of MVB/PVCs [47,51] but it does not

affect protein transport from the TGN to the plasma membrane [52,53]. *N. benthamiana* leaves were infiltrated either with Tyrphostin A23, Tyrphostin A51, Wortmannin or DMSO 4 hrs prior to agroinfiltration with A. tumefaciens Agl1 containing pCambiaTunos/$6K_2$:mCherry/GFP-HDEL. The drug concentrations used have been shown to block endocytotic pathway in plants [47,51] and inhibition of endocytosis of FM4-64 in the presence of Wortmannin was confirmed in our system (Fig. S1C). Four days after agroinfiltration, TuMV movement was examined by confocal microscopy. Fig. 4B-D shows TuMV propagation in the presence of the different drugs and none of the inhibitors affected the intercellular movement of the virus. Surface area measurements for mCherry-only expressing patches from twenty leaf samples for each treatment confirmed the lack of inhibitory effect of the different drugs on TuMV intercellular movement (Fig. 4E). These data then show that the endocytic pathway is not involved in TuMV intercellular movement.

We also investigated the association of TuMV-induced $6K_2$-tagged vesicles with Ara7 (AtRAB-F2b) and FM4-64. Intracellular trafficking of $6K_2$-tagged vesicles has been shown to be dependent on the secretory pathway and microfilaments [38,39,54] and these $6K_2$ vesicles have been shown to transit through Pds to move into neighboring cells (Grangeon et al., submitted). Ara7 is a Ras-related protein similar to Rab5 and Rab22 of mammals and to Ypt51/Ypt52/Ypt53 in yeast, and marks prevacuolar compartments and is involved in endocytic and vacuolar trafficking in plant cells [55,56]. Co-expression of Ara7 and pCambiaTunos/$6K_2$:mCherry in *N. benthamiana* leaves cells shows that there was no colocalization between Ara7 motile dots and $6K_2$-tagged vesicles (Fig. 5A). Moreover, a 40-min dipping of *N. benthamiana* leaves in FM4-64 at concentration of 1µg/µl allowed the internalization of the dye into endocytic vesicles from the plasma membrane but $6K_2$-tagged vesicles were never associated with FM4-64-labeled vesicles (Fig. 5B). Lack of co-localization of FM4-64 and Ara7 with TuMV-induced $6K_2$-tagged vesicles further indicates that these endocytic pathways are not important for TuMV cellular spread.

Intercellular movement of TuMV depends on myosin XI motors

Many viruses and individual virus proteins require the actomyosin system for their intracellular and/or intercellular movement [13,14,16-18,57]. However, a recent study showed that RNA viruses might have evolved differently in their requirements for actin and the associated myosin motors [20]. We first tested the effect of latrunculin B (LatB),

and cytochalasin D (CytD), which inhibit maintenance of microfilaments [58], on the intercellular spread of TuMV. Leaves were infiltrated with 5 μM LatB, 10 μM CytD, or DMSO 4 h before agroinfection. The disruption of actin by LatB or CytD was confirmed by confocal microscopy observation of microfilaments labeled with the actin-binding domain 2 of A. thaliana fimbrin fused to GFP (GFP-ABD2-GFP) [59] (Fig. S1D). TuMV intercellular movement was assessed by imaging *N. benthamiana* leaves 4 days post agroinfiltration with pCambiaTunos/$6K_2$:mCherry/GFP-HDEL. Inhibition of TuMV intercellular movement was observed with LatB and CytD (Fig. 6B-C). Surface area for mCherry-only expressing foci for 15 leaf samples were quantified and the data indicated greater spread for leaves treated with DMSO compared with those treated with LatB and CytD (Fig. 6D). The ratio of red to green fluorescence in dual expressing cells was unchanged between treatments indicating that virus replication was unaffected by these microfilament antagonists (Fig. 6E). These results indicate that an intact microfilament network was important for TuMV intercellular movement, but not for replication. The last assertion is in line with the prior observation that LatB treatment did not affect the production of TuMV-induced $6K_2$-tagged perinuclear structures and peripheral vesicles [38].

It was previously shown that overexpression of the myosin XI-K tail, a dominant negative mutant of this myosin species, inhibited the intracellular trafficking of TuMV $6K_2$ vesicles and reduced TuMV infection [60], indicating the involvement of this class of myosin in viral movement. We were also interested to see if other myosin classes could be involved. A series of Arabidopsis thaliana knockout lines for several myosins have been characterized. Single knockout mutants did not display developmental defect [62], which is likely the result of functional redundancy within myosin XIs that compensates the absence of any one of them since multiple knockout mutants showed stunted growth and delayed flowering [63]. Studies investigating the role of myosin in virus movement have used dominant-negative mutants [5,21,60]. Tobacco rattle virus-mediated virus-induced silencing (TRV-VIGS) was also adopted to determine the role of myosins on intercellular movement of TMV, potato virus X (PVX), tomato bushy stunt virus, and turnip vein-clearing virus [20]. One advantage in using TRV-VIGS is that it allows one to assay the consequence on a given event following the transiently knocking down of target genes. We thus used TRV-VIGS to silence individual myosin genes prior to TuMV infection. *N. benthamiana* leaves were first infected with TRV constructs and 15 days

later upper leaves were infiltrated with agrobacterium strain containing pCambiaTunos/6K_2:mCherry/GFP-HDEL. TuMV intercellular movement was quantified 5 days post infiltration. Quantitative RT-PCR confirmed that the transcriptional level of the target myosin genes was decreased in plants infected by the TRV silencing construct containing the corresponding genes (**Fig. 7A**). We then monitored TuMV intercellular movement by measuring the areas of foci expressing mCherry-only (n=10). Quantification indicated that there was no significant difference in TuMV intercellular movement in mock- and TRV-infected plants (**Fig. 7B**). Virus movement was not affected in myosin VIII-1 and VIII-2-silenced plants. However, silencing of myosin XI-2 reduced TuMV intercellular movement by a factor of 10 compared to the control. Slightly reduced TuMV movement was observed in myosin XI-F silenced plants, but was not found to be statistically significant. To be sure this effect on virus movement was specific to myosin XI-2 silencing, we analyzed the effect of silencing myosin XI-2 on the other myosins (**Fig. 7C**). Silencing myosin XI-2 had no significant effect on the transcript level of the other tested myosins. Results presented here indicate that myosin XI-2 is required for intercellular movement of TuMV, but not XI-F, VIII-1 and VIII-2.

Discussion

Studies on intercellular movement have shown that plant viruses may use different trafficking pathways to move from one cell to another (reviewed in [**2,12**]). In this study, by discriminating agroinfiltrated primary-infected cells from cells infected by intercellular virus movement, we were able to evaluate the contribution of the secretory pathway and the cytoskeleton for TuMV intercellular movement.

The first sign of infection was observed at around 60 hpi using the dual gene cassette construct described in this study (**Fig. 1**). This is the time frame normally observed when agroinfection is used [**63-65**]. Intercellular movement was noticed at approximately 72 hpi and an average rate of one cell infected every 3.0 hrs was calculated. This infection rate is very close to what has been estimated for TMV (3.5 hrs) [**4**]. TuMV intercellular movement cumulated in a systemic infection of the plant at 4-5 dpi. Viral replication is usually observed after 24 hrs and systemic infection 3 days later following leaf inoculation with a virus suspension [**32**]. The delay noted with agroinfection may be explained by the fact that a T-DNA copy of the viral RNA genome is delivered in

the cell. This T-DNA molecule needs to be transported to the nucleus and transcribed into RNA, which is then transported back in the cytoplasm. In the case of potyviruses, there is an additional delay because the RNA transcribed from the T-DNA is not linked to VPg. There is consequently a first round of translation that needs to take place before bona fide infection begins. However, past this initial delay, TuMV intercellular movement and systemic infection proceeded at the same rate as with infection using a virus inoculum. This indicates that the infiltrated agrobacterium did not cause a defense response by the plant, which might have affected the normal spread of TuMV. Consequently, the use of the dual cassette construct is a valid tool to study viral intercellular movement.

It was previously shown that intracellular motility of individual potyviral proteins was dependent on the early secretory pathway [15,37,54,60]. In present study, we show that in addition to the early secretory pathway, a post-Golgi component was involved for TuMV intercellular movement (Fig. 2-3). However, the endocytic pathway did not appear to be required (Fig. 4-5). In addition to ER, COPI and COPII coatamers, the Golgi apparatus has been shown to be recruited into virus factories [14,66,67] but the role of late secretory pathway in plant viral movement has not yet been investigated. We think that it is required for sorting the membrane-associated viral RNA-protein complex to Pds. Although ESCRT (endosomal sorting complexes required for transport) proteins, which have a major role in the sorting of cargo proteins, are recruited for tomato bushy stunt virus replication [68,69], it is not yet known if they have any involvement in virus movement.

Intercellular movement of TuMV was also depended on microfilaments (Fig. 6) and myosin motors (Fig. 7). In plant cells, myosins are classified into class VIII or class XI [70]. Among the four myosins tested in this study, myosin XI-2 was the principal driver for TuMV transport between the cells but not myosin VIIIs. Previously, myosin XI-K was shown to be involved in the intracellular movement of 6K2 vesicles [60]. Class XI myosins are then involved in TuMV movement, which is also the case for TMV [20] and GFLV [5]. Interestingly, although a cytoskeletal-dependent trafficking of a viral RNA-protein complex to PD is necessary for TMV, the related turnip vein clearing virus does not rely on this system [20]. On the other hand, class VIII myosins are required for Pd localization of a closterovirus Hsp70 homolog [21]. This suggests that more than one myosin-dependent mechanism of virus movement exist in plants. Interesting, not all

potyviral proteins that are targeted to Pd use the actinomyosin system. For instance, this system is not required for delivery of P3N-PIPO and CI to Pd [37]. Host proteins can also use different routes to reach Pds. Targeting of the Plasmodesmata Located Protein 1 (PDLP1) to Pd requires both the ER-Golgi secretory pathway and the actomyosin motility system [71] while the targeting of the plasmodesmata callose binding 1 (PDCB1) protein was shown not to depend on myosin motors [5]. Perhaps, P3N-PIPO and CI need to be targeted to Pd prior to the myosin-dependent moving viral RNA-protein complex comes into the vicinity of Pd in order to receive and anchor the complex to this organelle.

Disruption on the secretory pathway had no impact on TuMV accumulation in the initially infected cells. We showed previously that BFA treatment had no effect on the formation of TuMV-induced $6K_2$-tagged structures, although motile $6K_2$ vesicles showed a higher incidence of localizing with the COPII marker Sec24 [39]. Similarly, disruption of the early secretory trafficking by BFA did not modify the accumulation of melon necrotic spot virus (MNSV) but inhibited intercellular virus movement [14]. Coronavirus-induced remodeling of the ER and viral replication, albeit reduced, equally took place in the presence of BFA [72]. Breakdown of actin filaments also did not affect the formation of $6K_2$-tagged vesicles [38]. These results suggest that replication activities, despite their requirement for membranes, are influenced separately from those involved in movement, although aspects of both are likely coordinated [73].

In conclusion, we show in this study that the secretory pathway and the actinomyosin system are both important for the intercellular movement of TuMV. These host components are likely required by the virus to aid its movement out of the initially infected cell. Further work is necessary to identify host proteins within the secretory pathway and the actomyosin network that interact with the virus proteins and influence virus movement.

Materials and Methods

Fluorescent proteins and molecular clones

TuMV infectious clone pCambiaTunos/$6K_2$:mCherry was as described [38,74]. ARA7/RabF2b was as described [56]. The introduction of the 35S-GFP-HDEL gene

cassette into pCambiaTunos/6K_2:mCherry was completed as follows: pBIN/20-ER-gk [75] was digested with AseI and ligated with similarly digested pCambiaTunos/6KmCherry. Kanamycin-resistant Escherichia coli colonies were screened for pCambiaTunos/6K_2:mCherry/GFP-HDEL.

Protein expression in plants

Transient expression studies were performed by agroinfiltration on three-week-old *N. benthamiana* plants. Plasmids were introduced by electroporation into Agrobacterium tumefaciens AGL1 and selected on LB ampicillin-kanamycin plates. The pellet of an overnight culture was gently suspended in water supplemented with 10 mM MgCl2 and 150 µM acetosyringone and left at room temperature for 3 h. The solution was then diluted to an OD600 of 0.6 for pCambiaTunos/6KmCherry/GFP-HDEL; 0.1 for pARF1(Ni), pRAB-E1d(NI) and pYFP-RAB-F2b ; 1.5 for PTRV1 and PTRV2. For co-expression, 1:1 mixture of the two AGL1 bacteria containing the plasmids of interest were agroinfiltrated. Plants were kept for 3-5 days post-agroinfiltration (dpa) in a growth chamber until observation.

FM4-64 staining

Small pieces of *N. benthamiana* leaves were cut and dipped in 1 µg/µl of FM4-64 (Molecular Probes). Leaves were incubated at room temperature for 40-45 minutes and observed by confocal laser microscopy.

Inhibitor treatment

Stock solutions of latrunculin B (LatB: 2.5 mM Calbiochem) and cytochalasin D (CytD; 20 mM Calbiochem) were prepared in dimethyl sulfoxide (DMSO) and diluted to the desired concentration in water prior to their infiltration into 3-week-old *N. benthamiana* leaves. The final concentration of Brefeldin A (BFA), CMA, Tyrphostin A23, Tyrphostin A51 and Wortmannin were 10 µg/ml, 0.5 µM, 30 µM, 30 µM, and 20 µM, respectively. *N. benthamiana* leaves were agroinfiltrated with the inhibitors 4 hours before pCambiaTunos/6K_2:mCherry/GFP-HDEL agroinfiltration. The leaves were observed by confocal microscopy after a 96-hour incubation period.

VIGS and Quantitative RT-PCR

pTRV2 with myosin fragments was as described [20]. Virus-induced gene silencing (VIGS) studies were conducted as described previously [76,77]. vTRV infections were established in *N. benthamiana* by co-agroinfiltration of pTRV1 and

pTRV2. To confirm silencing of specific myosin transcripts, RNA was isolated from 20 day-old TRV-infected systemic leaves (two plants/construct) using the RNeasy plant mini kit (Qiagen). DNase-treated RNA (4 µg) was used to generate cDNA with iScript™cDNA Synthesis Kit. After a 15-fold dilution of the cDNA, 2 µL of solution was used for quantitative RT-PCR through a Rotor Gene 3000 real-time DNA detection system (Corbett Research). The following primers were used to detect

N. benthamiana myosins: VIII-1: 5'-GCCCGAGAGAGCAATGGA-3'and 5'-CCTCAGCTAATCGGCTTATAACACT-3'; VIII-2: 5'-ACTCCTATTGAATTTGCCAGCAA-3' and 5'-CTGCACATAAACTGCCATTATTCC-3'; XI-2: 5'-CAACTCCTACCCGCAAACCA-3' and 5'-TCCCATTGTCATTCTCCCAAA-3'; XI-F: 5'-GCACAGGGTTTTCGCTCAA-3' and 5'-CCCTCAATTCCGCTGTATCC-3'. Transcript levels were adjusted for loading differences after comparison with Actin-Binding Domain 2(ABD2) transcript internal control values and were calculated using the Delta-Delta CT METHOD. *N. benthamiana* leaves (x number of leaves above the original TRV-inoculated leaf(ves) were agroinfiltrated with pCambiaTunos/6KmCherry/GFP-HDEL 16 days after TRV infection. The leaves were observed 4 days later by confocal microscopy.

Confocal microscopy

Agroinfiltrated leaf sections were mounted on a depression microscope slide, aligning the leaf tissue in the well. Cells were observed using a 10X objective, 20X, 40X and 63X oil immersion objective on a LSM 510 Metaconfocal microscope (Zeiss) or on a LSM 780 Metaconfocal microscope (Zeiss). For LSM 510 Metaconfocal microscope experiments, argon and HeNe lasers were used to excite fluorescent proteins and for a LSM 780 Metaconfocal multiline argon and DPSS 561 were used. Data from both green and red channels were collected at the same time.

After acquisition, images were processed using Metamorph and/or ImageJ to quantify the average intensity of fluorescence, Carl Zeiss LSM Image Browser, and/or Adobe Photoshop software for post-capture imaging processes.

Statistical analyses

Graphpad Prism One-way analysis of variance (1 way ANOVA) was used to assess the overall statistical differences between the means of different groups. Following 1 way ANOVA, Tukey's Multiple Comparison Test was also used to assess

whether the mean of two particular groups were different from each other. P value summary ($P < 0.05$) shows statistically significant differences between different treatments.

Acknowledgments

We thank M. Desrosiers, J. Tremblay and J. Lacoste for helping with confocal microscopy. This study was supported by the Natural Sciences and Engineering Research Council of Canada and from Le Fonds de recherche du Québec – Nature et technologies to HZ and JFL.

References

1. Maule AJ, Benitez-Alfonso Y, Faulkner C (2011) Plasmodesmata - membrane tunnels with attitude. Curr Opin Plant Biol 14: 683-690.

2. Niehl A, Heinlein M (2011) Cellular pathways for viral transport through plasmodesmata. Protoplasma 248: 75-99.

3. Benitez-Alfonso Y, Faulkner C, Ritzenthaler C, Maule AJ (2010) Plasmodesmata: gateways to local and systemic virus infection. Mol Plant Microbe Interact 23: 1403-1412.

4. Kawakami S, Watanabe Y, Beachy RN (2004) Tobacco mosaic virus infection spreads cell to cell as intact replication complexes. Proc Natl Acad Sci U S A 101: 6291-6296.

5. Amari K, Lerich A, Schmitt-Keichinger C, Dolja VV, Ritzenthaler C (2011) Tubule-guided cell-to-cell movement of a plant virus requires class XI myosin motors. PLoS Pathog 7: e1002327.

6. Chen Q, Chen H, Mao Q, Liu Q, Shimizu T, et al. (2012) Tubular structure induced by a plant virus facilitates viral spread in its vector insect. PLoS Pathog 8: e1003032.

7. Pouwels J, Kornet N, van Bers N, Guighelaar T, van Lent J, et al. (2003) Identification of distinct steps during tubule formation by the movement protein of Cowpea mosaic virus. J Gen Virol 84: 3485-3494.

8. Vanlent J, Storms M, Vandermeer F, Wellink J, Goldbach R (1991) Tubular Structures Involved in Movement of Cowpea Mosaic-Virus Are Also Formed in Infected Cowpea Protoplasts. Journal of General Virology 72: 2615-2623.

9. Wada M, Suetsugu N (2004) Plant organelle positioning. Curr Opin Plant Biol 7: 626-631.

10. Taylor MP, Koyuncu OO, Enquist LW (2011) Subversion of the actin cytoskeleton during viral infection. Nat Rev Microbiol 9: 427-439.

11. Pena EJ, Heinlein M (2012) RNA transport during TMV cell-to-cell movement. Front Plant Sci 3: 193.

12. Schoelz JE, Harries PA, Nelson RS (2011) Intracellular Transport of Plant Viruses: Finding the Door out of the Cell. Molecular Plant 4: 813-831.

13. Xu Y, Zhou X (2012) Role of Rice Stripe Virus NSvc4 in Cell-to-Cell Movement and Symptom Development in Nicotiana benthamiana. Front Plant Sci 3: 269.

14. Genoves A, Navarro JA, Pallas V (2010) The Intra- and intercellular movement of Melon necrotic spot virus (MNSV) depends on an active secretory pathway. Mol Plant Microbe Interact 23: 263-272.

15. Cui X, Wei T, Chowda-Reddy RV, Sun G, Wang A (2010) The Tobacco etch virus P3 protein forms mobile inclusions via the early secretory pathway and traffics along actin microfilaments. Virology 397: 56-63.

16. Harries PA, Palanichelvam K, Yu W, Schoelz JE, Nelson RS (2009) The cauliflower mosaic virus protein P6 forms motile inclusions that traffic along actin microfilaments and stabilize microtubules. Plant Physiol 149: 1005-1016.

17. Prokhnevsky AI, Peremyslov VV, Dolja VV (2005) Actin cytoskeleton is involved in targeting of a viral Hsp70 homolog to the cell periphery. J Virol 79: 14421-14428.

18. Laporte C, Vetter G, Loudes AM, Robinson DG, Hillmer S, et al. (2003) Involvement of the secretory pathway and the cytoskeleton in intracellular targeting and tubule assembly of Grapevine fanleaf virus movement protein in tobacco BY-2 cells. Plant Cell 15: 2058-2075.

19. Yuan Z, Chen H, Chen Q, Omura T, Xie L, et al. (2011) The early secretory pathway and an actin-myosin VIII motility system are required for plasmodesmatal localization of the NSvc4 protein of Rice stripe virus. Virus Res 159: 62-68.

20. Harries PA, Park JW, Sasaki N, Ballard KD, Maule AJ, et al. (2009) Differing requirements for actin and myosin by plant viruses for sustained intercellular movement. Proc Natl Acad Sci U S A 106: 17594-17599.

21. Avisar D, Prokhnevsky AI, Dolja VV (2008) Class VIII myosins are required for plasmodesmatal localization of a closterovirus Hsp70 homolog. J Virol 82: 2836-2843.

22. Wei T, Shimizu T, Omura T (2008) Endomembranes and myosin mediate assembly into tubules of Pns10 of Rice dwarf virus and intercellular spreading of the virus in cultured insect vector cells. Virology 372: 349-356.

23. Vogel F, Hofius D, Sonnewald U (2007) Intracellular trafficking of Potato leafroll virus movement protein in transgenic Arabidopsis. Traffic 8: 1205-1214.

24. Andika IB, Zheng S, Tan Z, Sun L, Kondo H, et al. (2013) Endoplasmic reticulum export and vesicle formation of the movement protein of Chinese wheat mosaic virus are regulated by two transmembrane domains and depend on the secretory pathway. Virology 435: 493-503.

25. Haupt S, Cowan GH, Ziegler A, Roberts AG, Oparka KJ, et al. (2005) Two plant-viral movement proteins traffic in the endocytic recycling pathway. Plant Cell 17: 164-181.

26. Lewis JD, Lazarowitz SG (2010) Arabidopsis synaptotagmin SYTA regulates endocytosis and virus movement protein cell-to-cell transport. Proc Natl Acad Sci U S A 107: 2491-2496.

27. Pouwels J, Van Der Krogt GN, Van Lent J, Bisseling T, Wellink J (2002) The cytoskeleton and the secretory pathway are not involved in targeting the cowpea mosaic virus movement protein to the cell periphery. Virology 297: 48-56.

28. Schepetilnikov MV, Solovyev AG, Gorshkova EN, Schiemann J, Prokhnevsky AI, et al. (2008) Intracellular targeting of a hordeiviral membrane-spanning movement protein: sequence requirements and involvement of an unconventional mechanism. J Virol 82: 1284-1293.

29. Chung BY, Miller WA, Atkins JF, Firth AE (2008) An overlapping essential gene in the Potyviridae. Proc Natl Acad Sci U S A 105: 5897-5902.

30. Vijayapalani P, Maeshima M, Nagasaki-Takekuchi N, Miller WA (2012) Interaction of the trans-frame potyvirus protein P3N-PIPO with host protein PCaP1 facilitates potyvirus movement. Plos Pathogens 8: e1002639.

31. Rojas MR, Zerbini FM, Allison RF, Gilbertson RL, Lucas WJ (1997) Capsid Protein and Helper Component-Proteinase Function as Potyvirus Cell-to-Cell Movement Proteins. Virology 237: 283-295.

32. Dolja VV, Haldeman R, Robertson NL, Dougherty WG, Carrington JC (1994) Distinct functions of capsid protein in assembly and movement of tobacco etch potyvirus in plants. Embo Journal 13: 1482-1491.

33. Dolja VV, Haldeman-Cahill R, Montgomery AE, Vandenbosch KA, Carrington JC (1995) Capsid protein determinants involved in cell-to-cell and long distance movement of tobacco etch potyvirus. Virology 206: 1007-1016.

34. Carrington JC, Jensen PE, Schaad MC (1998) Genetic evidence for an essential role for potyvirus CI protein in cell-to-cell movement. Plant J 14: 393-400.

35. Rodriguez-Cerezo E, Findlay K, Shaw JG, Lomonossoff GP, Qiu SG, et al. (1997) The coat and cylindrical inclusion proteins of a potyvirus are associated with connections between plant cells. Virology 236: 296-306.

36. Roberts IM, Wang D, Findlay K, Maule AJ (1998) Ultrastructural and temporal observations of the potyvirus cylindrical inclusions (CIs) show that the CI protein acts transiently in aiding virus movement. Virology 245: 173-181.

37. Wei T, Zhang C, Hong J, Xiong R, Kasschau KD, et al. (2010) Formation of Complexes at Plasmodesmata for Potyvirus Intercellular Movement Is Mediated by the Viral Protein P3N-PIPO. PLoS Pathog 6: e1000962.

38. Cotton S, Grangeon R, Thivierge K, Mathieu I, Ide C, et al. (2009) Turnip mosaic virus RNA replication complex vesicles are mobile, align with microfilaments, and are each derived from a single viral genome. J Virol 83: 10460-10471.

39. Grangeon R, Agbeci M, Chen J, Grondin G, Zheng HQ, et al. (2012) Impact on the Endoplasmic Reticulum and Golgi Apparatus of Turnip Mosaic Virus Infection. J Virol 86: 9255-9265.

40. Patarroyo C, Laliberté J-F, Zheng H (2013) Hijack it, Change it: How do Plant Viruses Utilize the Host Secretory Pathway for Efficient Viral Replication and Spread? Front Plant Sci 3.

41. Tse YC, Lam SK, Jiang L (2007) Enigmatic brefeldin a. Plant Signal Behav 2: 199-202.

42. Gendre D, Oh J, Boutte Y, Best JG, Samuels L, et al. (2011) Conserved Arabidopsis ECHIDNA protein mediates trans-Golgi-network trafficking and cell elongation. Proc Natl Acad Sci U S A 108: 8048-8053.

43. Dettmer J, Hong-Hermesdorf A, Stierhof YD, Schumacher K (2006) Vacuolar H+-ATPase activity is required for endocytic and secretory trafficking in Arabidopsis. Plant Cell 18: 715-730.

44. Stefano G, Renna L, Chatre L, Hanton SL, Moreau P, et al. (2006) In tobacco leaf epidermal cells, the integrity of protein export from the endoplasmic reticulum and of ER export sites depends on active COPI machinery. Plant J 46: 95-110.

45. Zheng H, Camacho L, Wee E, Batoko H, Legen J, et al. (2005) A Rab-E GTPase mutant acts downstream of the Rab-D subclass in biosynthetic membrane traffic to the plasma membrane in tobacco leaf epidermis. Plant Cell 17: 2020-2036.

46. Banbury DN, Oakley JD, Sessions RB, Banting G (2003) Tyrphostin A23 Inhibits Internalization of the Transferrin Receptor by Perturbing the Interaction between

Tyrosine Motifs and the Medium Chain Subunit of the AP-2 Adaptor Complex. Journal of Biological Chemistry 278: 12022-12028.

47. Aniento F, Robinson DG (2005) Testing for endocytosis in plants. Protoplasma 226: 3-11.

48. Boutte Y, Frescatada-Rosa M, Men S, Chow CM, Ebine K, et al. (2010) Endocytosis restricts Arabidopsis KNOLLE syntaxin to the cell division plane during late cytokinesis. EMBO J 29: 546-558.

49. Spiro DJ, Boll W, Kirchhausen T, Wessling-Resnick M (1996) Wortmannin alters the transferrin receptor endocytic pathway in vivo and in vitro. Molecular Biology of the Cell 7: 355-367.

50. Bolte S, Talbot C, Boutte Y, Catrice O, Read ND, et al. (2004) FM-dyes as experimental probes for dissecting vesicle trafficking in living plant cells. Journal of Microscopy 214: 159-173.

51. Emans N, Zimmermann S, Fischer R (2002) Uptake of a fluorescent marker in plant cells is sensitive to brefeldin A and wortmannin. Plant Cell 14: 71-86.

52. Qi X, Kaneda M, Chen J, Geitmann A, Zheng H (2011) A specific role for Arabidopsis TRAPPII in post-Golgi trafficking that is crucial for cytokinesis and cell polarity. Plant J 68: 234-248.

53. Qi X, Zheng H (2012) Rab-A1c GTPase Defines a Population of the Trans-Golgi Network that Is Sensitive to Endosidin1 during Cytokinesis in Arabidopsis. Mol Plant.

54. Wei T, Wang A (2008) Biogenesis of cytoplasmic membranous vesicles for plant potyvirus replication occurs at endoplasmic reticulum exit sites in a COPI- and COPII-dependent manner. J Virol 82: 12252-12264.

55. Kotzer AM, Brandizzi F, Neumann U, Paris N, Moore I, et al. (2004) AtRabF2b (Ara7) acts on the vacuolar trafficking pathway in tobacco leaf epidermal cells. Journal of Cell Science 117: 6377-6389.

56. Haas TJ, Sliwinski MK, Martinez DE, Preuss M, Ebine K, et al. (2007) The Arabidopsis AAA ATPase SKD1 is involved in multivesicular endosome function and interacts with its positive regulator LYST-INTERACTING PROTEIN5. Plant Cell 19: 1295-1312.

57. Liu J-Z, Blancaflor EB, Nelson RS (2005) The Tobacco Mosaic Virus 126-Kilodalton Protein, a Constituent of the Virus Replication Complex, Alone or within the Complex Aligns with and Traffics along Microfilaments. Plant Physiology 138: 1853-1865.

58. Collings DA, Lill AW, Himmelspach R, Wasteneys GO (2006) Hypersensitivity to cytoskeletal antagonists demonstrates microtubule-microfilament cross-talk in the control of root elongation in Arabidopsis thaliana. New Phytol 170: 275-290.

59. Wang Y-S, Yoo C-M, Blancaflor EB (2008) Improved imaging of actin filaments in transgenic Arabidopsis plants expressing a green fluorescent protein fusion to the C- and N-termini of the fimbrin actin-binding domain 2. New Phytologist 177: 525-536.

60. Wei T, Huang TS, McNeil J, Laliberte JF, Hong J, et al. (2010) Sequential recruitment of the endoplasmic reticulum and chloroplasts for plant potyvirus replication. J Virol 84: 799-809.

61. Peremyslov VV, Prokhnevsky AI, Avisar D, Dolja VV (2008) Two class XI myosins function in organelle trafficking and root hair development in Arabidopsis. Plant Physiol 146: 1109-1116.

62. Peremyslov VV, Prokhnevsky AI, Dolja VV (2010) Class XI myosins are required for development, cell expansion, and F-Actin organization in Arabidopsis. Plant Cell 22: 1883-1897.

63. Eskelin K, Suntio T, Hyvarinen S, Hafren A, Makinen K (2010) Renilla luciferase-based quantitation of Potato virus A infection initiated with Agrobacterium infiltration of *N. benthamiana* leaves. J Virol Methods 164: 101-110.

64. Lacorte C, Ribeiro SG, Lohuis D, Goldbach R, Prins M (2010) Potatovirus X and Tobacco mosaic virus-based vectors compatible with the Gateway cloning system. J Virol Methods 164: 7-13.

65. Lindbo JA (2007) High-efficiency protein expression in plants from agroinfection-compatible Tobacco mosaic virus expression vectors. BMC Biotechnol 7: 52.

66. Grangeon R, Jiang J, Laliberte JF (2012) Host endomembrane recruitment for plant RNA virus replication. Curr Opin Virol 2: 677-684.

67. Tilsner J, Linnik O, Wright KM, Bell K, Roberts AG, et al. (2012) The TGB1 movement protein of Potato virus X reorganizes actin and endomembranes into the X-body, a viral replication factory. Plant Physiol 158: 1359-1370.

68. Barajas D, Jiang Y, Nagy PD (2009) A unique role for the host ESCRT proteins in replication of Tomato bushy stunt virus. PLoS Pathog 5: e1000705.

69. Barajas D, Nagy PD (2010) Ubiquitination of tombusvirus p33 replication protein plays a role in virus replication and binding to the host Vps23p ESCRT protein. Virology 397: 358-368.

70. Peremyslov VV, Klocko AL, Fowler JE, Dolja VV (2012) Arabidopsis Myosin XI-K Localizes to the Motile Endomembrane Vesicles Associated with F-actin. Front Plant Sci 3: 184.

71. Thomas CL, Bayer EM, Ritzenthaler C, Fernandez-Calvino L, Maule AJ (2008) Specific Targeting of a Plasmodesmal Protein Affecting Cell-to-Cell Communication. PLoS Biol 6: e7.

72. Knoops K, Swett-Tapia C, van den Worm SH, Te Velthuis AJ, Koster AJ, et al. (2010) Integrity of the early secretory pathway promotes, but is not required for, severe acute respiratory syndrome coronavirus RNA synthesis and virus-induced remodeling of endoplasmic reticulum membranes. J Virol 84: 833-846.

73. Tilsner J, Oparka KJ (2012) Missing links? - The connection between replication and movement of plant RNA viruses. Curr Opin Virol 2: 699-705.

74. Thivierge K, Cotton S, Dufresne PJ, Mathieu I, Beauchemin C, et al. (2008) Eukaryotic elongation factor 1A interacts with Turnip mosaic virus RNA-dependent RNA polymerase and VPg-Pro in virus-induced vesicles. Virology 377: 216-225.

75. Nelson BK, Cai X, Nebenführ A (2007) A multicolored set of in vivo organelle markers for co-localization studies in Arabidopsis and other plants. The Plant Journal 51: 1126-1136.

76. Lu R, Martin-Hernandez AM, Peart JR, Malcuit I, Baulcombe DC (2003) Virus-induced gene silencing in plants. Methods 30: 296-303.

77. Gould B, Kramer E (2007) Virus-induced gene silencing as a tool for functional analyses in the emerging model plant Aquilegia (columbine, Ranunculaceae). Plant Methods 3: 6.

Figures legends

Figure 1: TuMV intercellular movement time course. (A) Schematic representation of the plasmid pCambiaTunos/6K$_2$:mCherry/GFP-HDEL used to discriminate primary infected cells from secondary infected cells after agroinfiltration. (B) Schematic representation of the agroinfiltration procedure. Inoculation site is represented by light green circle and white rectangle indicates region visualized by confocal microscopy. (C) Three-dimensional rendering of 35 1-□m-thick confocal image sections that overlap by 0.5 □m at a high magnification showing the distribution of TuMV-induced 6K$_2$:mCherry-tagged structures and GFP-HDEL labeled ER. Scale bar = 20 □m. (D) Single-slice confocal microscope images of *N. benthamiana* leaf agroinfiltrated 60 hrs before with A. tumefaciens strain Agl1 containing the above plasmid. Left panel, red fluorescence channel imaging TuMV producing 6K$_2$:mCherry; middle panel, green fluorescence channel imaging GFP-HDEL; and right panel, merged images. Scale bar = 200 □m. (E) Confocal image of *N. benthamiana* leaf agroinfiltrated 72 hrs before with A. tumefaciens strain Agl1 containing the above plasmid. White line deliniates secondary infection front.

(F) Same leaf as in (E) but image was taken 17 hrs later. White line deliniates secondary infection front at time 0 and yellow line deliniates secondary infection front at time 17 hr. E and F are z-stacks of 5 opticle slices of 50 µm in thickness. Scale bar = 1 mm

Figure 2: The secretory pathway is required for intercellular movement. *N. benthamiana* leaves were infiltrated with DMSO (A), 10 µg/ml BFA (B) and 0.5 µM CMA (C) 4 hours before agroinfiltration with A. tumefaciens containing pCambiaTunos/6K_2:mCherry/GFP-HDEL. All images were taken at 4 dpi with a LSM 510 Meta confocal microscope. Scale bar = 200 µm. (D) Surface area of red-only fluorescent foci (n=20) was calculated and expressed in fluorescence units. (E) Fluorescence intensity ratio of red over green foci was calculated and expressed in fluorescence units. Bars represent means of one experiment and standard errors for 20 replicates per treatment. Experiments were repeated 3 times. One-way analysis of variance calculation followed by Tukey's Multiple Comparison Test allowed analysis of differences between means: **, 0.001<P value <0.01 .

Figure 3: Inhibition of TuMV intercellular movement by dominant negative mutants of secretory pathway factors. *N. benthamiana* leaves were agroinfiltrated with A. tumefaciens containing plasmids pCambiaTunos/6K_2:mCherry/GFP-HDEL alone (A) or with dominant negative mutant ARF1(NI) (B) or with RAB-E1d (NI) (C). All images were taken at 4 dpi with a LSM 510 Meta confocal microscope (Zeiss). Scale bar = 200 µm. (D) Surface area of red-only fluorescent foci (n=20) was calculated and expressed in fluorescence units. (E) Fluorescence intensity ratio of red over green foci was calculated and expressed in fluorescence units. Bars represent means of one experiment and standard errors per treatment. Experiments were repeated 3 times. One-way analysis of variance calculation followed by Tukey's Multiple Comparison Test allowed analysis of differences between means: ***, P value <0.0001.

Figure 4: TuMV intercellular movement does not depend on the endocytic pathway. *N. benthamiana* leaves were infiltrated with DMSO (A), 20 µM Wortmannin (B), 30 µM Tyrphostin A51 (C) and 30 µM Tyrphostin A23 (D) 4 hours before agroinfiltration with A. tumefaciens containing pCambiaTunos/6K_2:mCherry/GFP-HDEL. Images were taken at 4 dpi with a LSM 510 Meta confocal microscope (Zeiss). Scale bar = 200 µm. (E) Surface area of red-only fluorescent foci (n=15) was calculated and expressed in fluorescence units. Experiments were repeated 3 times. One-way analysis of variance

calculation followed by Tukey's Multiple Comparison Test allowed analysis of differences between means: NS, not significant.

Figure 5: TuMV $6K_2$-tagged vesicles do not colocalize with endocytic markers. Three-dimensional rendering of 22 1-µm-thick confocal images that overlap by 0.5 □m of *N. benthamiana* agroinfiltrated leaves. (A) shows the distribution of TuMV-induced $6K_2$-mCherry-tagged structures and YFP labeled Ara7 dots. Left panels; red fluorescence channel imaging TuMV producing $6K_2$-mCherry, middle panel; green fluorescence channel imaging YFP-RabF2b, and right panel; merged images. (B) shows the distribution of TuMV-induced $6K_2$:GFP-tagged structures and FM4-64 labeled vesicles. Left panel shows green fluorescence channel from TuMV producing $6K_2$:GFP, middle panel red fluorescence channel from FM4-64, and right merged panels. Images were taken at 4 dpi with a Zeiss LSM 780 confocal microscope. Scale bar = 20 µm.

Figure 6: Microfilament network is required for TuMV intercellular movement. *N. benthamiana* leaves were infiltrated with DMSO (A), 5 µM LatB (B), and 10 µM CytD (C) 4 hours before agroinfiltration with A. tumefaciens containing pCambiaTunos/$6K_2$:mCherry/GFP-HDEL. Images were taken at 4 dpi with a LSM 510 Meta confocal microscope (Zeiss). Scale bar = 200 µm. (F) Surface area of red-only fluorescent foci was calculated and expressed in fluorescence units. (G) Fluorescence intensity ratio of red over green foci was calculated and expressed in fluorescence units. Bars represent means of one experiment and standard errors for 20 replicates per treatment. Experiments were repeated 3 times. One-way analysis of variance calculation followed by Tukey's Multiple Comparison Test allowed analysis of differences between means: NS, not significant, **, 0.001<P value <0.01.

Figure 7: Myosin XI-2 is implicated in TuMV intercellular movement. (A) Quantitative RT-PCR was used to determine the relative expression ratio of target genes (myosin VIII-1, myosin VIII-2, myosin XI-2, and myosin XI-F) in *N. benthamiana* infected with the indicated TRV silencing constructs versus a TRV control not expressing a myosin fragment. (B) *N. benthamiana* leaves silenced for individual myosin genes (myosin VIII-1, myosinVIII-2, myosin XI-2, and myosin XI-F) were agroinfiltrated with pCambiaTunos/$6K_2$:mCherry/GFP-HDEL, and surface area of red-only fluorescent foci was calculated and expressed in fluorescence units 5 dpi. Wild-type TRV (TRV) or buffer (Mock) were used as controls. Bars represent means of one experiment and standard

errors for 10 replicates per treatment. Experiments were repeated 3 times. One-way analysis of variance calculation followed by Tukey's Multiple Comparison Test allowed analysis of differences between means: NS, not significant; *, $P < 0.05$. (C) Level of expression of non-target myosins in *N. benthamiana* leaves silenced for myosin XI-2. The internal loading control for each sample was actin-2. Expression analysis was performed on extracts from systemic leaves at 20 dpi with TRV constructs. Bars represent means of one experiment and standard errors for three replicates per treatment. One-way analysis of variance calculation followed by Tukey's Multiple Comparison Test allowed analysis of differences between means: = NS, not significant; *, $P < 0.05$. The experiment was repeated twice for each TRV silencing construct.

Figure S1: (A) The TuMV cassette in pCambianTunos/6K_2:mCherry/GFP-HDEL was replaced by 6K_2:mCherry cassette. Single-slice confocal microscope images of *N. benthamiana* leaf agroinfiltrated 4 days before with A. tumefaciens strain Agl1 containing the above plasmid. Left panel, red fluorescence channel imaging 6K_2:mCherry; middle panel, green fluorescence channel imaging GFP-HDEL; and right panel, merged images. Scale bar = 200 □m. (B) Single slice confocal microscopy images showing distribution of ERD2 in Golgi bodies (left panel) and its retention in ER following BFA treatment. Scale bar = 10 µm. (C) Single slice confocal microscopy images showing FM4-64-labeled endocytic vesicles (arrows, left panel) and inhibition of FM4-64-labeled endocytic vesicle formation by 20 µM worthmannin treatment 4h prior tostaining (right panel). Scale bar = 10 µm. (D) Single slice confocal microscopy images showing distribution of actin microfilaments in the presence of DMSO (left pane), 10 µM CytD (middle panel) and 5 µM LatB (right panel). Scale bar = 10 µm.

Movie S1. Time lapse series of confocal image of *N. benthamiana* leaf agroinfiltrated 72 hrs before with A. tumefaciens strain Agl1 containing the above plasmid. Images were taken every hour for 17 consecutive hours, indicated at upper left. Each image is a Z-stack of 5 opticle slices of 50 µm in thickness. Scale bar = 1 m

Figures

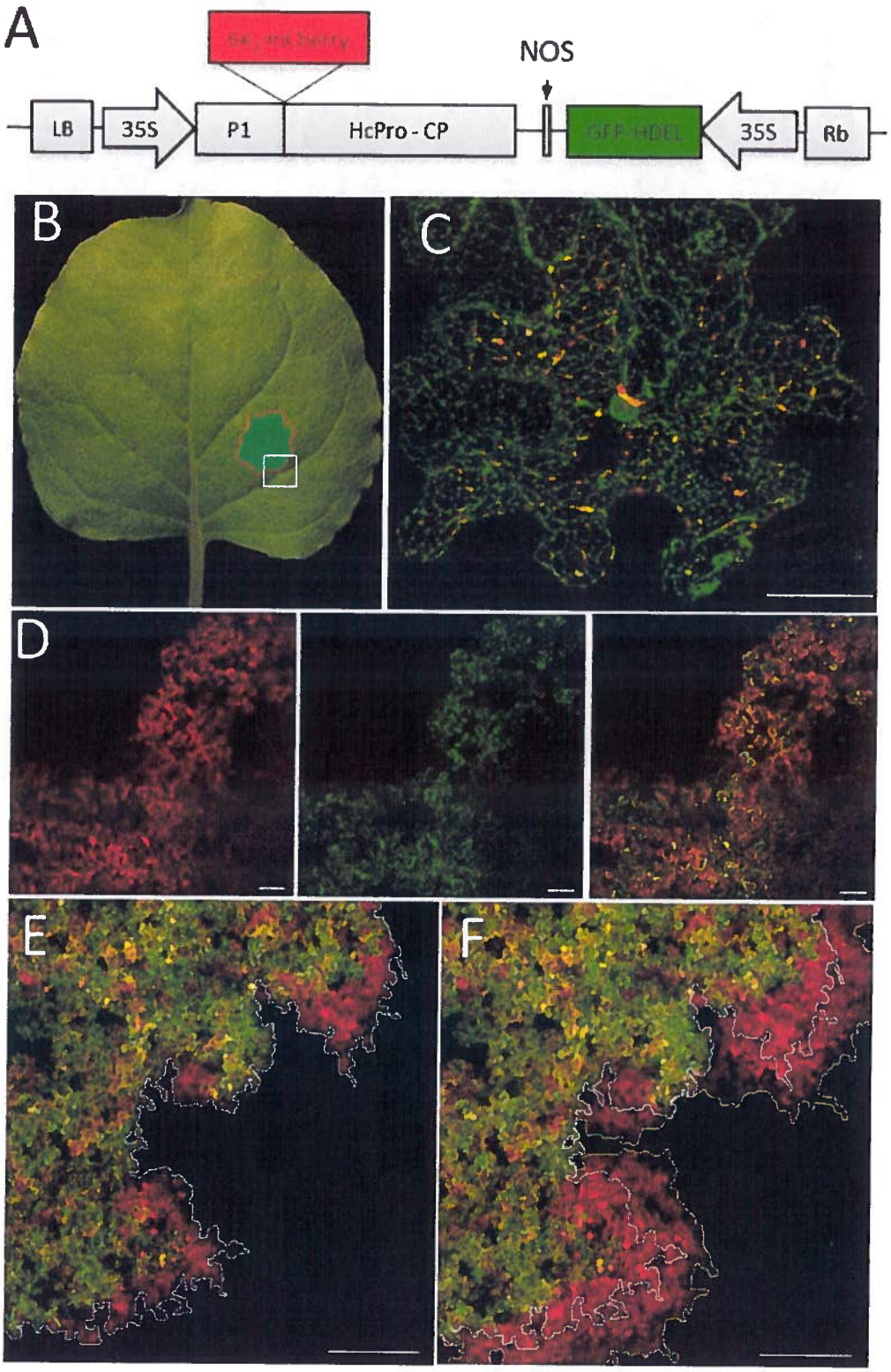

Figure 1: TuMV intercellular movement time course.

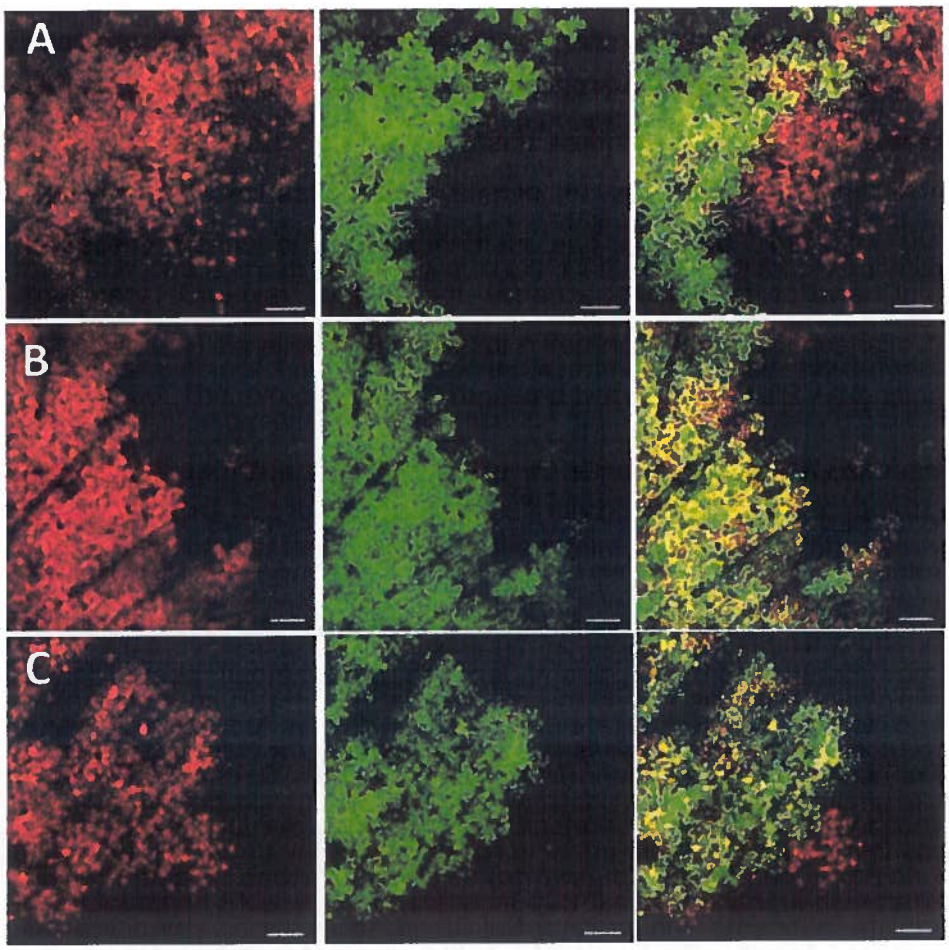

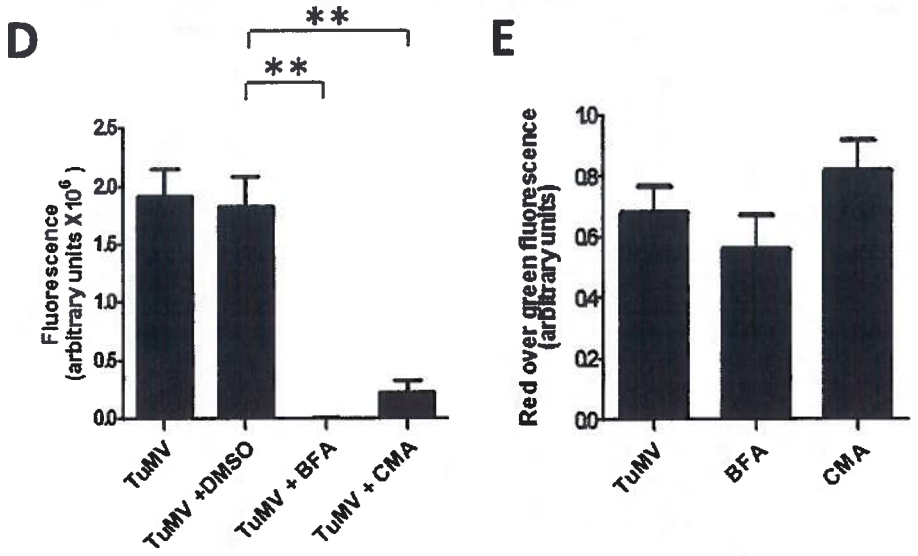

Figure 2: The secretory pathway is required for intercellular movement.

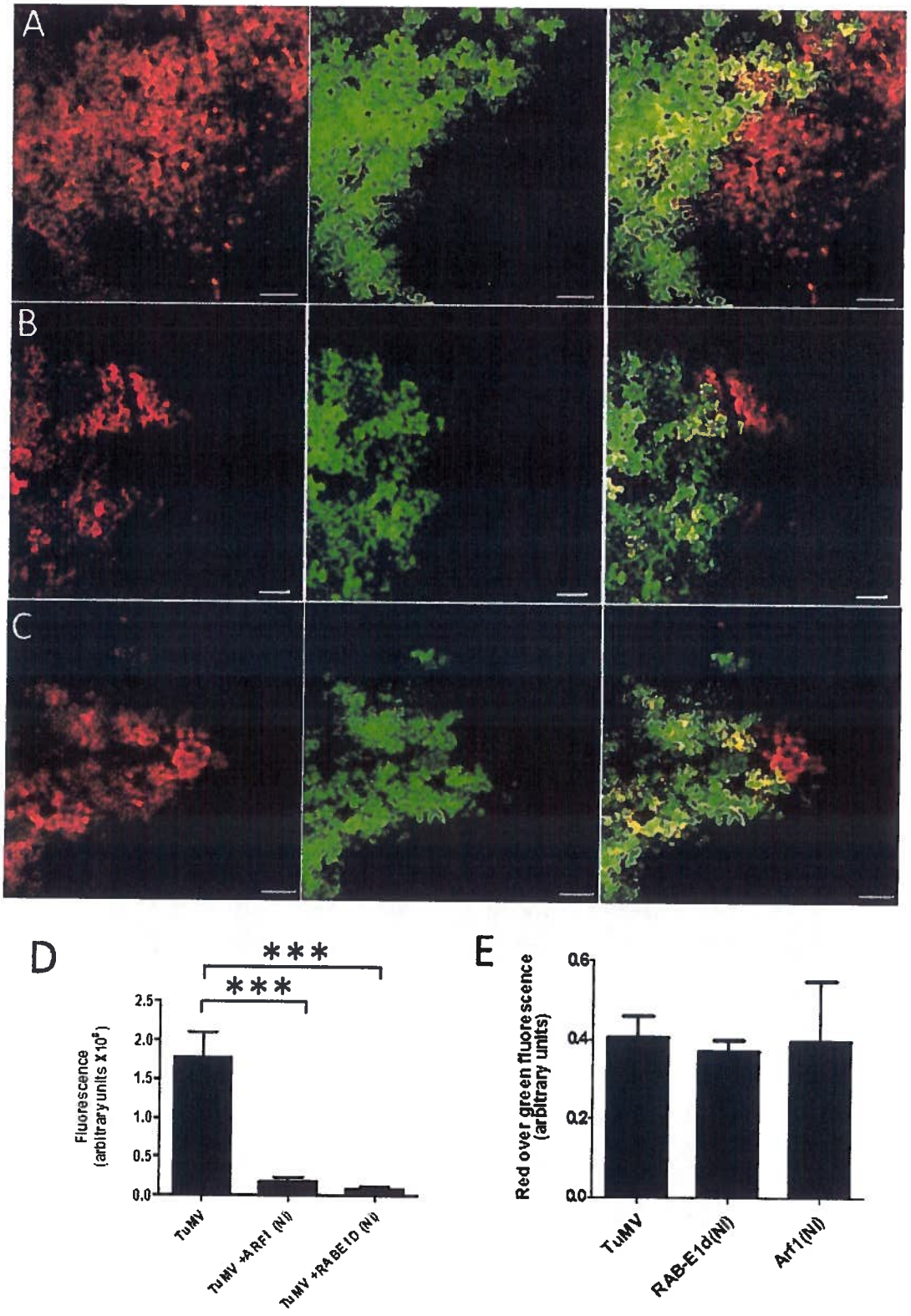

Figure 3: Inhibition of TuMV intercellular movement by dominant negative mutants of secretory pathway factors.

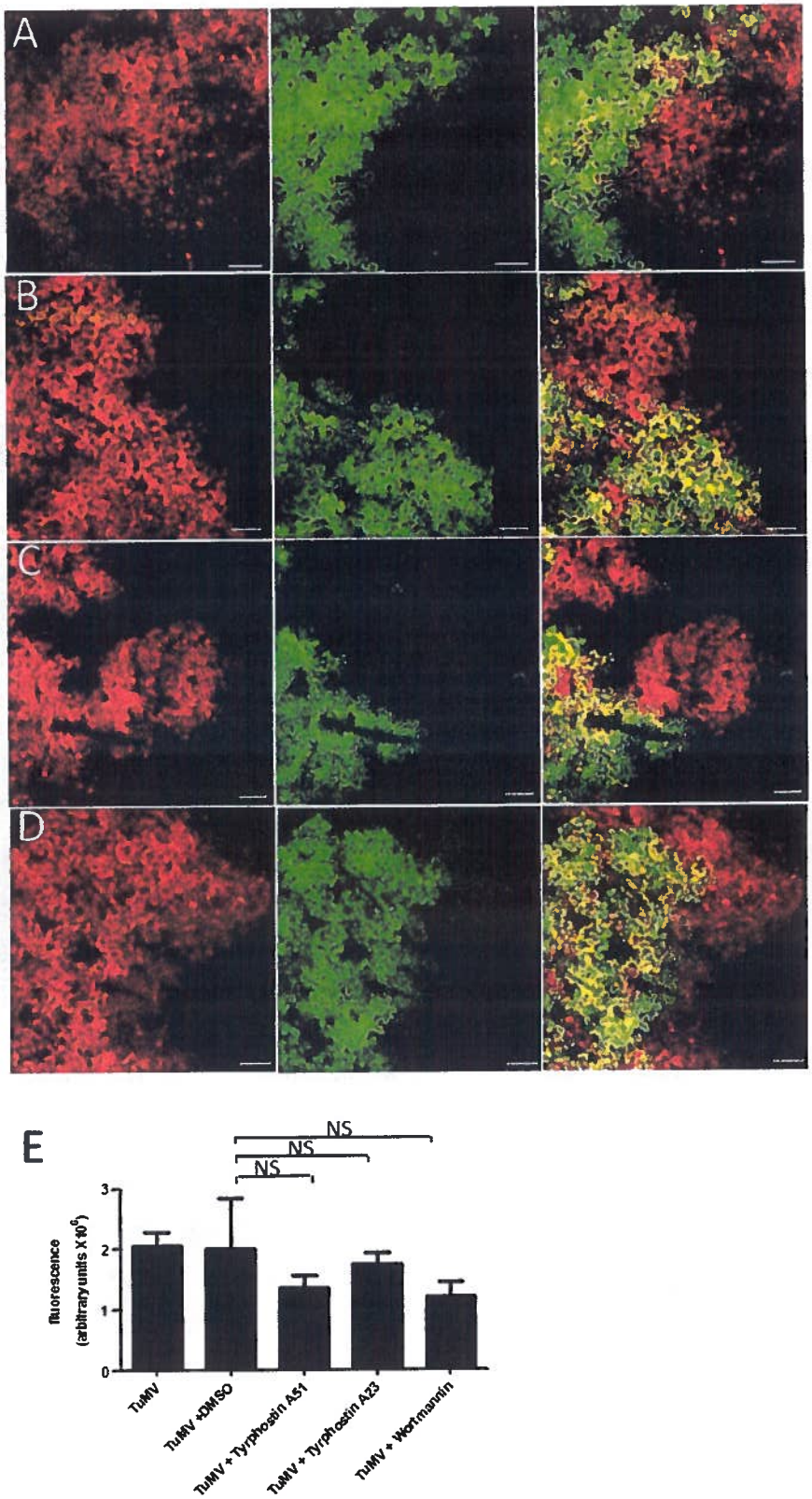

Figure 4: TuMV intercellular movement does not depend on the endocytic pathway.

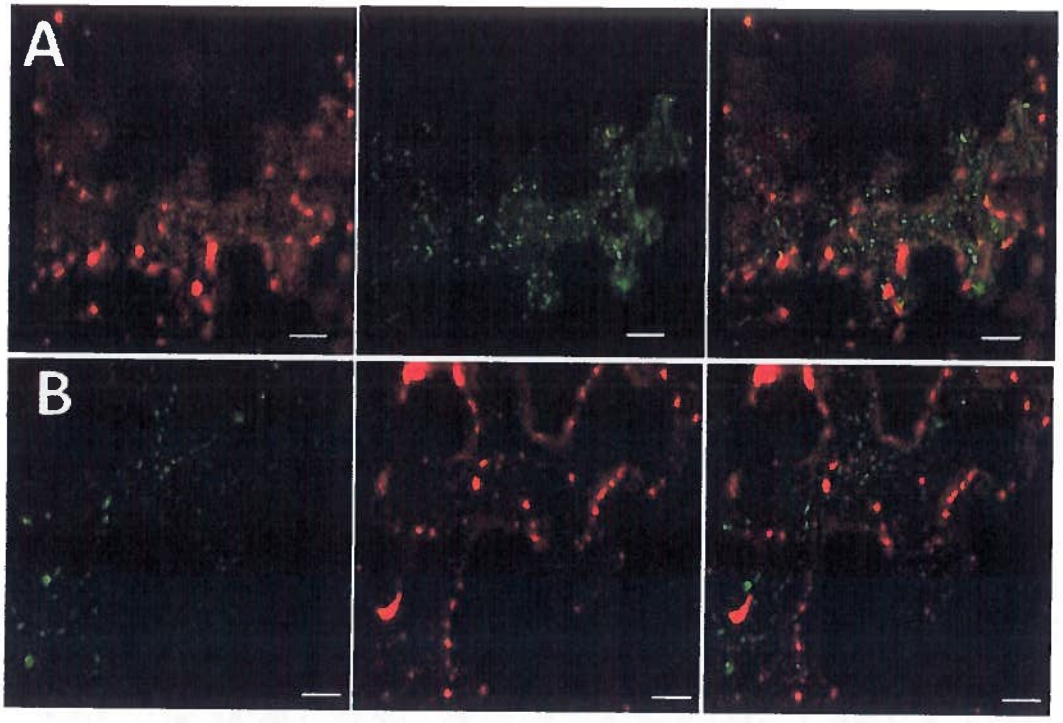

Figure 5: TuMV $6K_2$-tagged vesicles do not colocalize with endocytic markers.

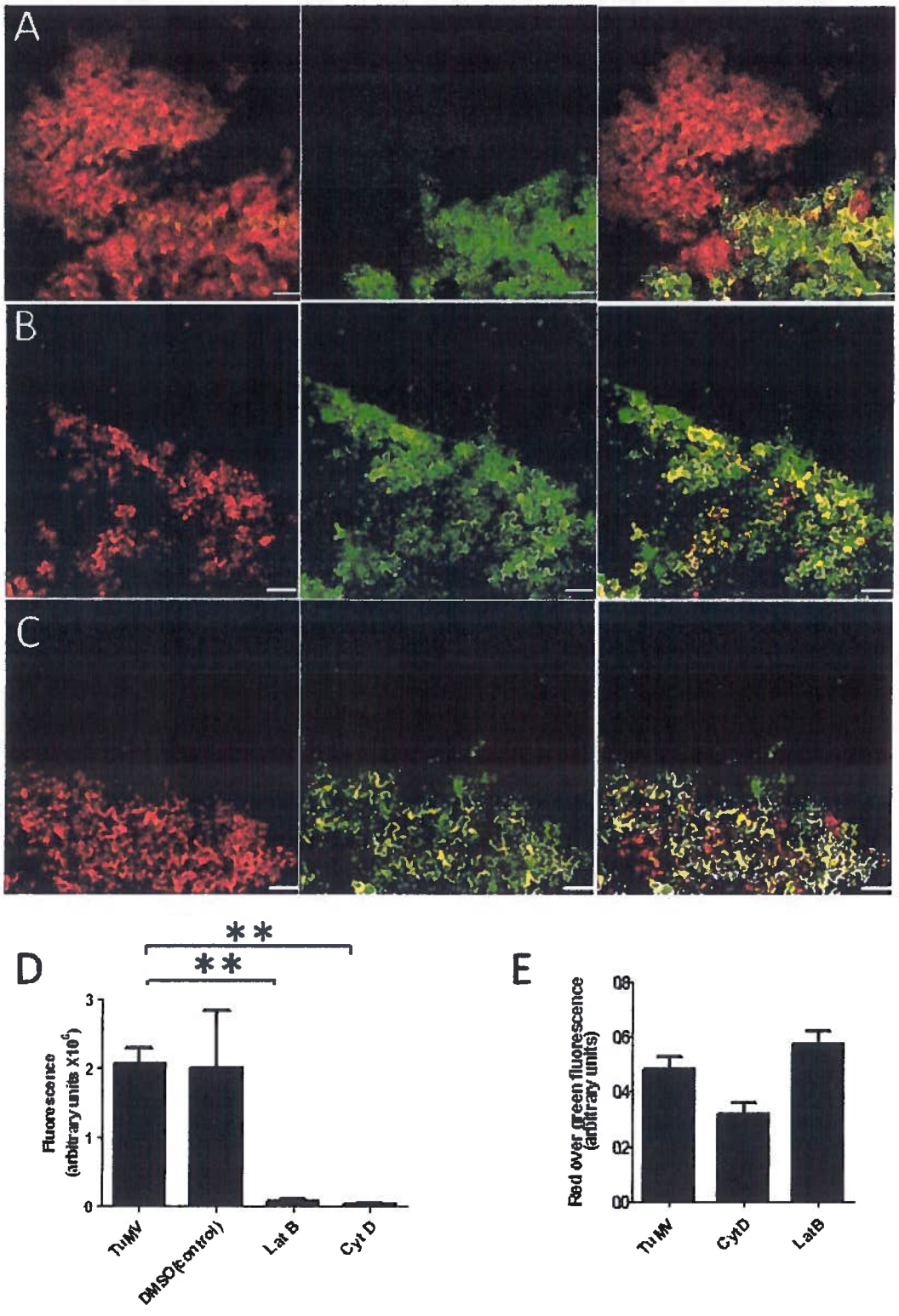

Figure 6: Microfilament network is required for TuMV intercellular movement.

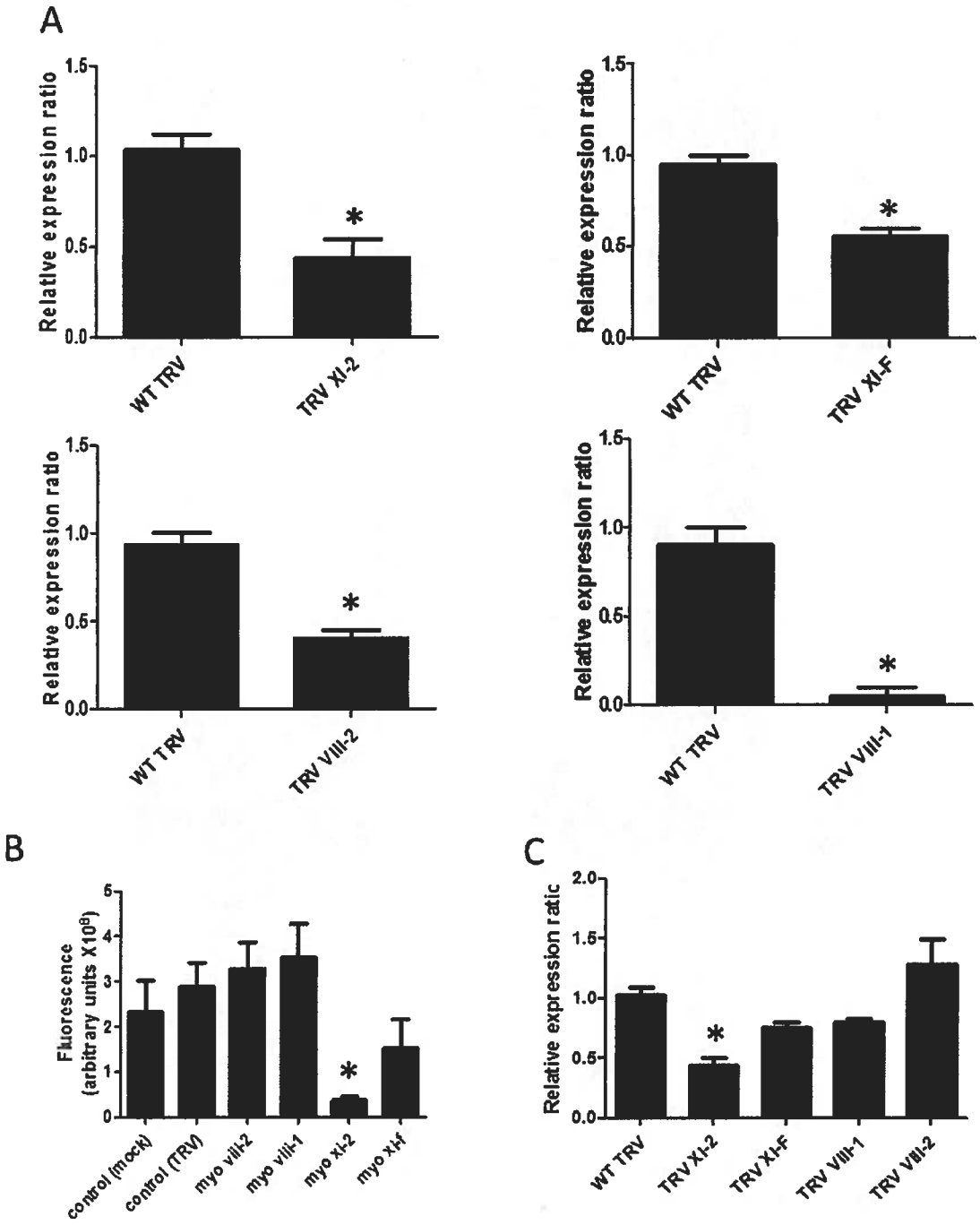

Figure 7: Myosin XI-2 is implicated in TuMV intercellular movement.

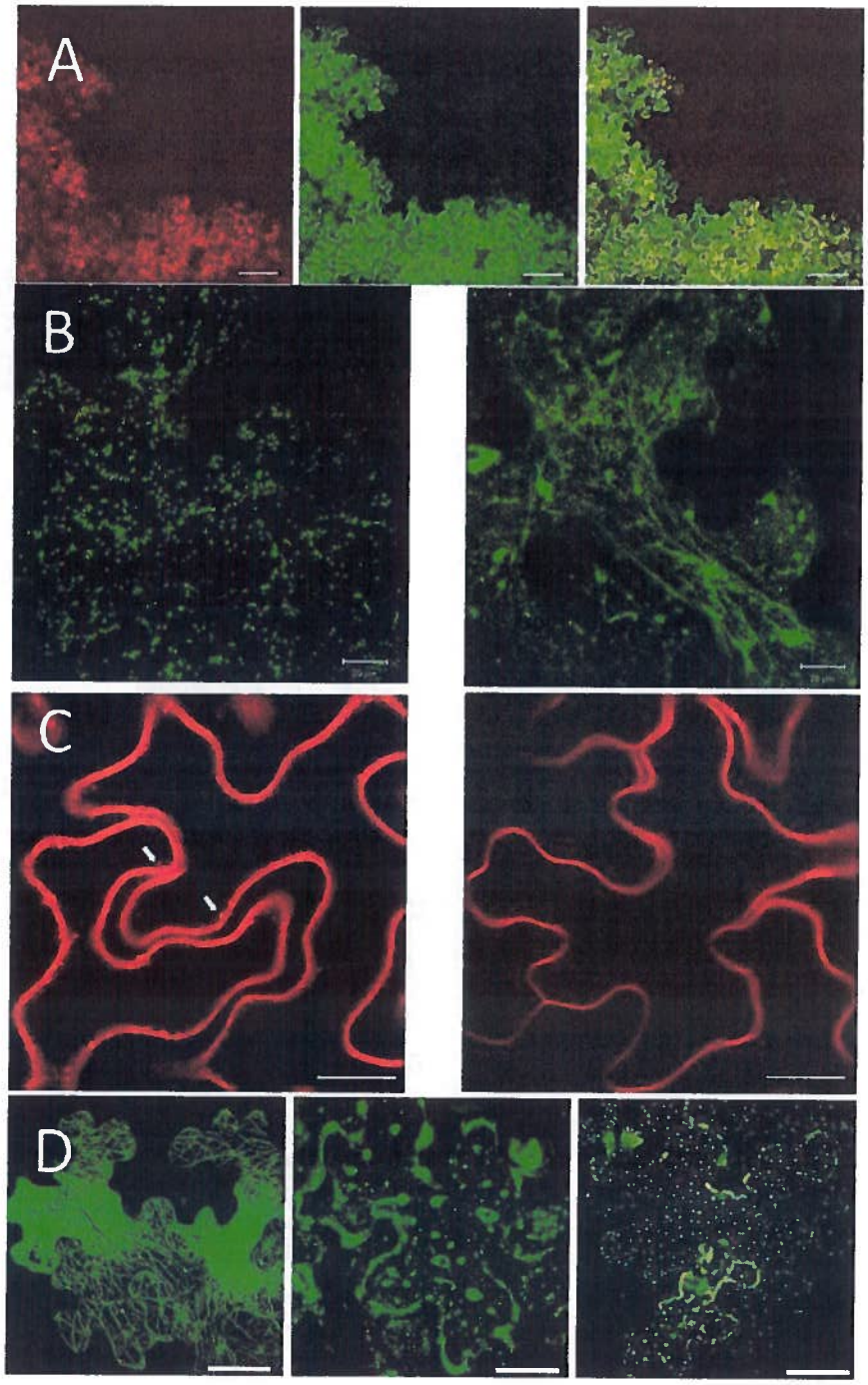

Figure S1

CHAPITRE 3: DISCUSSION

Ce projet de doctorat avait pour objectif de caractériser le mouvement intracellulaire des usines virales, d'étudier l'impact de leur biogenèse sur le système de sécrétion de la cellule, et de définir l'implication des usines virales dans le mouvement de cellule à cellule. Nos travaux ont mis en évidence le rôle fondamental joué par la protéine virale $6K_2$ lors de l'infection, mais ont aussi soulevé de nombreuses questions qui restent à élucider. Dans ce chapitre nous allons discuter des résultats obtenus, des questions qu'ils entraînent, et des projets menés dans notre laboratoire et qui prolongent ces travaux.

1. Couplage réplication et traduction virale

Les expériences de cette thèse se basent sur le développement d'un outil de génétique inverse, le clone infectieux TuMV-$6K_2$:mCherry ou GFP, qui permet de visualiser les usines virales induites par $6K_2$ grâce à une fusion avec une protéine fluorescente. Cet outil s'est avéré très utile, et il faut souligner que de nombreux laboratoires travaillant sur des virus de plantes ne disposent pas encore d'un clone infectieux leur permettant de visualiser le lieu de la réplication virale.

Grâce à cet outil, nous avons pu démontrer que les usines virales proviennent d'un seul génome (Cotton et al., 2009). En effet si on exprime un virus TuMV-$6K_2$:mCherry et un virus TuMV-$6K_2$:GFP dans la même cellule, lorsque les vésicules apparaissent nous n'observons que des vésicules rouges ou vertes. Plus tard au cours de l'infection on peut trouver des usines virales jaunes, suite à des évènements de fusions (Cotton et al., 2009;Grangeon et al., 2012). Cela signifie que la formation des usines virales se déroule dans un mécanisme en Cis, dans lequel il vas-y avoir formation d'usine virale dès qu'une quantité suffisante de la protéine $6K_2$ sera produite. La protéine $6K_2$ s'insère dans la membrane de façon co-traductionnelle et provoque la courbure des membranes. Cette observation suggère un couplage de la traduction et de la réplication dans les usines virales. Cette hypothèse est appuyée par la présence de nombreux facteurs hôtes de la traduction dans les usines virales, comme PABP, eIF(iso)4E, Hsc70, et eEF1A (Wittmann et al., 1997;Beauchemin et al., 2007;Beauchemin and Laliberté, 2007;Dufresne et al., 2008;Thivierge et al., 2008), et aussi la présence des protéines virales considérées comme nécessaires à la réplication de l'ARNv: VPg-Pro, RdRp, et CI (Cotton et al.,

2009). L'ARN double brin, un intermédiaire de la réplication virale, se localise également dans les usines virales.

L'ultrastructure des usines virales de certains virus d'animaux a été caractérisée par tomographie (Kopek et al., 2007;Knoops et al., 2008;Welsch et al., 2009) et a révélé la présence de ribosomes sur la face externe des usines virales. Des pores sont également présents, ce qui permet l'échange de molécules avec le cytoplasme. Il est probable que la traduction virale se déroule sur la face externe des vésicules, et que les protéines virales ainsi produites s'acheminent préférentiellement à l'intérieur des vésicules. Dans les schémas classiques du cycle viral des virus à ARN(+), on distingue généralement la traduction virale se déroulant dans le cytoplasme, de la réplication virale qui se déroule en association avec les membranes. Mais un couplage traduction et réplication a déjà été suggéré dans le cas des picornavirus (Andrea V. Gamarnik, 1998) et pour le RCNMV (Mizumoto et al., 2006). Un couplage traduction et réplication a également été observé pour les virus ambisens, qui possèdent dans le même segment une partie d'ARN de polarité positive et une autre de polarité négative (Nguyen and Haenni, 2003).

Dans le cas du TuMV, nous avons des indices qui suggèrent un tel couplage, comme la présence dans les usines virales de protéines de l'hôte impliquées dans la traduction. Mais il serait intéressant d'investiguer ce phénomène de façon plus approfondie. Des résultats préliminaires de microscopie électronique dans notre laboratoire ont révélé la présence de ribosomes sur la face externe des usines virales et sur les tubules du RE qui leurs donnent naissance (Juan Wan, communication personnelle). Les travaux de tomographie que nous menons, nous permettrons d'appuyer l'hypothèse d'un couplage réplication et traduction dans les usines virales.

2. Implication du système sécrétoire dans la biogenèse des usines virales et le mouvement du TuMV

Nous avons montré que le virus bloque la sécrétion de secGFP (Grangeon et al., 2012). La protéine SecGFP est normalement sécrétée dans l'apoplaste, mais en présence du TuMV, ou simplement de $6K_2$, cette protéine est retenue à l'interface du RE et du Golgi. Cette donnée suggère que $6K_2$ perturbe le

fonctionnement normal du système sécrétoire, et que cette perturbation intervient entre le RE et le Golgi.

Nos travaux ont également mis en évidence l'apparition de deux types de structures distinctes dans la cellule infectée. On observe autour du noyau la formation d'une structure d'environ 10µm de diamètre, qui est un amalgame de membranes issues du système sécrétoire de la cellule (RE, Golgi, vésicules COPII, et chloroplastes). Alors que l'on voit le long du RE du cortex la formation de vésicules de tailles inférieures à 1µm, et qui sont très mobiles. Ces deux types de structures sont fonctionnellement liées car nos résultats suggèrent que la structure périnucléaire donne naissance aux vésicules de plus petites tailles.

Bien que les membranes du système sécrétoire soient sollicitées pour former la structure périnucléaire, la structure caractéristique du RE du cortex en tubules et l'apparence des corps de Golgi ne semblent pas modifiées. De plus, les membranes de la structure périnucléaire sont en continuité avec le système sécrétoire, comme le montrent nos expériences de FRAP (Grangeon et al., 2012). La fonction exacte de cette structure périnucléaire n'est pas totalement comprise. Récemment, grâce à des anticorps dirigés contre les ARN double brin (ARNdb) nous avons observé que la structure périnucléaire contient des structures ponctuées, où l'on retrouve l'ARNdb (Juan Wan communication personnelle). Les vésicules de plus petites tailles en contiennent aussi, mais en plus faible quantité. Bien que nous ne puissions pas exclure qu'une activité de réplication virale se déroule dans les vésicules mobiles de petites tailles, le site principal de la réplication virale semble être la structure périnucléaire.

La formation des différentes usines virales du TuMV est due à l'action de la protéine $6K_2$, et un traitement à la BFA n'empêche pas la formation de la structure périnucléaire. Nous menons actuellement des travaux pour identifier les déterminants moléculaires de $6K_2$ qui sont responsables de la formation des usines virales. Nos résultats préliminaires montrent l'importance du domaine transmembranaire et de la queue N-terminale de la protéine (Figure 10).

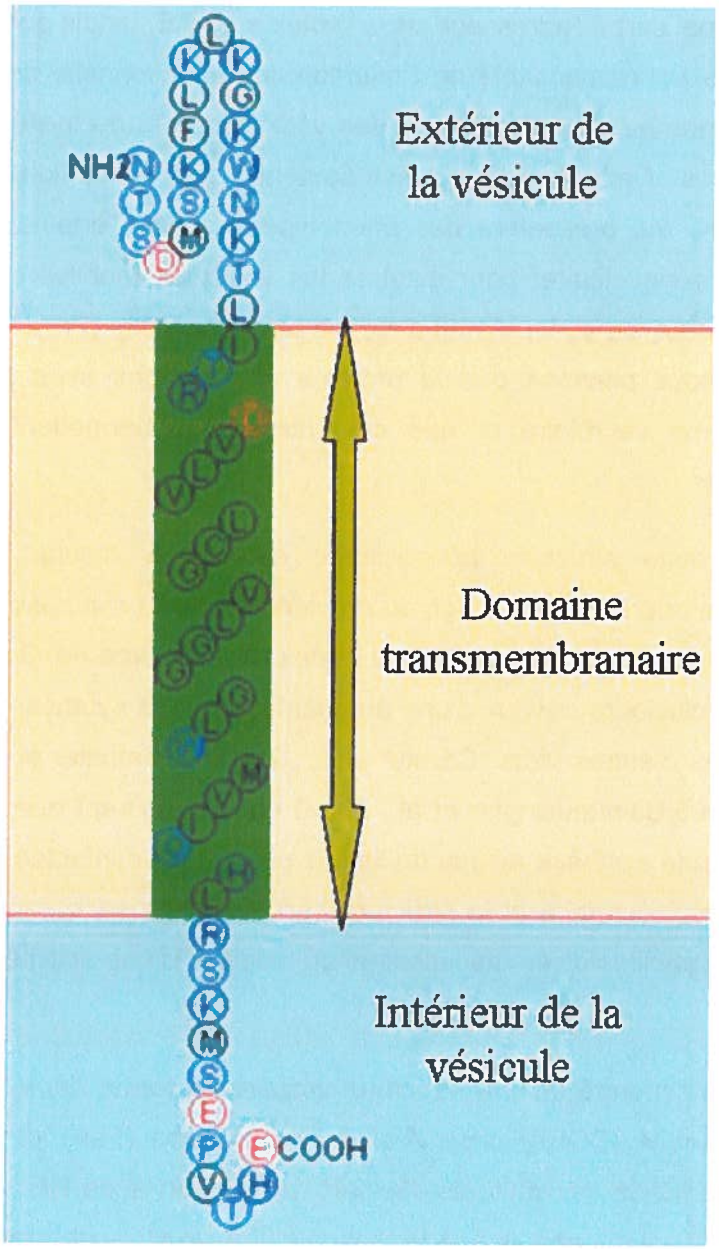

Figure 10: Prédiction de la structure secondaire de $6K_2$.

La protéine $6K_2$ possède un domaine N-terminal de 19 acides aminés, et un domaine transmembranaire. À l'extrémité C-terminale, $6K_2$ est lié avec la protéine VPg-Pro

Le domaine N-terminal sert à l'adressage de la protéine au RE, tandis que le domaine transmembranaire est responsable de l'insertion co-traductionnelle de la protéine dans les membranes et aussi de l'export des vésicules hors du système sécrétoire une fois matures. Cette hypothèse est soutenue par l'obtention de mutants de la protéine $6K_2$ qui présentent des phénotypes variés. Certains ne forment plus de structure périnucléaire, pour d'autres les vésicules mobiles sont retenues dans le RE du cortex, ou co-localisent avec les corps de Golgi (Projet de doctorat de Jun Jiang). Nous pensons que la protéine $6K_2$ interagit avec des protéines hôtes du système sécrétoire et que ces interactions permettent la biogenèse des usines virales.

La formation de cette structure périnucléaire est-elle le résultat de recrutement des membranes du RE et du Golgi, ou provient-elle de la synthèse *de novo* de lipides ? L'apparence inchangée du RE du cortex et des corps de Golgi, ainsi que la mention dans plusieurs travaux d'une augmentation de la synthèse *de novo* de lipides dans le cas d'autres virus (Carette et al., 2000;Ritzenthaler et al., 2002;Lee and Ahlquist, 2003;Bamunusinghe et al., 2009) nous suggèrent que les membranes proviennent d'une synthèse accrue de lipides par la cellule infectée. La connexion, entre le système sécrétoire et la structure périnucléaire permettrait de combler les besoins en métabolites divers nécessaires au maintien d'une activité de synthèse élevée.

Certaines études ont montré qu'une structure similaire se forme dans des mutants de la protéine Sec24 (COPII) chez *Arabidopsis thaliana* (Faso et al., 2009;Nakano et al., 2009). Chez ces mutants, l'export des protéines du RE vers l'appareil de Golgi est altéré, ce qui aboutit à la formation d'une structure aberrante. Pour cette raison Sec24 est un candidat potentiel pour interagir avec la protéine $6K_2$. Nous avons un projet en collaboration avec le professeur Hugo Zheng, de l'université McGill qui a pour objectif de faire un criblage d'interacteurs potentiels de $6K_2$ en utilisant le système du double hybride chez la levure. Les premiers résultats obtenus confirment l'interaction $6K_2$/Sec24 dans la levure, mais il y a vraisemblablement d'autres protéines hôtes ciblées par la $6K_2$ qui restent à découvrir.

La formation des usines virales périphériques ne semble pas non plus affectée par un traitement à la BFA, mais en revanche une plus grande proportion de ces vésicules co-localisent avec Sec24. Les vésicules se forment normalement aux ERES, dans une voie dépendante des vésicules COPI/COPII (Wei and Wang, 2008), mais la présence de BFA ralentit le processus de formation des vésicules sans changer drastiquement leur apparence. Selon nos observations, ce n'est pas la réplication qui serait affectée mais le mouvement cellule à cellule du virus. L'implication du système sécrétoire dans la propagation virale a été observée chez différents virus de plantes (Harries et al., 2009;Harries et al., 2010;Amari et al., 2011). Il semble que le mouvement intercellulaire du TuMV soit également dépendant du système sécrétoire. Pour répondre à cette hypothèse, nous avons créé un outil nous permettant d'observer le mouvement intercellulaire en même temps que la réplication. Cet outil s'avère très intéressant pour étudier l'effet de différents traitements sur le mouvement du TuMV. Nous avons développé une méthode d'observation en microscopie confocale qui nous permet de visualiser le mouvement du virus sur toute la zone agroinfiltrée (Figure 11).

Les expériences que nous avons menées, en utilisant des inhibiteurs et des mutants dominants négatifs qui perturbent le système sécrétoire, confirment le rôle des endomembranes dans la propagation virale (Agbeci, Grangeon, et al 2013 publication n°4). L'endocytose n'est pas sollicité mais l'interface RE/Golgi et le réseau d'actine sont impliqués dans le mouvement du TuMV.

Grâce à cet outil nous avons également pu estimer la vitesse de propagation du TuMV, qui infecte une cellule environ toute les 3 heures. Cette vitesse de propagation est du même ordre de grandeur que ce qui a été suggéré pour le TMV (Kawakami et al., 2004).

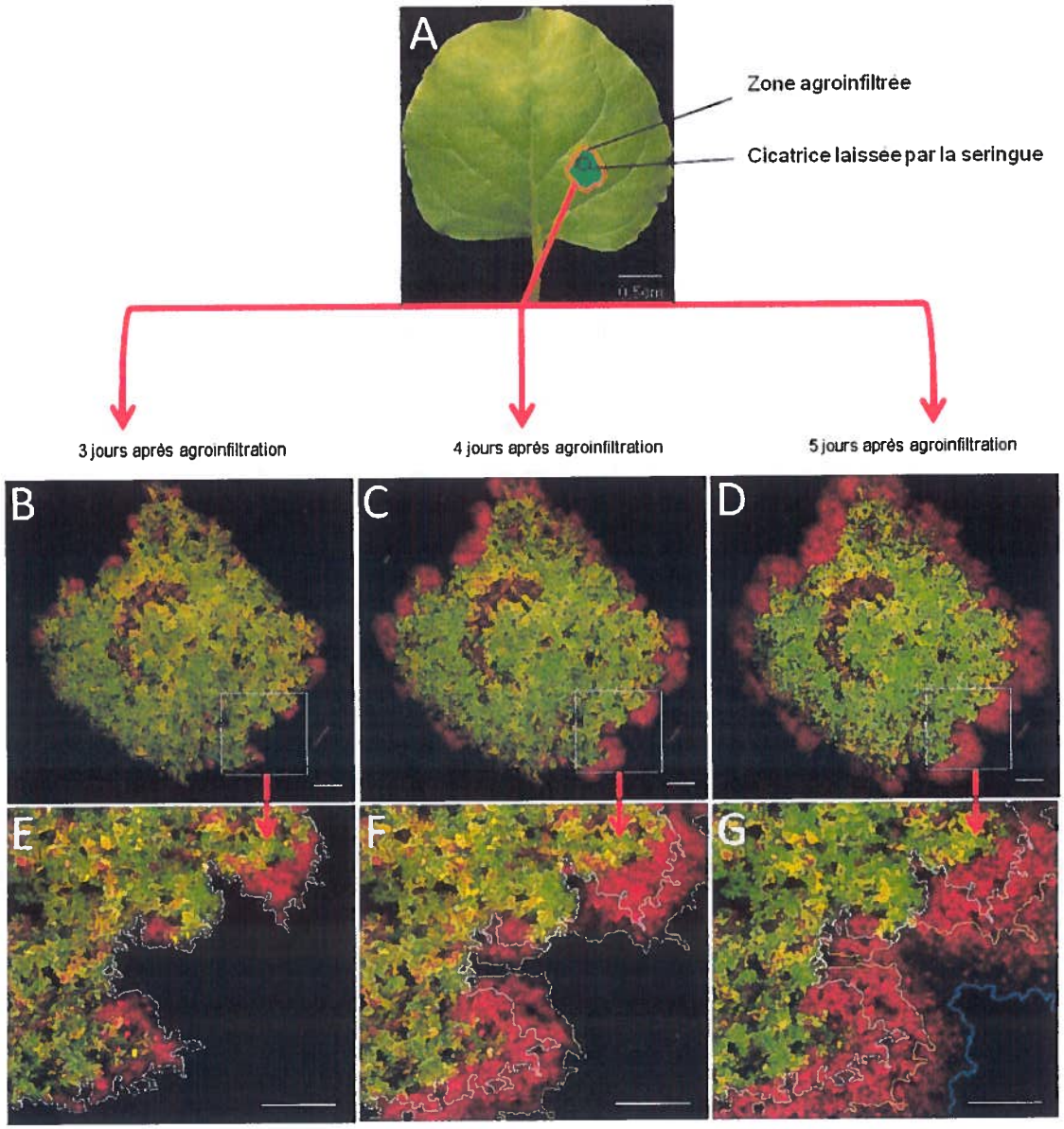

Figure 11: Visualisation du mouvement intercellulaire du TuMV en microscopie confocale

Observation en microscopie confocale de feuilles de *Nicotiana benthamiana* après agroinfiltration de la construction pCambiaTunos/6K$_2$:mCherry/GFP-HDEL. (A) représente une feuille de *N. benthamiana* sur laquelle nous avons dessiné la zone d'agroinfiltration. (B)(C)(D) sont des images de microscopie confocale obtenues avec l'objectif 10X de la totalité de la zone agroinfiltrée. Pour visualiser toute la zone agroinfiltrée nous avons utilisé la fonction "tile" et "Z-stack". Chaque image est une reconstitution de 10x10 images en XY, et de 5 images dans le Z. (E)(F)(G) sont des images de microscopie confocale obtenues avec l'objectif 20X d'une partie de la zone agroinfiltrée. Chaque image est une reconstitution de 5x5 images en XY, et de 4 images dans le Z (barre d'échelle = 1mm).

3. Mobilité des usines virales induites par $6K_2$

Un autre résultat important de cette thèse est la caractérisation du mouvement intracellulaire des usines virales induites par $6K_2$. Les usines virales sont des structures dynamiques, mobiles. Le cytoplasme est un milieu visqueux et encombré. Le mouvement des usines virales nécessite donc un transport actif qui implique le cytosquelette. Il semble pour certains virus que les microtubules soient impliqués dans le mouvement des usines virales (Greber and Way, 2006). Pour le TuMV nous avons observé que les usines virales se déplacent le long des microfilaments d'actine. Les usines virales bougent rapidement, s'immobilisent, puis repartent, leur vitesse moyenne de déplacement étant d'environ 0.45 µm/s. Lorsque les filaments d'actines sont dépolymérisés par un traitement à la latrunculine B, il n'y a plus de mouvement observé, et la production virale est diminuée de façon significative.

Au moment où nous avons fait ces observations, nous ne connaissions pas vraiment le rôle de ce mouvement intracellulaire dans le cycle viral du TuMV. Étant donné que la production de virus diminue drastiquement lorsque l'on dépolymérise les microfilaments, nous pensions que le mouvement des usines virales était impliqué dans la réplication. Mais en continuant mon projet de doctorat, nous avons vu que ces usines virales, qualifiées de périphériques, sont liées fonctionnellement avec la structure périnucléaire observée lors de l'infection. Certaines vésicules entrent et fusionnent avec la structure périnucléaire, d'autres vésicules en sortent, il y a un échange, une connexion.

Nous avons également observé que la destination finale dans la cellule de ce mouvement est la membrane plasmique. Les usines virales se rendent à la membrane plasmique pour se retrouver à proximité des PD, qui constituent la porte de sortie de la cellule pour le virus. De nombreuses études mentionnant le rôle des PD, des MP, de la voie de sécrétion, et du cytosquelette dans le mouvement des virus ont été publiées, mais l'entité virale qui circule n'a jamais été identifiée. En effet, nous avons montré que les vésicules peuvent s'accumuler le long de la membrane plasmique, et passer dans la cellule voisine comme il a été suggéré pour les usines virales du TMV par l'équipe du Dr Roger Beachy (Kawakami et al., 2004). Pour le TMV, le mouvement du complexe de réplication d'une cellule à une autre n'a pas été visualisé directement, mais a été estimé. Depuis ce résultat n'a jamais été

confirmé et la nature de l'entité virale qui circule de cellule en cellule fait toujours débat. Contrairement à l'équipe du D^r Beachy, nous avons directement visualisé le mouvement des usines virales qui passent d'une cellule à l'autre *in planta*. Les vésicules qui passent d'une cellule à l'autre mesurent environ 170nm ± 13 nm de diamètre, mais le TuMV augmente suffisamment la SEL des PD pour permettre leurs passages. Ce travail supporte l'idée que les PD sont modulables et que le TMV aussi pourrait circuler d'une cellule à l'autre sous forme d'usine virale intacte abritant l'ARNv et dont le mouvement serait facilité par les MP.

Un autre point important abordé dans cette thèse est la présence de vésicules marquées par $6K_2$ dans le xylème et contenant de l'ARNv. Ce résultat suggère qu'en plus d'être le véhicule pour passer d'une cellule à une autre, les vésicules formées par $6K_2$ sont également impliquées dans l'infection systémique. Le rôle de la protéine $6K_2$ apparaît bien plus important que ce que nous nous imaginions au départ. Le mouvement intracellulaire des usines virales que nous avons observé n'est en fait que la première étape du mouvement du TuMV, l'entité virale qui passe d'une cellule à l'autre est contenue dans une vésicule, enrobée par une membrane qui contient $6K_2$. Cependant, le contenu des usines virales qui passent d'une cellule à l'autre n'est toujours pas caractérisé. Notamment, il est important d'identifier les protéines hôtes associées à ces usines virales.

La présence d'un virus dans le xylème a déjà été rapportée (Opalka et al., 1998), mais il est plus commun pour un virus de plante d'utiliser le phloème pour se déplacer de façon systémique. Nous n'excluons pas la possibilité que les usines virales soient présentes dans le phloème également. Nous sommes en train d'explorer cette hypothèse en utilisant des plantes transgéniques qui expriment constitutivement des protéines fluorescentes sous contrôle d'un promoteur spécifique aux cellules du phloème. Des résultats très récents, qui ne sont pas encore publiés, montrent que les usines virales marquées par $6K_2$ peuvent être collectées dans la sève. Et lorsque l'on effectue une coloration négative de la sève collectée sur des plantes infectées par le TuMV, on observe en microscopie électronique la présence des particules virales (Daniel Garcia communication personnelle). Dans un futur proche, nous voulons isoler les vésicules marquées par $6K_2$ que l'on retrouve dans le xylème et faire une analyse protéomique afin de détecter les protéines hôtes associées aux vésicules. Un autre projet qui découle de

nos travaux, consiste à faire de la "cryofixation" sur la sève récoltée, et d'observer les usines virales et les particules virales en tomographie. La cryofixation est une technique de fixation qui en conserve l'ultrastructure des échantillons, spécialement les structures membranaires comme les vésicules $6K_2$

Les premiers résultats de tomographie que nous avons obtenus sur des cellules du mésophile de feuilles de *Nicotiana benthamiana* ont révélé la présence de particules virales qui s'accumulent dans la vacuole. Les particules virales sont entourées de membranes qui pourraient contenir la protéine $6K_2$. La présence de $6K_2$ reste à confirmer par des techniques immunologiques utilisant un anticorps secondaire couplé à des microparticules d'or ("immunogold"), mais si elle est confirmée cela voudrait dire que les lipides synthétisés de novo ne servent pas seulement à la traduction et à la réplication du TuMV, mais sont également impliquées dans le transport des particules virales.

4. Modèle illustrant la réplication et le transport du TuMV

À partir de nos résultats, nous avons élaboré un modèle qui décrit la réplication et le transport du TuMV (Figure 12). Après son entrée dans la cellule, le génome du TuMV est traduit et répliqué majoritairement dans la structure périnucléaire, bien que nous n'excluons pas la possibilité que les vésicules périphériques mobiles possèdent également une activité de traduction et de réplication virale. Les membranes de cette structure périnucléaire proviennent du système sécrétoire avec lequel elles entretiennent une connexion. Cette connexion est nécessaire au maintien de l'activité synthétique intense qui règne dans la structure périnucléaire. Des usines virales de plus petite taille vont se former à partir de la structure périnucléaire. Ces usines virales sont mobiles dans la cellule le long des TVS. Leur mouvement est soutenu par le réseau RE/actine et utilise préférentiellement la myosine XI-2.

Une fois arrivées à la membrane plasmique, les usines virales vont se retrouver à proximité des PD. Nous avons pu visualiser le passage des usines virales intactes d'une cellule à une autre. Le contenu de ces vésicules n'est pas encore totalement élucidé mais la RdRp, l'ARNv et 6K2 sont détectés.

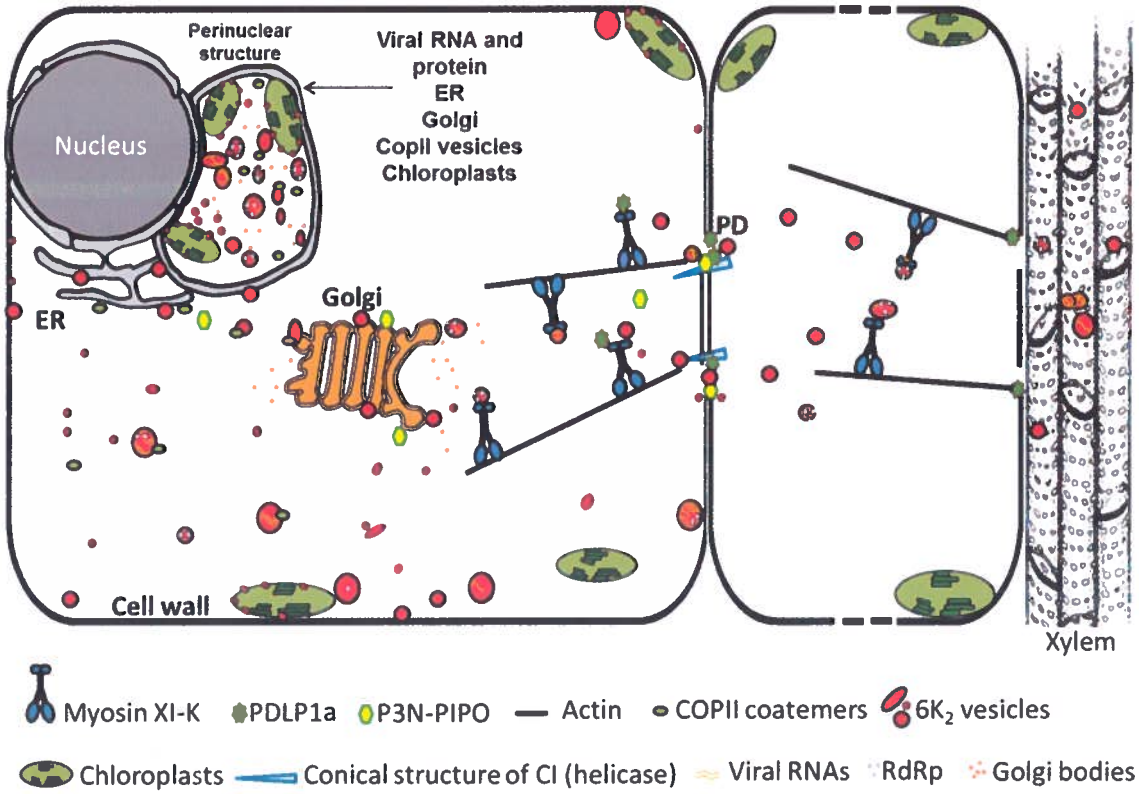

Figure 12: Modèle illustrant la réplication et le transport du TuMV.

Description de la figure dans le texte.

Ce mouvement à travers les PD est facilité par l'action de la protéine P3N-PIPO qui recrute PCAP1. La protéine virale CI semble aussi participer à ce mouvement de cellule à cellule en formant des structures coniques à proximité des PD.

Dans la cellule adjacente, le virus entame un nouveau cycle d'infection et va continuer son mouvement symplasmique jusqu'à atteindre le système vasculaire de la plante. Les vésicules marquées par $6K_2$ sont retrouvées dans le xylème, mais le mécanisme par lequel elles sont chargées dans le xylème reste méconnu. Il a été suggéré pour le virus de la panachure jaune du riz (RYMV, rice yellow mottle virus) qui se déplace également dans le xylème que le virus rentre dans les cellules du xylème lorsqu'elles sont en cours de différenciation (Opalka et al., 1998).

5. Conclusion

Dans la publication N°1 nous avons montré que les usines virales sont mobiles et contiennent de nombreux facteurs de traduction, ce qui suggère un couplage réplication/traduction dans les vésicules induites par $6K_2$. À cette époque il n'y avait pas beaucoup de groupes de recherches qui avaient émis cette hypothèse. De plus les travaux sur les mouvements intracellulaires des usines virales en étaient à leurs débuts.

Nos travaux sur les différents types d'usines virales que l'on retrouve dans les cellules infectées apportent une meilleure compréhension du cycle viral du TuMV. Pour la première fois concernant le TuMV nous avons mis en évidence la formation de deux types d'usines virales. La structure périnucléaire serait le lieu principal de la traduction et de la réplication, tandis que les petites usines virales mobiles serviraient à la propagation virale. Le rôle majeur joué par la protéine $6K_2$ a soulevé de nouvelles questions. Nous cherchons désormais à identifier les déterminants moléculaires de $6K_2$ qui permettent la formation de telles structures.

La visualisation du passage d'une usine virale intacte d'une cellule à une autre n'a jamais été observée auparavant, et remet en cause plusieurs dogmes en biologie végétale et en virologie. Je pense bien entendu à la taille d'exclusion des PD, qui apparaît comme extrêmement modulable par le virus, permettant le passage de vésicules d'environ 200nm. Une telle observation ouvre également la

porte à la possibilité d'un couplage de la réplication et du mouvement. Un tel couplage donne au virus un gain de temps considérable, et on peut penser que c'est ce mode de transport qui permet au virus d'infecter une nouvelle cellule tout les 3 heures.

La contribution du système sécrétoire à la création des usines virales et le besoin du cytosquelette de la cellule pour le mouvement du virus ont été démontrés. De plus, l'outil que nous avons mis au point pour étudier le mouvement cellule à cellule du TuMV s'est avéré très utile et pourra dans le futur permettre d'évaluer l'effet de certains traitements ou mutations sur le mouvement du TuMV.

BIBLIOGRAPHIE

Amari, K., Boutant, E., Hofmann, C., Schmitt-Keichinger, C., Fernandez-Calvino, L., Didier, P., Lerich, A., Mutterer, J., Thomas, C.L., Heinlein, M., Mély, Y., Maule, A.J., and Ritzenthaler, C. (2010). A Family of Plasmodesmal Proteins with Receptor-Like Properties for Plant Viral Movement Proteins. *PLoS Pathog* 6, e1001119.

Amari, K., Lerich, A., Schmitt-Keichinger, C., Dolja, V.V., and Ritzenthaler, C. (2011). Tubule-Guided Cell-to-Cell Movement of a Plant Virus Requires Class XI Myosin Motors. *PLoS Pathog* 7, e1002327.

Anandalakshmi, R., Pruss, G.J., Ge, X., Marathe, R., Mallory, A.C., Smith, T.H., and Vance, V.B. (1998). A viral suppressor of gene silencing in plants. *Proceedings of the National Academy of Sciences of the United States of America* 95, 13079-13084.

Andrea V. Gamarnik, R.A. (1998). Switch from translation to RNA replication in a positive-stranded RNAvirus. *Genes Dev.* 12, 2293–2304.

Anindya, R., Joseph J, Gowri Td, Savithri Hs. (2004). Complete genomic sequence of Pepper vein banding virus (PVBV): a distinct member of the genus Potyvirus. *Arch Virol.* 149, 625-632.

Anindya, R., and Savithri, H.S. (2004). Potyviral NIa Proteinase, a Proteinase with Novel Deoxyribonuclease Activity. *J. Biol. Chem.* 279, 32159-32169.

Astier, S., Robaglia, C., and Lecoq, H. (2006). Principles of plant virology. 472.

Bamunusinghe, D., Hemenway, C.L., Nelson, R.S., Sanderfoot, A.A., Ye, C.M., Silva, M.a.T., Payton, M., and Verchot-Lubicz, J. (2009). Analysis of potato virus X replicase and TGBp3 subcellular locations. *Virology* 393, 272-285.

Bamunusinghe, D., Seo, J.-K., and Rao, A.L.N. (2011). Subcellular Localization and Rearrangement of Endoplasmic Reticulum by Brome Mosaic Virus Capsid Protein. *Journal of Virology* 85, 2953-2963.

Barajas, D., Jiang, Y., and Nagy, P.D. (2009). A Unique Role for the Host ESCRT Proteins in Replication of Tomato bushy stunt virus. *PLoS Pathog* 5, e1000705.

Beauchemin, C., Boutet, N., and Laliberte, J.-F. (2007). Visualization of the Interaction between the Precursors of VPg, the Viral Protein Linked to the Genome of Turnip Mosaic Virus, and the Translation Eukaryotic Initiation Factor iso 4E In Planta. *J. Virol.* 81, 775-782.

Beauchemin, C., and Laliberté, J.-F. (2007). The Poly(A) Binding Protein Is Internalized in Virus-Induced Vesicles or Redistributed to the Nucleolus during Turnip Mosaic Virus Infection. *Journal of Virology* 81, 10905-10913.

Belov, G.A., Nair, V., Hansen, B.T., Hoyt, F.H., Fischer, E.R., and Ehrenfeld, E. (2012). Complex Dynamic Development of Poliovirus Membranous Replication Complexes. *Journal of Virology* 86, 302-312.

Brantley, J.D., and Hunt, A.G. (1993). The N-terminal protein of the polyprotein encoded by the potyvirus tobacco vein mottling virus is an RNA-binding protein. *J Gen Virol* 74, 1157-1162.

Browning, K.S. (2004). Plant translation initiation factors: It is not easy to be green. *Biochemical Society Transactions* 32, 589-591.

Byoung-Cheorl Kang, I.Y.J.D.F.J.F.M.M.M.J. (2005). The pvr1 locus in Capsicum encodes a translation initiation factor eIF4E that interacts with Tobacco etch virus VPg. *The Plant Journal* 42, 392-405.

Carette, J.E., Stuiver, M., Van Lent, J., Wellink, J., and Van Kammen, A. (2000). Cowpea Mosaic Virus Infection Induces a Massive Proliferation of Endoplasmic Reticulum but

Not Golgi Membranes and Is Dependent on De Novo Membrane Synthesis. *Journal of Virology* 74, 6556-6563.

Chen, S., Das, P., and And Hari, V. (1994). In situ localization of ATPase activity in cells of plants infected by maize dwarf mosaic potyvirus. . *Arch. Virol.* 134, pp. 433–439.

Choi, I.-R., Horken, K.M., Stenger, D.C., and French, R. (2005). An internal RNA element in the P3 cistron of Wheat streak mosaic virus revealed by synonymous mutations that affect both movement and replication. *Journal of General Virology* 86, 2605-2614.

Christensen, N., Tilsner, J., Bell, K., Hammann, P., Parton, R., Lacomme, C., and Oparka, K. (2009). The 5′ Cap of Tobacco Mosaic Virus (TMV) Is Required for Virion Attachment to the Actin/Endoplasmic Reticulum Network During Early Infection. *Traffic* 10, 536-551.

Chung, B.Y.-W., Miller, W.A., Atkins, J.F., and Firth, A.E. (2008). An overlapping essential gene in the Potyviridae. *Proceedings of the National Academy of Sciences* 105, 5897-5902.

Cotton, S., Grangeon, R., Thivierge, K., Mathieu, I., Ide, C., Wei, T., Wang, A., and Laliberté, J.-F. (2009). Turnip Mosaic Virus RNA Replication Complex Vesicles Are Mobile, Align with Microfilaments, and Are Each Derived from a Single Viral Genome. *Journal of Virology* 83, 10460-10471.

Covey, S.N., Al-Kaff, N.S., Langara, A., and Turner, D.S. (1997). Plants combat infection by gene silencing. *Nature* 385, 781-782.

Cronin, S., Verchot, J., Haldeman-Cahill, R., Schaad, M.C., and Carrington, J.C. (1995). Long-Distance Movement Factor: A Transport Function of the Potyvirus Helper Component Proteinase. *Plant Cell* 7, 549-559.

Daros, J.-A., Schaad, M.C., and Carrington, J.C. (1999). Functional Analysis of the Interaction between VPg-Proteinase (NIa) and RNA Polymerase (NIb) of Tobacco Etch Potyvirus, Using Conditional and Suppressor Mutants. *J. Virol.* 73, 8732-8740.

De Nova-Ocampo, M., Villegas-Sepúlveda, N., and Del Angel, R.M. (2002). Translation Elongation Factor-1[alpha], La, and PTB Interact with the 3' Untranslated Region of Dengue 4 Virus RNA. *Virology* 295, 337-347.

Den Boon, J.A., and Ahlquist, P. (2010). Organelle-Like Membrane Compartmentalization of Positive-Strand RNA Virus Replication Factories. *Annual Review of Microbiology* 64, 241-256.

Dufresne, P.J., Thivierge, K., Cotton, S., Beauchemin, C., Ide, C., Ubalijoro, E., Laliberté, J.-F., and Fortin, M.G. (2008). Heat shock 70 protein interaction with Turnip mosaic virus RNA-dependent RNA polymerase within virus-induced membrane vesicles. *Virology* 374, 217-227.

Duprat, A., Carole Caranta Frédéric Revers Benoît Menand Karen S. Browning Christophe Robaglia (2002). The Arabidopsis eukaryotic initiation factor (iso)4E is dispensable for plant growth but required for susceptibility to potyviruses. *The Plant Journal* 32, 927-934.

Eiamtanasate, S., Juricek, M., and Yap, Y.-K. (2007a). C-terminal hydrophobic region leads PRSV P3 protein to endoplasmic reticulum. *Virus Genes* 35, 611-617.

Eiamtanasate, S., Juricek, M., and Yap, Y.K. (2007b). C-terminal hydrophobic region leads PRSV P3 protein to endoplasmic reticulum. *Virus Genes* 35, 611-617.

Elena, S.F., and Rodrigo, G. (2012). Towards an integrated molecular model of plant–virus interactions. *Current Opinion in Virology* 2, 719-724.

Faso, C., Chen, Y.-N., Tamura, K., Held, M., Zemelis, S., Marti, L., Saravanan, R., Hummel, E., Kung, L., Miller, E., Hawes, C., and Brandizzi, F. (2009). A Missense Mutation in the Arabidopsis COPII Coat Protein Sec24A Induces the Formation of Clusters of the Endoplasmic Reticulum and Golgi Apparatus. *The Plant Cell Online* 21, 3655-3671.

Fauquet, C.M.M.a.M., J. Maniloff, U. Desselberger, and L.A. Ball (2005). Virus Taxonomy: VIIIth Report of the International Committee on Taxonomy of Viruses. *Elsevier Academic Press. San Diego.*

Fellers, J., Wan, J., Hong, Y., Collins, G.B., and Hunt, A.G. (1998). In vitro interactions between a potyvirus-encoded, genome-linked protein and RNA-dependent RNA polymerase. *J Gen Virol* 79, 2043-2049.

Flasinski, S.a.C., B. G. (1998). Potyvirus aphid transmission requires helper component and homologous coat protein for maximal efficiency *: Arch Virol.* 143(11).

Fridman, K., Mader, A., Zwerger, M., Elia, N., and Medalia, O. (2012). Advances in tomography: probing the molecular architecture of cells. *Nat Rev Mol Cell Biol* 13, 736-742.

Gao, Z., Eyers, S., Thomas, C., Ellis, N., and Maule, A. (2004). Identification of markers tightly linked to sbm recessive genes for resistance to Pea seed-borne mosaic virus. *TAG Theoretical and Applied Genetics* 109, 488-494.

Genovés, A., Navarro, J.A., and Pallás, V. (2010). The Intra- and Intercellular Movement of Melon necrotic spot virus (MNSV) Depends on an Active Secretory Pathway. *Molecular Plant-Microbe Interactions* 23, 263-272.

Goldbach, R. (1992). *The recombinative nature of potyviruses: implications for setting up true phylogenetic taxonomy, in "Potyvirus. "Taxonomy" Springer-Verlag Heidelberg, Berlin. (pp. 299-304)*

González-Jara, P., Fraile, A., Canto, T., and García-Arenal, F. (2009). The Multiplicity of Infection of a Plant Virus Varies during Colonization of Its Eukaryotic Host. *Journal of Virology* 83, 7487-7494.

Goodin, M., Yelton, S., Ghosh, D., Mathews, S., and Lesnaw, J. (2005). Live-Cell Imaging of Rhabdovirus-Induced Morphological Changes in Plant Nuclear Membranes. *Molecular Plant-Microbe Interactions* 18, 703-709.

Grangeon, R., Agbeci, M., Chen, J., Grondin, G., Zheng, H., and Laliberté, J.-F. (2012). Impact on the Endoplasmic Reticulum and Golgi Apparatus of Turnip Mosaic Virus Infection. *Journal of Virology* 86, 9255-9265.

Greber, U.F., and Way, M. (2006). A Superhighway to Virus Infection. *Cell* 124, 741-754.

Grzela, R., Strokovska, L., Andrieu, J.P., Dublet, B., Zagorski, W., and Chroboczek, J. (2006). Potyvirus terminal protein VPg, effector of host eukaryotic initiation factor eIF4E. *Biochimie* 88, 887-896.

Guo, D., Rajamaki, M.-L., Saarma, M., and Valkonen, J.P.T. (2001). Towards a protein interaction map of potyviruses: protein interaction matrixes of two potyviruses based on the yeast two-hybrid system. *J Gen Virol* 82, 935-939.

Gutiérrez, S., Yvon, M., Thébaud, G., Monsion, B., Michalakis, Y., and Blanc, S. (2010). Dynamics of the Multiplicity of Cellular Infection in a Plant Virus. *PLoS Pathog* 6, e1001113.

Hajimorad, M.R., Ding, X.S., Flasinski, S., Mahajan, S., Graff, E., Haldeman-Cahill, R., Carrington, J.C., and Cassidy, B.G. (1996). NIa and NIb of Peanut Stripe Potyvirus Are Present in the Nucleus of Infected Cells, but Do Not Form Inclusions. *Virology* 224, 368-379.

Han, S., and Sanfaçon, H. (2003). Tomato Ringspot Virus Proteins Containing the Nucleoside Triphosphate Binding Domain Are Transmembrane Proteins That Associate with the Endoplasmic Reticulum and Cofractionate with Replication Complexes. *Journal of Virology* 77, 523-534.

Hanton, S.L., Bortolotti, L.E., Renna, L., Stefano, G., and Brandizzi, F. (2005). Crossing the Divide – Transport Between the Endoplasmic Reticulum and Golgi Apparatus in Plants. *Traffic* 6, 267-277.

Harries, P.A., Park, J.-W., Sasaki, N., Ballard, K.D., Maule, A.J., and Nelson, R.S. (2009). Differing requirements for actin and myosin by plant viruses for sustained intercellular movement. *Proceedings of the National Academy of Sciences* 106, 17594-17599.

Harries, P.A., Schoelz, J.E., and Nelson, R.S. (2010). Intracellular Transport of Viruses and Their Components: Utilizing the Cytoskeleton and Membrane Highways. *Molecular Plant-Microbe Interactions* 23, 1381-1393.

Hatta, T., Bullivant, S., and Matthews, R.E.F. (1973). Fine Structure of Vesicles Induced in Chloroplasts of Chinese Cabbage Leaves by Infection with Turnip Yellow Mosaic Virus. *Journal of General Virology* 20, 37-50.

Haupt, S., Cowan, G.H., Ziegler, A., Roberts, A.G., Oparka, K.J., and Torrance, L. (2005). Two Plant–Viral Movement Proteins Traffic in the Endocytic Recycling Pathway. *The Plant Cell Online* 17, 164-181.

Hong, Y., and Hunt, A.G. (1996). RNA Polymerase Activity Catalyzed by a Potyvirus-Encoded RNA-Dependent RNA Polymerase. *Virology* 226, 146-151.

Hong, Y., Levay, K., Murphy, J.F., Klein, P.G., Shaw, J.G., and Hunt, A.G. (1995). A Potyvirus Polymerase Interacts with the Viral Coat Protein and VPg in Yeast Cells. *Virology* 214, 159-166.

Hsu, N.-Y., Ilnytska, O., Belov, G., Santiana, M., Chen, Y.-H., Takvorian, P.M., Pau, C., Van Der Schaar, H., Kaushik-Basu, N., Balla, T., Cameron, C.E., Ehrenfeld, E., Van Kuppeveld, F.J.M., and Altan-Bonnet, N. (2010). Viral Reorganization of the Secretory Pathway Generates Distinct Organelles for RNA Replication. *Cell* 141, 799-811.

Hyodo, K., Mine, A., Taniguchi, T., Kaido, M., Mise, K., Taniguchi, H., and Okuno, T. (2013). ADP ribosylation factor 1 plays an essential role in the replication of a plant RNA virus. *J Virol* 87, 163-176.

Jakubiec, A., Drugeon, G., Camborde, L., and Jupin, I. (2007). Proteolytic Processing of Turnip Yellow Mosaic Virus Replication Proteins and Functional Impact on Infectivity. *Journal of Virology* 81, 11402-11412.

Jiang, J., and Laliberté, J.-F. (2011). The genome-linked protein VPg of plant viruses-a protein with many partners. *Current Opinion in Virology* 1, 347-354.

Jonczyk, M., Pathak, K.B., Sharma, M., and Nagy, P.D. (2007). Exploiting alternative subcellular location for replication: Tombusvirus replication switches to the endoplasmic reticulum in the absence of peroxisomes. *Virology* 362, 320-330.

Kaido, M., Funatsu, N., Tsuno, Y., Mise, K., and Okuno, T. (2011). Viral cell-to-cell movement requires formation of cortical punctate structures containing Red clover necrotic mosaic virus movement protein. *Virology* 413, 205-215.

Kang Sh, L.W., Kim Kh. (2004). A protein interaction map of soybean mosaic virus strain G7H based on the yeast two-hybrid system. *Mol Cells.* 18(1), 122-126.

Kasschau, K.D., Cronin, S., and Carrington, J.C. (1997). Genome Amplification and Long-Distance Movement Functions Associated with the Central Domain of Tobacco Etch Potyvirus Helper Component-Proteinase. *Virology* 228, 251-262.

Kawakami, S., Watanabe, Y., and Beachy, R.N. (2004). Tobacco mosaic virus infection spreads cell to cell as intact replication complexes. *Proc Natl Acad Sci U S A* 101, 6291-6296.

Khan, M.A., Miyoshi, H., Ray, S., Natsuaki, T., Suehiro, N., and Goss, D.J. (2006). Interaction of Genome-linked Protein (VPg) of Turnip Mosaic Virus with Wheat Germ Translation Initiation Factors eIFiso4E and eIFiso4F. *J. Biol. Chem.* 281, 28002-28010.

Klein, P.G., Klein, R.R., Rodriguez-Cerezo, E., Hunt, A.G., and Shaw, J.G. (1994). Mutational Analysis of the Tobacco Vein Mottling Virus Genome. *Virology* 204, 759-769.

Knoops, K., Kikkert, M., Worm, S.H.E.V.D., Zevenhoven-Dobbe, J.C., Van Der Meer, Y., Koster, A.J., Mommaas, A.M., and Snijder, E.J. (2008). SARS-Coronavirus Replication Is Supported by a Reticulovesicular Network of Modified Endoplasmic Reticulum. *PLoS Biol* 6, e226.

Koenig, R., Lesemann, D.-E., and Pfeilstetter, E. (2009). New isolates of carnation Italian ringspot virus differ from the original one by having replication-associated proteins with a typical tombusvirus-like N-terminus and by inducing peroxisome- rather than mitochondrion-derived multivesicular bodies. *Archives of Virology* 154, 1695-1698.

Kopek, B.G., Perkins, G., Miller, D.J., Ellisman, M.H., and Ahlquist, P. (2007). Three-Dimensional Analysis of a Viral RNA Replication Complex Reveals a Virus-Induced Mini-Organelle. *PLoS Biol* 5, e220.

Laliberté, J.-F., Nicolas, O., Chatel, H., Lazure, C., and Morosoli, R. (1992). Release of a 22-kDa protein derived from the amino-terminal domain of the 49-kDa NIa of turnip mosaic potyvirus in Escherichia coli. *Virology* 190, 510-514.

Laliberté, J.-F., and Sanfaçon, H. (2010). Cellular Remodeling During Plant Virus Infection. *Annual Review of Phytopathology* 48, 69-91.

Langenberg, W.G., and Zhang, L. (1997). Immunocytology shows the presence of tobacco etch virus P3 protein in nuclear inclusions. *J Struct Biol* 118, 243-247.

Lee, W.-M., and Ahlquist, P. (2003). Membrane Synthesis, Specific Lipid Requirements, and Localized Lipid Composition Changes Associated with a Positive-Strand RNA Virus RNA Replication Protein. *Journal of Virology* 77, 12819-12828.

Lellis, A.D., Kasschau, K.D., Whitham, S.A., and Carrington, J.C. (2002). Loss-of-Susceptibility Mutants of Arabidopsis thaliana Reveal an Essential Role for eIF(iso)4E during Potyvirus Infection. *Current Biology* 12, 1046-1051.

Leonard, S., Viel, C., Beauchemin, C., Daigneault, N., Fortin, M.G., and Laliberte, J.-F. (2004). Interaction of VPg-Pro of Turnip mosaic virus with the translation initiation factor 4E and the poly(A)-binding protein in planta. *J Gen Virol* 85, 1055-1063.

Li, X.H., Valdez, P., Olvera, R.E., and Carrington, J.C. (1997). Functions of the tobacco etch virus RNA polymerase (NIb): subcellular transport and protein-protein interaction with VPg/proteinase (NIa). *J. Virol.* 71, 1598-1607.

Linnik, O., Liesche, J., Tilsner, J., and Oparka, K.J. (2013). Unraveling the structure of viral replication complexes at super-resolution. *Front Plant Sci* 4, 6.

Liu, C., and Nelson, R.S. (2013). The cell biology of Tobacco mosaic virus replication and movement. *Frontiers in Plant Science* 4.

Liu, L., Westler, W.M., Den Boon, J.A., Wang, X., Diaz, A., Steinberg, H.A., and Ahlquist, P. (2009). An Amphipathic α-Helix Controls Multiple Roles of Brome Mosaic Virus Protein 1a in RNA Replication Complex Assembly and Function. *PLoS Pathog* 5, e1000351.

Maia, I.G., Haenni, A.-L., and Bernardi, F. (1996). Potyviral HC-Pro: a multifunctional protein. *J Gen Virol* 77, 1335-1341.

Martínez-Gil, L., Saurí, A., Vilar, M., Pallás, V., and Mingarro, I. (2007). Membrane insertion and topology of the p7B movement protein of Melon Necrotic Spot Virus (MNSV). *Virology* 367, 348-357.

Maule, A.J., Benitez-Alfonso, Y., and Faulkner, C. (2011). Plasmodesmata – membrane tunnels with attitude. *Current Opinion in Plant Biology* 14, 683-690.

Mccartney, A., Greenwood, J., Fabian, M., White, K., and Mullen, R. (2005a). Localization of the tomato bushy stunt virus replication protein p33 reveals a peroxisome-to-endoplasmic reticulum sorting pathway. *Plant Cell* 17, 3513 - 3531.

Mccartney, A.W., Greenwood, J.S., Fabian, M.R., White, K.A., and Mullen, R.T. (2005b). Localization of the Tomato Bushy Stunt Virus Replication Protein p33 Reveals a Peroxisome-to-Endoplasmic Reticulum Sorting Pathway. *The Plant Cell Online* 17, 3513-3531.

Merits, A., Guo, D., and Saarma, M. (1998). VPg, coat protein and five non-structural proteins of potato A potyvirus bind RNA in a sequence-unspecific manner. *J Gen Virol* 79, 3123-3127.

Michon, T., Yannick Estevez Jocelyne Walter Sylvie German-Retana Olivier Gall (2006). The potyviral virus genome-linked protein VPg forms a ternary complex with the eukaryotic initiation factors eIF4E and eIF4G and reduces eIF4E affinity for a mRNA cap analogue. *FEBS Journal* 273, 1312-1322.

Mizumoto , H., Iwakawa, H.-O., Kaido, M., Mise, K., and Okuno, T. (2006). Cap-Independent Translation Mechanism of Red Clover Necrotic Mosaic Virus RNA2 Differs from That of RNA1 and Is Linked to RNA Replication. *Journal of Virology* 80, 3781-3791.

Mochizuki, T., Hirai, K., Kanda, A., Ohnishi, J., Ohki, T., and Tsuda, S. (2009). Induction of necrosis via mitochondrial targeting of Melon necrotic spot virus replication protein p29 by its second transmembrane domain. *Virology* 390, 239-249.

Nagy, P.D. (2008). Yeast as a Model Host to Explore Plant Virus-Host Interactions. *Annual Review of Phytopathology* 46, 217-242.

Nagy, P.D.P., Judit (2012). The dependence of viral RNA replication on co-opted host factors. *Nat Rev Micro* 10, 137-149.

Nakano, R.T., Matsushima, R., Ueda, H., Tamura, K., Shimada, T., Li, L., Hayashi, Y., Kondo, M., Nishimura, M., and Hara-Nishimura, I. (2009). GNOM-LIKE1/ERMO1 and SEC24a/ERMO2 Are Required for Maintenance of Endoplasmic Reticulum Morphology in Arabidopsis thaliana. *The Plant Cell Online* 21, 3672-3685.

Nguyen, M., and Haenni, A.-L. (2003). Expression strategies of ambisense viruses. *Virus Research* 93, 141-150.

Nicaise, V., Gallois, J.-L., Chafiai, F., Allen, L.M., Schurdi-Levraud, V., Browning, K.S., Candresse, T., Caranta, C., Le Gall, O., and German-Retana, S. (2007). Coordinated and selective recruitment of eIF4E and eIF4G factors for potyvirus infection in Arabidopsis thaliana. *FEBS Letters* 581, 1041-1046.

Nicaise, V., German-Retana, S., Sanjuan, R., Dubrana, M.-P., Mazier, M., Maisonneuve, B., Candresse, T., Caranta, C., and Legall, O. (2003). The Eukaryotic Translation Initiation Factor 4E Controls Lettuce Susceptibility to the Potyvirus Lettuce mosaic virus. *Plant Physiol.* 132, 1272-1282.

Nishikiori, M., Mori, M., Dohi, K., Okamura, H., Katoh, E., Naito, S., Meshi, T., and Ishikawa, M. (2011). A Host Small GTP-binding Protein ARL8 Plays Crucial Roles in Tobamovirus RNA Replication. *PLoS Pathog* 7, e1002409.

Oh, C.-S., and Carrington, J.C. (1989). Identification of essential residues in potyvirus proteinase HC-pro by site-directed mutagenesis. *Virology* 173, 692-699.

Opalka, N., Brugidou, C., Bonneau, C., Nicole, M., Beachy, R.N., Yeager, M., and Fauquet, C. (1998). Movement of rice yellow mottle virus between xylem cells through pit membranes. *Proceedings of the National Academy of Sciences* 95, 3323-3328.

Ortìn, J., and Parra, F. (2006). Structure and Function of RNA Replication. *Annual Review of Microbiology* 60, 305.

Pruss, G., Ge, X., Shi, X.M., Carrington, J.C., and Vance, V.B. (1997). Plant Viral Synergism: The Potyviral Genome Encodes a Broad-Range Pathogenicity Enhancer That Transactivates Replication of Heterologous Viruses. *Plant Cell* 9, 859-868.

Restrepo-Hartwig, M.A., and Carrington, J.C. (1992). Regulation of nuclear transport of a plant potyvirus protein by autoproteolysis. *J. Virol.* 66, 5662-5666.

Riechmann, J.L., Lain, S., and Garcia, J.A. (1992). Highlights and prospects of potyvirus molecular biology. *J Gen Virol* 73, 1-16.

Ritzenthaler, C. (2011). Parallels and distinctions in the direct cell-to-cell spread of the plant and animal viruses. *Current Opinion in Virology* 1, 403-409.

Ritzenthaler, C., Laporte, C., Gaire, F., Dunoyer, P., Schmitt, C., Duval, S., Piéquet, A., Loudes, A.M., Rohfritsch, O., Stussi-Garaud, C., and Pfeiffer, P. (2002). Grapevine Fanleaf Virus Replication Occurs on Endoplasmic Reticulum-Derived Membranes. *Journal of Virology* 76, 8808-8819.

Rodriguez-Cerezo, E., Ammar, E.D., Pirone, T.P., and Shaw, J.G. (1993). Association of the non-structural P3 viral protein with cylindrical inclusions in potyvirus-infected cells. *J Gen Virol* 74, 1945-1949.

Rojas, M.R., Zerbini, F.M., Allison, R.F., Gilbertson, R.L., and Lucas, W.J. (1997). Capsid Protein and Helper Component-Proteinase Function as Potyvirus Cell-to-Cell Movement Proteins. *Virology* 237, 283-295.

Rubino, L., and Russo, M. (1998). Membrane targeting sequences in tombusvirus infections. *Virology* 252, 431 - 437.

Rubino, L., Weber-Lofti, F., Dietrich, A., Stussi-Garaud, C., and Russo, M. (2001). The open reading frame 1-encoded ('36K') protein of carnation Italian ringspot virus localizes to mitochondria. *J Gen Virol* 82, 29 - 34.

Ruffel, S., Dussault M.H., Palloix, A., Moury, B., Bendahmane A., Robaglia C., Caranta, C. (2002). A natural recessive resistance gene against potato virus Y in pepper corresponds to the eukaryotic initiation factor 4E (eIF4E). *The Plant Journal* 32, 1067-1075.

Ruffel, S., Gallois, J., Lesage, M., and Caranta, C. (2005). The recessive potyvirus resistance gene pot-1 is the tomato orthologue of the pepper pvr2-eIF4E gene. *Molecular Genetics and Genomics* 274, 346-353.

Ruthardt, N., Gulde, N., Spiegel, H., Fischer, R., and Emans, N. (2005). Four-dimensional imaging of transvacuolar strand dynamics in tobacco BY-2 cells. *Protoplasma* 225, 205-215.

Salánki, K., Kiss, L., Gellért, Á., and Balázs, E. (2011). Identification a coat protein region of cucumber mosaic virus (CMV) essential for long-distance movement in cucumber. *Archives of Virology* 156, 2279-2283.

Schaad, M.C., Anderberg, R.J., and Carrington, J.C. (2000). Strain-Specific Interaction of the Tobacco Etch Virus NIa Protein with the Translation Initiation Factor eIF4E in the Yeast Two-Hybrid System. *Virology* 273, 300-306.

Schaad, M.C., Haldeman-Cahill, R., Cronin, S., and Carrington, J.C. (1996). Analysis of the VPg-proteinase (NIa) encoded by tobacco etch potyvirus: effects of mutations on subcellular transport, proteolytic processing, and genome amplification. *J. Virol.* 70, 7039-7048.

Schaad, M.C., Jensen, P.E., and Carrington, J.C. (1997). Formation of plant RNA virus replication complexes on membranes: role of an endoplasmic reticulum-targeted viral protein. *EMBO J* 16, 4049 - 4059.

Schaad, M.C., P E Jensen, and J C Carrington (1997). Formation of plant RNA virus replication complexes on membranes: role of an endoplasmic reticulum-targeted viral protein. *EMBO J.* 16(13), 4049–4059.

Schwartz, M., Chen, J., Lee, W.-M., Janda, M., and Ahlquist, P. (2004). Alternate, virus-induced membrane rearrangements support positive-strand RNA virus genome replication. *Proceedings of the National Academy of Sciences of the United States of America* 101, 11263-11268.

Sharma, M., Sasvari, Z., and Nagy, P.D. (2011). Inhibition of phospholipid biosynthesis decreases the activity of the tombusvirus replicase and alters the subcellular localization of replication proteins. *Virology* 415, 141-152.

Shukla, D.D., C. W. Ward (1989). Structure of potyvirus coat proteins and application in the taxonomy of the potyvirus group. *Adv. Virus Res.*, 273-314.

Soumounou, Y., and Laliberte, J.-F. (1994). Nucleic acid-binding properties of the P1 protein of turnip mosaic potyvirus produced in Escherichia coli. *J Gen Virol* 75, 2567-2573.

Staehelin, L.A. (1997). The plant ER: a dynamic organelle composed of a large number of discrete functional domains. *The Plant Journal* 11, 1151-1165.

Steil, B.P., and Barton, D.J. (2008). Cis-active RNA elements (CREs) and picornavirus RNA replication. *Virus Research* In Press, Corrected Proof.

Su, S., Liu, Z., Chen, C., Zhang, Y., Wang, X., Zhu, L., Miao, L., Wang, X.-C., and Yuan, M. (2010). Cucumber Mosaic Virus Movement Protein Severs Actin Filaments to Increase the Plasmodesmal Size Exclusion Limit in Tobacco. *The Plant Cell Online* 22, 1373-1387.

Suehiro, N., Natsuaki, T., Watanabe, T., and Okuda, S. (2004). An important determinant of the ability of Turnip mosaic virus to infect Brassica spp. and/or Raphanus sativus is in its P3 protein. *J Gen Virol* 85, 2087-2098.

Thivierge, K., Cotton, S., Dufresne, P.J., Mathieu, I., Beauchemin, C., Ide, C., Fortin, M.G., and Laliberté, J.-F. (2008). Eukaryotic elongation factor 1A interacts with Turnip mosaic virus RNA-dependent RNA polymerase and VPg-Pro in virus-induced vesicles. *Virology* 377, 216-225.

Tilsner, J., Linnik, O., Wright, K.M., Bell, K., Roberts, A.G., Lacomme, C., Santa Cruz, S., and Oparka, K.J. (2012). The TGB1 Movement Protein of Potato virus X Reorganizes Actin and Endomembranes into the X-Body, a Viral Replication Factory. *Plant Physiology* 158, 1359-1370.

Tilsner, J., and Oparka, K.J. (2012). Missing links? — The connection between replication and movement of plant RNA viruses. *Current Opinion in Virology* 2, 705-711.

Turner, K.A., Sit, T.L., Callaway, A.S., Allen, N.S., and Lommel, S.A. (2004). Red clover necrotic mosaic virus replication proteins accumulate at the endoplasmic reticulum. *Virology* 320, 276-290.

Urcuqui-Inchima, S., Haenni, A.-L., and Bernardi, F. (2001). Potyvirus proteins: a wealth of functions. *Virus Research* 74, 157-175.

Verchot-Lubicz, J., Torrance, L., Solovyev, A.G., Morozov, S.Y., Jackson, A.O., and Gilmer, D. (2010). Varied Movement Strategies Employed by Triple Gene Block–Encoding Viruses. *Molecular Plant-Microbe Interactions* 23, 1231-1247.

Verchot-Lubicz, J., Ye, C.-M., and Bamunusinghe, D. (2007). Molecular biology of potexviruses: recent advances. *Journal of General Virology* 88, 1643-1655.

Verchot, J., Herndon, K.L., and Carrington, J.C. (1992). Mutational analysis of the tobacco etch potyviral 35-kDa proteinase: Identification of essential residues and requirements for autoproteolysis. *Virology* 190, 298-306.

Vijayapalani, P., Maeshima, M., Nagasaki-Takekuchi, N., and Miller, W.A. (2012). Interaction of the Trans-Frame Potyvirus Protein P3N-PIPO with Host Protein PCaP1 Facilitates Potyvirus Movement. *PLoS Pathog* 8, e1002639.

Walsh, J.A., and Jenner, C.E. (2002). Turnip mosaic virus and the quest for durable resistance. *Molecular Plant Pathology* 3, 289-300.

Wang, X., Ullah, Z., and Grumet, R. (2000). Interaction between Zucchini Yellow Mosaic Potyvirus RNA-Dependent RNA Polymerase and Host Poly-(A) Binding Protein. *Virology* 275, 433-443.

Weber-Lotfi, F., Dietrich, A., Russo, M., and Rubino, L. (2002). Mitochondrial targeting and membrane anchoring of a viral replicase in plant and yeast cells. *J Virol*, 10485 - 10496.

Wei, T., Shimizu, T., Hagiwara, K., Kikuchi, A., Moriyasu, Y., Suzuki, N., Chen, H., and Omura, T. (2006). Pns12 protein of Rice dwarf virus is essential for formation of viroplasms and nucleation of viral-assembly complexes. *Journal of General Virology* 87, 429-438.

Wei, T., and Wang, A. (2008). Biogenesis of Cytoplasmic Membranous Vesicles for Plant Potyvirus Replication Occurs at Endoplasmic Reticulum Exit Sites in a COPI- and COPII-Dependent Manner. *Journal of Virology* 82, 12252-12264.

Wei, T., Zhang, C., Hong, J., Xiong, R., Kasschau, K.D., Zhou, X., Carrington, J.C., and Wang, A. (2010). Formation of Complexes at Plasmodesmata for Potyvirus Intercellular Movement Is Mediated by the Viral Protein P3N-PIPO. *PLoS Pathog* 6, e1000962.

Welsch, S., Miller, S., Romero-Brey, I., Merz, A., Bleck, C.K.E., Walther, P., Fuller, S.D., Antony, C., Krijnse-Locker, J., and Bartenschlager, R. (2009). Composition and Three-

Dimensional Architecture of the Dengue Virus Replication and Assembly Sites. *Cell Host & Microbe* 5, 365-375.

Wittmann, S., Chatel, H., Fortin, M.G., and Laliberté, J.-F. (1997). Interaction of the Viral Protein Genome Linked of Turnip Mosaic Potyvirus with the Translational Eukaryotic Initiation Factor (iso) 4E ofArabidopsis thalianaUsing the Yeast Two-Hybrid System. *Virology* 234, 84-92.

Zeenko, V.V., Ryabova, L.A., Spirin, A.S., Rothnie, H.M., Hess, D., Browning, K.S., and Hohn, T. (2002). Eukaryotic Elongation Factor 1A Interacts with the Upstream Pseudoknot Domain in the 3' Untranslated Region of Tobacco Mosaic Virus RNA. *J. Virol.* 76, 5678-5691.

CHAPITRE 4: AUTRES CONTRIBUTIONS

Revue n° 1

A model for the biogenesis of turnip mosaic virus replication factories

Communicative & Integrative Biology 3:4, 363-365; July/August 2010

Addendum to: Cotton S, Grangeon R, Thivierge K, Mathieu I, Ide C, Wei T, et al. Turnip mosaic virus RNA replication complex vesicles are mobile, align with microfilaments, and are each derived from a single viral genomeJ Virol2009831046010471 doi: 10.1128/JVI.00819-09.

Romain Grangeon, Sophie Cotton and Jean-François Laliberté*

Institut National de la Recherche Scientifique; INRS-Institut Armand-Frappier; Laval, QC Canada

* Corresponding author : Jean-François Laliberté
Email: jeanfrancois.laliberte@iaf.inrs.ca

Contribution

J'ai écrit 50% du texte, Sophie Cotton a écrit les 50% restant. Jean-François Laliberté a supervisé l'écriture et effectué les modifications finales.

Résumé

Des plants de *Nicotiana benthamiana* ont été agroinfiltrés avec un clone infectieux du virus de la mosaïque du navet (TuMV) qui a été conçu pour marquer les vésicules de réplication avec la GFP ou avec mCherry.Des structures ponctuées, appelées vésicules, ont été observées dans le cytoplasme des cellules infectées correspondant aux usines de réplication virale. Les vésicules sont très mobiles le long des microfilaments d'actine. L'utilisation de latrunculine B, un inhibiteur de polymérisation des microfilaments, réduit l'accumulation du virus, ce qui suggère que les microfilaments sont nécessaires à l'infection. Pour étudier la biogenèse des vésicules, des feuilles ont été infectées simultanément avec deux clones infectieux TuMV, un qui induit des vésicules marquées en rouge et l'autre en vert. Nous avons observé dans les cellules infectées par les deux virus des vésicules seulement rouges ou vertes, indiquant que la formation des usines virale ne provient que d'un seul génome. Dans certains cas, les vésicules présentent des secteurs contenant de fluorescence verte, rouge et jaune. Ce qui illustre la capacité que possèdent ces vésicules de fusionner entres elles`à un moment donné pendant l'infection. Sur la base de ces résultats, nous proposons un modèle pour la biogenèse de l'usine virale, où la traduction et la réplication virale sont étroitement couplées dans les vésicules induites par le virus.

Abstract

Nicotiana benthamiana plants were agroinfiltrated with an infectious clone of the Turnip mosaic virus (TuMV) that was engineered to tag replication vesicles with either GFP or mCherry fluorescent proteins. Punctuate vesicle structures were observed in the cytoplasm of infected cells corresponding to viral replication factories. The vesicles were highly motile and co-aligned with the microfilaments. Utilization of latrunculin B, an inhibitor of microfilament polymerization, reduced accumulation of the virus, suggesting that microfilaments are necessary during

infection. To investigate biogenesis of the vesicles, leaves were infected simultaneously with two recombinant TuMV infectious clones, one that labeled vesicles in red and one that labeled them in green. We observed cell with green only and red only vesicles indicating a single viral genome origin. In some cases, vesicles exhibited sectors of green, red and yellow fluorescence were also observed, demonstrating that fusion among individual vesicles is possible. Based on those results we propose a model for the biogenesis of viral factory, where viral translation and replication are tightly coupled within virus-induced vesicles.

Introduction

Over the past years, a large number of investigations have been devoted to understanding virus-host interactions at the molecular level. Concurrent to these molecular studies, an avenue of investigation at the interface of molecular virology and cell biology has emerged. These studies have shown that animal as well as plant RNA viruses induce substantial cellular remodeling during infection.1 Many of these virus-induced structures are organelles that house the RNA replication complex, and for that reason are given the generic term of replication factories. These factories contain positive and negative strand viral RNAs and the viral RNA-dependent RNA polymerase (RdRp), along with non-structural viral and host proteins. It has been proposed that virus-induced factories increase the local concentration of components required for replication, protect viral RNA from degradation and prevent the activation of host defense functions. Current questions centre on the membrane origins that give rise to the virus-induced factories and the molecular motors as well as pathways that are involved in their trafficking from their site of origin to their final destination. The origin and nature of these virus-induced membrane structures differ according to the virus families (1) In most cases, the modifications involve the formation of spherules, vesicles or multivesicular bodies derived from membranes of the endoplasmic reticulum (ER), mitochondria, peroxisomes, lysomes or chloroplasts. Electron tomography has recently been used for the generation of three-dimensional imaging of Dengue virus- and coronavirus-induced membrane alterations at high resolution. These alterations resulted in a reticulovesicular network of modified ER that integrates convoluted membranes, numerous interconnected double membrane vesicles and "vesicle packets"(2,3) The

three-dimensional renderings of these membrane networks show a spatio-temporal platform for the virus replication cycle, and suggest that not only RNA replication but also translation and virion assembly are associated with these virus-induced structures.

Turnip mosaic virus (TuMV) is an excellent model to study plant virus replication factory formation. TuMV has a positive-strand RNA genome of approximately 10 kb long, with a viral genomelinked protein (VPg) covalently linked to its 5′ end and a poly(A) tail at its 3′ end. The genomic RNA is translated into one polyprotein of 358 kDa that is processed into at least 10 mature proteins by viral proteases. Viral replication takes place in virus-induced vesicles derived from the ER (Fig. 1A) and the expression of a single viral protein (i.e., $6K_2$-VPg-Pro) is sufficient to induce vesicle formation (**4**). However, many questions are unresolved concerning TuMV vesicle biogenesis and content.

Vesicle Movement on Microfilaments

Virus replication factories are dynamic structures (**5–7**). We thus investigated the trafficking of TuMV-induced vesicles by confocal microscopy with an infectious clone that was engineered to tag replication vesicles with either GFP or mCherry fluorescent proteins. The observed vesicles were irregular in shape and varied in size, ranging from 0.6 to 4.3 μm in diameter. Interestingly, some vesicles were highly motile with an average velocity of 0.45 μm/s. Their movement was unidirectional and was characterized by a stop and go activity. Occasionally, fusion was observed between vesicles in the perinuclear zone. Because of the high viscosity of the cytoplasm, movement of large complexes requires an active transport with implication of cytoskeleton elements. When an actin marker fused to GFP was co-expressed, it was observed that the TuMV vesicles co-aligned with the microfilaments (Fig. 1B). When a low concentration (5 μM) of Latrunculin B (latB), which inhibits microfilament polymerization, was applied factory movement was stopped and virus production was significantly decreased.

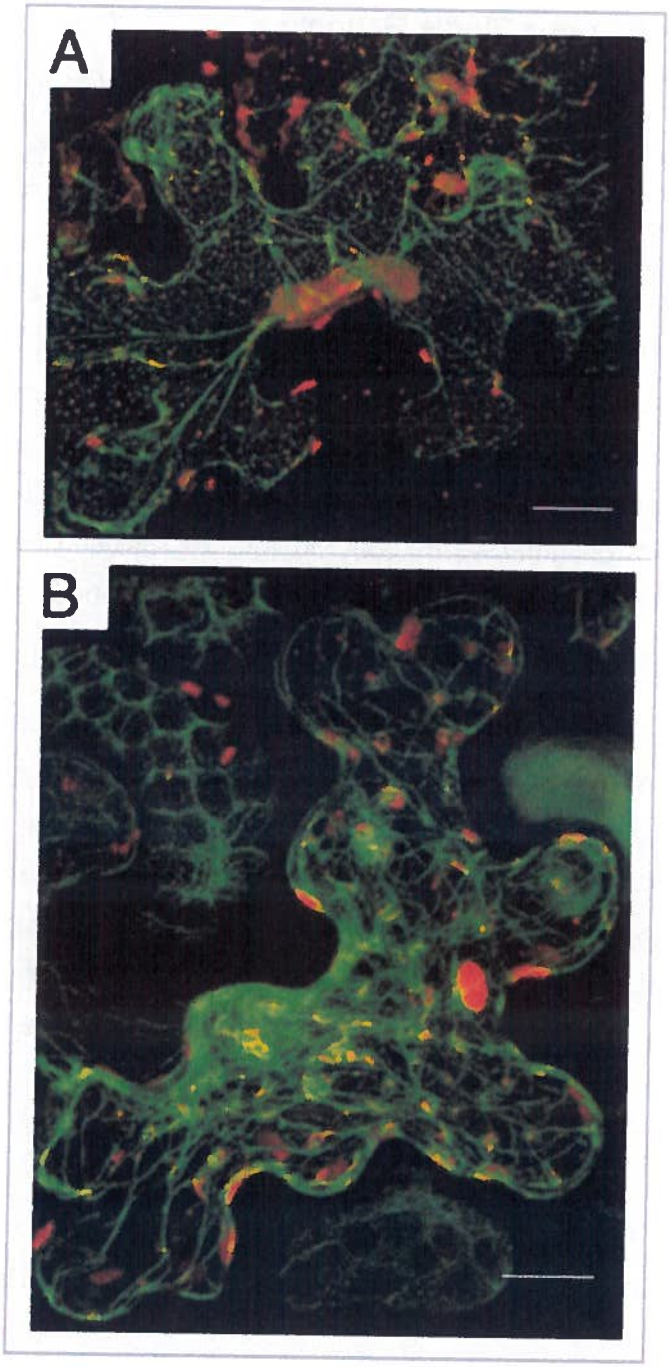

Figure 1: TuMV replication factories are associated with ER and co-allign with microfilaments.

Nicotiana benthamiana cells expressing mCherry-tagged TuMV-induced replication factories and ER -resident GFP (A) or the actin domain of fimbrin fused to GFP (B) observed by confocal microscopy at 4 days post-agroinfiltration. Photographs are a three-dimensional rendering of 40 1-µm thick slices that overlap by 0.5-µm. Scale bar, 10 µm.

Each Vesicle Derived from a Single Genome

One may also ask how viral proteins are imported within the replication factories. It is generally assumed that viral RNA translation is taking place in the cytoplasm and the newly synthesized proteins are exported in trans to virus-induced, pre-formed, vesicles. Since many translation factors have been found within the TuMV-induced vesicles (**8–10**) it is possible that translation instead occurs within the factories or is tightly associated with them. To resolve this issue, leaves were infected simultaneously with two recombinant TuMV infectious clones, one that labeled vesicles in red and one that labeled them in green. Following agro-infection, individual cells were screened for the expression of both green and red vesicles. The rational is that in a cell infected by both viruses, if translation happens in the cytoplasm and proteins are exported randomly to the vesicles, both green and red fluorescing vesicles should be observed.

However, if translation occurs within the vesicle, green- and red-only vesicles should be detected. What was observed were cells with individual green-only and red-only vesicles, suggesting a single-genome origin for each vesicle. Interestingly, vesicles exhibiting sectors of green, red and yellow colors were also observed, possibly resulting from a fusion between vesicles, a phenomenon that was noticed previously during vesicle trafficking. Formation of vesicles derived from a single viral genome indicates the existence of a cis mechanism that incorporates the proteins synthesized from a same viral RNA into the same vesicle. A mechanistic explanation is that viral RNA translation and replication occurs within the factories, and this was shown by the co-localization of several host translation factors with viral double-stranded RNA, a marker of viral RNA replication. This close coupling between viral replication and translation was recently suggested by Hafren and co-authors (**11**).

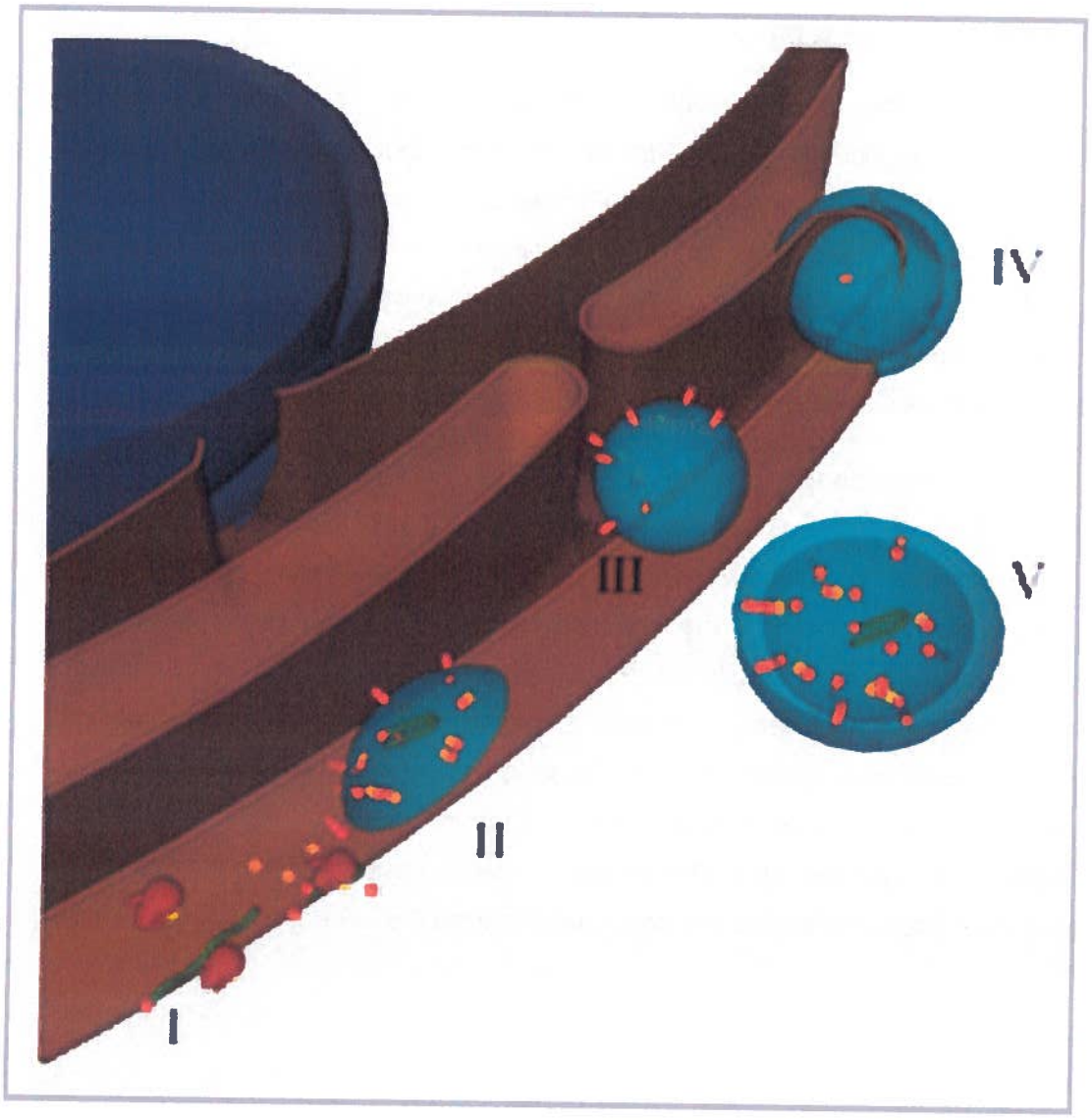

Figure 2: Model for the formation of virus-induced vesicles.

The blue sphere represents the nucleus, while the brown structure the ER. Partially transparent virus-induced vesicles are in light blue. Green ribbons and red spheres and rods depict viral RN As and proteins, respectively. Host proteins are the orange cubes, and the brown and yellow structures are ribosomes.

Factory Biogenesis: A Model

Based on the above results and those of others, a model where viral translation and replication is coupled within TuMV-induced vesicles is being proposed. The sequential steps can be schematized as follows (Fig. 2). Upon release of the genomic RNA into the cytoplasm, the host protein synthetic machinery is usurped for the production of viral proteins, on ER-associated ribosomes (step I in the figure). After several rounds of viral RNA translation, viral proteins accumulate in patches on the outer ER membrane and

initiate membrane curvature (II). During this process, the translation machinery through protein interaction with viral factors and viral RNA are trapped within the vesicles. Translation keeps going on within the vesicles and the newly produced proteins contribute to the size increase and maturation of the vesicles. A switch then happens from translation to replication to allow the viral RNA synthesis within in the same vesicles. Membrane curvature increases with accumulating replication components, which ultimately leads to the formation of single-membrane vesicles within the organelle lumen, which may or may not have a pore-like connection to the exterior (III). The clusters of large vesicles observed within the cytoplasm are produced during a second budding from the ER (IV-V).

Conclusion

Future issues will be to obtain a more refined 3-dimensional view of TuMV factories in order to better understand the interplay between virus RNA replication and various viral processes, such as translation and encapsidation. A corollary will be to determine the full content of host proteins and the mechanistic role for their presence in virus factories. Finally, trafficking and the fate of virus factories in cell-to-cell and long distance transport need to be investigated.

References

1. Miller S, Krijnse-Locker J. Modification of intracellular membrane structures for virus replication. Nat Rev Microbiol. 2008;6:363–374.

2. Knoops K, Kikkert M, Worm SH, Zevenhoven-Dobbe JC, van der Meer Y, et al. SARS-coronavirus replication is supported by a reticulovesicular network of modified endoplasmic reticulum. PLoS Biol.2008;6:226.

3. Welsch S, Miller S, Romero-Brey I, Merz A, Bleck CK, et al. Composition and three-dimensional architecture of the dengue virus replication and assembly sites. Cell Host Microbe. 2009;5:365–375.

4. Beauchemin C, Boutet N, Laliberté J-F. Visualization of the interaction between the precursors of VPg, the viral protein linked to the genome of turnip mosaic virus, and the translation eukaryotic initiation factor iso 4E in Planta. J Virol. 2007;81:775–782.

5. Harries PA, Palanichelvam K, Yu W, Schoelz JE, Nelson RS. The Cauliflower mosaic virus protein P6 forms motile inclusions that traffic along actin microfilaments and stabilize microtubules. Plant Physiol.2009;149:1005–1016.

6. Liu J-Z, Blancaflor EB, Nelson RS. The *Tobacco mosaic virus* 126-kilodalton protein, a constituent of the virus replication complex, alone of within the complex aligns with and traffics along microfilaments.Plant Physiol. 2005;138:1853–1865.

7. Lai C-K, Jeng K-S, Machida K, Lai MMC. Association of Hepatitis C virus replication complexes with microtubules and actin filaments is dependent on the interaction of NS3 and NS5A. J Virol.2008;82:8838–8848.

8. Beauchemin C, Laliberté J-F. The poly(A) binding protein is internalized in virus-induced vesicles or redistributed to the nucleolus during turnip mosaic virus infection. J Virol. 2007;81:10905–10913.

9. Dufresne PJ, Thivierge K, Cotton S, Beauchemin C, Ide C, et al. Heat shock 70 protein interaction with Turnip mosaic virus RNA-dependent RNA polymerase within virus-induced membrane vesicles.Virology. 2008;374:217–227.

10. Thivierge K, Cotton S, Dufresne PJ, Mathieu I, Beauchemin C, et al. Eukaryotic elongation factor 1A interacts with Turnip mosaic virus RNA-dependent RNA polymerase and VPg-Pro in virus-induced vesicles. Virology. 2008;377:216–225.

11. Hafren A, Hofius D, Ronnholm G, Sonnewald U, Makinen K. HSP70 and its cochaperone CPIP promote Potyvirus infection in *Nicotiana benthamiana* by regulating viral coat Protein functions. Plant Cell. 2010;22:523–535.

Revue n° 2

Host endomembrane recruitment for plant RNA virus replication

Current Opinion in Virology

Volume 2, Issue 6, December 2012, Pages 683–690

Romain Grangeon, Jun Jiang and Jean-François Laliberté

Institut National de la Recherche Scientifique; INRS-Institut Armand-Frappier; Laval, QC Canada

* Corresponding author : Jean-François Laliberté

Email: jeanfrancois.laliberte@iaf.inrs.ca

Contribution

J'ai écrit 60% du texte, et Jun Jiang a écrit les 40% restant. Jean-François Laliberté a supervisé l'écriture et effectué les modifications finales.

Résumé

Bien qu'il existe une quantité importante de littérature qui traite de l'identification des plantes protéines virales impliquées dans le remodelage de la membrane et la production de vésicules dans les cellules infectées, il ya très peu d'études qui rendent compte de l'impact que l'infection a sur l'architecture globale et sur la dynamique des membranes du système sécrétoire. Des études récentes ont montré que pour certains virus, le réticulum endoplasmique, l'appareil de Golgi et d'autres organites sont fortement recrutés pour former des structures périnucléaires. Ces structures ne sont pas des organites isolés et sont connectées de manière dynamique avec le système sécrétoire. Il existe un lien fonctionnel entre les vésicules mobiles périphériques impliquées dans le mouvement intracellulaire du virus et la structure périnucléaire. Les évènements qui déterminent le recrutement des endomembranes dans la formation de la structure périnucléaire restent à élucider, mais la réplication du génome viral et l'assemblage du virion se déroulent probablement au sein de ces structures.

Abstract

Although there is a significant amount of literature that deals with the identification of plant viral proteins involved in membrane remodeling and vesicle production in infected cells, there are very few investigations that report on the impact that infection has on the overall architecture and dynamics of the early secretory endomembranes. Recent investigations have shown that for some viruses the endoplasmic reticulum, Golgi bodies and other organelles are heavily recruited into virus-induced perinuclear structures. These structures are not isolated organelles and are dynamically connected to the bulk of non-modified endomembranes. They also have a functional link with peripheral motile vesicles involved in virus intracellular movement. The full molecular events that consubstantiate with this endomembrane recruitment in virus-induced structures remain to be elucidated but viral genome replication and virion assembly are likely taking place within these structures.

Introduction

Recent advances in cell fluorescent imaging and tomography coupled to electron microscopy are bringing growing interest in understanding the architecture and role of the cellular remodeling that is taking place upon infection by viruses (for extensive reviews on the subject, refer to [1,2]). Because most investigations on cellular remodeling in plant cells have been conducted using positive-sense (+) RNA viruses, this review will mainly focus on this class of viruses. Replication by plant (+) RNA viruses, like their vertebrate homologs, leads to the formation in the infected cell of elaborate membranous, organelle-like, platforms that sustain viral RNA synthesis and cell-to-cell movement. These membrane modifications are believed to increase the local concentrations of viral and host proteins needed to produce new genomes, which likely enhance replication efficiency, and possibly to provide protection from host defense response [3]. They also act as vehicles for the egress of viral RNA for systemic infection throughout the plant (for a review on the subject, refer to [4]).

Different plant virus groups induce the formation of diverse structures from host endomembranes, both in terms of architecture and membrane/organelle origin. Endomembranes is defined here as a system of interconnected membranes that fills the cell interior and connects the cell boundary with the double membraned organelles - nucleus, plastids and mitochondria. Essentially, every single organelle found in a plant cell is targeted by one virus or another. For example, Tomato bushy stunt virus (TBSV) replicates in peroxisomes [5], Carnation Italian ringspot virus in mitochondria [6] and Turnip yellow mosaic virus in chloroplasts [7]. The significance of this organellar diversity is unknown, but specific membrane targeting appears not to be a strict requirement for efficient viral infection as replication complexes can be redirected to an alternate sub-cellular localization [8,9]. There are also many examples indicating that membrane remodeling is the consequence of plant viruses replicating or moving on endoplasmic reticulum (ER)-derived membranes. This results in the formation of mini-organelles referred to as spherules, vesicles or multivesicular bodies [10-17]. These vesicles may be single or double membrane structures that are often connected to the cytosol by a narrow neck, allowing exchange of components needed for replication [18]. The ER is a major component of the cell's secretory pathway, which is a series of steps a cell uses to move host

components to their final functional location. The secretory pathway was thus shown to be used for intra- and intercellular viral movement [19-25]. Virus use of the secretory pathway not only has a morphological impact on ER, it also leads to an inhibition of protein secretion [26] and may promote specific lipid synthesis [27]. Although there is a significant amount of literature that deals with the identification of the viral proteins involved in membrane remodeling and vesicle production, there are very few investigations that report on the impact that plant virus infection has on the overall architecture and dynamics of the early secretory endomembranes. This review will look at recent works that show that Potato virus X (PVX) and Turnip mosaic virus (TuMV) infections lead to endomembrane recruitment into large perinuclear globular structures that are functionally linked to smaller peripherally located motile vesicles that ultimately become associated with plasmodesmata. This connection would provide an assembly line for viral genome replication and virus egress into neighboring cells.

Plant cell biology

Before looking at endomembrane recruitment during plant virus infections, it may be important to provide an overview of the general morphology of plant cells. For those interested in a more detailed account of plant cell morphology, they are invited to consult The Illuminated Plant Cell website (http://www.illuminatedcell.com/Home.html). First, it must be realized that for many plant cells there is limited free cytosolic space, which is restricted by the presence of large central vacuoles and by the sheer number of chloroplasts. Within this constricted space, the ER pervades the cell and has an extremely dynamic, multifunctional and pleomorphic nature [28,29]. Morphologically, it is characterized by a nuclear envelope-connected ER and a peripheral (cortical) tubular and cisternal ER juxtaposing the plasma membrane. Transvacuolar ER strands provide a direct link between the perinuclear and the cortical ER and act as distribution routes for metabolites, organelles [30] and are also thought to be involved in anchoring the nucleus within the cell [31]. The plant Golgi apparatus is present in the form of several motile bodies that are distributed throughout the cytoplasm and are associated with microfilaments [32]. Golgi bodies also move in close association with ER tubules and traffic rapidly within transvacuolar strands [33], whereas in animal cells the Golgi apparatus occupies a rather stationary perinuclear position

[34]. Another important difference is the absence in plant cells of an intermediate compartment between ER and the Golgi apparatus, which is present in mammalian cells and known as the ER-Golgi intermediate compartment (ERGIC) [35]. Finally, plant cells have plasmodesmata that provide cytoplasmic continuity between neighboring cells that supports the cell-to-cell and long-distance trafficking of small molecules as well as of a wide spectrum of endogenous proteins and ribonucleoprotein complexes. These plasma membrane lined channels contain ER-derived desmotubules and actin filaments and are used for virus cell-to-cell spread [for a review on the topic see [4,36]. These distinctive features may explain the relationship between ER-associated virus replication centers and virus egress through plasmodesmata [37].

Recruitment of endomembranes into virus-induced structures

Membrane-associated replication complexes contain viral RNA as well as viral and host replication factors but not much is known about their host endomembrane composition. This question has recently been addressed in the case of potato virus X (PVX, genus potexvirus). At late infection stages, PVX induces the formation of large inclusion bodies often localized next to the nucleus, which have historically been termed "X-bodies", that contain viral RNA [38], PVX replication proteins, virions and ribosomes [12,39]. Very recently, Tilsner et al. [40] have analyzed the contribution of endomembranes to these X-bodies. First, they found that the triple gene block protein 1 (TGBp1) forms the core of the X-bodies, which have a layered structure with TGBp1 aggregates at the center, vRNA in the middle and virions at the cytoplasmic periphery (Fig. 1). They found that the ER and Golgi (as well as actin filaments) are heavily recruited into these structures, apparently reorganized into densely stacked membranes (Fig. 1). Since TGB proteins are not needed for PVX replication, the authors propose that this elaborate structure provides a restricted environment that would link replication with movement and possibly encapsidation.

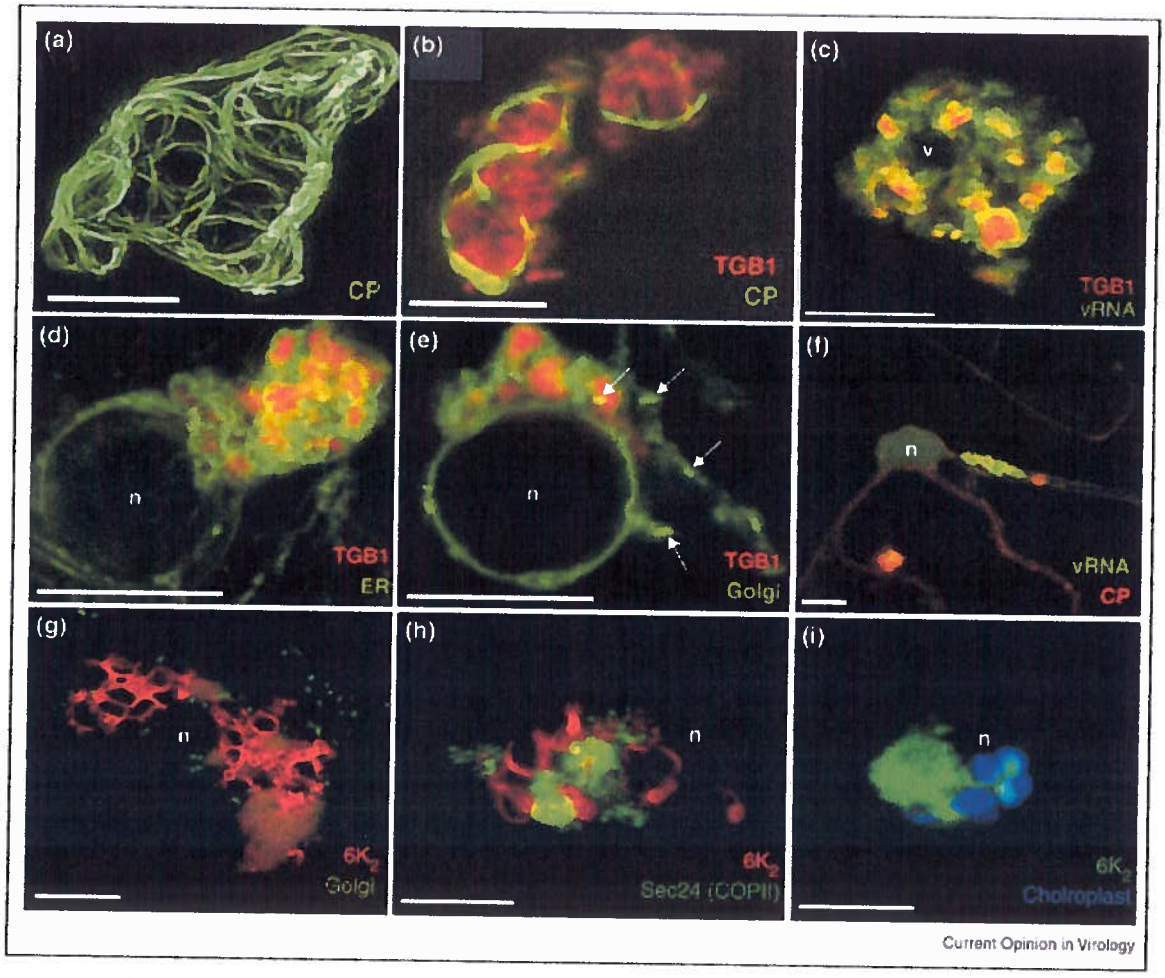

Figure 1: Recruitment of endomembranes into virus-induced structures.

(a)–(f) Distribution of viral and host components in the PVX X-body. (a) GFP-CP expressed from a green overcoat virus construct labels virions that form cages around the X-body. (b) Aggregates of TGB1-mCherry localize within the cage formed by GFP-CP-decorated virions in green overcoat PVX-infected tissue. (c) TGB1-mCherry is located within PUM-BiFC-labeled vRNA whorls. (d) Recruitment of ER by perinuclear TGBp1-mCherry aggregates in uninfected tissue. The ER is wrapped tightly around the aggregates. (e) Recruitment of Golgi membranes and disassembly of Golgi stacks by TGB1-mCherry. Similar to the ER, Golgi membranes are wrapped tightly around the perinuclear aggregates. A few individual Golgi stacks are visible (arrows). (f) X-body containing vRNA and CP near the nucleus. (g)–(i) Organelle recruitment in TuMV globular structure. TuMV-infected cells expressing $6K_2$-mCherry (g, h) or 6K2-GFP (i), co-expressed with ST-GFP a Golgi marker (g), sec24-YFP (h) or with chloroplast autofluorescence (i). Bar = 10 μm. (n) indicates nucleus position. (a)–(F) reproduced from [40] with permission of the American Society of Plant Biologists. (g)–(i) reproduced from [41] with permission of the American Society for Microbiology.

Grangeon et al [41] have reported that turnip mosaic virus (TuMV, genus potyvirus) infection also leads to the formation of perinuclear globular structures similar to X-bodies. The $6K_2$-VPg-Pro precursor protein of potyviruses has been shown to be a scaffold protein around which the viral replication complex assembles [15,42-46]. VPg binds several viral and host proteins, in particular translation factors (for a review, refer to [47]) while the $6K_2$ is responsible for membrane recruitment [47]. They examined the distribution of well characterized ER and Golgi organelle markers in TuMV-infected cells by confocal microscopy. In TuMV-infected cells, the cortical ER does not show any apparent modification but is speckled with $6K_2$-tagged vesicles (from now on designated as peripheral vesicles). On the other hand, the perinuclear ER is enlarged into a large irregular shaped globular-like structure that contained $6K_2$ and is linked to the cortical ER by transvacuolar strands. The ER is compacted within this structure and does not show a polygonal tubular pattern. Golgi bodies, COPII coatamers and chloroplasts are also recruited into this perinuclear globular structure (Fig. 1). Disruption of the early secretory pathway by Brefeldin A (BFA) or by co-expression of a dominant-negative mutant of Arf1, which regulates membrane traffic between the Golgi and ER, does not affect the formation of the globular structure. Similarly, BFA does not affect replication of Melon necrotic spot virus whereas it has a negative impact on cell-to-cell movement [**19**]. This situation is also observed during coronavirus infection where virus-induced remodeling of endoplasmic reticulum membranes and viral replication, albeit reduced, still take place in the presence of BFA [**48**].

However, despite their close association, ER and Golgi recruitment may not take place in tandem for all plant viruses. For instance, cowpea mosaic virus infection induces massive proliferation of ER and its recruitment into virus-induced vesicles, but not of Golgi membranes [**14**]. A similar situation is found for Grapevine fanleaf virus [**11**]. This noticeable dissimilarity suggests the existence of different mechanisms for host endomembrane recruitment during plant virus infection.

Dynamics of virus-induced structures

The plant ER and Golgi bodies are dynamic secretory organelles, constantly undergoing remodeling [**49,50**]. Since the perinuclear globular structure observed in TuMV-infected cells contains an amalgam of condensed ER and Golgi membranes, investigations have been performed to observe if this compartment is nevertheless

functionally linked to the bulk of non-modified endomembranes [41]. Fluorescence recovery after photobleaching (FRAP) experiments and the use of photoactivable GFP (PAGFP) [51] indicated that the TuMV-induced perinuclear structure is not an isolated subcellular compartment, Golgi and ER being connected to the bulk of the host cell endomembranes. It also appears that this compartment is a reservoir that can hold a large quantity of ER membranes. It has been reported that plant viral infections stimulate de novo membrane synthesis [14,52,53] and perhaps the bulk of newly synthesized lipids accumulate in these perinuclear structures. On the other hand, the perinuclear globular structure is not rapidly restocked in viral components following photobleaching, with no input of viral proteins from near-by perinuclear structures. Similarly, the internal architecture of Hepatitis C virus membranous webs appears relatively static, with limited exchange of viral proteins within and between neighboring replication complexes [54].

However, this apparent inactivity in restocking for viral components does not mean that the globular structure is a closed entity for viral proteins. PAGFP is used for fluorescent pulse labeling of fusion proteins at a specific position within a cell, which allows their subsequent cellular redistribution to be monitored [51]. When $6K_2$ was fused to PAGFP and expressed in infected cells and photoactivation performed within the globular structure, activated $6K_2$-PAGFP fluorescence was found to rapidly fill up the globular structure and motile $6K_2$-tagged vesicles were seen to originate and to move away from this same structure. These experiments then provide evidence for a functional link between the perinuclear globular structure and peripheral vesicles. Tilsner et al. [40] also demonstrated that there is continuity between the X-bodies and peripheral vesicles associated with movement proteins and thus viral egress.

TuMV peripheral vesicles show rapid trafficking along transvacuolar strands as if they were travelling on a highway out and into the perinuclear globular structure [41] (Fig. 2). This trafficking is likely brought by rearrangements in the actin cytoskeleton [30]. Several groups have looked at the contribution of the cytoskeleton in the intracellular trafficking of virus-induced structures (for a review on the subject, refer to [22,55]. For example, the group of Rick Nelson analyzed the association of tobacco mosaic virus-induced bodies with microfilaments [16].

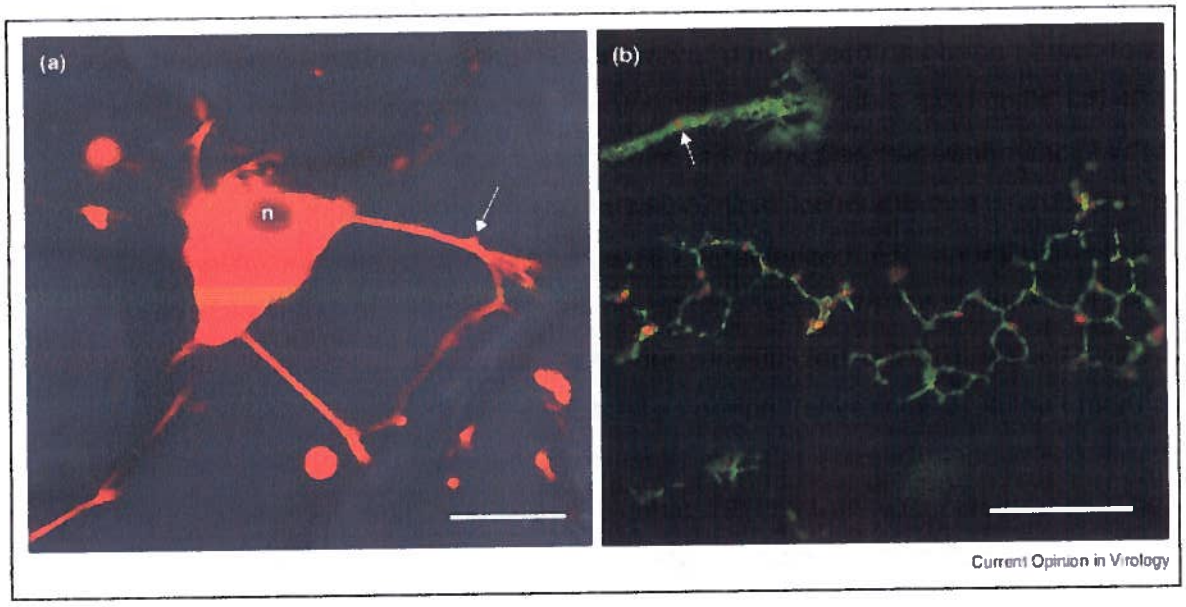

Figure 2: Dynamics of virus-induced structures

(a) TuMV-infected cells expressing $6K_2$-mCherry showing that transvacuolar strands provide a direct link between the perinuclear structure and the cell periphery highlighted by brightfield. (b) TuMV-infected cells expressing $6K_2$-mCherry showing association of peripheral vesicles with cortical ER (HDEL-GFP). n indicates nucleus position. Arrows indicate a peripheral vesicle moving within a transvacuolar strand. Bar = 10 µm.

Time-lapse imaging shows that the peripheral bodies traffic along microfilaments with average velocities of 1 μm/s with top speed approaching 8 μm/s. The movement of these bodies has subsequently been shown to depend on myosin motors [15,20,21]. Plasmodesmata are the ultimate destination of this trafficking.

Endomembranes are not only recruited to virus replication complexes, they are actively remodeled. For example, TBSV recruits ESCRT (endosomal sorting complexes required for transport) factors [3] and Brome mosaic virus (BMV) host reticulon proteins [56,57] to facilitate membrane curving during virus-induced structure formation.

Recruitment of endomembranes in Arabidopsis thaliana mutant lines

Interestingly, defects in the early secretory pathway can produce similar recruitment of endomembranes into perinuclear structures as those observed in PVX- and TuMV-infected cells. Faso et al. [58] characterized an A. thaliana mutant that partially accumulates Golgi membrane markers and a soluble secretory marker in perinuclear globular structures entwined with actin cables and composed of a mass of convoluted ER tubules that maintain a connection with the bulk ER. The mutation also leads to impaired traffic of proteins at the ER/Golgi interface. In the same vein, Nakano et al. [59] isolated two A. thaliana mutants with defects in ER morphology and designated them endoplasmic reticulum morphology1 (ermo1) and ermo2. The cells of both mutants develop a number of ER-derived spherical bodies, approximately 1 μm in diameter, that also contain Golgi bodies. The above lines have a defect in one of the Sec24 isomers that causes a partial loss of function for the binding of cargo protein intended for secretion. Faso et al. [58] hypothesized that if constitutive traffic is disrupted, inappropriate fusion of vesicles between the ER and the Golgi may occur, creating an aberrant compartment. It is then plausible that the formation of the perinuclear globular structure is the consequence of an interfering event between a viral protein and Sec24 or another host protein of that nature.

Such interfering events have been documented for vertebrate viruses. The viral proteins involved are membrane-associated and interact or interfere with

cellular membrane trafficking proteins of the early secretory pathway [60-63]. However, there is as yet no report showing a specific interaction with a plant viral protein and a host secretory pathway component but there is one investigation indicating that this may be the case. The triple gene block protein 3 (TGBp3) of Bamboo mosaic virus (genus potexvirus) induces by itself the production of peripheral vesicles that are associated with the cortical ER. Wu et al. [23] showed that mutations in the C-terminal region of the protein no longer formed vesicles in the cortical ER but exhibited perinuclear ER localization and concluded that C-terminal region of TGBp3 likely contains a sorting signal specifying cortical ER localization, implying interaction with a secretory pathway component. The tobacco etch virus (genus potyvirus) $6K_2$ protein may also have an ER export signal [64]. It will be interesting to see if these viral proteins target a component of the early secretory pathway at the ER/Golgi interface that leads to inhibition of protein secretion and formation of the perinuclear globular structure.

We suggest the following model to describe the cellular remodeling taking place during TuMV infection that shares many features with PVX replication (Fig. 3). Early in the infection process, the incoming viral RNA is translated and the viral gene products contribute to the formation of the perinuclear globular structure.Replication events (i.e. negative and positive-sense RNA transcription) take place within this globular structure and these events would still happen even if the ER-Golgi interface is disrupted during viral infection. After this step, viral egress is initiated by the budding of $6K_2$ vesicles at ERES in the globular structure, which then traffic along the ER/microfilaments towards the plasma membrane and plasmodesmata for ultimate delivery of the virus into neighboring cells.

Conclusion

The full molecular events that consubstantiate with this endomembrane recruitment in virus-induced structures remain however to be elucidated. Evidently viral genome replication and likely virion assembly are taking place within these structures. The fact that there is heavy recruitment of organelles into these structures would also reflect a need for sustained high synthetic activity that is required for virus production.

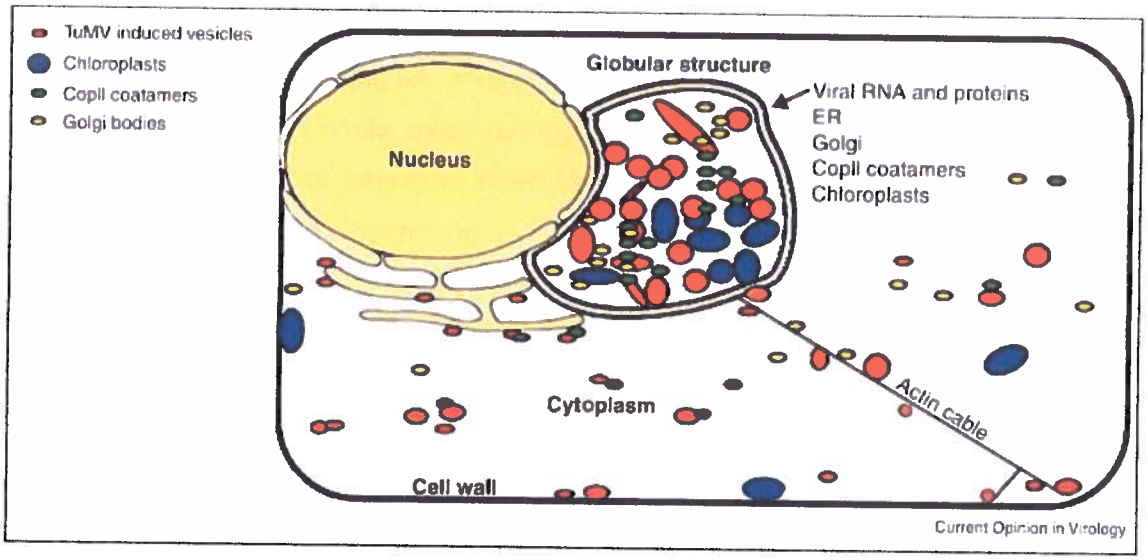

Figure 3: Model of perinuclear structure.

Early in the infection process, the incoming viral RNA is translated and the viral gene products contribute to the formation of the perinuclear globular structure. Following replication events (i.e., negative and positive-sense RNA transcription) that take place within this globular structure, viral egress is initiated by vesicle budding. Vesicles then traffic along the ER/microfilaments towards the plasma membrane and plasmodesmata for ultimate delivery of the virus into neighboring cells.

Future investigations will thus aim at identifying host proteins that are involved in the formation of the perinuclear structure. Additionally, considering the large size of these structures, other events may take place concomitantly. For instance, the unfolded protein response has been proposed to be an element of PVX infection [65]. The active role of the host endomembranes in other plant (+)RNA virus replication should also be explored to broaden our understanding of general and unique aspects of these membranes in supporting viral processes.

Acknowledgements

We thank the anonymous reviewer for his/her constructive comments. Studies in J-F Laliberté laboratory are supported by grants from the Natural Sciences and Engineering Research Council of Canada and from Le Fonds québécois de recherche sur la nature et les technologies.

References

Papers of particular interest have been highlighted as:

- * of special interest
- ** of outstanding interest

1. den Boon JA, Ahlquist P: Organelle-like membrane compartmentalization of positive-strand RNA virus replication Factories. Annual Review of Microbiology 2010, 64:241-256.

2. Laliberté J-F, Sanfaçon H: Cellular remodeling during plant virus infection. Annual Review of Phytopathology 2010, 48:69-91.

3. Barajas D, Jiang Y, Nagy PD: A unique role for the host ESCRT proteins in replication of Tomato bushy stunt virus. Plos Pathogens 2009, 5:e1000705.

4. Niehl A, Heinlein M: Cellular pathways for viral transport through plasmodesmata. Protoplasma 2011, 248:75-99.

5. McCartney AW, Greenwood JS, Fabian MR, White KA, Mullen RT: Localization of the tomato bushy stunt virus replication protein p33 reveals a peroxisome-to-endoplasmic reticulum sorting pathway. Plant Cell 2005, 17:3513-3531.

6. Hwang YT, McCartney AW, Gidda SK, Mullen RT: Localization of the Carnation Italian ringspot virus replication protein p36 to the mitochondrial outer membrane is mediated by an internal targeting signal and the TOM complex. BMC Cell Biol 2008, 9:54.

7. Prod'homme D, Jakubiec A, Tournier V, Drugeon G, Jupin I: Targeting of the turnip yellow mosaic virus 66K replication protein to the chloroplast envelope is mediated by the 140K protein. J Virol 2003, 77:9124-9135.

8. Jonczyk M, Pathak KB, Sharma M, Nagy PD: Exploiting alternative subcellular location for replication: tombusvirus replication switches to the endoplasmic reticulum in the absence of peroxisomes. Virology 2007, 362:320-330.

9. Miller DJ, Schwartz MD, Dye BT, Ahlquist P: Engineered retargeting of viral RNA replication complexes to an alternative intracellular membrane. J Virol 2003, 77:12193-12202.

10. Schwartz M, Chen J, Lee WM, Janda M, Ahlquist P: Alternate, virus-induced membrane rearrangements support positive-strand RNA virus genome replication. Proc Natl Acad Sci U S A 2004, 101:11263-11268.

11. Ritzenthaler C, Laporte C, Gaire F, Dunoyer P, Schmitt C, Duval S, Piequet A, Loudes AM, Rohfritsch O, Stussi-Garaud C, et al.: Grapevine fanleaf virus replication occurs on endoplasmic reticulum-derived membranes. Journal of Virology 2002, 76:8808-8819.

12. Ju HJ, Samuels TD, Wang YS, Blancaflor E, Payton M, Mitra R, Krishnamurthy K, Nelson RS, Verchot-Lubicz J: The potato virus X TGBp2 movement protein associates with endoplasmic reticulum-derived vesicles during virus infection. Plant Physiol 2005, 138:1877-1895.

13*. Bamunusinghe D, Seo J-K, Rao ALN: Subcellular localization and rearrangement of endoplasmic reticulum by brome mosaic virus capsid protein. J. Virol. 2011, 85:2953-2963.

14. Carette JE, Stuiver M, Van Lent J, Wellink J, Van Kammen AB: Cowpea mosaic virus infection induces a massive proliferation of endoplasmic reticulum but not Golgi membranes and is dependent on de novo membrane synthesis. Journal of Virology 2000, 74:6556-6563.

15*. Wei TY, Huang TS, McNeil J, Laliberte JF, Hong J, Nelson RS, Wang AM: Sequential Recruitment of the Endoplasmic Reticulum and Chloroplasts for Plant Potyvirus Replication. Journal of Virology 2010, 84:799-809.

16. Liu JZ, Blancaflor EB, Nelson RS: The tobacco mosaic virus 126-kilodalton protein, a constituent of the virus replication complex, alone or within the complex aligns with and traffics along microfilaments. Plant Physiology 2005, 138:1853-1865.

17. Kusumanegara K, Mine A, Hyodo K, Kaido M, Mise K, Okuno T: Identification of domains in p27 auxiliary replicase protein essential for its association with the endoplasmic reticulum membranes in Red clover necrotic mosaic virus. Virology 2012.

18. Pogany J, Nagy PD: Authentic replication and recombination of Tomato bushy stunt virus RNA in a cell-free extract from yeast. J Virol 2008, 82:5967-5980.

19. Genoves A, Navarro JA, Pallas V: The Intra- and intercellular movement of Melon necrotic spot virus (MNSV) depends on an active secretory pathway. Mol Plant Microbe Interact 2010, 23:263-272.

20*. Amari K, Lerich A, Schmitt-Keichinger C, Dolja VV, Ritzenthaler C: Tubule-Guided Cell-to-Cell Movement of a Plant Virus Requires Class XI Myosin Motors. Plos Pathogens 2011, 7.

21*. Harries PA, Park JW, Sasaki N, Ballard KD, Maule AJ, Nelson RS: Differing requirements for actin and myosin by plant viruses for sustained intercellular movement. Proceedings of the National Academy of Sciences of the United States of America 2009, 106:17594-17599.

22. Harries PA, Schoelz JE, Nelson RS: Intracellular Transport of Viruses and Their Components: Utilizing the Cytoskeleton and Membrane Highways. Molecular Plant-Microbe Interactions 2010, 23:1381-1393.

23**. Wu CH, Lee SC, Wang CW: Viral protein targeting to the cortical endoplasmic reticulum is required for cell-cell spreading in plants. Journal of Cell Biology 2011, 193:521-535.

24. Schepetilnikov MV, Solovyev AG, Gorshkova EN, Schiemann J, Prokhnevsky AI, Dolja VV, Morozov SY: Intracellular targeting of a hordeiviral membrane-spanning movement protein: Sequence requirements and involvement of an unconventional mechanism. Journal of Virology 2008, 82:1284-1293.

25. Haviv S, Moskovitz Y, Mawassi M: The ORF3-encoded proteins of vitiviruses GVA and GVB induce tubule-like and punctate structures during virus infection and localize to the plasmodesmata. Virus Research 2012, 163:291-301.

26. Wei TY, Wang AM: Biogenesis of Cytoplasmic Membranous Vesicles for Plant Potyvirus Replication Occurs at Endoplasmic Reticulum Exit Sites in a COPI- and COPII-Dependent Manner. Journal of Virology 2008, 82:12252-12264.

27. Zhang J, Diaz A, Mao L, Ahlquist P, Wang X: Host acyl coenzyme A binding protein regulates replication complex assembly and activity of a positive-strand RNA virus. J Virol 2012, 86:5110-5121.

28. Sparkes IA, Frigerio L, Tolley N, Hawes C: The plant endoplasmic reticulum: a cell-wide web. Biochemical Journal 2009, 423:145-155.

29. Staehelin LA: The plant ER: a dynamic organelle composed of a large number of discrete functional domains. Plant J 1997, 11:1151-1165.

30. Hoffmann A, Nebenführ A: Dynamic rearrangements of transvacuolar strands in BY-2 cells imply a role of myosin in remodeling the plant actin cytoskeleton. Protoplasma 2004, 224:201-210.

31*. Ruthardt N, Gulde N, Spiegel H, Fischer R, Emans N: Four-dimensional imaging of transvacuolar strand dynamics in tobacco BY-2 cells. Protoplasma 2005, 225:205-215.

32. Akkerman M, Overdijk EJR, Schel JHN, Emons AMC, Ketelaar T: Golgi Body Motility in the Plant Cell Cortex Correlates with Actin Cytoskeleton Organization. Plant and Cell Physiology 2011, 52:1844-1855.

33. Yang YD, Elamawi R, Bubeck J, Pepperkok R, Ritzenthaler C, Robinson DG: Dynamics of COPII vesicles and the Golgi apparatus in cultured Nicotiana tabacum BY-2 cells provides evidence for transient association of Golgi stacks with endoplasmic reticulum exit sites. Plant Cell 2005, 17:1513-1531.

34. Neumann U, Brandizzi F, Hawes C: Protein transport in plant cells: in and out of the Golgi. Ann Bot 2003, 92:167-180.

35. Hanton SL, Bortolotti LE, Renna L, Stefano G, Brandizzi F: Crossing the divide - Transport between the endoplasmic reticulum and Golgi apparatus in plants. Traffic 2005, 6:267-277.

36. Ueki S, Citovsky V: To Gate, or Not to Gate: Regulatory Mechanisms for Intercellular Protein Transport and Virus Movement in Plants. Molecular Plant 2011, 4:782-793.

37. Kawakami S, Watanabe Y, Beachy RN: Tobacco mosaic virus infection spreads cell to cell as intact replication complexes. Proc Natl Acad Sci U S A 2004, 101:6291-6296.

38. Tilsner J, Linnik O, Christensen NM, Bell K, Roberts IM, Lacomme C, Oparka KJ: Live-cell imaging of viral RNA genomes using a Pumilio-based reporter. Plant Journal 2009, 57:758-770.

39. Bamunusinghe D, Hemenway CL, Nelson RS, Sanderfoot AA, Ye CM, Silva MAT, Payton M, Verchot-Lubicz J: Analysis of potato virus X replicase and TGBp3 subcellular locations. Virology 2009, 393:272-285.

40**. Tilsner J, Linnik O, Wright KM, Bell K, Roberts AG, Lacomme C, Santa Cruz S, Oparka KJ: The TGB1 Movement Protein of Potato virus X Reorganizes Actin and Endomembranes into the X-Body, a Viral Replication Factory. Plant Physiology 2012, 158:1359-1370.

41**. Grangeon R, Agbeci M, Chen J, Grondin G, Zheng H, Laliberté J-F: Impact on the endoplasmic reticulum and Golgi apparatus during Turnip mosaic virus infection. Journal of Virology 2012.

42. Beauchemin C, Boutet N, Laliberte J-F: Visualization of the interaction between the precursors of VPg, the viral protein linked to the genome of turnip mosaic virus, and the translation eukaryotic initiation factor iso 4E in planta. J. Virol. 2007, 81:775-782.

43. Dufresne PJ, Thivierge K, Cotton S, Beauchemin C, Ide C, Ubalijoro E, Laliberté J-F, Fortin MG: Heat shock 70 protein interaction with Turnip mosaic virus RNA-dependent RNA polymerase within virus-induced membrane vesicles. Virology 2008, 374:217-227.

44. Thivierge K, Cotton S, Dufresne PJ, Mathieu I, Beauchemin C, Ide C, Fortin MG, Laliberte JF: Eukaryotic elongation factor 1A interacts with Turnip mosaic virus RNA-dependent RNA polymerase and VPg-Pro in virus-induced vesicles. Virology 2008, 377:216-225.

45. Cotton S, Grangeon R, Thivierge K, Mathieu I, Ide C, Wei T, Wang A, Laliberte JF: Turnip mosaic virus RNA replication complex vesicles are mobile, align with microfilaments, and are each derived from a single viral genome. Journal of Virology 2009, 83:10460-10471.

46. Huang TS, Wei T, Laliberte JF, Wang A: A host RNA helicase-like protein, AtRH8, interacts with the potyviral genome-linked protein, VPg, associates with the virus accumulation complex, and is essential for infection. Plant Physiol 2010, 152:255-266.

47. Jiang J, Laliberté J-F: The genome-linked protein VPg of plant viruses—a protein with many partners. Current Opinion in Virology 2011, 1:347-354.

48. Knoops K, Swett-Tapia C, van den Worm SHE, Velthuis AJWT, Koster AJ, Mommaas AM, Snijder EJ, Kikkert M: Integrity of the Early Secretory Pathway Promotes, but Is Not Required for, Severe Acute Respiratory Syndrome Coronavirus RNA Synthesis and Virus-Induced Remodeling of Endoplasmic Reticulum Membranes. Journal of Virology 2010, 84:833-846.

49. Boevink P, Oparka K, Cruz SS, Martin B, Betteridge A, Hawes C: Stacks on tracks: the plant Golgi apparatus traffics on an actin/ER network. Plant Journal 1998, 15:441-447.

50. Nebenfuhr A, Gallagher LA, Dunahay TG, Frohlick JA, Mazurkiewicz AM, Meehl JB, Staehelin LA: Stop-and-go movements of plant Golgi stacks are mediated by the acto-myosin system. Plant Physiology 1999, 121:1127-1141.

51. Runions J, Brach T, Kuhner S, Hawes C: Photoactivation of GFP reveals protein dynamics within the endoplasmic reticulum membrane. Journal of Experimental Botany 2006, 57:43-50.

52. Lee WM, Ahlquist P: Membrane synthesis, specific lipid requirements, and localized lipid composition changes associated with a positive-strand RNA virus RNA, replication protein. Journal of Virology 2003, 77:12819-12828.

53. Sharma M, Sasvari Z, Nagy PD: Inhibition of phospholipid biosynthesis decreases the activity of the tombusvirus replicase and alters the subcellular localization of replication proteins. Virology 2011, 415:141-152.

54. Wolk B, Buchele B, Moradpour D, Rice CM: A dynamic view of Hepatitis C virus replication complexes. J. Virol. 2008, 82:10519-10531.

55. Schoelz JE, Harries PA, Nelson RS: Intracellular Transport of Plant Viruses: Finding the Door out of the Cell. Molecular Plant 2011, 4:813-831.

56. Diaz A, Ahlquist P: Role of host reticulon proteins in rearranging membranes for positive-strand RNA virus replication. Curr Opin Microbiol 2012, 15:519-524.

57. Diaz A, Wang X, Ahlquist P: Membrane-shaping host reticulon proteins play crucial roles in viral RNA replication compartment formation and function. Proc Natl Acad Sci U S A 2010, 107:16291-16296.

58. Faso C, Chen Y-N, Tamura K, Held M, Zemelis S, Marti L, Saravanan R, Hummel E, Kung L, Miller E, et al.: A Missense Mutation in the Arabidopsis COPII Coat Protein Sec24A Induces the Formation of Clusters of the Endoplasmic Reticulum and Golgi Apparatus. The Plant Cell Online 2009, 21:3655-3671.

59**. Nakano RT, Matsushima R, Ueda H, Tamura K, Shimada T, Li L, Hayashi Y, Kondo M, Nishimura M, Hara-Nishimura I: GNOM-LIKE1/ERMO1 and SEC24a/ERMO2 are required for maintenance of endoplasmic reticulum morphology in Arabidopsis thaliana. Plant Cell 2009, 21:3672-3685.

60*. Sharp TM, Guix S, Katayama K, Crawford SE, Estes MK: Inhibition of Cellular Protein Secretion by Norwalk Virus Nonstructural Protein p22 Requires a Mimic of an Endoplasmic Reticulum Export Signal. PLoS ONE 2010, 5:e13130.

61. Moffat K, Knox C, Howell G, Clark SJ, Yang H, Belsham GJ, Ryan M, Wileman T: Inhibition of the Secretory Pathway by Foot-and-Mouth Disease Virus 2BC Protein Is Reproduced by Coexpression of 2B with 2C, and the Site of Inhibition Is Determined by the Subcellular Location of 2C. J. Virol. 2007, 81:1129-1139.

62. Belov GA, Altan-Bonnet N, Kovtunovych G, Jackson CL, Lippincott-Schwartz J, Ehrenfeld E: Hijacking Components of the Cellular Secretory Pathway for Replication of Poliovirus RNA. J. Virol. 2007, 81:558-567.

63. Belov GA, Feng Q, Nikovics K, Jackson CL, Ehrenfeld E: A Critical Role of a Cellular Membrane Traffic Protein in Poliovirus RNA Replication. PLoS Pathog 2008, 4:e1000216.

64. Lerich A, Langhans M, Sturm S, Robinson DG: Is the 6 kDa tobacco etch viral protein a bona fide ERES marker? Journal of Experimental Botany 2011, 62:5013-5023.

65. Ye C, Dickman MB, Whitham SA, Payton M, Verchot J: The Unfolded Protein Response Is Triggered by a Plant Viral Movement Protein. Plant Physiology 2011, 156:741-755.

Revue n° 3

Remodelage cellulaire par les phytovirus

Soumis à la revue virologie le 22 avril 2013

Romain Grangeon et Jean-François Laliberté

Institut National de la Recherche Scientifique; INRS-Institut Armand-Frappier; Laval, QC Canada

* Corresponding author : Jean-François Laliberté

Email: jeanfrancois.laliberte@iaf.inrs.ca

Contribution

J'ai écrit le texte, et Jean-François Laliberté m'a supervisé et effectué les modifications finales. Comme cette revue a été écrite en français elle a été intégralement ajoutée dans la partie de l'introduction intitulée : Remodelage cellulaire par les phytovirus.

Résumé

Lorsqu'une plante est infectée par un virus, les cellules sont reprogrammées et subissent des modifications morphologiques importantes. Ces modifications conduisent à partir de membranes cellulaires à la formation d'usines qui sont requises pour la réplication virale. Cette revue discute de la biogenèse des différentes usines qui sont observées et de l'impact de leur formation sur le fonctionnement de la cellule. L'implication de ces usines dans le mouvement des virus de cellule à cellule et la modification des plasmodesmes sont également abordées.

Abstract

The plant cell is reprogrammed and undergoes drastic morphological alterations during infection by viruses. Infection leads to the formation of viral factories, derived from host cell membranes for viral replication. This review discusses the biogenesis of the different viral replication factories that are observed and the impact of their formation on the cell metabolism. The involvement of viral factories in cell-to-cell movement of the virus and modifications of plasmodesmata are also described.